UNIVERSITÀ DEGLI STUDI DI MESSINA

DOTTORATO DI RICERCA IN FISICA

XXXIII CICLO

Open Hybrid Quantum Systems in the Ultra-Strong Coupling Regime

Alessio Settineri

Alessio Settineri

Coordinatore Dottorato:

Chiar.ma Prof.ssa V. Crupi

Relatore:

Chiar.mo Prof. S. Savasta

S. Savasta

Triennio 2017/2020

Contents

List of Publications

I. **Dissipation and thermal noise in hybrid quantum systems in the ultrastrong-coupling regime**
Alessio Settineri, Vincenzo Macrí, Alessandro Ridolfo, Omar Di Stefano, Anton Frisk Kockum, Franco Nori, Salvatore Savasta
Physical Review A ***95***, 053834 (2019)

II. **Conversion of mechanical noise into correlated photon pairs: Dynamical Casimir effect from an incoherent mechanical drive**
Alessio Settineri, Vincenzo Macrí, Luigi Garziano, Omar Di Stefano, Franco Nori, Salvatore Savasta
*Physical Review A****100***, 022501 (2019)

III. **Interaction of mechanical oscillators mediated by the exchange of virtual photon pairs**
Omar Di Stefano, Alessio Settineri, Vincenzo Macrí, Alessandro Ridolfo, Roberto Stassi, Anton Frisk Kockum, Salvatore Savasta, Franco Nori
Physical Review Letters ***122***, 030402 (2019)

IV. **Resolution of gauge ambiguities in ultrastrong-coupling cavity quantum electrodynamics**
Omar Di Stefano, Alessio Settineri, Vincenzo Macrì, Luigi Garziano, Roberto Stassi, Salvatore Savasta, Franco Nori
Nature Physics ***15***, 803−808 (2019)

V. **Gauge invariance of the Dicke and Hopfield models**
Luigi Garziano, Alessio Settineri, Omar Di Stefano, Salvatore Savasta, Franco Nori,
Physical Review A **102**, 023718, (2020)

VI. **Gauge freedom, quantum measurements, and time-dependent interactions in cavity and circuit QED**
Alessio Settineri, Omar Di Stefano, David Zueco, Stephen Hughes, Salvatore Savasta, Franco Nori
arXiv:, 1912.08548 (2019)

VII. **Gauge Principle and Gauge Invariance in Quantum Two-Level Systems**
Salvatore Savasta, Omar Di Stefano, Alessio Settineri, David Zueco, Stephen Hughes, Franco Nori
arXiv:2002.04241, (2020)

I. **Near-field imaging of surface-plasmon vortex-modes around a single elliptical nanohole in a gold film**
Claudia Triolo, Salvatore Savasta, Alessio Settineri, Sebastiano Trusso, Rosalba Saija, Nisha Rani Agarwal, Salvatore Patanè
Scientific Reports **9**, 5320 (2020)

Acknowledgements

First of all I would like to express my sincere gratitude and thanks to my supervisor Salvatore Savasta for giving me the chance to work and explore the wonderful world of quantum optics in the ultrastrong light-matter coupling regime. Thank you for your infinite enthusiasm and for sharing with me your knowledge. A special thanks goes also to Omar Di Stefano who has been much more than a colleague, you are a good friend of mine. I would like to thank both of you for encouraging me every day allowing me not only to grow as a research scientist but also as a person. Last but not least I would like to thank my colleagues and friends Luigi Garziano, Vincenzo Macrì, Roberto Stassi and Alessandro Ridolfo for the stimulating discussions and for all the time we spent together in these three years. I want you to know that I will carry forever a lot of wonderful memories of all the good moments we had together.

I also acknowledge support by the Army Research Office (ARO) (Grant No. W911NF1910065).

Messina, September 2020 Alessio Settineri

Introduction

Quantum mechanics has always provided a conceptual framework for the description of microscopic phenomena and has been applied to explain properties and behaviour of a wide range of natural systems. In particular, the main developments have been achieved through the first half of the twentieth century thanks to the understanding of the interaction of matter with electromagnetic fields. Several achievements in the understanding of these properties have been obtained treating the electromagnetic field classically. However, in order to fully understand the light-matter interactions a full quantum theory is required. For example, quantum mechanics allowed to understand the transport and optical properties of materials. Nowadays, the field studying these light-matter interactions using a fully quantum description for both light and matter is the so called Quantum Optics. This widespread field is attracting great growing interest and is driving the second quantum revolution. Indeed, during the last several decades much efforts have been directed at exploiting the most puzzling effects of quantum mechanics, like, for example, the quantum superpositions and the entanglement, for the development of practical technologies. As part of this research direction, devices for high-precision sensing [1–4], secure communication [5,6] and quantum information processing [7], have been implemented in several types of systems. The driving force behind all these developments is the ability to experimentally manipulate and control quantum dynamics in a large variety of systems ranging from single photons [5, 8], atoms and ions [9, 10], individual electron and nuclear spins [11–13], to mesoscopic superconducting circuits [14, 15] and nanomechanical devices [16, 17]. In particular, each of these systems possesses physical properties that make it better suited than others for specific tasks; for example is well-known that, photons are best suited for transmitting quantum information, weakly interacting spins may

be used as long-lived quantum memories, while superconducting circuits can rapidly process information encoded in their quantum states.

The main goal of the quantum technologies is the implementation of devices that can simultaneously perform several of these tasks in the most efficient way. This goal, can be achieved by combining different systems in order to build a new "hybrid" system able to hopefully inherit only the advantages of each one of its components and to provide the required multitasking capabilities [18–20]. Specifically, the fundamental property of a functional hybrid quantum system (HQS) is the ability to communicate, with high fidelity, quantum states and properties between its different components. Clearly, even if the idea behind a hybrid quantum system is conceptually simple the experimental realization of such a device requires careful planning and several challenges may arise. For example, if the energy scales of the coupled components are too different, even in the presence of a good interaction, the swap processes between the subsystems may not take place. Another obstacle arises when the effective coupling strength g_{eff} between the subsystems is too weak. In this case, the fidelity of the communication between the components results very low. Notice that the minimal coupling strength required for a functional hybrid quantum system is determined by the coherence time, that is the time over which quantum superposition states survive. It follows that the effective coupling rate g_{eff} between the subsystems must be large enough to allow quantum state transfer between them within the shortest coherence time T_{min} of the two, *i.e.*, $g_{\text{eff}}\, T_{\text{min}} \gg 1$.

The first ideas of hybrid quantum systems derive from quantum information processing and were inspired by the progresses in circuit quantum electrodynamics (circuit QED), where superconducting qubits are coupled to high-quality microwave resonators [21–26]. Superconducting artificial atoms based on Josephson junctions are well-controlled quantum systems but, differently than natural atoms, they suffer from short coherence times since they are very sensitive to environmental noise from extrinsic and intrinsic decohering elements. A better design of the qubits [27–30] and the surrounding circuitry could reduce decoherence caused by extrinsic elements such as the local electromagnetic environment. On the other hand, coherence is limited

by more intrinsic elements, like the low-frequency noise, that are very hard to avoid. However, superconducting quantum circuits present different advantages. For example, as they can be designed with specific parameters, the strong-coupling limit for one or more superconducting qubits in a coplanar waveguide resonator can be attained much more easily than for natural atoms in an optical cavity (cavity QED system) [31]. Moreover, by taking advantage of the large kinetic inductance of a Josephson junction in the center conductor of a resonator, it has been possible to experimentally achieve the so-called ultrastrong coupling regime [31–34], where the light-matter coupling strength is comparable to the energy scales of the system components (in this case, qubit and photon). For relatively large Josephson energies ($E_J > 1000\,\mathrm{GHz}$), the coupling energy can easily reach values of ~ 1000 MHz and beyond, corresponding to several tens of percent of the resonator frequency [32]. As long as the Josephson inductance is small compared to that of the qubit, this coupling can be increased further by lowering the Josephson energy of the inserted junction.

The importance of the ultrastrong coupling regime in this specific type of hybrid systems does not rely only in the possibility to get better performances from new promising quantum computing technologies [35]. Indeed, this light-matter regime presents a great variety of new exciting phenomena that cannot be observed in the conventional weak and strong coupling regimes [33, 34, 36–38]. Most of them derive from the fact that in this ultrastrong coupling regime, the rotating wave approximation of the Jaynes Cummings model [39], well describing many cavity QED experiments in the standard weak and strong coupling regimes, breaks down and the counter-rotating terms in the interaction Hamiltonian lead to observable experimental consequences [33, 34]. In this situation, the total number of excitations in the system is no more conserved, even if the parity is [40]. The most important consequence of this fact is that the ground state of the system is now a squeezed vacuum containing a finite number of virtual qubit(s)-resonator excitations [36, 41] that cannot be experimentally detected unless a time-dependent perturbation is applied to the system [36]. Other hybrid systems with a great potential for the development of new quantum tech-

nologies are the so-called optomechanical systems, in which a mechanical resonator interacts with an optical cavity [42–45]. The typical experimental setup is constituted by an optical cavity in which one of the mirrors can move serving as mechanical harmonic oscillator. If the vibrational energy of the movable mirror becomes larger than the thermal energy k_BT, the mechanical oscillation can behave quantum mechanically and the resulting quantized vibrations of the mirror can couple to the photons in the cavity due to radiation pressure. This kind of setup has been realized in a large variety of systems in recent years [46–50]. However, the experimental observation of this quantum behavior is challenging since it requires the cooling of the mechanical resonator to extremely low temperatures and the ability to generate nonclassical states. It is possible to realize an analogue of a cavity optomechanical system exploiting superconducting circuits without the necessity of using any moving part [51]. In this case, the circuit consists of a coplanar transmission line with an electrical length that can be changed at a few percent of the speed of light by modulating the inductance of a superconducting quantum interference device (SQUID) composed by two Josephson junctions which form a loop [52]. The movement is then simulated by tuning the magnetic field passing through the SQUID loop. Using this type of superconducting systems, it has been possible to observe the creation of real photons out of vacuum fluctuations [53] as in the dynamical Casimir effect (DCE), where a mobile mirror undergoing relativistic motion convert virtual photons into directly observable real photons [54]. In this case, however, the boundary conditions of the system are modulated by an effective motion, producing a parametric amplification of vacuum fluctuations (*parametric*-DCE [55–59]). Thus, these optical experiment do not demonstrate the conversion of mechanical energy into photons as predicted by the dynamical Casimir effect. Recently, much effort has been directed by many groups towards this type of hybrid quantum system and various designs/applications have been explored. Among all these studies we could highlight the generation of quantum entanglement [60], quantum measurement [61], high precision displacement detection [62], and cooling [63–65]. Moreover, since quantum superpositions are the main resources for quantum information processing, many theoretical

proposals and experimental demonstrations have been presented in order to generate arbitrary superpositions of different mechanical Fock states [66–69].

Overview and Results

The thesis is structured as follows. After an introductory part giving an overview of the field and providing the general context in which my research activity has taken place, a brief description of the theoretical tools is presented.

In Chapter 1, the quantum theory of light-matter interaction in cavity QED is presented . After a brief review of the weak and strong coupling regimes, the peculiarities of the ultrastrong coupling regime are shown. In particular, it is pointed out that in this regime the rotating wave approximation cannot be safely made and counter-rotating terms in the interaction Hamiltonian must be taken into account. This evidence has two important consequences, namely that the total number of excitations in the system is no more conserved and the dressed ground state now contains a finite number of virtual excitations.

Chapter 2 is devoted to describe the theoretical model behind the interaction between optical and mechanical resonators. The canonical quantization of both the field and the motion of the mirror, in order to derive a nonrelativistic Hamiltonian of a one-dimensional mirror-field coupled system in a cavity configuration, is discussed. This approach leads to a more detailed description of a typical cavity optomechanical setup in terms of an Hamiltonian known as "Law Hamiltonian" [70]. This theoretical framework provides a more fundamental explanation of the Casimir dynamic effect, and opens the door to a possible experimental observation of light emission from mechanical motion.

Chapter 3 is devoted to describe the standard formulation of dissipation in the ultrastrong coupling regime. In particular, it has been demonstrated that, while the standard quantum optical master equation can be safely used to describe the dynamics of the system in the weak and strong coupling

regimes, in the ultrastrong coupling regime this standard approach fails to correctly describe the dissipation processes and leads to unphysical results as well [71]. For example, an incautious application of the standard relations for a system in its dressed ground state, which now contains a finite number of photons due to the counter-rotating terms in the Rabi Hamiltonian, would result in a prediction of an unphysical stream of output photons from the vacuum even in the absence of any external driving. The dressed master equation approach presented in this chapter has been used as starting point to derive a generalized approach in Paper 5.1

Chapter 4 is devoted to introduce the Gauge Principle in quantum mechanics. In particular, after a brief general introduction, I provide a review of the issues recently pointed out by several groups claiming that this fundamental principle is violated when the light-matter system enters the ultrastrong or deepstrong coupling regime.

Chapter 5 and Chapter 6 provide an overview of my publications in chronological order.

In particular, Chapter 5 is mainly centered on papers studying the dynamics of open Hybrid Quantum Systems (HQSs). According to quantum mechanics, a closed system always displays a reversible evolution. However, no quantum system is completely isolated from its environment; for example, control and readout of a quantum system requires a coupling to the outside world, which leads to dissipation and decoherence. For this reason, realistic quantum systems should be regarded as open. The standard approaches to describe the HQSs dynamics neglect the interaction among the system components when considering their coupling to the environment. This approximation, as has been shown for cavity-QED [71] and optomechanical [72] systems, leads to unphysical predictions when the interaction strength becomes large as in the ultrastrong-coupling regime. In Paper 5.1 we went beyond these previous derivations and presented a general master equation approach for arbitrary hybrid quantum systems interacting with thermal reservoirs. This approach has been used to study the influence of temperature on multiphoton vacuum Rabi oscillations in circuit QED and the conversion of mechanical energy into photon pairs in an optomechanical

system.

In Paper 5.2 we studied the dynamical Casimir effect (DCE) in the ultrastrong cavity optomechanics. Specifically, by adopting a fully quantum-mechanical approach for both the cavity field and the oscillating mirror [73], and by using the generalized master equation (presented in Paper 5.1) we found that the dynamical Casimir effect can be observed also when the movable mirror is excited by and incoherent drive removing one of the major obstacles for the experimental observation of this long-sought effect.

In Paper 5.3 we considered a generalized optomechanical system consisting of two vibrating mirrors constituting an optical resonator. Specifically, we found that motional forces can determine noticeable coupling rates between the two spatially separated vibrating mirrors. It follows that, by tuning the two mechanical oscillators into resonance, it is possible to observe an energy exchange between them, enabled by virtual photon pairs (Casimir photon pairs). Thus, the electromagnetic quantum vacuum is able to transfer mechanical energy, acting somewhat like an ordinary fluid.

Papers in Chapter 6 are, instead, mainly centered on the resolution of the ambiguities recently arose on the validity of the Gauge invariance principle in the USC regime. Gauge invariance is the cornerstone of modern quantum field theory. When the light-matter interaction becomes very strong, different gauges can lead to drastically different predictions, leading to several controversies [74–78]. Recently, it has been claimed that the quantum Rabi model (see Chapter 1), describing the dipolar coupling between a two-level atom and a quantized electromagnetic field, violates this principle giving different predictions depending on the chosen gauge [79]. This failure is attributed to the finite-level truncation of the matter system. In Paper 6.1 we show that a careful application of the gauge principle is able to restore gauge invariance of the quantum Rabi model even for extreme light-matter interaction regimes. The resulting Hamiltonian in the Coulomb gauge significantly differs from the standard model and provides the same physical results obtained by using the dipole gauge. It turns out that it contains field operators to all orders that cannot be neglected when the coupling strength is high. These results shed light on several subtleties of gauge invariance in nonperturbative and

extreme interaction regimes, which are now experimentally accessible, and solve all the long-lasting controversies arising from gauge ambiguities in the quantum Rabi and Dicke models.

In Paper 6.2 we focused on the resolution of serveral fundamental issues like the proper definition of subsystems and their quantum measurements, the structure of light-matter ground states, or the analysis of time-dependent interactions arising when considering high coupling strength regimes like the ultrastrong and the deep strong.

In Paper 6.3 we studied the gauge invariance of the USC Dicke model, which describes the dipolar coupling between N two-level atoms and a quantized electromagnetic field. Specifically, we have shown that, while the two-level approximation can work well in the dipole gauge, the Coulomb gauge fails to provide the correct spectra in the ultrastrong coupling regime. However, taking into account the non-locality of the atomic potential induced by the two-level approximation, gauge invariance is fully restored for arbitrary interaction strengths, even in the limit of N going to infinity. Finally, we expressed the Hopfield model, a general description based on the quantization of a linear dielectric medium, in a manifestly gauge-invariant form, and showed that the Dicke model in the dilute regime can be regarded as a particular case of the more general Hopfield model.

In conclusion, in Paper 6.4 we provided an alternative derivation of the results obtained in Paper 6.1, based on the implementation of the gauge principle in two-level systems. The adopted procedure can be regarded as the two-site version of the general method used to implement the gauge principle in lattice gauge theories. Applying this method, we have also obtained the gauge-invariant quantum Rabi model for asymmetric two-state systems, and the multi-mode gauge-invariant quantum Rabi model beyond the dipole approximation.

Chapter 1

Cavity QED

Quantum electrodynamics (QED) studies the interaction of atoms with the quantum fluctuations of the electromagnetic field. The general description of this kind of interactions is pretty complex and should involve both the internal structure of the system (atom, molecule, solid, etc.) and the infinite number of modes of the electromagnetic field, which can be easily described as a collection of independent harmonic oscillators. However, in cavity QED the atoms are placed inside a resonant cavity which supports only discrete modes of the electromagnetic field whose resonance frequencies can be properly adjusted with respect to the transition frequency of the atoms. Thus, the problem can be considerably simplified by considering one cavity mode of frequency ω_c and a two level atom $|g\rangle$ and $|e\rangle$ with energy separation $E_\mathrm{e} - E_\mathrm{g} = \hbar(\omega_e - \omega_g) \equiv \hbar\omega_q$ such that $\omega_c \simeq \omega_q$, while all the other cavity modes can be disregarded since do not couple to the atom due to the large frequency mismatch. Such an approach is still valid in many physical experiments and allows one to describe the light-matter interaction in its simplest form. Within this simplified model the system can be depicted as in Fig. 1.1.

In order to properly describe a QED system it is important to define the atom-cavity field coupling rate g, resulting from the interaction between the atom and the zero-point fluctuations of the electromagnetic field in the cavity, which is given by [80]:

$$g = \sqrt{\frac{d_{eg}^2 \omega_c}{2\hbar\epsilon_0 V_0}}, \tag{1.1}$$

where ω_c is the angular cavity frequency, ϵ_0 is the electric permittivity, V_0 is the cavity volume and d_{eg} is the dipole moment associated to the atomic transition.

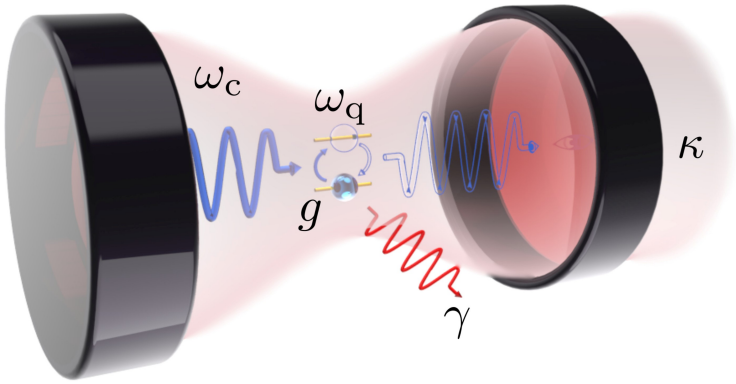

Figure 1.1: Two-level atom inside a single-mode resonant cavity. The light-matter interaction is described by three parameters: the atom-field interaction strength g, the cavity photon decay rate κ and the atomic decay rate into non-cavity modes γ.

When the atom-cavity interaction rate is slower than all the loss rates ($g << \kappa, \gamma$), the system is in the weak coupling regime and photons emitted by the atom escape the cavity before being reabsorbed in a process analogous to the spontaneous emission in the free-space. On the contrary, when $g >> \kappa, \gamma$, the system enters the so-called strong coupling regime, in which the periodic exchange of the excitation between the atom and the cavity is faster than the *irreversible* processes given by the photon losses into non-cavity modes. In this case, the photon emission is a *reversible* process in which the photon is absorbed by the atom before it can leave the cavity. In the strong coupling regime, the energy eigenstates of the system are no longer the bare states of the atom and the cavity mode, but they are instead coherent superpositions of atom and photon excitations (dressed energy eigenstates), also known as polaritons. Moreover, the atom and cavity resonances exhibit an avoided crossing and the resulting splitting is referred to as the "vacuum-Rabi" splitting, as predicted by the well known Jaynes-Cummings model [39, 81, 82]. When the qubit-cavity coupling strength becomes comparable to the transition frequency of the qubit or the resonance

frequency of the cavity mode $g/\omega_{c,q} \simeq 0.1$, the system enters the ultrastrong coupling regime (USC) which displays a great variety of new exciting effects that are not observed in the conventional weak and strong-coupling regimes [36–38]. Recently, due to the experimental progress in the development of circuit quantum electrodynamics (circuit QED) systems, where superconducting artificial qubits are coupled to on-chip cavities, it has been possible to experimentally achieve the USC regime [31–34]. This regime has also been achieved with photochromic molecules [83], by using intersubband transitions in semiconductor structures [84, 85] or by coupling the cyclotron transition of a high-mobility two-dimensional electron gas to the photonic modes of an array of electronic split-ring resonators [86]. When the coupling rates exceed the transition frequencies of the bare components we reach the so-called deep-strong-coupling (DSC) [40]. This extremely high interaction regime have been recently obtained in both a circuit QED setup [87] and with a two-dimensional electron gas [88].

1.0.1 Quantum Rabi Model

In order to describe the interaction of a qubit with the quantized field of a cavity, let us introduce the Pauli spin operators $\hat{\sigma}_z, \hat{\sigma}_y, \hat{\sigma}_x$ expressed in the bare basis $\{|g\rangle, |e\rangle\}$:

$$\hat{\sigma}_z = \hat{\sigma}_+\hat{\sigma}_- - \hat{\sigma}_-\hat{\sigma}_+ = \begin{pmatrix} 1 & 0 \\ 0 & -1 \end{pmatrix} = |e\rangle\langle e| - |g\rangle\langle g| \tag{1.2}$$

$$\hat{\sigma}_x = \hat{\sigma}_- + \hat{\sigma}_+ = \begin{pmatrix} 0 & 1 \\ 1 & 0 \end{pmatrix} = |g\rangle\langle e| + |e\rangle\langle g| \tag{1.3}$$

$$\hat{\sigma}_y = i(\hat{\sigma}_- - \hat{\sigma}_+) = \begin{pmatrix} 0 & -i \\ i & 0 \end{pmatrix} = i(|g\rangle\langle e| - |e\rangle\langle g|) \tag{1.4}$$

and the raising and lowering operators $\hat{\sigma}_+$ and $\hat{\sigma}_-$,

$$\hat{\sigma}_+ = \begin{pmatrix} 0 & 1 \\ 0 & 0 \end{pmatrix} = |e\rangle\langle g| \tag{1.5}$$

$$\hat{\sigma}_- = \begin{pmatrix} 0 & 0 \\ 1 & 0 \end{pmatrix} = |g\rangle\langle e| \tag{1.6}$$

$$\tag{1.7}$$

The raising operators $\hat{\sigma}_+$ produces a transition from the lower to the upper state and the lowering operator $\hat{\sigma}_-$ has the opposite effect. The $\hat{\sigma}_z$ operator coincides with the corresponding Pauli spin matrix, while the pseudo-spin raising and lowering operators can be related to the Pauli matrices through the relation $\hat{\sigma}_\pm = \frac{1}{2}\left[\hat{\sigma}_x \pm i\hat{\sigma}_y\right]$.

The total Hamiltonian for the system,

$$\hat{H} = \hat{H}_{\mathrm{Q}} + \hat{H}_{\mathrm{C}} + \hat{V} \tag{1.8}$$

contains three terms: $\hat{H}_{\mathrm{C}}$ and $\hat{H}_{\mathrm{Q}}$, describing the cavity field and the qubit, respectively, and the qubit-cavity interaction $\hat{V}$. In terms of the qubit operators, the qubit Hamiltonian is given by

$$\hat{H}_{\mathrm{Q}} = \frac{1}{2}\hbar\omega_{\mathrm{q}}\hat{\sigma}_z = \frac{1}{2}\hbar\omega_{\mathrm{q}}\,|e\rangle\langle e| - \frac{1}{2}\hbar\omega_{\mathrm{q}}\,|g\rangle\langle g| \tag{1.9}$$

In Eq. (1.9) the zero point of energy has been chosen half-way between levels $|e\rangle$ and $|g\rangle$, so that the energy of the state $|e\rangle$ is $E_{\mathrm{e}} = \frac{1}{2}\hbar\omega_{\mathrm{q}}$ and that of $|g\rangle$ is $E_{\mathrm{g}} = -\frac{1}{2}\hbar\omega_{\mathrm{q}}$. The Hamiltonian for the cavity field is

$$\hat{H}_{\mathrm{C}} = \hbar\omega_{\mathrm{c}}\hat{a}^\dagger\hat{a}, \tag{1.10}$$

where $\hat{a}^\dagger$ and $\hat{a}$ are, respectively, the bosonic creation and annihilation operators for the cavity mode. Finally, in the dipole approximation, the qubit-cavity interaction has the standard form

$$\hat{V} = -d \cdot E = -d \cdot \epsilon E(\mathbf{r_0})(\hat{a} + \hat{a}^\dagger), \tag{1.11}$$

where $E(\mathbf{r_0})$ is the the electric field at the qubit position $\mathbf{r_0}$ and $\epsilon = (\hbar\omega_c/\epsilon_0 V_0)^{\frac{1}{2}}$ is the field per photon within the cavity volume V_0. The dipole-moment operator can be expressed as

$$d = |g\rangle\langle g|\, d\, |e\rangle\langle e| + |e\rangle\langle e|\, d\, |g\rangle\langle g| = d_{ge}\hat{\sigma}_- + d_{eg}\hat{\sigma}_+ \tag{1.12}$$

If we assume, without loss of generality, that the matrix elements of the dipole-moment operator are real ($\langle g\,|d|\,e\rangle = \langle e\,|d|\,g\rangle$) and define the qubit-cavity coupling strength as

$$\hbar g \equiv -\langle e\,|d\cdot\epsilon|\,g\rangle\, E(r_0), \tag{1.13}$$

we can write the the qubit-cavity interaction Hamiltonian as

$$\hat{V} = \hbar g(\hat{\sigma}_+ + \hat{\sigma}_-)(\hat{a} + \hat{a}^\dagger) = \hbar g\hat{\sigma}_x(\hat{a} + \hat{a}^\dagger). \tag{1.14}$$

Thus, the total Hamiltonian for the system becomes:

$$H = \frac{1}{2}\hbar\omega_q\hat{\sigma}_z + \hbar\omega_c\hat{a}^\dagger\hat{a} + \hbar g(\hat{\sigma}_+ + \hat{\sigma}_-)(\hat{a} + \hat{a}^\dagger) \tag{1.15}$$

known as *Quantum Rabi Hamiltonian*. Eq. (1.15) describes the full qubit-cavity interaction without any approximation. In the latter, the interaction term $\hat{a}^\dagger\hat{\sigma}_-$ corresponds to the process in which the atom loses its excitation creating one photon, while the term $\hat{a}\hat{\sigma}_+$ describes the inverse process. Both processes are near-resonant and oscillate at frequencies $\pm(\omega_c - \omega_q)$. On the other hand, the terms $\hat{a}\hat{\sigma}_-$ and $\hat{a}^\dagger\hat{\sigma}_+$ (counter-rotating terms), which in the interaction picture oscillate with the sum frequencies $\pm(\omega_c + \omega_q)$, describe the nonresonant processes in which the atom and the field are excited or de-excited simultaneously. These terms do not conserve the total energy of the system. Indeed, for $E_e > E_g$, the operator combination $\hat{a}\hat{\sigma}_-$ annihilates a photon and induces a transition from the higher energy state $|e\rangle$ to the lower energy state $|g\rangle$, while $\hat{a}^\dagger\hat{\sigma}_+$, creates a photon during the transition $|g\rangle \to |e\rangle$. In analogy with the classical case, these nonresonant terms are usually dropped performing the so-called rotating wave approximation

(RWA). However, these terms can be neglected only in the case in which the ratio $g/\omega_c \ll 1$, and this can be understood considering that the counter rotating terms couples the states $|g, n\rangle$ and $|e, n+1\rangle$ that differ by two excitations

$$\langle e, n+1| \hbar g(\hat{a}\hat{\sigma}_- + \hat{a}^\dagger\hat{\sigma}_+) |g, n\rangle = \langle g, n| \hbar g(\hat{a}\hat{\sigma}_- + \hat{a}^\dagger\hat{\sigma}_+) |e, n+1\rangle \approx \hbar g, \tag{1.16}$$

while the energy difference between the bare states (at resonance) is

$$\langle e, n+1| \hat{H}_0 |e, n+1\rangle - \langle g, n| \hat{H}_0 |g, n\rangle \approx 2\hbar\omega_c, \tag{1.17}$$

where $\hat{H}_0 = \frac{1}{2}\hbar\omega_q\hat{\sigma}_z + \hbar\omega_c\hat{a}^\dagger\hat{a}$.

Comparing Eq. (1.16) and Eq. (1.17), it is easy to observe that the counter-rotating terms become relevant only when the coupling strength g becomes comparable to or much larger than the transition frequency of the atom or the resonance frequency of the cavity mode.
In this situation, $[\hat{H}_R, \hat{\mathcal{N}}_{exc}] \neq 0$, the total number of excitations is not conserved, even though the parity is [40]. Indeed, under the unity parity operator $\hat{\mathcal{P}} = e^{i\pi\hat{\mathcal{N}}_{exc}}$ the field annihilation operator $\hat{a}$ and the atomic operator $\hat{\sigma}_x = \hat{\sigma}_+ + \hat{\sigma}_-$ transform, respectively, as $\hat{\mathcal{P}}^\dagger\hat{a}\hat{\mathcal{P}} = -\hat{a}$ and $\hat{\mathcal{P}}^\dagger\hat{\sigma}_x\hat{\mathcal{P}} = -\hat{\sigma}_x$, so that the commutation relation $[\hat{\mathcal{P}}, \hat{H}_R] = 0$ immediately follows. An important consequence of the non conservation of the total number of excitations is that the ground state of the system is no longer the vacuum state $|g, 0\rangle$ of the JC model, but a new state $|G\rangle$ which now contains both atom and resonator excitations:

$$|G\rangle = \sum_{k=0}^{\infty}(c^G_{g,2k}|g, 2k\rangle + c^G_{e,2k+1}|e, 2k+1\rangle). \tag{1.18}$$

This excitations are regarded as virtual and can be experimentally detected only by turning them into real by applying a time-dependent perturbation to the light-matter coupling [36]. It follows that the number of virtual photons bound in the dressed ground state is not independent of the coupling strength but, actually, increases for increasing values of g. The other dressed states

of the Rabi Hamiltonian can be expanded in terms of the bare states as

$$|j,+\rangle = \sum_{k=0}^{\infty}(c_{\mathrm{g},2k}^{j^+}|\mathrm{g},2k\rangle + c_{\mathrm{e},2k+1}^{j^+}|\mathrm{e},2k+1\rangle), \tag{1.19}$$

$$|j,-\rangle = \sum_{k=0}^{\infty}(c_{\mathrm{g},2k+1}^{j^-}|\mathrm{g},2k+1\rangle + c_{\mathrm{e},2k}^{j^-}|\mathrm{e},2k\rangle), \tag{1.20}$$

where $|j,+\rangle$ and $|j,-\rangle$ indicate, respectively, the even- and odd-parity eigenstates. Although the analytical spectrum of $\hat{H}_{\mathrm{R}}$ has recently been found [89], it is defined in terms of the power series of a transcendental function. An approximate, but more simple form, can be found in the intermediate regime (referred to as the Bloch-Siegert regime) where the coupling strength g is small with respect to $\Sigma \equiv \omega_{\mathrm{c}} + \omega_{\mathrm{q}}$, with the system still being in the ultrastrong coupling regime. This is done using the unitary transformation

$$\hat{U} = e^{[\Lambda\left(\hat{a}\hat{\sigma}_- - \hat{a}^\dagger\hat{\sigma}_+\right)+\xi\left(\hat{a}^2-\hat{a}^{\dagger 2}\right)\hat{\sigma}_z]}, \tag{1.21}$$

where $\Lambda = g/\Sigma$, and $\xi = g\Lambda/2\omega_{\mathrm{c}}$. This yields the Bloch-Siegert Hamiltonian

$$\hat{U}^\dagger\hat{H}_{\mathrm{R}}\hat{U} \simeq \hat{H}_{\mathrm{BS}} = \left(\omega_{\mathrm{c}} + \mu\hat{\sigma}_z\right)\hat{a}^\dagger\hat{a} + \frac{\tilde{\omega}_{\mathrm{q}}}{2}\hat{\sigma}_z + g\hat{I}_+, \tag{1.22}$$

where $\hat{I}_+ = \hat{a}\hat{\sigma}_+ + \hat{a}^\dagger\hat{\sigma}_-$, $\tilde{\omega}_{\mathrm{q}} = \omega_{\mathrm{q}} + \mu$, and $\mu = g^2/\Sigma$.

This Hamiltonian is similar to the Jaynes-Cummings Hamiltonian, but contains Bloch-Siegert shifts μ on qubit and resonator frequencies. Since the Bloch-Siegert Hamiltonian in Eq. (1.22) is block diagonal, its eigenstates can be found exactly to be

$$|n,+\rangle = -\sin\theta_n\,|e,n-1\rangle + \cos\theta_n\,|g,n\rangle\,, \tag{1.23}$$

$$|n,-\rangle = \cos\theta_n\,|e,n-1\rangle + \sin\theta_n\,|g,n\rangle\,, \tag{1.24}$$

where θ_n is Bloch-Siegert mixing angle

$$\theta_n = \arctan\left[\frac{\Delta_n^{\mathrm{BS}} - \sqrt{(\Delta_n^{\mathrm{BS}})^2 + 4g^2n}}{2g\sqrt{n}}\right], \tag{1.25}$$

and $\Delta_n^{\mathrm{BS}} = \omega_{\mathrm{q}} - \omega_{\mathrm{c}} + 2\mu n$. To second order in Λ, the excited eigenstates $\widetilde{|n,\pm\rangle}$ of the Rabi Hamiltonian in the bare basis are then given by

$$\widetilde{|n,\pm\rangle} = U\,|n,\pm\rangle\,, \tag{1.26}$$

while the ground state takes the form

$$|G\rangle = U|g,0\rangle \simeq \left(1 - \frac{\Lambda^2}{2}\right)|g,0\rangle - \Lambda|e,1\rangle + \xi\sqrt{2}|g,2\rangle. \tag{1.27}$$

As mentioned before, the ground state $|G\rangle$ is different from the simple ground state $|g,0\rangle$ of the JC model, as it is a squeezed vacuum containing a finite number of virtual photons. This is one of the most important feature of the ultrastrong coupling regime as, for example, in the presence of nonadiabatic modulations [36], induced Raman transitions [90], spontaneous decay mechanisms [37], or sudden on-off switches of the light-matter interaction [91], these virtual photons can be converted to real ones, giving rise to a stream of quantum vacuum radiation. Moreover, in the ultrastrong coupling regime the resonator field $\hat{X} = \hat{a} + \hat{a}^\dagger$ can display a non-zero vacuum first-order coherence ($|\langle G\,|\hat{a}|\,G\rangle\,|^2 / \langle G\,|\hat{a}^\dagger\hat{a}|\,G\rangle \neq 0$), a situation that does not occur in the JC model, where the vacuum first-order coherence is strictly zero (*e.g.*, $|\langle g,0\,|\hat{a}|\,g,0\rangle\,|^2 = 0$). This property is very important in circuit QED systems constituted by a flux qubit coupled to an on-chip coplanar resonator, as a non-zero expectation value of the resonator field in the system ground state $|G\rangle$ can lead to a vacuum-induced parity-symmetry breaking on an additional artificial atom [92].

The quantum Rabi model (QRM) here described is the fundamental theoretical model used to derive most of the original results presented in this thesis. Specifically, in Paper 5.1, we used the QRM to test our generalized master equation approach. In particular, we investigated the temperature dependence of the two-photon Rabi oscillation process. This exotic effect, peculiar to the USC regime, describes the simultaneous exchange of two excitations between atom and cavity. In Paper 6.2 we presented the solution to several fundamental ambiguities regarding this type of systems in the USC

and DSC regimes. In particular, we shed light on the proper definition of subsystem and its quantum measurement, the structure of light-matter ground state and the analysis of time-dependent interactions. In Papers 6.1 and 6.3 we investigated, respectively, the validity of the gauge invariance principle in the USC regime both for the quantum Rabi and Dicke model. The latter is a generalization of the QRM which takes into account multiple emitters coupled to the cavity.

Chapter 2

Cavity Optomechanics

Light carries momentum which gives rise to radiation pressure forces. The research field which explores the interaction (via radiation pressure) between the electromagnetic field in an optical resonator and a mechanical oscillator at a fundamental level is called cavity optomechanics. During the '90s, several aspects of quantum cavity optomechanical systems such as the squeezing of light [93, 94] and quantum nondemolition (QND) detection of the light intensity [95], which exploit the effective Kerr nonlinearity generated by the optomechanical interaction, have been theoretically studied. Moreover, in the last few years optomechanical systems have been implemented in several designs by many groups [45, 96, 97] and, in particular, this type of HQSs have been promising for the study of fundamental quantum effects on a macroscopic or mesoscopic scale, such as the dynamical Casimir effect (DCE) which [54, 73, 98–100] predicts the generation of photons from the quantum vacuum due to rapid changes of the system geometry. In particular, it has been shown that this fundamental physical process originates from *avoided-level crossings* involving also states with different excitations number [73]. Furthermore, it has also been shown that radiation pressure can be used to entangle macroscopic oscillators like movable mirrors and the achievable entanglement is robust against thermal noise [101].

2.1 The optomechanical Hamiltonian

The system Hamiltonian derived by C.K. Law [70] is a non-relativistic Hamiltonian describing the interaction, due to the radiation pressure, between an

oscillating mirror and the cavity field, derived directly from the canonical quantization of both the cavity field and the oscillating mirror by using the equation of motion of the mirror (regarded as a mechanical harmonic oscillator) and the wave equation (with appropriate boundary conditions) of the field.

Let us consider a one-dimensional cavity formed by two perfectly reflecting mirrors one fixed at $x = 0$ and the other one able to move in a potential well $V(q)$ acting as an infinite wall which prevents the movable mirror from penetrating through the fixed mirror. The cavity field vector potential $A(x,t)$ is then defined in the region $0 \leqslant x \leqslant q(t)$ corresponding to the whole cavity effective length and obeys the wave equation ($c = 1$),

$$\frac{\partial^2 A(x,t)}{\partial x^2} = \frac{\partial^2 A(x,t)}{\partial t^2}\,. \tag{2.1}$$

Notice that we labelled $q(t)$ the position of the movable mirror. By applying the time-dependent boundary conditions $A(0,t) = A(q(t),t) = 0$ ensuring that the electric field is always zero in the rest frame of the mirror surface the non-relativistic equation of motion of the mirror is given by

$$m\ddot{q} = -\frac{\partial V(q)}{\partial q} + \frac{1}{2}\left(\frac{\partial A(x,t)}{\partial x}\right)^2_{x=q(t)}\,, \tag{2.2}$$

where m is the mirror mass. The second term on the right side of Eq. (2.2) is the radiation pressure force that can be derived from the radiation pressure force appearing in the rest frame of the movable mirror. We can now define a set of generalized coordinates Q_k:

$$Q_k = \sqrt{\frac{2}{q(t)}}\int_0^{q(t)} dx A(x,t)\sin\left(\frac{k\pi x}{q(t)}\right) \qquad k\,\epsilon\,\mathbb{N}\,. \tag{2.3}$$

obtained by the modal decomposition of the field in the the basis determined by the instantaneous position of the mirror. By using Eq. (2.3) and the completeness relation of the mode functions, the vector potential can be

written as:

$$A(x,t) = \sum_{k=1}^{\infty} Q_k(t) \sqrt{\frac{2}{q(t)}} \sin\left(\frac{k\pi x}{q(t)}\right) . \tag{2.4}$$

Exploiting Eq. (2.4) and the orthogonality of the mode functions $Q_k(t)$, Eq. (2.1) and Eq. (2.2) read:

$$\begin{aligned} \ddot{Q}_k =& -\omega_k^2 Q_k + 2\frac{\dot{q}}{q}\sum_j g_{kj}\dot{Q}_j + \frac{\ddot{q}q - \dot{q}^2}{q^2}\sum_j g_{kj}Q_j + \frac{\dot{q}^2}{q^2}\sum_{jl} g_{jk}g_{jl}Q_l \,, \\ m\ddot{q} =& -\frac{\partial V(q)}{\partial q} + \frac{1}{q}\sum_{kj}(-1)^{k+j}\omega_k\omega_j Q_k Q_j \,, \end{aligned} \tag{2.5}$$

where the position-dependent frequencies ω_k and the dimensionless coefficients g_{kj} are given by

$$\begin{aligned} \omega_k(q) =& \frac{k\pi}{q}, \\ g_{kj} =& \begin{cases} (-1)^{k+j}\frac{2kj}{j^2-k^2} & , k \neq j \\ 0 & , k = j \end{cases} \end{aligned} \tag{2.6}$$

Starting from Eq. (2.5), we can construct the system Lagrangian $\mathcal{L}$ as

$$\begin{aligned} \mathcal{L}(q,\dot{q},Q_k,\dot{Q}_k) =& \frac{1}{2}\sum_k \left[\dot{Q}_k^2 - \omega_k^2(q)Q_k^2\right] + \frac{1}{2}m\dot{q}^2 - v(q) \\ & -\frac{\dot{q}}{q}\sum_{jk} g_{kj}\dot{Q}_k Q_j + \frac{\dot{q}^2}{2q^2}\sum_{jkl} g_{kj}g_{kl}Q_l Q_j . \end{aligned} \tag{2.7}$$

corresponding to the Hamiltonian:

$$\mathcal{H}(P_k,Q_j,p,q) = \frac{1}{2m}\left(p + \frac{1}{q}\sum_{jk} g_{kj}P_k Q_j\right)^2 + V(q) + \frac{1}{2}\sum_k \left[P_k^2 + \omega_k^2 Q_k^2\right] , \tag{2.8}$$

where P_k and p are canonical momenta conjugate to Q_k and q, defined as

$$\begin{aligned} P_k &= \dot{Q}_k - \frac{\dot{q}}{q}\sum_{jk} g_{kj} P_k Q_j \,, \\ p &= m\dot{q} - \frac{1}{q}\sum_{jk} g_{kj} P_k Q_j \,. \end{aligned} \tag{2.9}$$

It is important to notice that, since the mirror is included as a dynamical degree of freedom, the Hamiltonian in Eq. (2.8) allows us to consider the effects of radiation pressure. Following the canonical quantization procedure, we promote the canonical momenta (P_k, p) and their conjugate variables (Q_k, q) to operators, satisfying the commutation relations

$$\begin{aligned} &\left[\hat{q}, \hat{Q}_j\right] = \left[\hat{q}, \hat{P}_k\right] = \left[\hat{p}, \hat{Q}_j\right] = \left[\hat{p}, \hat{P}_k\right] = 0 \\ &[\hat{q}, \hat{p}] = i\hbar \qquad \left[\hat{Q}_j, \hat{P}_k\right] = i\hbar \end{aligned} \tag{2.10}$$

and define the cavity-length-dependent creation and annihilation operators for each cavity mode as

$$\begin{aligned} \hat{a}_k(\hat{q}) &= \sqrt{\frac{1}{2\hbar\omega_k(\hat{q})}}\left[\omega_k(\hat{q})\hat{Q}_k + i\hat{P}_k\right] \,, \\ \hat{a}_k^\dagger(\hat{q}) &= \sqrt{\frac{1}{2\hbar\omega_k(\hat{q})}}\left[\omega_k(\hat{q})\hat{Q}_k - i\hat{P}_k\right] \,, \end{aligned} \tag{2.11}$$

where the dependence on the operator $\hat{q}$ indicates that, for each position of the mirror, there is a set of *Fock* states associated with that position. However, these creation and annihilation operators are not defined when the cavity has zero length ($q = 0$). This issue can be easily solved by imposing the boundary condition implying the wave function to be identically zero at $q = 0$. Using the operators in Eq. (2.11), the Hamiltonian can be written as:

$$\hat{H}' = \frac{(\hat{p} + \hat{\Gamma})^2}{2m} + V(\hat{q}) + \hbar\sum_k \omega_k(\hat{q})\left[\hat{a}_k^\dagger \hat{a}_k + \frac{1}{2}\right] \,, \tag{2.12}$$

where

$$\hat{\Gamma} = \frac{i\hbar}{2\hat{q}} \sum_{kj} g_{kj} \left[\frac{k}{j}\right]^{\frac{1}{2}} \left[\hat{a}_k^\dagger \hat{a}_j^\dagger - \hat{a}_k \hat{a}_j + \hat{a}_k^\dagger \hat{a}_j - \hat{a}_j^\dagger \hat{a}_k\right] . \tag{2.13}$$

As expected, the vacuum field energy appearing in Eq. (2.12) is divergent and it is the origin of the Casimir force. However, following the usual procedure [102], the Casimir energy results to be finite ($\hbar\pi/24q$ for one-dimensional space) because of the cancellation of the divergent parts of the vacuum pressure from both sides of the mirror [103]. However, this result is obtained considering only the static part (the Casimir effect) of the interaction between the mirror and the outside field and neglecting the dynamical part which describes the change of the field outside the cavity. Nevertheless, this is a good approximation in most physical situations where the cavity field is dominant. At this point we can consider the cavity optomechanical case, in which the movable mirror motion corresponds to the motion of a mechanical resonator (see Fig. 2.1).

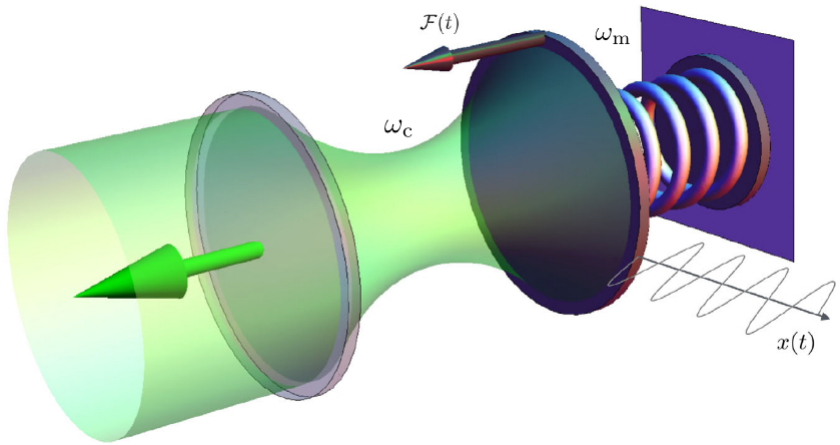

Figure 2.1: Schematic of a generic optomechanical system: a mechanical oscillator with frequency ω_m is coupled via radiation pressure, with a single-mode cavity with frequency ω_c.

In this case, the mirror is bounded by a potential $V(\hat{q})$ which keeps the mirror's range of motion around a certain equilibrium position l_0, and the radiation pressure force acts as a small perturbation. When the mobile mirror displacement $\hat{X} = \hat{q} - l_0$ is small compared with l_0, one can write $\hat{\Gamma} \approx$

$\hat{\Gamma}|_{\hat{q}=l_0} = \hat{\Gamma}_0$, which is the operator $\hat{\Gamma}$ evaluated at the equilibrium position. Furthermore, for small values of $\hat{X}/l_0$ the annihilation operators and the mirror oscillation frequency can be expanded as:

$$\begin{aligned} \hat{a}_k(\hat{q}) &\approx \hat{a}_{k0} - \frac{\hat{X}}{2l_0}\hat{a}_k^\dagger \\ \omega_k(\hat{q}) &\approx \omega_{k0}\left(1 - \frac{\hat{X}}{l_0}\right) . \end{aligned} \tag{2.14}$$

By using the latter relations and performing the unitary transformation with the operator $\hat{U} = \exp(i\hat{X}\Gamma_0/\hbar)$, the Hamiltonian in Eq. (2.12) becomes:

$$\hat{H} = \frac{\hat{p}^2}{2m} + V(\hat{X}) + \hbar\sum_k \omega_{k0}\hat{a}_{k0}^\dagger\hat{a}_{k0} - \hat{X}\hat{F}_0 \,, \tag{2.15}$$

where $\hat{F}_0$ is the normally ordered radiation pressure force

$$\hat{F}_0 = \frac{\hbar}{2l_0}\sum_{kj}(-1)^{k+j}\sqrt{\omega_{k0}\omega_{j0}}\left[\hat{a}_{k0}^\dagger\hat{a}_{j0}^\dagger + \hat{a}_{k0}\hat{a}_{j0} + \hat{a}_{k0}^\dagger\hat{a}_{j0} + \hat{a}_{j0}^\dagger\hat{a}_{k0}\right] . \tag{2.16}$$

Considering only one cavity mode ($k = j = 1$) and expressing the mobile mirror energy and displacement in terms of the creation and annihilation phonon operator

$$\begin{aligned} \hat{b} &= \sqrt{\frac{1}{2\hbar\omega_m}}\left[\omega_m\hat{X} + i\hat{p}\right] , \\ \hat{b}^\dagger &= \sqrt{\frac{1}{2\hbar\omega_m}}\left[\omega_m\hat{X} - i\hat{p}\right] , \end{aligned} \tag{2.17}$$

Eq. (2.15) can be written as

$$\hat{H} = \hbar\omega_c\hat{a}^\dagger\hat{a} + \hbar\omega_m\hat{b}^\dagger\hat{b} + \hbar g(\hat{b}^\dagger + \hat{b})(\hat{a}^\dagger + \hat{a})^2, \tag{2.18}$$

where $\omega_{\mathrm{c(m)}}$ is the cavity (mechanical) frequency and $g = Gx_{zpf}$ is the optomechanical coupling strength with x_{zpf} the amplitude of the mirror zero-point fluctuations and G a coupling parameter. When the mechanical fre-

quency is much smaller than the cavity frequency (which is the most common experimental situation) the quadratic term in Eq. (2.18) can be neglected, because it connects bare states with an energy difference $2\hbar\omega_R \pm \hbar\omega_m$. With this approximation, the resulting Hamiltonian is

$$\hat{H} = \hbar\omega_c \hat{a}^\dagger \hat{a} + \hbar\omega_m \hat{b}^\dagger \hat{b} + \hbar g \hat{a}^\dagger \hat{a}(\hat{b}^\dagger + \hat{b})\,. \tag{2.19}$$

This Hamiltonian, which conserves the number of photons and can be analytically diagonalized, is referred to as standard optomechanical Hamiltonian.

Eq. (2.18) is employed in Papers 5.1 and 5.2 in order to describe, respectively, the influence of temperature on the conversion of mechanical energy into photon pairs and to show that the dynamical Casimir effect can be observed even when the mean value of the mechanical displacement is zero. Furthermore, a generalization of Eq. (2.18), describing a system in which both the mirrors constituting the optical cavity are able to move, has been used in Paper 5.3 to demonstrate that, the quantum vacuum allows the transfer of mechanical excitations between two spatially separated mirrors. In particular, it turns out that this transfer is possible thanks to virtual photon pairs generated by the DCE

Chapter 3

Open Quantum system dynamics

Like in classical physics, any realistic quantum system is subjected to a coupling to an environment which influences it in a non-negligible way. It follows that realistic quantum mechanical systems must always be regarded as open systems. Moreover, a more fundamental reason for introducing the notion of an open system in quantum theory is that quantum mechanics is essentially a probabilistic theory and any test of the statistical predictions on a quantum system requires to couple it to a measurement apparatus which, usually, influences the quantum system being measured. In other words we can say that quantum mechanics contains in itself the notion of an open system through the action of the measurement process. In order to study such a complex system, a fully microscopical description including all the degrees of freedom would be highly desirable. However, a complete microscopic description of a system interacting with an environment is often not feasible and we are forced to seek for a simpler probabilistic description of an open system dynamics. In particular, we need a theory that allows the treatment of complex systems (which involve even an infinite number of degrees of freedom) by restricting the mathematical formulation to a small number of relevant variables. The theoretical tool able to achieve such a desired result is the so-called master-equation approach, in which the dynamics of an open system is formulated by means of an appropriate equation of motion for its density matrix operator. In the following section I will present the dressed master equation approach [71] used as starting point to obtain the

generalized master equation presented in Paper 5.1.

3.1 The dressed Master Equation

Let us consider a system S coupled to another system B usually called *reservoir* modelled as an infinite collection of harmonic oscillators (see Fig. 3.1). Trivially, since both the systems are coupled together the evolution of S will be influenced by B. This interaction leads to a certain system-environment correlations such that the resulting changes in the state of S can no longer be represented in terms of unitary Hamiltonian dynamics. The total Hamil-

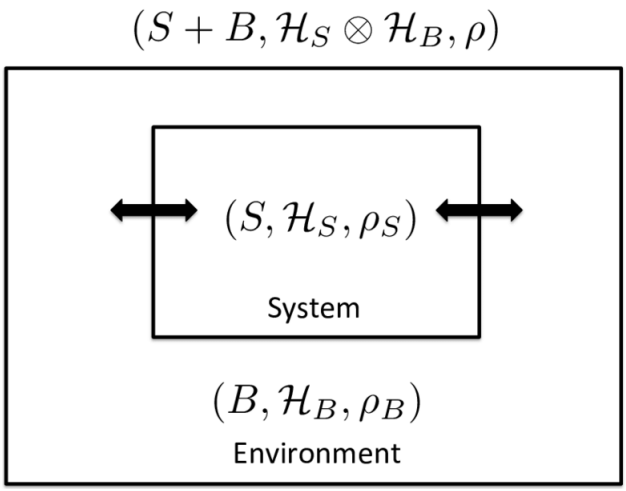

Figure 3.1: Schematic picture of an open quantum system.

tonian of the system in Fig. 3.1 can be written as:

$$\hat{H} = \hat{H}_{\mathrm{S}} + \hat{H}_{\mathrm{B}} + \hat{H}_{\mathrm{SB}}, \tag{3.1}$$

where $\hat{H}_{\mathrm{S}}$ and $\hat{H}_{\mathrm{B}}$ are, respectively, the free Hamiltonian of the system S and of the *reservoir* B while $\hat{H}_{\mathrm{SB}}$ describes the interaction Hamiltonian between the two components. If we denote by $\hat{\chi}(t)$ the density operator of the total system $S+B$ the reduced density operator $\hat{\rho}(t)$ can be obtained through:

$$\hat{\rho}(t) = tr_B[\hat{\chi}(t)], \tag{3.2}$$

where we have taken the partial trace over the *reservoir* degrees of freedom. Once the density operator $\hat{\rho}(t)$ is known, if we consider a generic operator $\hat{O}$ of the system S, its average can be calculated in the Schrödinger picture as:

$$\langle \hat{O} \rangle = tr_{(S\otimes B)}[\hat{O}\,\hat{\chi}(t)] = tr_S\{\hat{O}\,tr_B[\hat{\chi}(t)]\} = tr_S[\hat{O}\hat{\rho}(t)]. \tag{3.3}$$

It follows that the fundamental task of the master-equation approach is to isolate and determine the interesting physical properties of the system S by obtaining an equation for $\hat{\rho}(t)$ containing the properties of the *reservoir* as parameters. Let us start considering the Schrödinger equation for $\hat{\chi}(t)$:

$$\dot{\hat{\chi}} = \frac{1}{i\hbar}[\hat{H}, \hat{\chi}]\,, \tag{3.4}$$

where $\hat{H}$ is given by Eq. (3.1). It is convenient to separate the rapid motion generated by $\hat{H}_{\rm S} + \hat{H}_{\rm B}$ from the slow motion generated by the interaction $\hat{H}_{\rm SB}$. This can be done by rewriting Eq. (3.4) in the interaction picture (note that from now on we will use the tilde symbol to indicate operators in this picture):

$$\dot{\tilde{\chi}} = \frac{1}{i\hbar}[\tilde{H}_{\rm SB}(t), \tilde{\chi}], \tag{3.5}$$

where

$$\tilde{\chi}(t) = e^{\frac{i}{\hbar}(\hat{H}_{\rm S}+\hat{H}_{\rm B})t}\,\hat{\chi}\,e^{-\frac{i}{\hbar}(\hat{H}_{\rm S}+\hat{H}_{\rm B})t}, \tag{3.6}$$

and $\tilde{H}_{\rm SB}(t)$ is explicity time-dependent

$$\tilde{H}_{\rm SB}(t) = e^{\frac{i}{\hbar}(\hat{H}_{\rm S}+\hat{H}_{\rm B})t}\,\hat{H}_{\rm SB}\,e^{-\frac{i}{\hbar}(\hat{H}_{\rm S}+\hat{H}_{\rm B})t}. \tag{3.7}$$

By formally integrating Eq. (3.5) and substituting $\tilde{\chi}(t)$ in the commutator we obtain:

$$\dot{\tilde{\chi}}(t) = \frac{1}{i\hbar}[\tilde{H}_{\rm SB}(t), \tilde{\chi}(0)] - \frac{1}{\hbar^2}\int_0^t dt'\,[\tilde{H}_{\rm SB}(t), [\tilde{H}_{\rm SB}(t'), \tilde{\chi}(t')]]\,. \tag{3.8}$$

The latter is written in a convenient form in order to identify some reasonable assumptions. The first one is that the interaction is turned on at $t = 0$, so

that no correlations exist between the system and the *reservoir* before this initial time. It follows that the total system density matrix $\chi(0) = \tilde{\chi}(0)$ can be factorized as

$$\tilde{\chi}(0) = \tilde{\rho}(0)B_0, \tag{3.9}$$

where B_0 is the initial *reservoir* density operator. After tracing over the *reservoir*, Eq. (3.8) reads

$$\dot{\tilde{\rho}} = -\frac{1}{\hbar^2}\int_0^t dt'\, tr_B\{[\tilde{H}_{\rm SB}(t), [\tilde{H}_{\rm SB}(t'), \tilde{\chi}(t')]]\}, \tag{3.10}$$

where we assumed that $tr_B[\tilde{H}_{\rm SB}(t)B_0] = 0$, a result that is guaranteed if the *reservoir* operators coupled to S have zero mean in B_0. It is important to notice that, even if the system and the *reservoir* are not supposed to interact at $t = 0$, at later times correlations may arise due to the system-bath coupling through the interaction Hamiltonian $\tilde{H}_{\rm SB}$. However, if the coupling is weak $\tilde{\chi}(t)$ will only show deviations of the order of $\tilde{H}_{\rm SB}$ from an uncorrelated state. The second assumption to be taken into account (*Born approximation*) is that the state of B remains unaffected by the coupling with S. The latter is a very reasonable assumption since the bath B is very large, and allows us to write

$$\tilde{\chi}(t) = \tilde{\rho}(t)B_0 + \mathcal{O}(\tilde{H}_{\rm SB}). \tag{3.11}$$

where the higher order terms $\tilde{H}_{\rm SB}$ can be neglected when considering a weak system-reservoir interaction [104]. By using the results in Eq. (3.11) the equation of motion of the reduced density operator can be re-written as:

$$\dot{\tilde{\rho}} = -\frac{1}{\hbar^2}\int_0^t dt'\, tr_B\{[\tilde{H}_{\rm SB}(t), [\tilde{H}_{\rm SB}(t'), \tilde{\rho}(t')B_0]]\}. \tag{3.12}$$

By carefully analyzing the latter result we can notice that the future evolution of $\tilde{\rho}(t)$ depends on its past history through the integration over $\tilde{\rho}(t')$ (not-Markovian behaviour). However, if the *reservoir* is a large system maintained at thermal equilibrium, it is not expected to preserve the minor changes induced by its interaction with S for very long and for sure not for long

enough to significantly affect the future evolution of S. On the basis of these physical grounds, one can expect a Markovian behaviour and can perform the so-called *Markov approximation* by substituting $\tilde{\rho}(t')$ to $\tilde{\rho}(t)$ in Eq. (3.12) to obtain the *Born-Markov master equation*

$$\dot{\tilde{\rho}} = -\frac{1}{\hbar^2}\int_0^t dt'\, tr_B\{[\tilde{H}_{\rm SB}(t),[\tilde{H}_{\rm SB}(t'),\tilde{\rho}(t)B_0]]\}. \tag{3.13}$$

In order to derive the dressed master equation approach [71] let us consider a more practical system, e.g., an arbitrary qubit-resonator system in the ultrastrong coupling regime described by the Rabi Hamiltonian Eq. (1.15).

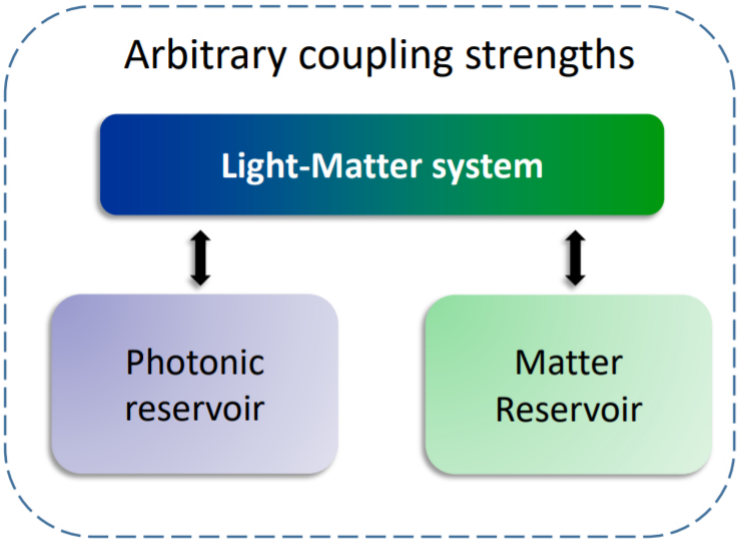

Figure 3.2: Schematic picture of an open QED system. Each component is individually coupled to a reservoir and the coupling between the subsystems is directly taken into account while deriving the dissipators.

In this case, let us consider the qubit and the resonator to be weakly coupled to two independent baths of quantum harmonic oscillators (see Fig. 3.2), each one described by the free Hamiltonian ($\hbar = 1$):

$$\hat{H}_{\rm B} = \sum_l \nu_l \hat{b}_l^\dagger \hat{b}_l, \tag{3.14}$$

where $\hat{b}_l^\dagger, \hat{b}_l$ are ladder operators for the bath mode l with frequency ν_l. The

system-bath interaction Hamiltonian is given by

$$\hat{H}_{\mathrm{SB}} = \sum_l \alpha_l (\hat{c} + \hat{c}^\dagger)(\hat{b}_l + \hat{b}_l^\dagger), \tag{3.15}$$

where α_l is the coupling strength to bath mode l, $\hat{c}, \hat{c}^\dagger \rightarrow \hat{\sigma}_-, \hat{\sigma}_+$ for the qubit and $\hat{c}, \hat{c}^\dagger \rightarrow \hat{a}, \hat{a}^\dagger$ for the resonator. The latter can be rewritten in the interaction picture with respect to the free system and bath Hamiltonians by using the transformation operator $\hat{U} = e^{i\hat{H}_{\mathrm{S}}t}$ as

$$\tilde{H}_{\mathrm{SB}}(t) = \sum_l \alpha_l e^{i\hat{H}_{\mathrm{S}}t}(\hat{c} + \hat{c}^\dagger)e^{-i\hat{H}_{\mathrm{S}}t}(\hat{b}_l e^{-i\nu_l t} + \hat{b}_l^\dagger e^{i\nu_l t}). \tag{3.16}$$

Developing the calculations considering that $\hat{H}_{\mathrm{S}}$ is the total system Hamiltonian which can be expressed in the dressed basis of its energy eigenstates as

$$\hat{H}_{\mathrm{S}} = \sum_j E_j \left|j\right\rangle\!\left\langle j\right|, \tag{3.17}$$

we obtain:

$$\tilde{H}_{\mathrm{SB}}(t) = \sum_{jkl} \alpha_l C_{jk} \left|j\right\rangle\!\left\langle k\right| (\hat{c} + \hat{c}^\dagger)(\hat{b}_l e^{-i\nu_l t} + \hat{b}_l^\dagger e^{i\nu_l t})e^{i\Delta_{jk}t}, \tag{3.18}$$

where $C_{jk} = \left\langle j \left| (\hat{c} + \hat{c}^\dagger) \right| k \right\rangle$ and $\Delta_{jk} = E_j - E_k$. The sum in Eq. (3.18) can be split in three parts as

$$\begin{aligned}\tilde{H}_{\mathrm{SB}}(t) = &\sum_{l,j} \alpha_l C_{jj} \left|j\right\rangle\!\left\langle j\right| (\hat{b}_l e^{-i\nu_l t} + \hat{b}_l^\dagger e^{i\nu_l t}) \\ &+ \left\{ \sum_l \sum_{j,k>j} + \sum_l \sum_{j,k<j} \right\} \alpha_l C_{jk} \left|j\right\rangle\!\left\langle k\right| \left(\hat{b}_l e^{-i(\nu_l - \Delta_{jk})t} + \hat{b}_l^\dagger e^{i(\nu_l + \Delta_{jk})t}\right).\end{aligned} \tag{3.19}$$

The latter equation seems to be very complicated since it involves several terms. However, taking into account that $C_{kj} = C_{jk}^*$ and that $C_{jj} = 0$ due

to the well-defined parity of the eigenstates $|j\rangle$, it can be simplified as

$$\tilde{H}_{\mathrm{SB}}(t) = \tilde{s}(t)\tilde{B}^{\dagger}(t) + \tilde{s}^{\dagger}(t)\tilde{B}(t), \tag{3.20}$$

where we defined

$$\tilde{s}(t) = \sum_{j,k>j} C_{jk}\,|j\rangle\langle k|\,e^{i\Delta_{jk}t}, \tag{3.21}$$

and

$$\tilde{B}(t) = \sum_{l} \alpha_l \hat{b}_l e^{-i\nu_l t}. \tag{3.22}$$

By substituting Eq. (3.20) in Eq. (3.13) we obtain

$$\begin{aligned}
\dot{\tilde{\rho}}(t) = &\int_0^t dt' \,[\tilde{s}(t')\tilde{\rho}(t')\tilde{s}(t) - \tilde{s}(t)\tilde{s}(t')\tilde{\rho}(t')]\langle\tilde{B}^{\dagger}(t)\tilde{B}^{\dagger}(t')\rangle \\
&+ \int_0^t dt' \,[\tilde{s}^{\dagger}(t')\tilde{\rho}(t')\tilde{s}^{\dagger}(t) - \tilde{s}^{\dagger}(t)\tilde{s}^{\dagger}(t')\tilde{\rho}(t')]\langle\tilde{B}(t)\tilde{B}(t')\rangle \\
&+ \int_0^t dt' \,[\tilde{s}^{\dagger}(t')\tilde{\rho}(t')\tilde{s}(t) - \tilde{s}(t)\tilde{s}^{\dagger}(t')\tilde{\rho}(t')]\langle\tilde{B}^{\dagger}(t)\tilde{B}(t')\rangle \\
&+ \int_0^t dt' \,[\tilde{s}(t')\tilde{\rho}(t')\tilde{s}^{\dagger}(t) - \tilde{s}^{\dagger}(t)\tilde{s}(t')\tilde{\rho}(t')]\langle\tilde{B}(t)\tilde{B}^{\dagger}(t')\rangle + H.c.
\end{aligned} \tag{3.23}$$

The *reservoir* correlation functions in Eq. (3.23) can be evaluated explicitly as

$$\langle\tilde{B}(t)\tilde{B}(t')\rangle = \langle\tilde{B}^{\dagger}(t)\tilde{B}^{\dagger}(t')\rangle = 0, \tag{3.24}$$

$$\langle\tilde{B}^{\dagger}(t)\tilde{B}(t')\rangle = \int_0^{\infty} d\nu\, g(\nu)|\alpha(\nu)|^2\,\bar{n}(\nu,T)e^{i\nu(t-t')}, \tag{3.25}$$

$$\langle\tilde{B}(t)\tilde{B}^{\dagger}(t')\rangle = \int_0^{\infty} d\nu\, g(\nu)|\alpha(\nu)|^2\,\left[\bar{n}(\nu,T)+1\right]e^{-i\nu(t-t')}, \tag{3.26}$$

where $\bar{n}(\nu_l,T) = \left[e^{(\hbar\nu_l/k_{\mathrm{B}}T)}-1\right]^{-1}$ is the mean photon number for an oscillator with frequency ν_l in thermal equilibrium at temperature T. It is important to note that the nonvanishing reservoir correlation functions should involve a summation over the reservoir oscillators. However, this summation has been turned to an integration by introducing the density of states $g(\nu)$, so that $g(\nu)d\nu$ gives the number of oscillators with frequencies in the interval ν to

$\nu + d\nu$. Considering Eqs. (3.24)-(3.26), the only relevant terms in the master equation are:

$$\begin{aligned}\dot{\tilde{\rho}}(t) = &\int_0^t dt' \,[\tilde{s}^\dagger(t')\tilde{\rho}(t')\tilde{s}(t) - \tilde{s}(t)\tilde{s}^\dagger(t')\tilde{\rho}(t')]\langle\tilde{B}^\dagger(t)\tilde{B}(t')\rangle \\ &+ \int_0^t dt' \,[\tilde{s}(t')\tilde{\rho}(t')\tilde{s}^\dagger(t) - \tilde{s}^\dagger(t)\tilde{s}(t')\tilde{\rho}(t')]\langle\tilde{B}(t)\tilde{B}^\dagger(t')\rangle \\ &+ \int_0^t dt' \,[\tilde{s}^\dagger(t)\tilde{\rho}(t')\tilde{s}(t') - \tilde{\rho}(t')\tilde{s}(t')\tilde{s}^\dagger(t)]\langle\tilde{B}^\dagger(t')\tilde{B}(t)\rangle \\ &+ \int_0^t dt' \,[\tilde{s}(t)\tilde{\rho}(t')\tilde{s}^\dagger(t') - \tilde{\rho}(t')\tilde{s}^\dagger(t')\tilde{s}(t)]\langle\tilde{B}(t')\tilde{B}^\dagger(t)\rangle.\end{aligned} \tag{3.27}$$

By using Eqs. (3.21)-(3.22) and making the change of variable $\tau = t - t'$, we obtain:

$$\dot{\tilde{\rho}}(t) = \sum_{j,k>j}\sum_{j',k'>j'} C^*_{j'k'}C_{jk}\Big[\mathcal{A}_{j,j',k,k'}(t) + \mathcal{B}_{j,j',k,k'}(t) + \mathcal{C}_{j,j',k,k'}(t) + \mathcal{D}_{j,j',k,k'}(t)\Big], \tag{3.28}$$

where

$$\begin{aligned}\mathcal{A}_{j,j',k,k'}(t) = &\int_0^t d\tau\, e^{i(\Delta_{jk}-\Delta_{j'k'})t}\, e^{i\Delta_{j'k'}\tau}\Big(|k'\rangle\langle j'|\,\tilde{\rho}(t)\,|j\rangle\langle k| - |j\rangle\langle k|\,k'\rangle\langle j'|\tilde{\rho}(t)\Big) \\ &\times \int_0^\infty d\nu\, g(\nu)|\alpha(\nu)|^2\,\bar{n}(\nu,T)e^{i\nu\tau},\end{aligned} \tag{3.29}$$

$$\begin{aligned}\mathcal{B}_{j,j',k,k'}(t) = &\int_0^t d\tau\, e^{i(\Delta_{jk}-\Delta_{j'k'})t}\, e^{-i\Delta_{jk}\tau}\Big(|j\rangle\langle k|\,\tilde{\rho}(t)\,|k'\rangle\langle j'| - |k'\rangle\langle j'|\,j\rangle\langle k|\tilde{\rho}(t)\Big) \\ &\times \int_0^\infty d\nu\, g(\nu)|\alpha(\nu)|^2\,\big[\bar{n}(\nu,T)+1\big]e^{-i\nu\tau},\end{aligned} \tag{3.30}$$

$$\begin{aligned}\mathcal{C}_{j,j',k,k'}(t) = &\int_0^t d\tau\, e^{i(\Delta_{jk}-\Delta_{j'k'})t}\, e^{-i\Delta_{jk}\tau}\Big(|k'\rangle\langle j'|\,\tilde{\rho}(t)\,|j\rangle\langle k| - \tilde{\rho}(t)\,|j\rangle\langle k|\,k'\rangle\langle j'|\Big) \\ &\times \int_0^\infty d\nu\, g(\nu)|\alpha(\nu)|^2\,\bar{n}(\nu,T)e^{-i\nu\tau}\,,\end{aligned} \tag{3.31}$$

$$\mathcal{D}_{j,j',k,k'}(t) = \int_0^t d\tau\, e^{i(\Delta_{jk}-\Delta_{j'k'})t}\, e^{i\Delta_{j'k'}\tau}\Big(|j\rangle\langle k|\,\tilde{\rho}(t)\,|k'\rangle\langle j'| - \tilde{\rho}(t)\,|k'\rangle\langle j'|\,j\rangle\langle k|\Big) \times \int_0^\infty d\nu\, g(\nu)|\alpha(\nu)|^2\left[\bar{n}(\nu,T)+1\right]e^{i\nu\tau}. \tag{3.32}$$

Note that in Eq. (3.28) the *Markov approximation* has been made by replacing $\tilde{\rho}(t-\tau)$ by $\tilde{\rho}(t)$. In each term of the *Born-Markov master equation* [Eq. (3.28)], we find oscillating exponentials of the form $\exp[i(\Delta_{jk}-\Delta_{j'k'}t)]$. However, since $k>j$ and $k'>j'$, the arguments of these exponentials will be zero for $j=j'$ and $k=k'$, and more in general for any pairs of different transitions in the system occurring at the same frequency. In practice, we are often interested only in a subset of the energy levels of the system for which all transitions have different frequencies. For this reason we usually perform the so-called *secular approximation* by setting $j=j'$ and $k=k'$ in Eq. (3.28). Within this approximation, by extending the τ integration to infinity and evaluating the integrals neglecting the *Lamb-Shift* terms, we obtain the *dressed master equation* in the interaction picture:

$$\dot{\tilde{\rho}}(t) = \sum_{j,k>j}\Gamma^{jk}\bar{n}(\Delta_{kj},T)\mathcal{D}[|k\rangle\langle j|]\tilde{\rho}(t) + \sum_{j,k>j}\Gamma^{jk}(1+\bar{n}(\Delta_{kj},T))\mathcal{D}[|j\rangle\langle k|]\tilde{\rho}(t)\,, \tag{3.33}$$

where

$$\Gamma^{jk} = 2\pi g(\Delta_{kj})|\alpha(\Delta_{kj})|^2|C_{jk}|^2, \tag{3.34}$$

$$\Gamma(\nu) = 2\pi g(\nu)|\alpha(\nu)|^2, \tag{3.35}$$

are the relaxation rates and $\mathcal{D}[\hat{O}]\hat{\rho} = \frac{1}{2}(2\hat{O}\hat{\rho}\,\hat{O}^\dagger - \rho\,\hat{O}^\dagger\hat{O} - \hat{O}^\dagger\hat{O}\hat{\rho})$ is the *Lindblad* superoperator.

Eq. (3.33) has been obtained (within the usual Born-Markov approximation) considering the coupling between the subsystems while deriving the dissipators. It turns out that this procedure allows to correctly describe the systems dynamics in the USC regime [71]. However, due to the secular approximation performed in its derivation, it is not able to describe dissipation

or decoherence in open quantum systems with mixed harmonic-anharmonic or quasi-harmonic spectra (e.g, for cavity QED in the dispersive regime and cavity optomechanics). In Chapter 5.1 we relaxed this approximation and we developed a generalized master equation approach able to describe dissipation in this two commonly studied systems and, more in general, able to describe open system dynamics without any restriction on the energy level spectrum, independently by the coupling strength.

Chapter 4

The Gauge principle

The gauge invariance principle plays a key role in the Standard Model which describes electroweak and strong interactions of elementary particles. Its origins can be traced to Vladimir Fock who extended the known freedom of choosing the electromagnetic potentials in classical electrodynamics to the quantum mechanics of charged particles interacting with electromagnetic fields. This fundamental principle has been then generalized and refined trough the years and, nowadays, it is considered to be a fundamental principle of nature, stating that different forms of potentials yield the same physical description. The gauge principle can be regarded as the cornerstone of the standard model, and it is used to introduce all the fundamental interactions in the model. Here we limit to discuss quantum electrodynamics, and are interested to discuss the gauge principle in the framework of the non-relativistic quantum theory. According to gauge invariance, different potentials, as long as they are related to each other by gauge transformations, describe the same electromagnetic fields [105]. Gauge transformation can be written in a general form as

$$A \rightarrow A' = A + \Delta F \tag{4.1}$$

$$U \rightarrow U' = U - \frac{\partial F}{\partial t} \tag{4.2}$$

where A and U are, respectively, the electromagnetic vector and scalar potentials and F is an arbitrary function, which depends on space-time coordinates. When considering quantum electrodynamics, the gauge invariance is obtained by transforming the wave functions under local unitary trans-

formations, resulting in different Hamiltonians in the corresponding time dependent Schrödinger equations (TDSE). For example, the wave function transforms as:

$$\psi^{(1)}(x) \rightarrow \psi^{(2)}(x) = e^{iqF(x)}\psi^{(1)}(x) \tag{4.3}$$

where $\psi^{(1,2)}$ are the wavefunctions in two different gauges and q is the particle charge. However, it is important to notice that unitary transformations can result also into "representations" which are not considered as "gauge" transformations. In particular, the fundamental property for a unitary transformation to be regarded as a gauge transformation is that the dynamics must be invariant [105]. It follows that, according to the gauge principle, all the physical observables are gauge invariant. In quantum mechanics, an observable $\hat{O}$ is defined as an operator acting in the system's Hilbert space (for example, the momentum and spin operators). We can easily change the representation in which the observable is defined performing the transformation

$$\hat{O}^{(2)} = e^{iqF(x)}\hat{O}^{(1)}e^{-iqF(x)} \,. \tag{4.4}$$

If the latter is a gauge transformation the expectation value of the observable will be also gauge invariant thus, will obey to the relation:

$$\left\langle \psi^{(1)} \right| \hat{O}^{(1)} \left| \psi^{(1)} \right\rangle = \left\langle \psi^{(2)} \right| \hat{O}^{(2)} \left| \psi^{(2)} \right\rangle \,. \tag{4.5}$$

However, one could argue that it is possible to construct Hermitian operators which transform differently from Eq. (4.4) under gauge transformations still remaining quantum observables according to the interpretation laws of quantum mechanics. The answer is that, according to the gauge principle, they are not considered "true" quantum observables because they cannot be phisically measured. Notice that a physical quantity cannot depend on the gauge choice, otherwise, it could take any arbitrary value. Often, the evaluation of the physical (gauge invariant) observables involve the evaluation of gauge dependent quantities, e. g., the expression of the electron wave function depends on the chosen gauge. If the exact analytical solution of the TDSE is known, it is possible to move from one gauge to the other without

any problem since all the gauges will yield the same physical results (in this case, the gauge choice is simply a matter of convenience since it may be easier to solve the problem in one specific gauge). On the contrary, when approximations are involved the gauge invariance of the physical observables may be lost as the error induced by the approximation scheme may not transform in the same way as the full solution. In order to make this fundamental concept clear let us consider a single electron in interaction with an electromagnetic field expressed in two different gauges such that our system can be described equivalently by the following wave functions:

$$\psi^{(1)} = \tilde{\psi}^{(1)} + R^{(1)} \tag{4.6}$$

$$\psi^{(2)} = \tilde{\psi}^{(2)} + R^{(2)} \tag{4.7}$$

where $\psi^{(1,2)}$ are the exact wavefunctions in the two gauges, while $\tilde{\psi}^{(1,2)}$ and $R^{(1,2)}$ are, respectively, the approximated wavefunctions and the errors. Typically, $R^{(1,2)} \simeq g^n$ for perturbation theory (where g is a small parameter). The two exact wave functions are as always related by a gauge transformation such that we can move from a gauge to the other by applying a unitary operator and that Eq. (4.5) is verified. If the approximate wave functions obey the same gauge transformation as the full solution the approximated observable will also be gauge invariant. However, this is not the general scenario since they usually transform differently yielding:

$$\left\langle \tilde{\psi}^{(1)} \right| \hat{O}^{(1)} \left| \tilde{\psi}^{(1)} \right\rangle \neq \left\langle \tilde{\psi}^{(2)} \right| \hat{O}^{(2)} \left| \tilde{\psi}^{(2)} \right\rangle \tag{4.8}$$

Therefore, we have lost gauge invariance by approximating the wave function. As the approximate wave functions get closer to the exact solution, the observables calculated in two different gauges converge towards each other and gauge invariance is recovered in the limit of the exact solution when $R^{(1,2)} \to 0$. In conclusion, it is clear that approximating a gauge independent quantity (a physical observable) by implementing an approximation of a gauge dependent quantity (the wave function) may destroy the gauge independence of the former however the breaking of the gauge invariance is

an artifact of the approximation method. For this reason one should always choose the gauge giving the best approximation of the physical quantity under consideration. This issue has been extensively studied. For instance, it was remarked by Lamb in his celebrated study of the Hydrogen atom fine structure, that the theoretical results obtained in the so-called length and velocity gauges differ in perturbation theory [106]. This ambiguity was resolved when it was observed that the perturbation theory is not gauge invariant and that special care is required to calculate observables in a gauge independent way. Recently this kind of issues have been raised also in the field of quantum optics. In particular, it has been shown by several authors [106–110] that approximate models for light-matter interactions derived in different gauges may lead to different predictions. Specifically, it has been argued that truncations of the atomic Hilbert space, to obtain a two-level description of the matter system, violate the gauge principle [78, 79] and that such violations become particularly relevant in the USC and DSC regimes. Among all these closely related works, De Bernardis et al. [78] have shown that, while in the electric dipole gauge, the two-level approximation can be performed as long as the Rabi frequency remains much smaller than the energies of all higher-lying levels, it can drastically fail in the Coulomb gauge, even for systems with an extremely anharmonic spectrum. This unexpected result is particularly unsatisfactory, since the general procedure to derive the multipolar gauge consists of using the minimal coupling replacement first, and then applying the Coulomb gauge [111]. The impact of the truncation of the Hilbert space of the matter system to only two states has been studied also by Stokes and Nazir [79], by introducing a one-parameter (α) set of gauge transformations. In particular, investigating a matter system with a lower anharmonicity (with respect to that considered in [78]) and by using the gauge parameter α as a sort of fit parameter they found the surprising result that, in several circumstances, the optimal gauge is the so-called Jaynes-Cummings (JC) gauge, a gauge in which the counter-rotating terms giving raise to the exotic effect typical of the USC and DSC regime (e.g., the virtual excitations in the system ground state) are automatically absent. However, ambiguities are not limited to those properties dependent on virtual excitations, but also affect

physical detectable photons. This issue originates from the gauge dependence of the field canonical momentum (see, e.g., Refs. [112–114]). According to the Glauber's photodetection theory [115], the detection rate for photons polarized along a direction i is proportional to $\langle\psi|\hat{E}_i^{(-)}\hat{E}_i^{(+)}|\psi\rangle$, where $\hat{\mathbf{E}}^{(\pm)}$ are the positive and negative frequency components of the electric-field operator. In the Coulomb gauge, $\hat{\mathbf{E}}$ is proportional to the field canonical momentum and can be expanded in terms of photon operators. On the contrary, in the multipolar gauge, the canonical momentum that can be expanded in terms of photon operators is not $\hat{\mathbf{E}}$ but the displacement operator $\hat{\mathbf{D}}$. This subtlety is generally disregarded, and the usual procedure is to obtain the system states in the dipole gauge (the multipolar gauge after the electric-dipole approximation) $|\psi_D\rangle$, and to calculate the photodetection rate ignoring that in this gauge the electric field operator is not a canonical momentum. It follows that this procedure, when applied to the quantum Rabi model, can lead to strongly incorrect predictions.

In 1970, Ref. [108] pointed out that gauge ambiguities in the calculation of atomic oscillator strengths, originate from the occurrence of nonlocal potentials determined by the approximation procedures. Since a nonlocal potential in the coordinate representation is an integral operator, it does not commute with the coordinate operator. Indeed, it is easy to show that it can be expressed as a local momentum-dependent operator $V(\hat{r},\hat{p})$. Specifically, in order to introduce the coupling of the matter system with the electromagnetic field, the minimal replacement rule $\hat{p}\rightarrow\hat{\Pi}=\hat{p}-A(\hat{r},t)$ has to be applied not only to the kinetic energy terms, but also to the potentials in the effective Hamiltonian of the particles in the system. By applying such a procedure, the ambiguities in the calculation of approximate matrix elements for electric dipole transitions can be removed [108]. Moreover, it has been demonstrated that taking into account the nonlocality of the approximate potential, two-photon transition rates involving Wannier excitons in semiconductors become gauge invariant [109]. Also the microscopic quantum theory of excitonic polaritons is affected by the presence of nonlocal potentials. Specifically, the application of the standard minimal coupling replacement leads to a total Hamiltonian which, besides the usual $\hat{A}\hat{p}$ term, displays an additional dia-

magnetic term e $2e^2\hat{A}^2/2m$, where e and m are the electron charge and mass respectively. If a limited number of exciton levels are explicitly included in the model, the long wavelength solution of the polariton dispersion cannot be recovered without introducing ad-hoc the Thomas-Reiche-Kuhn sum rule and truncating the summation consistently [116]. This procedure presents some ambiguity and appears to be rather artificial. However, if the nonlocality of the approximate potential is taken into account and the resulting additional terms are included, up to second order in the vector potential, the correct dispersion relation is automatically recovered [117,118]. In summary, it seems that the concept of approximation-induced nonlocal potentials, together with an expansion of the interaction Hamiltonian up to second order in the vector potential, is able to overcome gauge ambiguities.

In Paper 6.1 the source of gauge violation in the QRM has been identified, and a general method for the derivation of light-matter Hamiltonians in truncated Hilbert spaces able to produce gauge-invariant physical results has been developed. The gauge invariance has been restored by solving the nonlocality issues arising from the two-level truncation of the matter potential in the effective Hamiltonian. The resulting quantum Rabi Hamiltonian in the Coulomb gauge differs significantly from the standard one, but, as expected, it provides exactly the same energy levels obtained by using the dipole gauge, because physical observable quantities must be gauge-invariant. In Paper 6.4, the same result has been obtained with an alternative derivation based on the implementation of the gauge principle in two-level systems. This approach allowed us to obtain the QRM beyond the dipole approximation. In Paper 6.3 we studied and solved the gauge ambiguities in the Dicke model with a similar procedure. Specifically we demonstrated that, by employing the correct procedure shown in Papers 6.3 - 6.4, gauge invariance is fully restored for arbitrary interaction strengths, even when the number of emitters tends to infinity. Finally, in Paper 6.2 we focus on the resolution of ambiguities, not necessarily related to approximations, which can arise while considering USC and DSC cavity- and circuit-QED systems. For example, we discuss the proper definition of subsystems and their quantum measurements, the structure of light-matter ground states, and the analysis of time-dependent

interactions.

Chapter 5

Open Quantum Systems Dynamics in the USC regime

5.1 Dissipation and thermal noise in hybrid quantum systems in the ultrastrong-coupling regime

Dissipation and thermal noise in hybrid quantum systems in the ultrastrong-coupling regime

Alessio Settineri,[1] Vincenzo Macrí,[2] Alessandro Ridolfo,[2] Omar Di Stefano,[2]
Anton Frisk Kockum,[2,3] Franco Nori,[2,4] and Salvatore Savasta[1,2]

[1]*Dipartimento di Scienze Matematiche e Informatiche, Scienze Fisiche e Scienze della Terra, Università di Messina, I-98166 Messina, Italy*
[2]*Theoretical Quantum Physics Laboratory, RIKEN Cluster for Pioneering Research, Wako-shi, Saitama 351-0198, Japan*
[3]*Wallenberg Centre for Quantum Technology, Department of Microtechnology and Nanoscience, Chalmers University of Technology, 412 96 Gothenburg, Sweden*
[4]*Physics Department, The University of Michigan, Ann Arbor, Michigan 48109-1040, USA*

(Received 18 July 2018; published 20 November 2018)

The interaction among the components of a hybrid quantum system is often neglected when considering the coupling of these components to an environment. However, if the interaction strength is large, this approximation leads to unphysical predictions, as has been shown for cavity-QED and optomechanical systems in the ultrastrong-coupling regime. To deal with these cases, master equations with dissipators retaining the interaction between these components have been derived for the quantum Rabi model and for the standard optomechanical Hamiltonian. In this article, we go beyond these previous derivations and present a general master equation approach for arbitrary hybrid quantum systems interacting with thermal reservoirs. Specifically, our approach can be applied to describe the dynamics of open hybrid systems with harmonic, quasiharmonic, and anharmonic transitions. We apply our approach to study the influence of temperature on multiphoton vacuum Rabi oscillations in circuit QED. We also analyze the influence of temperature on the conversion of mechanical energy into photon pairs in an optomechanical system, which has been recently described at zero temperature. We compare our results with previous approaches, finding that these sometimes overestimate decoherence rates and underestimate excited-state populations.

DOI: 10.1103/PhysRevA.98.053834

I. INTRODUCTION

According to quantum mechanics, a closed system always displays a reversible evolution. However, no quantum system is completely isolated from its environment; for example, control and readout of a quantum system requires some coupling to the outside world, which leads to dissipation and decoherence (see, e.g., Refs. [1–4]). Realistic quantum systems should thus be regarded as open, taking into account the coupling to their environments. However, using an exact microscopic approach to include the environment (or reservoir) with its many degrees of freedom is often not feasible. Hence it is highly desirable to model open quantum systems using a small number of variables. An adequate description of the time evolution of an open quantum system can be provided by the equation of motion for its density matrix: a quantum master equation [5,6]. Another useful approach is based on the Heisenberg Langevin equation (see, e.g., Refs. [7–9]). Microscopic derivations of master equations start from the Hamiltonian dynamics of the total density matrix (for the system plus the environment). Then, tracing out the reservoir degrees of freedom, and introducing some approximations, a master equation can be derived describing the time evolution of the reduced density matrix only for the system [10]. It turns out that the resulting evolution, in general, is no longer unitary, and the open quantum system evolves into mixed states (see, e.g., Ref. [11]).

A hybrid quantum system combines two or more physical components or subsystems [12–14], with the goal of exploiting the advantages and strengths of the different systems in order to explore new phenomena and potentially bring about new quantum technologies. An important requirement for the realization of a functional hybrid quantum system is the ability to transfer, with high fidelity, quantum states and properties between its different components. Specifically, the effective coupling rate between the subsystems must be large enough to allow quantum state transfers between them within the shortest coherence time of the two subsystems [14]. This interaction regime is usually called the strong-coupling regime [15]. Cavity quantum electrodynamics (QED) in the strong-coupling regime has demonstrated great capability and potential for the control and manipulation of quantum states [3,13,15]. Further increasing the coupling strength, a hybrid quantum system enters the ultrastrong-coupling (USC) regime when the interaction rate becomes comparable to the transition frequency of at least one of the subsystems [3,16,17].

It has been shown that USC can give rise to several interesting physical effects [18–34]. Ultrastrong coupling has been achieved in a variety of cavity-QED and other hybrid condensed-matter systems, including semiconductor polaritons in quantum wells [35–39], superconducting quantum circuits [40–53], a terahertz metamaterial coupled to the cyclotron resonance of a two-dimensional electron gas (2DEG) [54–58], organic molecules [59–64], and in an optomechanical system, where a plasmonic picocavity was coupled to vibrations in a molecule [65]. In particular, in the case of superconducting quantum circuits, it is possible to reach the USC regime with even just a single artificial atom coupling to an electromagnetic resonator [40,41,52,53,66,67]. Recently, coupling rates exceeding the transition frequencies

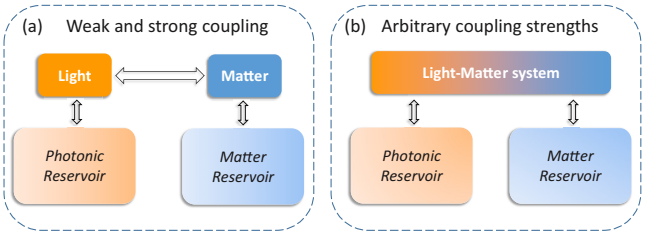

FIG. 1. (a) Master-equation approach valid in the weak- and strong-coupling regimes. The light-matter coupling is neglected while deriving the dissipators. (b) The master-equation approach considering the light-matter coupling. As the coupling strength between the two subsystems increases, it becomes necessary to treat dissipation effects including the coupling between the subsystems. This can be done by developing the system operators describing the coupling to the reservoirs in the eigenbasis of the coupled light-matter system.

of the components (deep-strong-coupling regime [20]) have been obtained in both a circuit-QED setup [46,50] and with a 2DEG [58].

Although the Hamiltonian of a coupled light-matter system contains the so-called counter-rotating terms, allowing the simultaneous creation or annihilation of an excitation in both the matter system and the cavity mode, these terms can be safely neglected for small coupling rates, if the components interact resonantly or almost resonantly. However, when the coupling strength becomes a significant fraction of the cavity frequency (or of the emitter's transition frequency), this often-invoked rotating-wave approximation (RWA) is no longer applicable and the antiresonant terms in the interaction Hamiltonian significantly change the standard cavity-QED physics [35]. For example, the number of excitations in the cavity-emitter system is no longer conserved [30], even in the absence of drives and dissipation, and the system states become dressed by the presence of virtual excitations [68]. It has also been demonstrated [69] that counter-rotating terms can induce anomalous qubit transitions (which do not conserve the excitation number) in a superconducting qubit-resonator system detuned from resonance.

When deriving the master equation for a hybrid quantum system, the interaction between the subsystems is usually neglected when considering their coupling to the environment [see Fig. 1(a)]. This results in the standard quantum-optical master equation [5,6] (see Sec. II A). This procedure works well in the weak-coupling regime, and can also be safely applied in the strong-coupling regime, when the density of states of the reservoirs and the system-bath interaction strengths are approximately flat (frequency independent) on the scale of the energy-level splittings induced by the interaction between the subsystems. However, it has been shown that when the light-matter interaction increases up to the breakdown of the RWA, this approach leads to unphysical predictions, e.g., excitations in the system even at zero temperature [21]. A closely related problem arising in the USC regime is the failure of standard input-output theory [22,24,70–72], which predicts an unphysical output of photons when the hybrid quantum system is in its ground state.

In order to overcome the problems in the description of dissipation of cavity-QED systems in the USC regime, a master equation taking into account the non-Markovian nature of the baths has been developed [73]. Furthermore, Ref. [21] showed that a master equation working properly in the USC regime of cavity QED can be obtained by including the light-matter coupling in the derivation of dissipative terms of the master equation [see Fig. 1(b)]. This approach does not require the introduction of non-Markovian baths. The decoherence rates entering the modified master equation instead depend on the bath noise spectrum evaluated at the dressed transition frequencies of the light-matter system. Since this modified master equation is obtained after a post-trace RWA, it can only be applied to nonlinear interacting quantum systems with anharmonicity larger than the transition linewidths. This prevents the application of this approach to cavity-QED systems in the USC dispersive regime (see Sec. III A), and to other hybrid quantum systems displaying a coexistence of harmonic (or quasiharmonic) and anharmonic transitions, e.g., optomechanical systems. In order to describe the losses through the mirror of a cavity embedding matters, a master equation of a non-Lindblad form was also derived [74]. For optomechanical systems in the USC regime, an analogous *dressed-state* master-equation approach has been developed [75], but it also has limitations (see Sec. III B). A zero-temperature master equation able to describe systems with both anharmonic and (quasi-) harmonic transitions has been introduced to study a cavity-QED system in the USC and dispersive regimes [76]. However, a finite-temperature master equation is an essential tool for a precise analysis of experimental results, which, to some degree, are always affected by thermal noise. A master equation without the post-trace RWA has been derived to describe a general spin-boson problem mapped into a finite-temperature Rabi model in ultrastrong coupling in Ref. [77].

The main purpose of this article is to provide a general approach for the description of dissipation in arbitrary hybrid quantum systems with arbitrary coupling strengths between its components. We do this by presenting a generalized master equation able to describe systems with both harmonic and anharmonic transitions, also valid for non-zero-temperature reservoirs. The only key assumption in our derivation is a weak system-bath interaction, such that the usual second-order Born approximation can be applied (recently, different approaches where this assumption can be relaxed have been developed in Refs. [78–81].

In particular, we decompose the system operators in terms of the dressed states of the hybrid quantum system and derive the master equation without performing the usual secular approximation. Finally, we take care of possible numerical instabilities due to the presence of fast oscillating terms.

The outline of this article is as follows. We begin in Sec. II by briefly reviewing the standard quantum-optical master equation (Sec. II A) and the dressed master equation for anharmonic systems (Sec. II B). Section II C is devoted to the presentation of a non-Lindblad generalized master equation, able to overcome the limitations of the dressed approach of Sec. II B and to take into account non-zero-temperature reservoirs. We also give a suitable solution for some numerical stability problems of our generalized master equation. In Secs. III A and III B, we apply this generalized master equation to calculate the dynamics of a circuit-QED system and an optomechanical system, respectively, at nonzero

temperatures, comparing the obtained results with the standard approaches used previously. We conclude in Sec. IV. In the Appendix A, we present more details for the derivation of the generalized dressed master equation.

II. MASTER EQUATIONS

In this section, we introduce dissipation for hybrid quantum systems following three different approaches. We start with the standard master equation, generally used for the description of open systems in quantum optics. Then we introduce the dressed master equation [21]. Finally, we consider a generalized dressed approach, able to describe the dissipation of hybrid quantum systems with arbitrary coupling strength, valid for systems displaying harmonic, quasiharmonic, and anharmonic transitions, while also considering non-zero-temperature reservoirs.

We begin by considering a generic system consisting of N interacting components or subsystems. Each ith component is weakly coupled to an independent bath, modeled as a collection of quantum harmonic oscillators, described by the free Hamiltonian ($\hbar = 1$ throughout this article)

$$\hat{H}_{\mathrm{B}}^{(i)} = \sum_{l} \nu_l \hat{b}_{i,l}^{\dagger} \hat{b}_{i,l}, \tag{1}$$

where $\hat{b}_{i,l}$ ($\hat{b}_{i,l}^{\dagger}$) are bosonic annihilation (creation) operators for the lth bath mode with frequency ν_l of the ith reservoir. The system-bath (denoted by the subscript SB) interaction Hamiltonian is given by

$$\hat{H}_{\mathrm{SB}} = \sum_{i,l} \alpha_{i,l} (\hat{s}_i + \hat{s}_i^{\dagger})(\hat{b}_{i,l} + \hat{b}_{i,l}^{\dagger}), \tag{2}$$

where $\hat{s}_i$ ($\hat{s}_i^{\dagger}$) are annihilation (creation) operators of the ith subsystem, mediating the interaction with the reservoirs. We denoted the coupling strength of the ith subsystem to the bath mode l of the ith reservoir by $\alpha_{i,l}$. In the interaction picture, the system-bath interaction Hamiltonian takes the form

$$\hat{\tilde{H}}_{\mathrm{SB}} = \sum_{i,l} \alpha_{i,l} e^{\iota \hat{H}_S t} (\hat{s}_i + \hat{s}_i^{\dagger}) e^{-\iota \hat{H}_S t} (\hat{b}_{i,l} e^{-\iota \nu_{i,l} t} + \hat{b}_{i,l}^{\dagger} e^{\iota \nu_{i,l} t}), \tag{3}$$

where $\hat{H}_S$ is the system Hamiltonian and ι is the imaginary unit.

A. Standard master equation

In the standard approach, the components or subsystems are assumed to be independent while obtaining the dissipation. The coupling between the components is afterwards introduced in the system Hamiltonian. This leads to the Schrödinger-picture standard master equation

$$\dot{\hat{\rho}} = -\iota [\hat{H}_{\mathrm{S}}, \hat{\rho}] + \mathcal{L}_{\mathrm{bare}} \hat{\rho}, \tag{4}$$

where $\hat{\rho}$ is the density matrix of the system and

$$\mathcal{L}_{\mathrm{bare}} \hat{\rho} = \sum_i \{\gamma_i [1 + n(\omega_i, T_i)] \mathcal{D}[\hat{s}_i] \hat{\rho} + \gamma_i n(\omega_i, T_i) \mathcal{D}[\hat{s}_i^{\dagger}] \hat{\rho}\}, \tag{5}$$

with the generic dissipator

$$\mathcal{D}[\hat{O}]\hat{\rho} = \tfrac{1}{2}(2\hat{O}\hat{\rho}\hat{O}^{\dagger} - \hat{\rho}\hat{O}^{\dagger}\hat{O} - \hat{O}^{\dagger}\hat{O}\hat{\rho}). \tag{6}$$

In Eq. (5), the γ_i's describe the leakage rates and $n(\omega_i, T_i)$ is the average thermal population of the ith reservoir at temperature T_i and the frequency ω_i at which $\hat{s}_i$ rotates in the interaction picture. Pure dephasing effects can be included by adding to Eq. (5) the additional term $(\gamma_{\phi_i}/2)\mathcal{D}[\hat{d}_i]\hat{\rho}$, where $\hat{d}_i$ are system operators that do not change the energy of the system and γ_{ϕ_i} are the pure dephasing rates.

The master equation provided in Eq. (4) can be used to describe many cavity- and circuit-QED experiments in the weak- and strong-coupling regimes [3,5,6]. However, it has been shown that when the coupling between the components or subsystems increases beyond the point where the RWA is applicable, this approach leads to *unphysical* predictions, e.g., production of excitations in the system even at zero temperature [21].

B. Master equations in the dressed picture

Master equation for anharmonic systems

In order to overcome the limitations of the standard approach, Ref. [21] developed a dressed master equation, taking into account the coupling between all the components of the system. They also considered that transitions in the hybrid system occur between dressed eigenstates, not between the eigenstates of the free Hamiltonians of the components. In the following, we briefly show some key points of the dressed master equation derivation. We first express the system Hamiltonian in the dressed basis of its energy eigenstates. We then switch to the interaction picture, writing the system operators as

$$\hat{\tilde{S}}_i(t) = \sum_{j,k>j} C_{jk} |j\rangle\langle k| e^{\iota \Delta_{jk} t}, \tag{7}$$

with

$$C_{jk} = \langle j | (\hat{s}_i + \hat{s}_i^{\dagger}) | k \rangle, \tag{8}$$

$$\Delta_{jk} = E_j - E_k, \tag{9}$$

and the reservoir operators as

$$\hat{\tilde{B}}(t) = \sum_{i,l} \alpha_{i,l} \hat{b}_{i,l} e^{-\iota \nu_l t}. \tag{10}$$

In this way, the system operators $\hat{s}_i$ are expressed as a sum over transition operators $|j\rangle\langle k|$, which cause transitions (with frequency Δ_{jk}) between eigenstates of the hybrid quantum system $\{|j\rangle, |k\rangle\}$. Note that "˜" identifies the operators in the interaction picture. With these new dressed operators, Eq. (3) can be split into two parts, one each for the dressed system operators with positive and negative frequencies:

$$\hat{\tilde{H}}_{\mathrm{SB}} = \sum_i \{\hat{\tilde{S}}_i(t) \hat{\tilde{B}}_i^{\dagger}(t) + \hat{\tilde{S}}_i^{\dagger}(t) \hat{\tilde{B}}_i(t)\}. \tag{11}$$

Note that, as shown in Ref. [21], the fast oscillating terms $\hat{S}_i^{\dagger}(t)\hat{B}_i^{\dagger}(t)$ and $\hat{S}_i(t)\hat{B}_i(t)$ have been dropped by an initial RWA and the diagonal terms arising from degenerate transitions with $j = k$ are neglected considering a system

displaying parity symmetry (in this case $C_{jj} = 0$). By following the standard procedure [5] (second-order Born approximation, Markov approximation, assuming reservoirs with a continuum of frequencies, and performing the secular approximation), as shown in detail in Ref. [21], for this simplified version of Eq. (3), we obtain a dressed master equation that in the Schrödinger picture can be written as

$$\dot{\hat{\rho}} = -\imath[\hat{H}_S, \hat{\rho}] + \mathcal{L}_{\text{dressed}}\hat{\rho}, \tag{12}$$

with the Lindbladian superoperator

$$\mathcal{L}_{\text{dressed}}\hat{\rho} = \sum_i \sum_{j,k<j} \{\Gamma_i^{jk} n(\Delta_{jk}, T_i)\mathcal{D}[|j\rangle\langle k|]\hat{\rho} + \Gamma_i^{jk}[1 + n(\Delta_{jk}, T_i)]\mathcal{D}[|k\rangle\langle j|]\hat{\rho}\}, \tag{13}$$

where the thermal populations are ($k_B = 1$ throughout this article)

$$n(\Delta_{jk}, T_i) = [\exp\{\Delta_{jk}/T_i\} - 1]^{-1} \tag{14}$$

and the damping rates are

$$\Gamma_i^{jk} = 2\pi g_i(\Delta_{jk})|\alpha_i(\Delta_{jk})|^2|C_{jk}|^2, \tag{15}$$

with $g(\Delta_{jk})$ being the reservoir density of states and $\alpha(\Delta_{jk})$ the system-reservoir coupling strength.

As shown by several studies [21–24,29,71,82–85], the Lindbladian in Eq. (13) can correctly describe the dynamics of anharmonic cavity-QED systems in the USC regime. At $T = 0$, rather than exciting the system, the dissipators give relaxation to the true dressed ground state. At $T \neq 0$, these dissipators correctly describe the relaxation to the thermal-equilibrium density matrix for the interacting system [71]. However, because of the secular approximation used in the derivation of Eq. (13), this standard approach is *not* able to describe dissipation or decoherence in open quantum systems with mixed harmonic-anharmonic or quasiharmonic spectra [21], e.g., for cavity QED in the dispersive regime and cavity optomechanics.

C. Generalized master equation

1. Derivation

In this section, we extend the previous treatment in order to derive a generalized dressed master equation able to describe both harmonic and mixed harmonic-anharmonic systems coupled to non-zero-temperature reservoirs. Moreover, the present derivation is not limited to systems with parity symmetry.

We start expressing the system Hamiltonian in the dressed basis of its energy eigenstates. We then switch to the interaction picture, writing the system operators as

$$\hat{\tilde{S}}_i(t) = \sum_{\epsilon'-\epsilon=\omega} \hat{\Pi}(\epsilon)(\hat{s}_i + \hat{s}_i^\dagger)\hat{\Pi}(\epsilon')e^{-\imath\omega t} = \sum_{\epsilon'-\epsilon=\omega} \hat{S}_i(\omega)e^{-\imath\omega t}, \tag{16}$$

and the reservoir operators as in Eq. (10), labelling the eigenvalues of $\hat{H}_S$ by ϵ and denoting the projectors onto the respective eigenspaces by $\hat{\Pi}(\epsilon) \equiv |\epsilon\rangle\langle\epsilon|$. Recall that the tilde symbol identifies interaction-picture operators. In this way, the system operators $\hat{s}_i$ are expressed as a sum over transition operators, which cause transitions (with transition frequency ω) between energy eigenstates of the hybrid quantum system. For $\omega > 0$, $\hat{S}_i(\omega)$ is a positive-frequency operator that takes the system from an eigenstate with higher energy to one with lower energy. Conversely, for $\omega < 0$, $\hat{S}_i(\omega)$ is a negative-frequency operator which produces a transition to a higher-energy eigenstate. In the following, to emphasize these properties, we introduce the notation

$$\begin{aligned} \hat{S}_i^{(+)}(\omega) &= \hat{S}_i(\omega) \qquad \text{for } \omega > 0, \\ \hat{S}_i^{(-)}(\omega) &= \hat{S}_i(-\omega) \qquad \text{for } \omega > 0, \\ \hat{S}_i^{(0)} &= \hat{S}_i(\omega) \qquad \text{for } \omega = 0. \end{aligned} \tag{17}$$

With these new dressed operators, Eq. (3) can be rewritten in a way that makes it easy to derive the Born-Markov master equation for the system:

$$\hat{\tilde{H}}_{\text{SB}} = \sum_i \hat{\tilde{S}}_i(t)[\hat{\tilde{B}}_i^\dagger(t) + \hat{\tilde{B}}_i(t)]. \tag{18}$$

Following the standard procedure (see the Appendix A) the generalized dressed master equation can be obtained evaluating the double integrals in Eq. (A4) of the Appendix A without assuming parity symmetry, and evaluating the two integrals without introducing the secular approximation $\omega = \omega'$. In this case, we obtain a Liouvillian superoperator $\mathcal{L}$ that, considering all the different subsystems, in the Schrödinger picture, can be written in the general form

$$\begin{aligned} \mathcal{L}_{\text{gme}}\hat{\rho} = \frac{1}{2}\sum_i \sum_{\omega,\omega'} \{&\Gamma_i(-\omega')n(-\omega', T_i)[\hat{S}_i(\omega')\hat{\rho}(t)\hat{S}_i(\omega) - \hat{S}_i(\omega)\hat{S}_i(\omega')\hat{\rho}(t)] + \Gamma_i(\omega)n(\omega, T_i)[\hat{S}_i(\omega')\hat{\rho}(t)\hat{S}_i(\omega) \\ &- \hat{\rho}(t)\hat{S}_i(\omega)\hat{S}_i(\omega')] + \Gamma_i(\omega)[n(\omega, T_i) + 1][\hat{S}_i(\omega)\hat{\rho}(t)\hat{S}_i(\omega') - \hat{S}_i(\omega')\hat{S}_i(\omega)\hat{\rho}(t)] \\ &+ \Gamma_i(-\omega')[n(-\omega', T_i) + 1][\hat{S}_i(\omega)\hat{\rho}(t)\hat{S}_i(\omega') - \hat{\rho}(t)\hat{S}_i(\omega')\hat{S}_i(\omega)]\}, \end{aligned} \tag{19}$$

where

$$\Gamma_i(\omega) = 2\pi g_i(\omega)|\alpha_i(\omega)|^2, \tag{20}$$

and "gme" refers to generalized master equation.

Equation (19) contains several terms since both the transition frequencies ω and ω' can be positive, negative, and zero, although both $\Gamma_i(\omega)$ and $n(\omega, T_i)$ are nonzero for positive frequencies only. Moreover, only a few of these terms are relevant in order to correctly describe the system dynamics. Indeed, the terms with oscillation frequencies significantly larger than the damping rates Γ_i of the system provide negligible contributions when integrating the master equation.

Equation (19) also contains terms with $\omega' = \omega = 0$, originating from diagonal transition operators or, more generally, operators describing zero-frequency transitions. These terms give rise to additional pure dephasing contributions. Note that these terms can be regarded as a generalization of those appearing in the master equation for optomechanical systems in the USC regime [75].

Expanding Eq. (19), we obtain terms oscillating at frequencies $\pm(\omega' \pm \omega)$ arising from products of $\hat{S}_i^{(-)}$ and $\hat{S}_i^{(+)}$. We also obtain terms oscillating at frequencies $-\omega'$, $+\omega$ arising from products of $\hat{S}_i^{(-)}$ or $\hat{S}_i^{(+)}$ with $\hat{S}_i^{(0)}$ and nonoscillating terms arising from products between zero-frequency operators $\hat{S}_i^{(0)}$. Moreover, considering a system with well separated energy levels ($\omega \gg \Gamma_i$), the terms oscillating at $\pm(\omega + \omega')$, $+\omega$, and $-\omega'$ can be considered as rapidly oscillating and can be neglected. Including only those terms providing non-negligible contributions to the dynamics, the Liouvillian in Eq. (19) can be written as

$$\begin{aligned}\mathcal{L}_{\rm gme}\hat{\rho} = \frac{1}{2}\sum_i \sum_{(\omega,\omega')>0} &\{\Gamma_i(\omega')n(\omega', T_i)[\hat{S}_i^{(-)}(\omega')\hat{\rho}(t)\hat{S}_i^{(+)}(\omega) - \hat{S}_i^{(+)}(\omega)\hat{S}_i^{(-)}(\omega')\hat{\rho}(t)] + \Gamma_i(\omega)n(\omega, T_i)[\hat{S}_i^{(-)}(\omega')\hat{\rho}(t)\hat{S}_i^{(+)}(\omega)\\ &- \hat{\rho}(t)\hat{S}_i^{(+)}(\omega)\hat{S}_i^{(-)}(\omega')] + \Gamma_i(\omega)[n(\omega, T_i)+1][\hat{S}_i^{(+)}(\omega)\hat{\rho}(t)\hat{S}_i^{(-)}(\omega') - \hat{S}_i^{(-)}(\omega')\hat{S}_i^{(+)}(\omega)\hat{\rho}(t)]\\ &+ \Gamma_i(\omega')[n(\omega', T_i)+1][\hat{S}_i^{(+)}(\omega)\hat{\rho}(t)\hat{S}_i^{(-)}(\omega') - \hat{\rho}(t)\hat{S}_i^{(-)}(\omega')\hat{S}_i^{(+)}(\omega)] + \Omega_i^{+}(T_i)\big[\hat{S}_i^{(0)}\hat{\rho}(t)\hat{S}_i^{(0)} - \hat{S}_i^{(0)}\hat{S}_i^{(0)}\hat{\rho}(t)\big]\\ &+ \Omega_i^{'+}(T_i)\big[\hat{S}_i^{(0)}\hat{\rho}(t)\hat{S}_i^{(0)} - \hat{\rho}(t)\hat{S}_i^{(0)}(\omega')\hat{S}_i^{(0)}\big] + \Omega_i^{-}(T_i)\big[\hat{S}_i^{(0)}\hat{\rho}(t)\hat{S}_i^{(0)} - \hat{\rho}(t)\hat{S}_i^{(0)}\hat{S}_i^{(0)}\big]\\ &+ \Omega_i^{'-}(T_i)\big[\hat{S}_i^{(0)}\hat{\rho}(t)\hat{S}_i^{(0)} - \hat{S}_i^{(0)}\hat{S}_i^{(0)}\hat{\rho}(t)\big]\},\end{aligned} \tag{21}$$

with

$$\Omega_i^{'\pm}(T_i) = \int_0^t d\tau \int_0^\infty d\nu\, g_i(\nu)|\alpha_i(\nu)|^2[n(\nu, T_i)+1]e^{\pm\imath\nu\tau}, \tag{22}$$

$$\Omega_i^{\pm}(T_i) = \int_0^t d\tau \int_0^\infty d\nu\, g_i(\nu)|\alpha_i(\nu)|^2 n(\nu, T_i)e^{\pm\imath\nu\tau}. \tag{23}$$

We also observe that, for the particular case of an Ohmic bath, where

$$g_i(\nu)|\alpha_i(\nu)|^2 = \frac{\gamma_i \nu}{2\pi f_i}, \tag{24}$$

with γ_i and f_i being, respectively, the damping and the frequency of the considered subsystem, we obtain

$$\Gamma_i(\omega) = \frac{\gamma_i \omega}{f_i}, \tag{25}$$

and all the pure dephasing rates give the same result:

$$\Omega_i^{'\pm}(T_i) = \Omega_i^{\pm}(T_i) = \Omega(T_i), \tag{26}$$

$$\Omega(T_i) = \frac{\gamma_i}{4 f_i} T_i. \tag{27}$$

In the next section, we apply this generalized dressed master equation to two hybrid quantum systems, comparing the obtained numerical results with previous approaches.

2. Stability problems

We observe that the dissipator in Eq. (21) is not in Lindblad form and, consequently, properties like the positivity of the density matrix and the conservation of the probability cannot be guaranteed. Furthermore, in this framework, some useful theorems [86] on the steady-state behavior have not been proven yet.

Actually, a careful inspection of Eq. (21) shows that it can be regarded as approximately Lindblad-like. Specifically, if we consider the interaction picture, each term of Eq. (21) (except the last) oscillates at frequencies $\pm(\omega - \omega')$. If $(\omega - \omega')$ is significantly larger than the damping rates Γ_i of the system, these terms provide negligible contributions when integrating the master equation. Hence $|\omega - \omega'|$ can be assumed to be of the order of the system linewidths. It is thus reasonable to assume for the thermal populations of the reservoirs $n(\omega, T_i) \simeq n(\omega', T_i)$ and for the dampings $\Gamma_i(\omega) \simeq \Gamma_i(\omega')$. This analysis shows that, within a very good approximation, the dissipator in Eq. (21) can be regarded to be in Lindblad form.

Although the fast oscillating terms arising in Eq. (21), produced from transitions with high frequency differences (not present after the post-trace RWA), should not provide a significant contribution for $|\omega - \omega'| > \Gamma_i$, they can strongly increase the computation time and lead to computational instabilities. In order to overcome these difficulties, we use numerical filtering with a steplike function that sets to zero all the dissipator terms involving frequency differences higher than a certain value Λ. More specifically, the filtered Liouvillian takes the form

$$\mathcal{L}_{\rm gme}^{\rm filt}\hat{\rho} = \mathcal{L}_{\rm gme}\hat{\rho} \times F(\omega, \omega'), \tag{28}$$

where the filter function $F(\omega, \omega')$ can be written in a generalized form as

$$F(\omega, \omega') = \Theta(|\omega - \omega'|) - \Theta(|\omega - \omega'| - \Lambda), \tag{29}$$

with Θ the Heaviside step function and Λ the bandwidth of the filter.

III. DISSIPATION IN THE USC REGIME

In this section, we apply the generalized master equation presented in the previous section to study the influence of temperature on the dynamics of two open hybrid quantum systems in the USC regime. Specifically, we reexamine the dynamics of the two systems presented in Refs. [27] and [87]. The first example is a circuit-QED system in the dispersive regime, displaying multiphoton quantum Rabi oscillations.

For this setup, we also compare the results obtained with the generalized master equation to those obtained using the dressed approach for anharmonic systems [21].

The second example is an optomechanical system with coexisting harmonic and anharmonic spectra. Specifically, we consider an ultra-high-frequency mechanical oscillator ultrastrongly coupled to a microwave resonator. Very recently, considering zero-temperature reservoirs, it has been shown [88] that this system is promising for the observation of the dynamical Casimir effect (DCE), which converts mechanical energy into photon pairs [89]. Here we analyze the influence of temperature on this fundamental quantum effect. Moreover, in order to understand the impact of the generalized master equation on the dynamics of hybrid quantum systems, we compare the obtained numerical results with those obtained using a previously developed approach for USC optomechanics [75]. Note that all the numerical results are displayed in the laboratory frame.

A. Circuit QED beyond the RWA

In this circuit-QED example, we study a flux qubit coupled to a single-mode resonator [27]. The bare qubit Hamiltonian can be written as

$$\hat{H}_q = \omega_q \hat{\sigma}_z/2, \tag{30}$$

where the qubit resonance frequency is $\omega_q = \sqrt{\Delta^2 + (2I_p\delta\Phi_x)^2}$, with Δ the qubit energy gap, I_p the persistent current corresponding to the minima of the qubit potential, and $\delta\Phi_x$ the flux offset. The bare resonator Hamiltonian is

$$\hat{H}_c = \omega_c \hat{a}^\dagger \hat{a}, \tag{31}$$

where ω_c is the frequency of the resonator mode and $\hat{a}$ ($\hat{a}^\dagger$) is the bosonic annihilation (creation) operator for that mode. The total quantum system is described by the generalized quantum Rabi Hamiltonian

$$\hat{H}_S = \hat{H}_q + \hat{H}_c + g\hat{X}[\cos(\theta)\hat{\sigma}_x + \sin(\theta)\hat{\sigma}_z], \tag{32}$$

where the flux dependence is encoded in $\cos(\theta) = \Delta/\omega_q$, $\hat{X} = \hat{a} + \hat{a}^\dagger$, and $\hat{\sigma}_x$, $\hat{\sigma}_z$ are Pauli matrices.

As shown in Ref. [27], the lowest energy levels of this system display a well-known avoided level crossing arising for $\omega_q \simeq \omega_c$ (vacuum Rabi splitting). This avoided crossing is due to the coherent coupling of the states $|e,0\rangle$ and $|g,1\rangle$, where g (e) indicates the ground (excited) state of the qubit and the second entry in the kets represents the photon number. However, when the RWA breaks down, the counter-rotating terms in Eq. (32) must be taken into account and the total number of excitations in the system is no longer conserved [41,69]. As a consequence, the coherent coupling between states with different numbers of excitations, not allowed in the standard Jaynes-Cummings model [90,91], becomes possible through virtual transitions mediated by the counter-rotating terms [31]. This generates several additional avoided level crossings between states with different excitation numbers, e.g., between $|e,0\rangle$ and $|g,2\rangle$ [27].

For our numerical calculations, we consider, as in Ref. [27], $\omega_c/2\pi = 4.0\,GHz$ and a resonator-qubit coupling strength $g/\omega_c = 0.157$. We focus on the avoided crossing arising at $\omega_q \simeq 2\omega_c$ between the states $|\psi_\pm\rangle \simeq \frac{1}{\sqrt{2}}(|e,0\rangle \pm |g,2\rangle)$. We set $\omega_q/2\pi = 7.97$ GHz (obtained using the qubit parameters $\Delta/h = 2.25\,GHz$, $2I_p = 1.97\,nA$, and $\delta\Phi_x = 3.88\,\Phi_0$); this is where the splitting reaches its minimum [27]. The minimum splitting $2\Omega_{\rm eff}$ provides a direct measurement of the effective resonant coupling $\Omega_{\rm eff}$ between the states $|e,0\rangle$ and $|g,2\rangle$.

In order to probe this avoided crossing, we consider, as in Ref. [27], the case where the qubit is directly excited by a Gaussian π pulse,

$$\hat{H}_p = \mathcal{E}(t)\cos(\omega t)\hat{\sigma}_x, \tag{33}$$

where $\mathcal{E}(t) = \Omega\,\exp[-(t-t_0)^2/2\tau^2]/(\tau\sqrt{2\pi})$. Here, τ is the standard deviation and $\Omega/\omega_c = (\pi/3)\times 10^{-1}$ the amplitude of the pulse. The center frequency of the pulse corresponds to the middle of the avoided crossing considered here. Specifically, $\omega = (\omega_{3,0} + \omega_{2,0})/2$, with $\omega_{i,j} = \omega_i - \omega_j$, where we labeled the energy values and the eigenstates of the hybrid system as ω_l and $|l\rangle$, with $l = 0, 1, \ldots$, such that $\omega_k > \omega_j$ for $k > j$.

The system dynamics is then evaluated using the generalized master equation (gme)

$$\dot{\hat{\rho}} = -\imath[\hat{H}_S + \hat{H}_p, \hat{\rho}] + \mathcal{L}_{\rm gme}\hat{\rho}, \tag{34}$$

where, considering an Ohmic bath, the Liouvillian dissipator can be written as

$$\begin{aligned}\mathcal{L}_{\rm gme}\hat{\rho} = \sum_{(\omega,\omega')>0} \frac{1}{2}\Bigg\{ & \frac{\gamma\omega'}{\omega_q} n(\omega', T_\gamma)[\hat{P}^{(-)}(\omega')\hat{\rho}\hat{P}^{(+)}(\omega) - \hat{P}^{(+)}(\omega)\hat{P}^{(-)}(\omega')\hat{\rho}] + \frac{\gamma\omega}{\omega_q}[n(\omega, T_\gamma)+1][\hat{P}^{(+)}(\omega)\hat{\rho}\hat{P}^{(-)}(\omega') \\ & - \hat{P}^{(-)}(\omega')\hat{P}^{(+)}(\omega)\hat{\rho}] + \frac{\gamma\omega}{\omega_q} n(\omega, T_\gamma)[\hat{P}^{(-)}(\omega')\hat{\rho}\hat{P}^{(+)}(\omega) - \hat{\rho}\hat{P}^{(+)}(\omega)\hat{P}^{(-)}(\omega')] + \frac{\gamma\omega'}{\omega_q}[n(\omega', T_\gamma)+1] \\ & \times [\hat{P}^{(+)}(\omega)\hat{\rho}\hat{P}^{(-)}(\omega') - \hat{\rho}\hat{P}^{(-)}(\omega')\hat{P}^{(+)}(\omega)] + \frac{\kappa\omega'}{\omega_c} n(\omega', T_\kappa)[\hat{A}^{(-)}(\omega')\hat{\rho}\hat{A}^{(+)}(\omega) - \hat{A}^{(+)}(\omega)\hat{A}^{(-)}(\omega')\hat{\rho}] \\ & + \frac{\kappa\omega}{\omega_c}[n(\omega, T_\kappa)+1][\hat{A}^{(+)}(\omega)\hat{\rho}\hat{A}^{(-)}(\omega') - \hat{A}^{(-)}(\omega')\hat{A}^{(+)}(\omega)\hat{\rho}] + \frac{\kappa\omega}{\omega_c} n(\omega, T_\kappa)[\hat{A}^{(-)}(\omega')\hat{\rho}\hat{A}^{(+)}(\omega) \\ & - \hat{\rho}\hat{A}^{(+)}(\omega)\hat{A}^{(-)}(\omega')] + \frac{\kappa\omega'}{\omega_c}[n(\omega', T_\kappa)+1][\hat{A}^{(+)}(\omega)\hat{\rho}\hat{A}^{(-)}(\omega') - \hat{\rho}\hat{A}^{(-)}(\omega')\hat{A}^{(+)}(\omega)]\Bigg\}. \end{aligned} \tag{35}$$

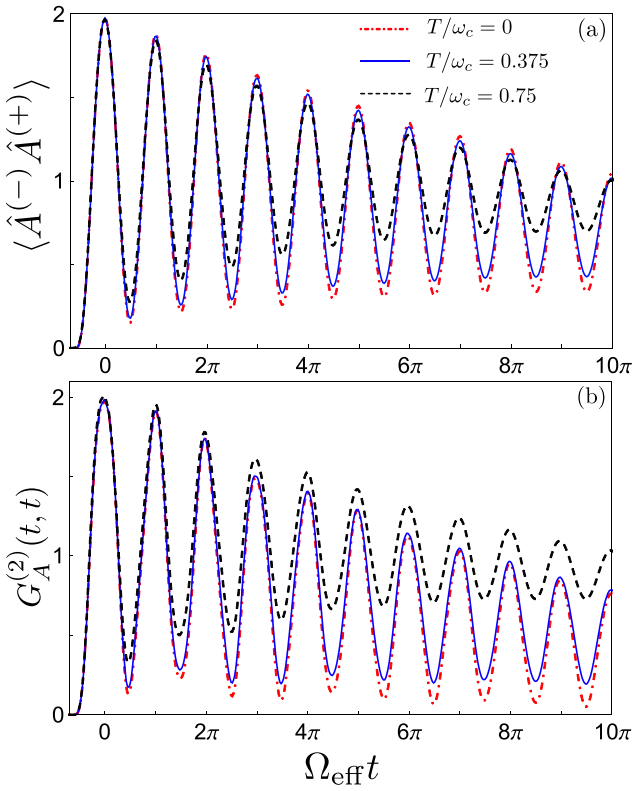

FIG. 2. Dynamics of anomalous two-photon vacuum Rabi oscillations. Results obtained using the generalized-master-equation approach, varying the temperature of both subsystems. (a) Time evolution of the mean cavity photon number $\langle \hat{A}^{(-)}\hat{A}^{(+)}\rangle$ after the arrival of a Gaussian π pulse to the qubit. The system starts in the ground state. (b) Two-photon correlation function for the cavity, obtained with the same parameters and conditions. After the arrival of the pulse, independent of the temperature of the reservoirs, the system undergoes vacuum Rabi oscillations showing the reversible exchange of photon pairs between the qubit and the resonator. However, when raising the temperature, due to the increasing decoherence, the oscillations become more damped and the correlation function reaches higher stationary values due to larger incoherent, thermal contributions. Note that the second and the fifth dips are shallower because of some spurious effects generated by other transitions excited by the coherent pulse. All parameters for the simulations are given in the text. $\Omega_{\rm eff}$ on the x axis indicates the effective resonant coupling.

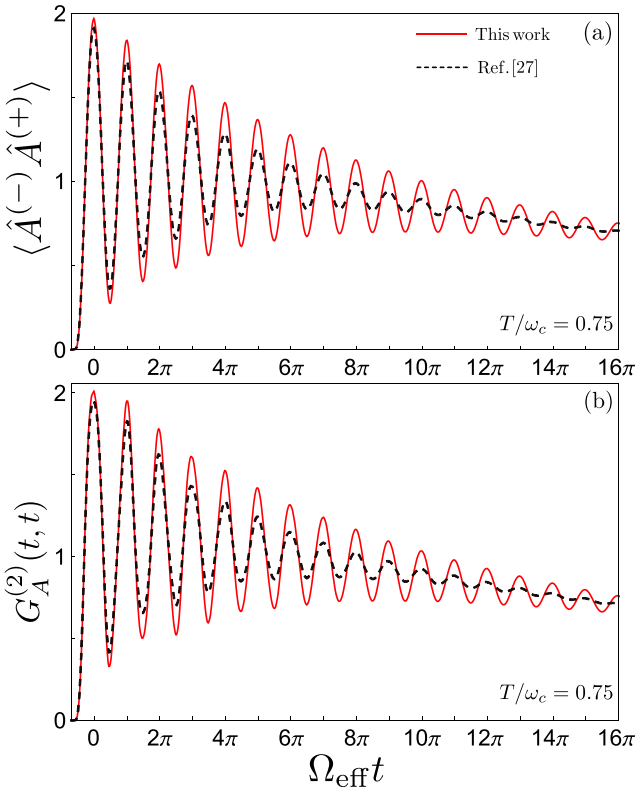

FIG. 3. Comparison between the results obtained using the generalized-master-equation approach (red solid curves) and the standard dressed master equation (black dashed curves). (a) Time evolution of the mean cavity photon number $\langle \hat{A}^{(-)}\hat{A}^{(+)}\rangle$ at temperature $T/\omega_c = 0.75$ with all other parameters the same as in Fig. 2. (b) Two-photon correlation functions, obtained with the same parameters and conditions. After the arrival of the pulse, both approaches show the system undergoing two-photon Rabi oscillations and relaxing to thermal equilibrium. However, with the standard dressed master equation, the coherence losses are slightly overestimated (because of the post-trace RWA), so the oscillations are more damped and the stationary value is reached sooner.

Here κ and γ are the qubit and cavity damping rates, respectively, $\hat{A}^{(+)}$ and $\hat{A}^{(-)}$ are the positive- and negative-frequency dressed cavity operators ($\hat{s}_i = \hat{a}$), and $\hat{P}^{(+)}$ and $\hat{P}^{(-)}$ are the positive- and negative-frequency dressed qubit operators ($\hat{s}_i = \hat{\sigma}_-$). We neglected the very small pure dephasing term in the dissipator [see Eq. (21)]and we did not apply any filtering procedure.

Figure 2 displays the dynamics of the mean cavity photon number $\langle \hat{A}^{(-)}\hat{A}^{(+)}\rangle$ (a) and of the zero-delay two-photon correlation function $G_A^{(2)}(t,t) = \langle \hat{A}^{(-)}(t)\hat{A}^{(-)}(t)\hat{A}^{(+)}(t)\hat{A}^{(+)}(t)\rangle$ (b) after the arrival of a Gaussian π pulse, evaluated for different temperatures and starting the dynamics with the system in its ground state. We used $T_\gamma/\omega_c = T_\kappa/\omega_c$ and the decoherence rates $\gamma/\omega_c = \kappa/\omega_c = 3.75 \times 10^{-4}$. Note that the output photon flux is proportional to $\langle \hat{A}^{(-)}\hat{A}^{(+)}\rangle$. At $T = 0$ our approach reproduces the two-photon vacuum Rabi oscillations shown in Ref. [27]. Here we study the influence of nonzero temperature on the this anomalous atom-cavity energy exchange. Increasing the temperature, the oscillations become more damped and the energy exchange becomes less effective. This effect is even more pronounced for the two-photon correlation $G_A^{(2)}(t,t)$, which displays a stronger thermal sensitivity. These results help to set a limit on the system temperature for the observation of two-photon vacuum Rabi oscillations.

In order to further show the impact of the generalized approach presented in this paper on the dissipative dynamics of cavity-QED systems in the USC regime, we compare the numerical results obtained with the generalized dressed master equation with those obtained using the standard dressed approach of Ref. [21].

Figure 3 shows the mean cavity photon number (a) and the two-photon correlation function (b) evaluated using the generalized dressed master equation (red solid curves) and the

standard dressed master equation [21] (black dashed curves), calculated with the atom and cavity reservoirs at temperature $T/\omega_c = 0.75$. Both approaches show the system undergoing multiphoton Rabi oscillations and the signals reaching the same stationary values, corresponding to the equilibrium thermal populations.

We observe that the standard approach overestimates decoherence effects. In the dispersive regime of cavity QED, pairs of photonlike transitions partially overlap, reducing decoherence effects during the time evolution. This effect is completely neglected in the standard dressed master equation. Further calculations, not shown here, indicate that these discrepancies increase with temperature. These effects lead to an overestimation of the coherence losses of the system, which also can be seen in the behavior of the two-photon correlation function [Fig. 3(b)].

It is also important to note that the generalized master equation is able to overcome another limit of validity of the standard dressed approach. As reported in Ref. [21], the standard dressed master equation breaks down in the limit of high excitation numbers, where more transitions might accidentally have the same frequency. The generalized master equation can handle such degenerate transitions well.

B. Cavity optomechanics beyond the RWA

1. Full optomechanical Hamiltonian

In Sec. III A, we demonstrated that our generalized approach is able to correctly describe systems with quasiharmonic spectra. In this section, we explore a mixed harmonic-anharmonic behavior, considering a simple optomechanical system [87], where a single cavity mode of frequency ω_c is coupled by radiation pressure to a single mechanical mode of a mirror vibrating at frequency ω_m.

Denoting the mechanical bosonic operators $\hat{b}$, $\hat{b}^\dagger$ and the cavity bosonic operators $\hat{a}$, $\hat{a}^\dagger$, the system Hamiltonian can be written as [92]

$$\hat{H}_S = \hat{H}_0 + \hat{V}_{\rm om} + \hat{V}_{\rm DCE}, \tag{36}$$

where

$$\hat{H}_0 = \omega_c \hat{a}^\dagger \hat{a} + \omega_m \hat{b}^\dagger \hat{b} \tag{37}$$

is the unperturbed Hamiltonian,

$$\hat{V}_{\rm om} = g \hat{a}^\dagger \hat{a} (\hat{b} + \hat{b}^\dagger) \tag{38}$$

is the standard optomechanical interaction Hamiltonian, and

$$\hat{V}_{\rm DCE} = \frac{g}{2} (\hat{a}^2 + \hat{a}^{\dagger 2})(\hat{b} + \hat{b}^\dagger) \tag{39}$$

describes the emission of photon pairs induced by the mechanical motion predicted by the DCE [89,93,94]. When treating most optomechanics experiments until now, $\hat{V}_{\rm DCE}$ has been neglected. This is a very good approximation when the mechanical frequency is much smaller than the cavity frequency (which is the most common experimental situation), because $\hat{V}_{\rm DCE}$ connects bare states with an energy difference $2\omega_c \pm \omega_m$ which then is much larger than the coupling strength g. With this approximation, the resulting Hamiltonian, $\hat{H}_0 + \hat{V}_{\rm om}$, conserves the number of photons and can be analytically diagonalized. However, when considering ultra-high-frequency mechanical oscillators, with resonance frequencies in the GHz spectral range, coupled to a microwave resonator, $\hat{V}_{\rm DCE}$, which does not conserve the photon number, cannot be neglected any more [87].

As shown in Ref. [87], such a system displays an energy-level spectrum with a ladder of avoided level crossings arising from the coherent coupling induced by $\hat{V}_{\rm DCE}$ between the states $|n, k_n\rangle$ and $|n+2, (k-q)_{n+2}\rangle$, occurring when the energies of the initial and final states coincide ($2\omega_c \simeq q\omega_m$). Here the first number in the ket denotes photon number and the second denotes phonon number (with the photon number as a subscript since the photons displace the mechanical Fock state). For example, with $q = 1$, we have the standard resonance condition for the DCE ($2\omega_c \simeq \omega_m$ [95]), in which case $\hat{V}_{\rm DCE}$ gives rise to a resonant coupling between the states $|0, k\rangle$ and $|2, (k-1)_2\rangle$ with $k \geqslant 1$, converting a phonon into a photon pair.

When $\hat{V}_{\rm DCE}$ is taken into account, the system Hamiltonian does not conserve the number of photons (the phonon number is not conserved even in the standard optomechanical Hamiltonian). For example, the ground state of $\hat{H}_S$ contains photons, i.e., $\langle E_0|\hat{a}^\dagger a|E_0\rangle \neq 0$. Therefore, in analogy to USC cavity QED, a careful treatment of dissipation and input-output theory is required. If the standard photon and phonon operators were used to describe the interaction with the outside world, unphysical effects would arise.

2. Impact of temperature on the dynamical Casimir effect

It has been shown [87] that this system can be used to demonstrate the conversion of mechanical energy into photon pairs (DCE). The calculations in Ref. [87] were performed using a dressed master equation without the post-trace RWA, developed only for the case of zero-temperature reservoirs. Here we instead apply the generalized master equation presented in Sec. II C, in order to study the influence of temperature on the energy conversion from phonons to photons.

For our numerical calculation we consider a normalized optomechanical coupling $g/\omega_m = 0.1$, a mechanical damping rate $\gamma/\omega_m = 0.05$, and a cavity damping rate $\kappa = \gamma/2$. We focus on the avoided level crossing between the states $|0, 2\rangle$ and $|2, 0_2\rangle$ at $\omega_m \simeq \omega_c$. We consider the resonant condition, corresponding to the minimum level splitting: $\omega_c/\omega_m = 1.016$.

As in Ref. [87], we consider a continuous coherent drive of the mechanical oscillator,

$$\hat{H}_d = \Omega(\hat{b}\, e^{-\imath\omega_m t} + \hat{b}^\dagger e^{\imath\omega_m t}), \tag{40}$$

with frequency resonant with the oscillating mirror and amplitude $\Omega = \gamma/2$. The dynamics giving rise to the DCE is then described by the filtered generalized master equation ($\Lambda = 10\gamma$)

$$\dot{\hat{\rho}} = -i[\hat{H}_S + \hat{H}_d, \hat{\rho}] + \mathcal{L}^{\rm filt}_{\rm gme}\hat{\rho}, \tag{41}$$

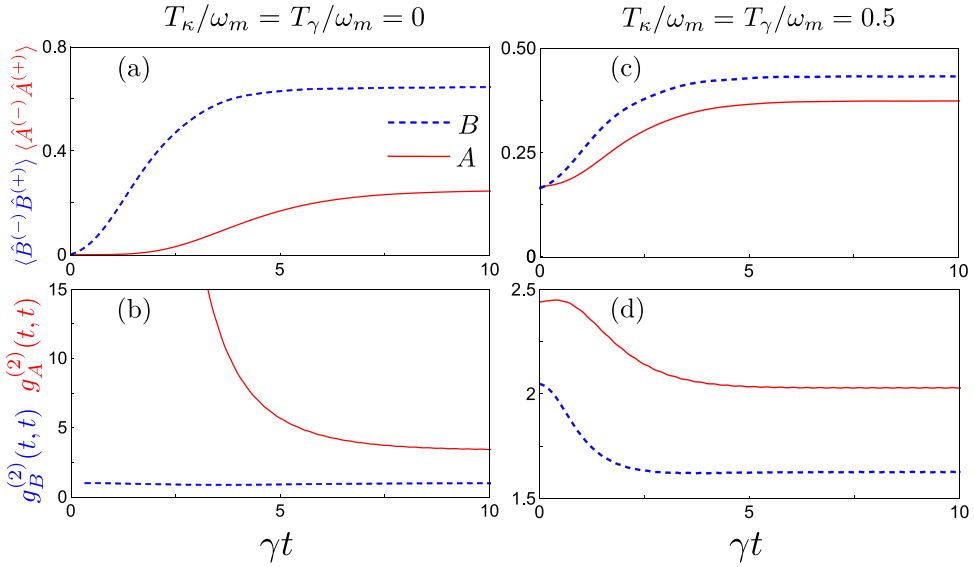

FIG. 4. Results for the DCE at different temperatures, obtained using the generalized-master-equation approach. (a), (b) System dynamics for $\omega_c \simeq \omega_m$, under coherent mechanical pumping, in perfect cooling conditions $T_\gamma = T_\kappa = 0$, starting the dynamics from the ground state. (c), (d) The same, but with $T_\gamma/\omega_m = T_\kappa/\omega_m = 0.5$ and the initial state being the thermal state with $T/\omega_m = 0.5$. The blue dashed curves show the mean phonon number $\langle \hat{B}^{(-)}\hat{B}^{(+)}\rangle$ in (a), (c) and the phonon-phonon correlation function $g_B^{(2)}(t,t)$ in (b), (d). The red solid curves describe the mean cavity photon number $\langle \hat{A}^{(-)}\hat{A}^{(+)}\rangle$ in (a), (c) and the zero-delay normalized photon-photon correlation function $g_A^{(2)}(t,t)$ in (b), (d). All parameters for the simulations are given in the text.

where the Liouvillian superoperator can be written as

$$\begin{aligned}\mathcal{L}_{\rm gme}^{\rm filter}\hat{\rho} = \sum_{(\omega,\omega')>0} \frac{1}{2}\{&\gamma n(\omega', T_\gamma)[\hat{B}^{(-)}(\omega')\hat{\rho}\hat{B}^{(+)}(\omega) - \hat{B}^{(+)}(\omega)\hat{B}^{(-)}(\omega')\hat{\rho}] + \gamma[n(\omega, T_\gamma)+1][\hat{B}^{(+)}(\omega)\hat{\rho}\hat{B}^{(-)}(\omega')\\ &- \hat{B}^{(-)}(\omega')\hat{B}^{(+)}(\omega)\hat{\rho}] + \gamma n(\omega, T_\gamma)[\hat{B}^{(-)}(\omega')\hat{\rho}\hat{B}^{(+)}(\omega) - \hat{\rho}\hat{B}^{(+)}(\omega)\hat{B}^{(-)}(\omega')] + \gamma[n(\omega', T_\gamma)+1]\\ &\times[\hat{B}^{(+)}(\omega)\hat{\rho}\hat{B}^{(-)}(\omega') - \hat{\rho}\hat{B}^{(-)}(\omega')\hat{B}^{(+)}(\omega)] + \kappa n(\omega', T_\kappa)[\hat{A}^{(-)}(\omega')\hat{\rho}\hat{A}^{(+)}(\omega) - \hat{A}^{(+)}(\omega)\hat{A}^{(-)}(\omega')\hat{\rho}]\\ &+\kappa[n(\omega, T_\kappa)+1][\hat{A}^{(+)}(\omega)\hat{\rho}\hat{A}^{(-)}(\omega') - \hat{A}^{(-)}(\omega')\hat{A}^{(+)}(\omega)\hat{\rho}] + \kappa n(\omega, T_\kappa)[\hat{A}^{(-)}(\omega')\hat{\rho}\hat{A}^{(+)}(\omega)\\ &- \hat{\rho}\hat{A}^{(+)}(\omega)\hat{A}^{(-)}(\omega')] + \kappa[n(\omega', T_\kappa)+1][\hat{A}^{(+)}(\omega)\hat{\rho}\hat{A}^{(-)}(\omega') - \hat{\rho}\hat{A}^{(-)}(\omega')\hat{A}^{(+)}(\omega)]\}F(\omega,\omega'), \end{aligned} \tag{42}$$

where $\hat{A}^{(+)}$ and $\hat{A}^{(-)}$ are the positive- and negative-frequency dressed cavity operators ($\hat{s}_i = \hat{a}$), and $\hat{B}^{(+)}$ and $\hat{B}^{(-)}$ are the positive- and negative-frequency dressed mechanical operators ($\hat{s}_i = \hat{b}$).

In Fig. 4, we show the photonic and phononic populations, $\langle \hat{A}^{(-)}\hat{A}^{(+)}\rangle$ and $\langle \hat{B}^{(-)}\hat{B}^{(+)}\rangle$, and the relative two-photon and two-phonon correlation functions,

$$g_A^{(2)}(t,t) = \frac{\langle \hat{A}^{(-)}(t)\hat{A}^{(-)}(t)\hat{A}^{(+)}(t)\hat{A}^{(+)}(t)\rangle}{\langle \hat{A}^{(-)}(t)\hat{A}^{(+)}(t)\rangle^2}, \tag{43}$$

$$g_B^{(2)}(t,t) = \frac{\langle \hat{B}^{(-)}(t)\hat{B}^{(-)}(t)\hat{B}^{(+)}(t)\hat{B}^{(+)}(t)\rangle}{\langle \hat{B}^{(-)}(t)\hat{B}^{(+)}(t)\rangle^2}. \tag{44}$$

Figures 4(a) and 4(b) display the results of calculations done with zero-temperature reservoirs for both subsystems and starting the dynamics from the ground state. Figures 4(c) and 4(d) display the results of calculations for reservoirs with $T_\gamma/\omega_m = T_\kappa/\omega_m = 0.5$ and with the system initially in thermal equilibrium with those reservoirs.

At $T = 0$, with the system starting in its ground state, the photonic and phononic populations start from zero and, due to the coherent pumping, reach nonzero stationary values. The photonic correlation function $g_A^{(2)}(t,t)$ is initially much higher than two, suggesting photon-pair emission. As time goes on, $g_A^{(2)}(t,t)$ decreases significantly due to losses which affect the photon-photon correlations, and also due to the increase of the mean photon number [note that $g_A^{(2)}(t,t)$, owing to the squared denominator, is an intensity-dependent quantity]. The mechanical correlation function $g_B^{(2)}(t,t)$, on the contrary, has an almost constant value [$g_B^{(2)}(t,t) \approx 1$], showing that the mechanical system is mainly in the coherent state produced by the pumping.

For reservoirs with nonzero temperature, the phonon and photon populations, starting from their thermal-equilibrium values, equilibrate to lower steady-state values. This reduction of both populations originates from the increase of the decay rate of the coherent contributions with increasing temperature. We also note that the difference between the two steady-state values is reduced at higher temperatures, due to the thermal

contributions. At $T \neq 0$, a fraction of the observed photons, as expected, does not come from the mechanical-to-optical energy conversion, but, trivially, from the photonic thermal reservoir.

This picture is confirmed by comparing the dynamics of the higher-order correlation functions [Figs. 4(c) and 4(d)]. Specifically, at higher temperature, we observe a strong decrease of $g_A^{(2)}(t,t)$, showing that a reduced fraction of photons is emitted in pairs. However, the photon-photon correlation functions remains, even in the steady state, *higher* than the thermal value $g_A^{(2)}(t,t) = 2$. The phonon-phonon correlation starts from a value $\simeq 2$ corresponding to the initial incoherent thermal state and, as time goes on, decays to a stationary value higher than one due to the incoherent thermal excitations provided by the interaction with the thermal reservoirs.

Furthermore, in Fig. 4(d), the photon-photon and the phonon-phonon correlation functions do not start from the same initial value. This effect is due to the $\hat{V}_{\rm DCE}$ term which, owing to its nonbilinear form, modifies the thermodynamic equilibrium of the initial state of the system. The $\hat{V}_{\rm DCE}$ contribution leads to a separation of the correlation-function values with size proportional to the temperature. This separation thus vanishes trivially for $T = 0$, when the $\hat{V}_{\rm DCE}$ term becomes negligible.

The results obtained clearly show that the generalized dressed master equation provided here is able to describe dissipation in hybrid quantum systems with coexisting coherent phases (provided, e.g., by means of a continuous drive) and incoherent phases (provided, e.g., by thermal reservoirs or thermal-like pumping). The behavior of the one- and two-photon correlation functions show that signatures of the DCE can be observed even in the presence of a non-negligible amount of thermal noise. It thus demonstrates that this effect can be observed in a real experimental setup, where perfect cooling conditions cannot be reached. Although the number of Casimir photon pairs produced depends on the thermal noise injected into the system, our results here show that the DCE remains detectable even at relatively high temperatures.

3. Comparison to other approaches

As already mentioned in the Introduction, and demonstrated in Ref. [21], the use of a master equation with a dissipator not taking into account the interaction between the subsystems can lead to unphysical results. Hu *et al.* derived [75] a dressed master equation specifically developed to describe dissipation in optomechanical systems characterized by the standard optomechanical Hamiltonian, $\hat{H}_S = \hat{H}_0 + \hat{V}_{\rm om}$, in the USC regime. Here we show that this master equation *fails* when considering the complete optomechanical Hamiltonian $\hat{H}_S = \hat{H}_0 + \hat{V}_{\rm om} + \hat{V}_{\rm DCE}$.

In Fig. 5, we display results obtained describing the dynamics of our optomechanical system in perfect cooling conditions, without any pumping, with the master equation provided in Ref. [75], including the $\hat{V}_{\rm DCE}$ term as a perturbation in the dynamics. In these conditions, evaluating the dynamics with the system initially in the ground state (an eigenstate of the system), zero population is expected in the states

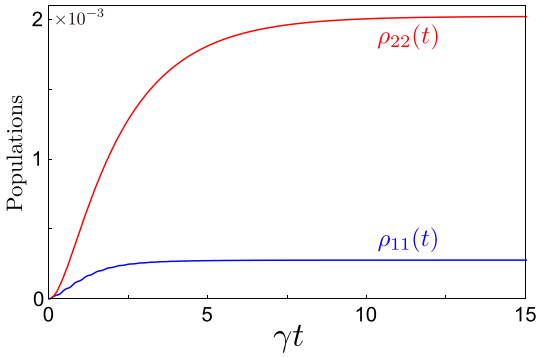

FIG. 5. State populations obtained using the master-equation approach of Ref. [75]. The red (blue) solid curve shows the time evolution of the population of the one-photon state $|1,0\rangle$ (the one-phonon state $|0,1\rangle$) labeled $\rho_{22}(t)$ [$\rho_{11}(t)$] under perfect cooling conditions $T_\gamma = T_\kappa = 0$ and without any pumping. The initial state is the ground state $|0,0\rangle$. All other parameters are the same as in Fig. 4. In these conditions, without any external driving or thermal excitations, the system is expected to remain in the ground state. However, the plot clearly shows a nonzero population in both the one-photon and one-phonon states. This indicates that this approach is *not* able to correctly describe optomechanical systems when the $\hat{V}_{\rm DCE}$ contribution no longer can be neglected.

with one photon, $|1,0\rangle$, and one phonon, $|0,1\rangle$. However, Fig. 5 clearly shows nonzero populations. This anomalous effect occurs because, due to the additional $\hat{V}_{\rm DCE}$ term, the number of photons is no longer conserved and consequently the eigenstates of the Hamiltonian changes. In this case, the master equation provided in Ref. [75] does not describe interactions between subsystems and reservoirs in terms of the correct eigenstates, which leads to an unphysical evolution of the initial ground state. This result shows once more the importance of expressing the system operators in the basis of the system eigenstates when describing interactions with reservoirs to derive a correct master equation.

IV. CONCLUSIONS

We have presented a generalized dressed master equation, valid for arbitrary open hybrid quantum system interacting with thermal reservoirs and for arbitrary strength of the coupling between the components of the hybrid system. Our approach was derived within the Born-Markov approximation, including the pure dephasing terms and without performing the usual post-trace RWA. Therefore, our approach is able to handle dynamics in systems with both harmonic, quasiharmonic, and anharmonic transitions. Moreover, this approach is not limited to systems displaying parity symmetry. Unfortunately the dissipator obtained includes rapidly oscillating terms that can cause numerical instabilities. In order to fix this problem, we introduced a filtering procedure which eliminates the fast-oscillating terms which do not contribute to the coarse-grained dynamics. This filtering has the added benefit of reducing computation times.

We applied our generalized approach to study the influence of temperature on multiphoton vacuum Rabi oscillation in a circuit-QED system in the dispersive regime. We compared

our results with those obtained using the dressed master equation of Ref. [21]. We found that both approaches describe multiphoton Rabi oscillations and reach the same stationary state (the thermal equilibrium). However, the standard master equation overestimates decoherence effects since it does not take into account the partial overlap of photonlike transitions, which reduces the decoherence during the time evolution.

We also studied the influence of temperature on the conversion of mechanical energy into photon pairs (DCE) in an optomechanical system, recently described in Ref. [87] for zero-temperature reservoirs. In this case, we showed that the DCE can be observed also in the presence of a significant amount of thermal noise.

Finally, we demonstrated that the master-equation approach provided in Ref. [75] for optomechanical systems with ultrastrong coupling fails when considering the full optomechanical Hamiltonian including the $\hat{V}_{\rm DCE}$ term. Specifically, under these conditions, the master equation provided in Ref. [75] does not describe interactions between the components and reservoirs correctly in terms of transitions between eigenstates of the hybrid system. Because of this shortcoming, that approach leads to an unphysical evolution of the initial ground state to excited states even at zero temperature and without any external pumping. This example clearly shows that the general master-equation approach provided here is necessary to describe dissipation of general open hybrid quantum systems interacting with thermal reservoirs.

ACKNOWLEDGMENTS

F.N. is supported in part by the MURI Center for Dynamic Magneto-Optics via the Air Force Office of Scientific Research (AFOSR) (FA9550-14-1-0040), Army Research Office (ARO) (Grant No. W911NF-18-1-0358), Asian Office of Aerospace Research and Development (AOARD) (Grant No. FA2386-18-1-4045), Japan Science and Technology Agency (JST) (Q-LEAP program, the ImPACT program and CREST Grant No. JP-MJCR1676), Japan Society for the Promotion of Science (JSPS) (JSPS-RFBR Grant No. 17-52-50023 and JSPS-FWO Grant No. VS.059.18N), RIKEN-AIST Challenge Research Fund, and the John Templeton Foundation.

APPENDIX: DERIVATION OF THE DRESSED MASTER EQUATION

Starting from the system-bath Hamiltonian in Eq. (18), and following the standard procedure [5], i.e., performing the second-order Born approximation, the Markov approximation, and considering reservoirs with a continuum of frequencies, we obtain

$$\begin{aligned}\dot{\hat{\rho}}(t) = &\int_0^t dt'[\hat{\tilde{S}}_i(t')\hat{\rho}(t')\hat{\tilde{S}}_i(t) - \hat{\tilde{S}}_i(t)\hat{\tilde{S}}_i(t')\hat{\rho}(t')]\langle\hat{\tilde{B}}_i^\dagger(t)\hat{\tilde{B}}_i(t')\rangle + \int_0^t dt'[\hat{\tilde{S}}_i(t)\hat{\rho}(t)\hat{\tilde{S}}_i(t') - \hat{\rho}(t')\hat{\tilde{S}}_i(t')\hat{\tilde{S}}_i(t)]\langle\hat{\tilde{B}}_i^\dagger(t')\hat{\tilde{B}}_i(t)\rangle \\ &+ \int_0^t dt'[\hat{\tilde{S}}_i(t')\hat{\rho}(t)\hat{\tilde{S}}_i(t) - \hat{\tilde{S}}_i(t)\hat{\tilde{S}}_i(t')\hat{\rho}(t')]\langle\hat{\tilde{B}}_i(t)\hat{\tilde{B}}_i^\dagger(t')\rangle + \int_0^t dt'[\hat{\tilde{S}}_i(t)\hat{\rho}(t')\hat{\tilde{S}}_i(t') - \hat{\rho}(t')\hat{\tilde{S}}_i(t')\hat{\tilde{S}}_i(t)]\langle\hat{\tilde{B}}_i(t')\hat{\tilde{B}}_i^\dagger(t)\rangle,\end{aligned} \tag{A1}$$

where $\langle\hat{\tilde{B}}_i^\dagger(t)\hat{\tilde{B}}_i(t')\rangle$ and $\langle\hat{\tilde{B}}_i^\dagger(t')\hat{\tilde{B}}_i(t)\rangle$ are the reservoir correlation functions

$$\langle\hat{\tilde{B}}_i^\dagger(t)\hat{\tilde{B}}_i(t')\rangle = \int_0^\infty d\nu\, g_i(\nu)|\alpha_i(\nu)|^2 n(\nu, T_i)e^{\imath\nu(t-t')}, \tag{A2}$$

$$\langle\hat{\tilde{B}}_i(t)\hat{\tilde{B}}_i^\dagger(t')\rangle = \int_0^\infty d\nu\, g_i(\nu)|\alpha_i(\nu)|^2 [n(\nu, T_i)+1]e^{-\imath\nu(t-t')}, \tag{A3}$$

with $g(\nu)$ being the reservoir density of states and $\alpha(\nu)$ the system-reservoir coupling strength. Substituting Eqs. (A2) and (A3) into Eq. (A1), and performing the change of variable $\tau = t - t'$, we obtain

$$\dot{\hat{\rho}}(t) = \sum_i \sum_{\omega,\omega'} \big[\hat{A}^i_{\omega,\omega'}(t) + \hat{B}^i_{\omega,\omega'}(t) + \hat{C}^i_{\omega,\omega'}(t) + \hat{D}^i_{\omega,\omega'}(t)\big], \tag{A4}$$

where

$$\begin{aligned}\hat{A}^i_{\omega,\omega'}(t) &= \int_0^t d\tau\, e^{-\imath(\omega+\omega')t}e^{\imath\omega'\tau}[\hat{S}_i(\omega')\hat{\rho}(t)\hat{S}_i(\omega) - \hat{S}_i(\omega)\hat{S}_i(\omega')\hat{\rho}(t)]\int_0^\infty d\nu\, g_i(\nu)|\alpha_i(\nu)|^2 n(\nu, T_i)e^{\imath\nu\tau}, \\ \hat{B}^i_{\omega,\omega'}(t) &= \int_0^t d\tau\, e^{-\imath(\omega+\omega')t}e^{\imath\omega\tau}[\hat{S}_i(\omega')\hat{\rho}(t)\hat{S}_i(\omega) - \hat{\rho}(t)\hat{S}_i(\omega)\hat{S}_i(\omega')]\int_0^\infty d\nu\, g_i(\nu)|\alpha_i(\nu)|^2 n(\nu, T_i)e^{-\imath\nu\tau}, \\ \hat{C}^i_{\omega,\omega'}(t) &= \int_0^t d\tau\, e^{-\imath(\omega+\omega')t}e^{\imath\omega\tau}[\hat{S}_i(\omega)\hat{\rho}(t)\hat{S}_i(\omega') - \hat{S}_i(\omega')\hat{S}_i(\omega)\hat{\rho}(t)]\int_0^\infty d\nu\, g_i(\nu)|\alpha_i(\nu)|^2 [n(\nu, T_i)+1]e^{-\imath\nu\tau}, \\ \hat{D}^i_{\omega,\omega'}(t) &= \int_0^t d\tau\, e^{-\imath(\omega+\omega')t}e^{\imath\omega'\tau}[\hat{S}_i(\omega)\hat{\rho}(t)\hat{S}_i(\omega') - \hat{\rho}(t)\hat{S}_i(\omega')\hat{S}_i(\omega)]\int_0^\infty d\nu\, g_i(\nu)|\alpha_i(\nu)|^2 [n(\nu, T_i)+1]e^{\imath\nu\tau}.\end{aligned} \tag{A5}$$

Assuming that the integrands decay on a much shorter time scale than that of the reservoir correlation functions, we can extend the τ integration to infinity. Evaluating both the integrals without performing any approximation except for the Born-Markov

approximation, the master equation in the Schrödinger picture can be written

$$\dot{\hat{\rho}} = -i[\hat{H}_S, \hat{\rho}] + \mathcal{L}_{\rm gme}\hat{\rho}, \tag{A6}$$

with the Lindbladian superoperator that in the most general form can be written as

$$\begin{aligned}\mathcal{L}_{\rm gme}\hat{\rho} = \frac{1}{2}\sum_i \sum_{\omega,\omega'} \{&\Gamma_i(-\omega')n(-\omega', T_i)[\hat{S}_i(\omega')\hat{\rho}(t)\hat{S}_i(\omega) - \hat{S}_i(\omega)\hat{S}_i(\omega')\hat{\rho}(t)] + \Gamma_i(\omega)n(\omega, T_i)\\ &\times [\hat{S}_i(\omega')\hat{\rho}(t)\hat{S}_i(\omega) - \hat{\rho}(t)\hat{S}_i(\omega)\hat{S}_i(\omega')] + \Gamma_i(\omega)[n(\omega, T_i) + 1][\hat{S}_i(\omega)\hat{\rho}(t)\hat{S}_i(\omega') - \hat{S}_i(\omega')\hat{S}_i(\omega)\hat{\rho}(t)]\\ &+ \Gamma_i(-\omega')[n(-\omega', T_i) + 1][\hat{S}_i(\omega)\hat{\rho}(t)\hat{S}_i(\omega') - \hat{\rho}(t)\hat{S}_i(\omega')\hat{S}_i(\omega)]\}.\end{aligned} \tag{A7}$$

Both $\Gamma_i(\omega)$ and $n(\omega, T_i)$ are nonzero only for $\omega > 0$; thus, using the definitions in Eq. (17), Eq. (A7) can be written as

$$\begin{aligned}\mathcal{L}_{\rm gme}\hat{\rho} = \frac{1}{2}\sum_i \sum_{(\omega,\omega')>0} \{&\Gamma_i(\omega')n(\omega', T_i)[\hat{S}_i^{(-)}(\omega')\hat{\rho}(t)\hat{S}_i^{(+)}(\omega) - \hat{S}_i^{(+)}(\omega)\hat{S}_i^{(-)}(\omega')\hat{\rho}(t)] + \Gamma_i(\omega)n(\omega, T_i)[\hat{S}_i^{(-)}(\omega')\hat{\rho}(t)\hat{S}_i^{(+)}(\omega)\\ &- \hat{\rho}(t)\hat{S}_i^{(+)}(\omega)\hat{S}_i^{(-)}(\omega')] + \Gamma_i(\omega)[n(\omega, T_i) + 1][\hat{S}_i^{(+)}(\omega)\hat{\rho}(t)\hat{S}_i^{(-)}(\omega') - \hat{S}_i^{(-)}(\omega')\hat{S}_i^{(+)}(\omega)\hat{\rho}(t)] + \Gamma_i(\omega')[n(\omega', T_i) + 1]\\ &\times [\hat{S}_i^{(+)}(\omega)\hat{\rho}(t)\hat{S}_i^{(-)}(\omega') - \hat{\rho}(t)\hat{S}_i^{(-)}(\omega')\hat{S}_i^{(+)}(\omega)] + \Gamma_i(\omega')n(\omega', T_i)[\hat{S}_i^{(-)}(\omega')\hat{\rho}(t)\hat{S}_i^{(-)}(\omega) - \hat{S}_i^{(-)}(\omega)\hat{S}_i^{(-)}(\omega')\hat{\rho}(t)]\\ &+ \Gamma_i(\omega')[n(\omega', T_i) + 1][\hat{S}_i^{(-)}(\omega)\hat{\rho}(t)\hat{S}_i^{(-)}(\omega') - \hat{\rho}(t)\hat{S}_i^{(-)}(\omega')\hat{S}_i^{(-)}(\omega)] + \Gamma_i(\omega)n(\omega, T_i)[\hat{S}_i^{(+)}(\omega')\hat{\rho}(t)\hat{S}_i^{(+)}(\omega)\\ &- \hat{\rho}(t)\hat{S}_i^{(+)}(\omega)\hat{S}_i^{(+)}(\omega')] + \Gamma_i(\omega)[n(\omega, T_i) + 1][\hat{S}_i^{(+)}(\omega)\hat{\rho}(t)\hat{S}_i^{(+)}(\omega') - \hat{S}_i^{(+)}(\omega')\hat{S}_i^{(+)}(\omega)\hat{\rho}(t)]\\ &+ \Gamma_i(\omega')n(\omega', T_i)\big[\hat{S}_i^{(-)}(\omega')\hat{\rho}(t)\hat{S}_i^{(0)} - \hat{S}_i^{(0)}\hat{S}_i^{(-)}(\omega')\hat{\rho}(t)\big] + \Gamma_i(\omega')[n(\omega', T_i) + 1]\big[\hat{S}_i^{(0)}\hat{\rho}(t)\hat{S}_i^{(-)}(\omega') - \hat{\rho}(t)\hat{S}_i^{(-)}(\omega')\hat{S}_i^{(0)}\big]\\ &+ \Gamma_i(\omega)n(\omega, T_i)\big[\hat{S}_i^{(0)}\hat{\rho}(t)\hat{S}_i^{(+)}(\omega) - \hat{\rho}(t)\hat{S}_i^{(+)}(\omega)\hat{S}_i^{(0)}\big] + \Gamma_i(\omega)[n(\omega, T_i) + 1]\big[\hat{S}_i^{(+)}(\omega)\hat{\rho}(t)\hat{S}_i^{(0)} - \hat{S}_i^{(0)}\hat{S}_i^{(+)}(\omega)\hat{\rho}(t)\big]\\ &+ \Omega_i^{+}(T_i)\big[\hat{S}_i^{(0)}\hat{\rho}(t)\hat{S}_i^{(0)} - \hat{S}_i^{(0)}\hat{S}_i^{(0)}\hat{\rho}(t)\big] + \Omega_i^{'+}(T_i)\big[\hat{S}_i^{(0)}\hat{\rho}(t)\hat{S}_i^{(0)} - \hat{\rho}(t)\hat{S}_i^{(0)}(\omega')\hat{S}_i^{(0)}\big]\\ &+ \Omega_i^{-}(T_i)\big[\hat{S}_i^{(0)}\hat{\rho}(t)\hat{S}_i^{(0)} - \hat{\rho}(t)\hat{S}_i^{(0)}\hat{S}_i^{(0)}\big] + \Omega_i^{'-}(T_i)\big[\hat{S}_i^{(0)}\hat{\rho}(t)\hat{S}_i^{(0)} - \hat{S}_i^{(0)}\hat{S}_i^{(0)}\hat{\rho}(t)\big]\}, \end{aligned} \tag{A8}$$

with thermal populations

$$n(\omega, T_i) = [\exp\{\omega/T_i\} - 1]^{-1}, \tag{A9}$$

damping rates

$$\Gamma_i(\omega) = 2\pi g_i(\omega)|\alpha_i(\omega)|^2, \tag{A10}$$

and pure dephasing damping rates

$$\Omega_i^{'\pm}(T_i) = \int_0^t d\tau \int_0^\infty d\nu\, g_i(\nu)|\alpha_i(\nu)|^2[n(\nu, T_i) + 1]e^{\pm i\nu\tau}, \tag{A11}$$

$$\Omega_i^{\pm}(T_i) = \int_0^t d\tau \int_0^\infty d\nu\, g_i(\nu)|\alpha_i(\nu)|^2 n(\nu, T_i)e^{\pm i\nu\tau}. \tag{A12}$$

Specifically, the terms in the first four lines of Eq. (A8) oscillate at frequencies $\pm(\omega - \omega')$. If $(\omega - \omega')$ is significantly larger than the damping rates Γ_i of the system, these terms provide negligible contributions when integrating the master equation. In the generalized approach, these terms are then eliminated by the numerical filtering. The terms in the next four lines of Eq. (A8) oscillate at $\pm(\omega' + \omega)$. These terms are clearly rapidly oscillating and thus provide negligible contributions. The terms in the following four lines, oscillating at $+\omega$, $-\omega'$, are fast oscillating when considering systems displaying well-separated energy levels with $\omega \gg \Gamma_i$ and, in these cases, can be neglected. Finally, the terms in the last four lines arise from degenerate transitions and describe pure dephasing. The contribution of these terms becomes negligible at very low temperatures in the particular case of Ohmic baths. Furthermore, it is important to note that, applying the post-trace RWA without considering any parity symmetry of the system, Eq. (A7) can be rewritten in a form equal to the standard dressed master equation as in Ref. [21], with a few additional terms provided by the zero-frequency operators $\hat{S}_i^{(0)} \neq 0$.

[1] M. Brune, E. Hagley, J. Dreyer, X. Maître, A. Maali, C. Wunderlich, J. M. Raimond, and S. Haroche, Observing the Progressive Decoherence of the "Meter" in a Quantum Measurement, Phys. Rev. Lett. **77**, 4887 (1996).

[2] M. Hofheinz, H. Wang, M. Ansmann, R. C. Bialczak, E. Lucero, M. Neeley, A. D. O'Connell, D. Sank, J. Wenner, J. M. Martinis, and A. N. Cleland, Synthesizing arbitrary quantum states in a superconducting resonator, Nature (London) **459**, 546 (2009).

[3] X. Gu, A. F. Kockum, A. Miranowicz, Y.-X. Liu, and F. Nori, Microwave photonics with superconducting quantum circuits, Phys. Rep. **718-719**, 1 (2017).

[4] S. N. A. Duffus, V. M. Dwyer, and M. J. Everitt, Open quantum systems, effective Hamiltonians, and device characterization, Phys. Rev. B **96**, 134520 (2017).

[5] H. P. Breuer and F. Petruccione, *The Theory of Open Quantum Systems* (Oxford University Press, Oxford, 2002).

[6] C. W. Gardiner and P. Zoller, *Quantum Noise*, 3rd ed. (Springer, New York, 2004).

[7] M. D. Kostin, On the Schrödinger-Langevin equation, J. Chem. Phys. **57**, 3589 (1972).

[8] G. W. Ford and M. Kac, On the quantum Langevin equation, J. Stat. Phys. **46**, 803 (1987).

[9] S. Portolan, O. Di Stefano, S. Savasta, F. Rossi, and R. Girlanda, Nonequilibrium Langevin approach to quantum optics in semiconductor microcavities, Phys. Rev. B **77**, 035433 (2008).

[10] F. Haake, in *Statistical Treatment of Open Systems by Generalized Master Equations*, edited by G. Höhler, Springer Tracts in Modern Physics (Springer, Berlin, Heidelberg, 1973), pp. 98–168.

[11] N. Shammah, S. Ahmed, N. Lambert, S. De Liberato, and F. Nori, Open quantum systems with local and collective incoherent processes: Efficient numerical simulation using permutational invariance, arXiv:1805.05129 [Phys. Rev. A (to be published)].

[12] M. Wallquist, K. Hammerer, P. Rabl, M. Lukin, and P. Zoller, Hybrid quantum devices and quantum engineering, Phys. Scr. **T137**, 014001 (2009).

[13] Z.-L. Xiang, S. Ashhab, J. Q. You, and F. Nori, Hybrid quantum circuits: Superconducting circuits interacting with other quantum systems, Rev. Mod. Phys. **85**, 623 (2013).

[14] G. Kurizki, P. Bertet, Y. Kubo, K. Mølmer, D. Petrosyan, P. Rabl, and J. Schmiedmayer, Quantum technologies with hybrid systems, Proc. Natl. Acad. Sci. USA **112**, 3866 (2015).

[15] S. Haroche, Nobel lecture: Controlling photons in a box and exploring the quantum to classical boundary, Rev. Mod. Phys. **85**, 1083 (2013).

[16] A. F. Kockum, A. Miranowicz, S. De Liberato, S. Savasta, and F. Nori, Ultrastrong coupling between light and matter, arXiv:1807.11636 [Nat. Rev. Phys. (to be published)].

[17] P. Forn-Díaz, L. Lamata, E. Rico, J. Kono, and E. Solano, Ultrastrong coupling regimes of light-matter interaction, arXiv:1804.09275.

[18] S. De Liberato, C. Ciuti, and I. Carusotto, Quantum Vacuum Radiation Spectra from a Semiconductor Microcavity with a Time-Modulated Vacuum Rabi Frequency, Phys. Rev. Lett. **98**, 103602 (2007).

[19] S. Ashhab and F. Nori, Qubit-oscillator systems in the ultrastrong-coupling regime and their potential for preparing nonclassical states, Phys. Rev. A **81**, 042311 (2010).

[20] J. Casanova, G. Romero, I. Lizuain, J. J. García-Ripoll, and E. Solano, Deep Strong Coupling Regime of the Jaynes-Cummings Model, Phys. Rev. Lett. **105**, 263603 (2010).

[21] F. Beaudoin, J. M. Gambetta, and A. Blais, Dissipation and ultrastrong coupling in circuit QED, Phys. Rev. A **84**, 043832 (2011).

[22] A. Ridolfo, M. Leib, S. Savasta, and M. J. Hartmann, Photon Blockade in the Ultrastrong Coupling Regime, Phys. Rev. Lett. **109**, 193602 (2012).

[23] R. Stassi, A. Ridolfo, O. Di Stefano, M. J. Hartmann, and S. Savasta, Spontaneous Conversion from Virtual to Real Photons in the Ultrastrong-Coupling Regime, Phys. Rev. Lett. **110**, 243601 (2013).

[24] L. Garziano, A. Ridolfo, R. Stassi, O. Di Stefano, and S. Savasta, Switching on and off of ultrastrong light-matter interaction: Photon statistics of quantum vacuum radiation, Phys. Rev. A **88**, 063829 (2013).

[25] S. De Liberato, Light-Matter Decoupling in the Deep Strong Coupling Regime: The Breakdown of the Purcell Effect, Phys. Rev. Lett. **112**, 016401 (2014).

[26] E. Sanchez-Burillo, D. Zueco, J. J. Garcia-Ripoll, and L. Martin-Moreno, Scattering in the Ultrastrong Regime: Nonlinear Optics with One Photon, Phys. Rev. Lett. **113**, 263604 (2014).

[27] L. Garziano, R. Stassi, V. Macrì, A. F. Kockum, S. Savasta, and F. Nori, Multiphoton quantum Rabi oscillations in ultrastrong cavity QED, Phys. Rev. A **92**, 063830 (2015).

[28] L. Garziano, V. Macrì, R. Stassi, O. Di Stefano, F. Nori, and S. Savasta, One Photon Can Simultaneously Excite Two or More Atoms, Phys. Rev. Lett. **117**, 043601 (2016).

[29] M. Cirio, S. De Liberato, N. Lambert, and F. Nori, Ground State Electroluminescence, Phys. Rev. Lett. **116**, 113601 (2016).

[30] A. F. Kockum, A. Miranowicz, V. Macrì, S. Savasta, and F. Nori, Deterministic quantum nonlinear optics with single atoms and virtual photons, Phys. Rev. A **95**, 063849 (2017).

[31] A. F. Kockum, V. Macrì, L. Garziano, S. Savasta, and F. Nori, Frequency conversion in ultrastrong cavity QED, Sci. Rep. **7**, 5313 (2017).

[32] R. Stassi, V. Macrì, A. F. Kockum, O. Di Stefano, A. Miranowicz, S. Savasta, and F. Nori, Quantum nonlinear optics without photons, Phys. Rev. A **96**, 023818 (2017).

[33] W. Qin, A. Miranowicz, P. B. Li, X. Y. Lü, J. Q. You, and F. Nori, Exponentially Enhanced Light-Matter Interaction, Cooperativities, and Steady-State Entanglement Using Parametric Amplification, Phys. Rev. Lett. **120**, 093601 (2018).

[34] A. Ridolfo, G. Falci, F. M. D. Pellegrino, and E. Paladino, Photon pair production by STIRAP in ultrastrongly coupled matter-radiation systems, arXiv:1805.07079.

[35] A. A. Anappara, S. De Liberato, A. Tredicucci, C. Ciuti, G. Biasiol, L. Sorba, and F. Beltram, Signatures of the ultrastrong light-matter coupling regime, Phys. Rev. B **79**, 201303 (2009).

[36] G. Günter, A. A. Anappara, J. Hees, A. Sell, G. Biasiol, L. Sorba, S. De Liberato, C. Ciuti, A. Tredicucci, A. Leitenstorfer, and R. Huber, Sub-cycle switch-on of ultrastrong light–matter interaction, Nature (London) **458**, 178 (2009).

[37] Y. Todorov, A. M. Andrews, R. Colombelli, S. De Liberato, C. Ciuti, P. Klang, G. Strasser, and C. Sirtori, Ultrastrong Light-Matter Coupling Regime with Polariton Dots, Phys. Rev. Lett. **105**, 196402 (2010).

[38] M. Geiser, F. Castellano, G. Scalari, M. Beck, L. Nevou, and J. Faist, Ultrastrong Coupling Regime and Plasmon Polaritons in Parabolic Semiconductor Quantum Wells, Phys. Rev. Lett. **108**, 106402 (2012).

[39] B. Askenazi, A. Vasanelli, A. Delteil, Y. Todorov, L. C. Andreani, G. Beaudoin, I. Sagnes, and C. Sirtori, Ultra-strong light-matter coupling for designer Reststrahlen band, New J. Phys. **16**, 043029 (2014).

[40] P. Forn-Díaz, J. Lisenfeld, D. Marcos, J. J. García-Ripoll, E. Solano, C. J. P. M. Harmans, and J. E. Mooij, Observation of the Bloch-Siegert Shift in a Qubit-Oscillator System in the Ultrastrong Coupling Regime, Phys. Rev. Lett. **105**, 237001 (2010).

[41] T. Niemczyk, F. Deppe, H. Huebl, E. P. Menzel, F. Hocke, M. J. Schwarz, J. J. Garcia-Ripoll, D. Zueco, T. Hümmer, E. Solano, A. Marx, and R. Gross, Circuit quantum electrodynamics in the ultrastrong-coupling regime, Nat. Phys. **6**, 772 (2010).

[42] A. Baust, E. Hoffmann, M. Haeberlein, M. J. Schwarz, P. Eder, J. Goetz, F. Wulschner, E. Xie, L. Zhong, F. Quijandría, D. Zueco, J.-J.G. Ripoll, L. García-Álvarez, G. Romero, E. Solano, K. G. Fedorov, E. P. Menzel, F. Deppe, A. Marx, and R. Gross, Ultrastrong coupling in two-resonator circuit QED, Phys. Rev. B **93**, 214501 (2016).

[43] P. Forn-Díaz, G. Romero, C. J. P. M. Harmans, E. Solano, and J. E. Mooij, Broken selection rule in the quantum Rabi model, Sci. Rep. **6**, 26720 (2016).

[44] S. J. Bosman, M. F. Gely, V. Singh, A. Bruno, D. Bothner, and G. A. Steele, Multi-mode ultra-strong coupling in circuit quantum electrodynamics, npj Quantum Inf. **3**, 46 (2017).

[45] F. Yoshihara, T. Fuse, S. Ashhab, K. Kakuyanagi, S. Saito, and K. Semba, Characteristic spectra of circuit quantum electrodynamics systems from the ultrastrong- to the deep-strong-coupling regime, Phys. Rev. A **95**, 053824 (2017).

[46] F. Yoshihara, T. Fuse, S. Ashhab, K. Kakuyanagi, S. Saito, and K. Semba, Superconducting qubit-oscillator circuit beyond the ultrastrong-coupling regime, Nat. Phys. **13**, 44 (2017).

[47] N. K. Langford, R. Sagastizabal, M. Kounalakis, C. Dickel, A. Bruno, F. Luthi, D. J. Thoen, A. Endo, and L. DiCarlo, Experimentally simulating the dynamics of quantum light and matter at deep-strong coupling, Nat. Commun. **8**, 1715 (2017).

[48] J. Braumüller, M. Marthaler, A. Schneider, A. Stehli, H. Rotzinger, M. Weides, and A. V. Ustinov, Analog quantum simulation of the Rabi model in the ultra-strong coupling regime, Nat. Commun. **8**, 779 (2017).

[49] L. Magazzù, P. Forn-Díaz, R. Belyansky, J.-L. Orgiazzi, M. A. Yurtalan, M. R. Otto, A. Lupascu, C. M. Wilson, and M. Grifoni, Probing the strongly driven spin-boson model in a superconducting quantum circuit, Nat. Commun. **9**, 1403 (2018).

[50] F. Yoshihara, T. Fuse, Z. Ao, S. Ashhab, K. Kakuyanagi, S. Saito, T. Aoki, K. Koshino, and K. Semba, Inversion of Qubit Energy Levels in Qubit-oscillator Circuits in the Deep-strong-coupling Regime, Phys. Rev. Lett. **120**, 183601 (2018).

[51] J. P. Martinez, S. Leger, N. Gheereart, R. Dassonneville, L. Planat, F. Foroughi, Y. Krupko, O. Buisson, C. Naud, W. Guichard, S. Florens, I. Snyman, and N. Roch, Probing a transmon qubit via the ultra-strong coupling to a Josephson waveguide, arXiv:1802.00633.

[52] P. Forn-Díaz, J. J. García-Ripoll, B. Peropadre, J.-L. Orgiazzi, M. A. Yurtalan, R. Belyansky, C. M. Wilson, and A. Lupascu, Ultrastrong coupling of a single artificial atom to an electromagnetic continuum in the nonperturbative regime, Nat. Phys. **13**, 39 (2017).

[53] Z. Chen, Y. Wang, T. Li, L. Tian, Y. Qiu, K. Inomata, F. Yoshihara, S. Han, F. Nori, J. S. Tsai, and J. Q. You, Single-photon-driven high-order sideband transitions in an ultrastrongly coupled circuit-quantum-electrodynamics system, Phys. Rev. A **96**, 012325 (2017).

[54] V. M. Muravev, I. V. Andreev, I. V. Kukushkin, S. Schmult, and W. Dietsche, Observation of hybrid plasmon-photon modes in microwave transmission of coplanar microresonators, Phys. Rev. B **83**, 075309 (2011).

[55] G. Scalari, C. Maissen, D. Turcinkova, D. Hagenmuller, S. De Liberato, C. Ciuti, C. Reichl, D. Schuh, W. Wegscheider, M. Beck, and J. Faist, Ultrastrong coupling of the cyclotron transition of a 2D electron gas to a THz metamaterial, Science **335**, 1323 (2012).

[56] C. Maissen, G. Scalari, F. Valmorra, M. Beck, J. Faist, S. Cibella, R. Leoni, C. Reichl, C. Charpentier, and W. Wegscheider, Ultrastrong coupling in the near field of complementary split-ring resonators, Phys. Rev. B **90**, 205309 (2014).

[57] Q. Zhang, M. Lou, X. Li, J. L. Reno, W. Pan, J. D. Watson, M. J. Manfra, and J. Kono, Collective non-perturbative coupling of 2D electrons with high-quality-factor terahertz cavity photons, Nat. Phys. **12**, 1005 (2016).

[58] A. Bayer, M. Pozimski, S. Schambeck, D. Schuh, R. Huber, D. Bougeard, and C. Lange, Terahertz light-matter interaction beyond unity coupling strength, Nano Lett. **17**, 6340 (2017).

[59] T. Schwartz, J. A. Hutchison, C. Genet, and T. W. Ebbesen, Reversible Switching of Ultrastrong Light-Molecule Coupling, Phys. Rev. Lett. **106**, 196405 (2011).

[60] S. Kéna-Cohen, S. A. Maier, and D. D. C. Bradley, Ultrastrongly coupled exciton-polaritons in metal-clad organic semiconductor microcavities, Adv. Opt. Mater. **1**, 827 (2013).

[61] S. Gambino, M. Mazzeo, A. Genco, O. Di Stefano, S. Savasta, S. Patanè, D. Ballarini, F. Mangione, G. Lerario, D. Sanvitto, and G. Gigli, Exploring light-matter interaction phenomena under ultrastrong coupling regime, ACS Photon. **1**, 1042 (2014).

[62] C. R. Gubbin, S. A. Maier, and S. Kéna-Cohen, Low-voltage polariton electroluminescence from an ultrastrongly coupled organic light-emitting diode, Appl. Phys. Lett. **104**, 233302 (2014).

[63] M. Mazzeo, A. Genco, S. Gambino, D. Ballarini, F. Mangione, O. Di Stefano, S. Patanè, S. Savasta, D. Sanvitto, and G. Gigli, Ultrastrong light-matter coupling in electrically doped microcavity organic light emitting diodes, Appl. Phys. Lett. **104**, 233303 (2014).

[64] J. George, T. Chervy, A. Shalabney, E. Devaux, H. Hiura, C. Genet, and T. W. Ebbesen, Multiple Rabi Splittings under Ultrastrong Vibrational Coupling, Phys. Rev. Lett. **117**, 153601 (2016).

[65] F. Benz, M. K. Schmidt, A. Dreismann, R. Chikkaraddy, Y. Zhang, A. Demetriadou, C. Carnegie, H. Ohadi, B. de Nijs, R. Esteban, J. Aizpurua, and J. J. Baumberg, Single-molecule optomechanics in "picocavities", Science **354**, 726 (2016).

[66] M. H. Devoret, S. Girvin, and R. Schoelkopf, Circuit-QED: How strong can the coupling between a Josephson junction atom and a transmission line resonator be? Ann. Phys. (Leipzig) **16**, 767 (2007).

[67] J. Bourassa, J. M. Gambetta, A. A. Abdumalikov, O. Astafiev, Y. Nakamura, and A. Blais, Ultrastrong coupling regime of cavity QED with phase-biased flux qubits, Phys. Rev. A **80**, 032109 (2009).

[68] O. Di Stefano, R. Stassi, L. Garziano, A. F. Kockum, S. Savasta, and F. Nori, Feynman-diagrams approach to the quantum Rabi model for ultrastrong cavity QED: stimulated emission and reabsorption of virtual particles dressing a physical excitation, New J. Phys. **19**, 053010 (2017).

[69] D. Sank, Z. Chen, M. Khezri, J. Kelly, R. Barends, B. Campbell, Y. Chen, B. Chiaro, A. Dunsworth, A. Fowler, E. Jeffrey, E. Lucero, A. Megrant, J. Mutus, M. Neeley, C. Neill, P. J. J. O'Malley, C. Quintana, P. Roushan, A. Vainsencher, T. White, J. Wenner, A. N. Korotkov, and J. M. Martinis, Measurement-Induced State Transitions in a Superconducting Qubit: Beyond the Rotating Wave Approximation, Phys. Rev. Lett. **117**, 190503 (2016).

[70] C. Ciuti and I. Carusotto, Input-output theory of cavities in the ultrastrong coupling regime: The case of time-independent cavity parameters, Phys. Rev. A **74**, 033811 (2006).

[71] A. Ridolfo, S. Savasta, and M. J. Hartmann, Nonclassical Radiation from Thermal Cavities in the Ultrastrong Coupling Regime, Phys. Rev. Lett. **110**, 163601 (2013).

[72] L. Garziano, A. Ridolfo, S. De Liberato, and S. Savasta, Cavity QED in the ultrastrong coupling regime: Photon bunching from the emission of individual dressed qubits, ACS Photon. **4**, 2345 (2017).

[73] S. De Liberato, D. Gerace, I. Carusotto, and C. Ciuti, Extracavity quantum vacuum radiation from a single qubit, Phys. Rev. A **80**, 053810 (2009).

[74] M. Bamba and N. Imoto, Maxwell boundary conditions imply non-Lindblad master equation, Phys. Rev. A **94**, 033802 (2016).

[75] D. Hu, S.-Y. Huang, J.-Q. Liao, L. Tian, and H.-S. Goan, Quantum coherence in ultrastrong optomechanics, Phys. Rev. A **91**, 013812 (2015).

[76] K. K. W. Ma and C. K. Law, Three-photon resonance and adiabatic passage in the large-detuning Rabi model, Phys. Rev. A **92**, 023842 (2015).

[77] J. Iles-Smith, N. Lambert, and A. Nazir, Environmental dynamics, correlations, and the emergence of noncanonical equilibrium states in open quantum systems, Phys. Rev. A **90**, 032114 (2014).

[78] J. Iles-Smith, A. G. Dijkstra, N. Lambert, and A. Nazir, Energy transfer in structured and unstructured environments: Master equations beyond the Born-Markov approximations, J. Chem. Phys. **144**, 044110 (2016).

[79] P. Strasberg, G. Schaller, N. Lambert, and T. Brandes, Nonequilibrium thermodynamics in the strong coupling and non-Markovian regime based on a reaction coordinate mapping, New J. Phys. **18**, 073007 (2016).

[80] S. De Liberato, Virtual photons in the ground state of a dissipative system, Nat. Commun. **8**, 1465 (2017).

[81] D. Zueco and J. García-Ripoll, Ultrastrongly dissipative quantum Rabi model, arXiv:1806.01952 [Phys. Rev. A (to be published)].

[82] F. Altintas and R. Eryigit, Dissipative dynamics of quantum correlations in the strong-coupling regime, Phys. Rev. A **87**, 022124 (2013).

[83] D. Pagel, A. Alvermann, and H. Fehske, Nonclassical light from few emitters in a cavity, Phys. Rev. A **91**, 043814 (2015).

[84] A. Le Boité, M.-J. Hwang, H. Nha, and M. B. Plenio, Fate of photon blockade in the deep strong-coupling regime, Phys. Rev. A **94**, 033827 (2016).

[85] R. Stassi and F. Nori, Long-lasting quantum memories: Extending the coherence time of superconducting artificial atoms in the ultrastrong-coupling regime, Phys. Rev. A **97**, 033823 (2018).

[86] B. Kraus, H. P. Büchler, S. Diehl, A. Kantian, A. Micheli, and P. Zoller, Preparation of entangled states by quantum Markov processes, Phys. Rev. A **78**, 042307 (2008).

[87] V. Macrì, A. Ridolfo, O. Di Stefano, A. F. Kockum, F. Nori, and S. Savasta, Nonperturbative Dynamical Casimir Effect in Optomechanical Systems: Vacuum Casimir-Rabi Splittings, Phys. Rev. X **8**, 011031 (2018).

[88] G. T. Moore, Quantum theory of the electromagnetic field in a variable-length one-dimensional cavity, J. Math. Phys. **11**, 2679 (1970).

[89] P. D. Nation, J. R. Johansson, M. P. Blencowe, and Franco Nori, Colloquium: Stimulating uncertainty: Amplifying the quantum vacuum with superconducting circuits, Rev. Mod. Phys. **84**, 1 (2012).

[90] E. T. Jaynes and F. W. Cummings, Comparison of quantum and semiclassical radiation theories with application to the beam maser, Proc. IEEE **51**, 89 (1963).

[91] B. W. Shore and P. L. Knight, The Jaynes-Cummings model, J. Mod. Opt. **40**, 1195 (1993).

[92] C. K. Law, Interaction between a moving mirror and radiation pressure: A Hamiltonian formulation, Phys. Rev. A **51**, 2537 (1995).

[93] J. R. Johansson, G. Johansson, C. M. Wilson, and F. Nori, Dynamical Casimir effect in superconducting microwave circuits, Phys. Rev. A **82**, 052509 (2010).

[94] C. M. Wilson, G. Johansson, A. Pourkabirian, M. Simoen, J. R. Johansson, T. Duty, F. Nori, and P. Delsing, Observation of the dynamical Casimir effect in a superconducting circuit, Nature (London) **479**, 376 (2011).

[95] A. Lambrecht, M.-T. Jaekel, and S. Reynaud, Motion Induced Radiation from a Vibrating Cavity, Phys. Rev. Lett. **77**, 615 (1996).

5.2 Conversion of mechanical noise into correlated photon pairs: Dynamical Casimir effect from an incoherent mechanical drive

Conversion of mechanical noise into correlated photon pairs: Dynamical Casimir effect from an incoherent mechanical drive

Alessio Settineri,[1,2] Vincenzo Macrì,[2] Luigi Garziano,[2] Omar Di Stefano,[2] Franco Nori,[2,3] and Salvatore Savasta[1,2]
[1]*Dipartimento di Scienze Matematiche e Informatiche, Scienze Fisiche e Scienze della Terra, Università di Messina, 98166 Messina, Italy*
[2]*Theoretical Quantum Physics Laboratory, RIKEN Cluster for Pioneering Research, Wako-shi, Saitama 351-0198, Japan*
[3]*Physics Department, University of Michigan, Ann Arbor, Michigan 48109-1040, USA*

(Received 21 March 2019; published 1 August 2019)

We show that the dynamical Casimir effect in an optomechanical system can be achieved under incoherent mechanical pumping. We adopt a fully quantum-mechanical approach for both the cavity field and the oscillating mirror. The dynamics is then evaluated using a recently developed master-equation approach in the dressed picture, including both zero- and finite-temperature photonic reservoirs. This analysis shows that the dynamical Casimir effect can be observed even when the mean value of the mechanical displacement is zero. This opens up possibilities for the experimental observation of this effect. We also calculate cavity emission spectra in both the resonant and the dispersive regimes, providing useful information on the emission process.

DOI: 10.1103/PhysRevA.100.022501

I. INTRODUCTION

One of the most surprising predictions of quantum field theory is that the vacuum of space is not empty, but it has plenty of short-lived virtual particles. Real observable particles can be produced out from the quantum vacuum providing energy to its fluctuations [1–5]. Vacuum fluctuations have measurable consequences, such as the Lamb shift of atomic spectra [6] and the modification of the electron magnetic moment [7], even when real particles are not generated. For years, scientists and researchers wondered if it was possible to achieve a direct observation of the virtual particles composing the quantum vacuum or at least if their conversion into real particles was achievable. The answer arrived when Moore [2] suggested that a variable length cavity undergoing relativistic motion would be able to convert virtual photons into real ones. This phenomenon was later called the dynamical Casimir effect (DCE). Fulling and Davies [3] demonstrated that photons can also be generated by a single mirror subjected to a nonuniform acceleration. The DCE was first studied in the context of electromagnetic resonators with oscillating walls or containing a dielectric medium with time-modulated internal properties [8–11].

This concept was later generalized for other bosonic fields, e.g., cold atoms [12], phononic excitation of ion chains [13], optomechanical systems [14], and Bose-Einstein condensates [15,16]. Moreover, it has been shown that photon pairs can be emitted from the vacuum by switching or modulating the light-matter-coupling strength in cavity QED systems [17–21]. It was shown [22] that a significant number of photons can be produced also in realistic high-Q cavities with moderate mirror speeds, taking advantage of resonance-enhancement effects. Unfortunately, the resonance conditions require the mechanical frequency ω_m to be at least twice the first cavity mode frequency ω_c, i.e., $\omega_m \simeq 2n\omega_c$, where $n \in \mathbb{N}$. This is a significant obstacle for experimental observations.

Additional theoretical studies on the DCE have been presented in, e.g., [3,23–29]. Some of these proposals suggested the use of alternative experimental setups where the boundary conditions of the electromagnetic field are modulated by an effective motion [17,30–35]. Specifically, the link between the DCE and superconducting circuits was theoretically proposed for the first time in Ref. [36] and elaborated later on in Ref. [37]. In this context, it did not take long for the experimental results to arrive. In fact, the emission of photon pairs was observed in a coplanar transmission line terminated by a superconducting quantum interference device whose inductance was modulated at high frequency [38]. The experimental realization of the DCE gives further evidence of the quantum nature of the dynamical Casimir radiation, indicating that the produced radiation can be strictly nonclassical with a measurable amount of intermode entanglement [39]. Reference [40] reviews vacuum amplification phenomena with superconducting circuits. Photon pairs were also produced by rapidly modulating the refractive index of a Josephson metamaterial embedded in a microwave cavity [41]. However, these do not demonstrate the conversion of mechanical energy into photon pairs, so these experiments can also be regarded as quantum simulator. A new type of optomechanical dynamical coupling based on the DCE has also been proposed in trapped Rydberg atoms interacting with a dynamical mirror whose refractive index can be periodically varied [42]. A significant emission of photon pairs has also been predicted in Mott insulators of coherently dressed three-level atoms by parametric amplification of the polaritonic zero-point fluctuations in the presence of a fast time modulation of the dressing amplitude [43].

Most theoretical studies on the DCE are based on a *quantum*-mechanical description of the electromagnetic field and a *classical* description of the time-dependent boundary conditions. Recently, the DCE in cavity optomechanical systems has been investigated without linearizing the dynamics *and* describing *quantum* mechanically *both* the cavity field and the vibrating mirror [44–46]. Within this full quantum description, it turns out that the resonant generation of photons

from the vacuum is determined by several ladders of mirror-field vacuum Rabi-like splittings. The resulting general resonance condition for the photon-pair production is $k\omega_m \simeq 2n\omega_c$ ($k, n \in \mathbb{N}$). This corresponds to processes where k phonons in the mechanical oscillator are converted into n cavity photon pairs. This generalized resonance condition enables a resonant production of photons out from the vacuum even for mechanical frequencies lower than the lowest cavity-mode frequency, thus removing one of the major obstacles for the experimental observation of this effect.

In addition, it has been shown that a vibrating mirror prepared in an excited state (mechanical Fock state) can spontaneously emit photons like a quantum emitter. In this case, however, a photon pair is emitted instead of a single photon.

Moreover, it has been recently demonstrated that virtual Casimir photon pairs can be used to enable a coherent motional coupling between two spatially separated movable mirrors, allowing this kind of optomechanical system to also operate as a mechanical parametric down-converter even at very weak excitations [47]. Entangled photons from the vacuum can also be generated by using microwave circuit-acoustic resonators [48].

The approach considered in Ref. [46] also extends the investigation of the DCE to the optomechanical ultrastrong-coupling regime, where the optomechanical coupling rate is comparable to the mechanical frequency [49–55]. This regime, which attracted great interest also in cavity QED giving rise to a great variety of novel quantum effects [20,56–58], turned out to be an essential feature for the realization of new interesting proposals in quantum optomechanics [59–61].

Temperature effects also play an important role in the generation of photons in a resonantly vibrating cavity [62–65]. Specifically, it turns out that the thermal contributions in these systems under the influence of time-dependent boundary conditions lead to a strong enhancement of photon-pair production at finite temperatures.

Encouraged by the results obtained in Ref. [46], here we investigate the dynamics of an optomechanical system in a fully quantum-mechanical framework, under incoherent mechanical excitation, using a master-equation approach. This allows us to demonstrate that a remarkable Casimir photon-pair flux is produced even considering a thermal-like noise source coupled only to the mechanical degree of freedom. For ultrastrongly coupled hybrid quantum systems [66–70], the standard quantum-optical master equation breaks down and a dressed master-equation approach is needed [56,71,72]. Furthermore, if the energy-level spectrum displays a quasiharmonic behavior [51], like in optomechanical systems, a new dressed master equation [73,74] not involving the usual secular approximation is required.

The outline of this article is as follows. In Sec. II we briefly introduce the theoretical model and the dressed master-equation approach for quasiharmonic hybrid systems. Section III is devoted to the presentation of the energy-level structure, focusing the attention on the avoided level crossings giving rise to the DCE. In Sec. IV we apply the generalized master equation [74] to calculate the dynamics of the system at finite temperatures and, using the quantum regression theorem, we present the power spectra in the weak- and strong-light-matter-coupling regimes. We summarize in Sec. V.

FIG. 1. Schematic of a generic optomechanical system. One of the mirrors of the optical cavity is coupled to a noise source with effective temperature T_γ and can vibrate at frequency ω_m. This system can generate Casimir photon pairs.

II. MODEL

We study a standard optomechanical system composed of an optical cavity with a movable end mirror (see Fig. 1). Moreover, we consider a radiation pressure coupling between the first cavity mode and a single mechanical mode.

The system Hamiltonian can be written as

$$\hat{H}_S = \hat{H}_0 + \hat{V}_{\rm om} + \hat{V}_{\rm DCE}, \tag{1}$$

where ($\hbar = 1$ throughout the paper)

$$\hat{H}_0 = \omega_c \hat{a}^\dagger \hat{a} + \omega_m \hat{b}^\dagger \hat{b} \tag{2}$$

is the uncoupled Hamiltonian and

$$\hat{V}_{\rm om} = g\hat{a}^\dagger \hat{a}(\hat{b} + \hat{b}^\dagger) \tag{3}$$

is the standard optomechanical interaction Hamiltonian. Here ω_c is the resonator frequency, ω_m is the mechanical frequency, g is the optomechanical coupling strength, and $\hat{a}$ ($\hat{b}$) and $\hat{a}^\dagger$ ($\hat{b}^\dagger$) are, respectively, the bosonic creation (annihilation) operators for the cavity and mechanical modes. Finally, the perturbation term determining the DCE is

$$\hat{V}_{\rm DCE} = \frac{g}{2}(\hat{a}^2 + \hat{a}^{\dagger 2})(\hat{b} + \hat{b}^\dagger). \tag{4}$$

Since in this case the $\hat{V}_{\rm DCE}$ term only couples bare states having energy differences $2\omega_c \pm \omega_m$ much larger than the coupling strength g, it can be neglected. Also, this interaction term is often neglected when describing most of the experimental optomechanical systems, where the mechanical frequency is much smaller than the cavity frequency.

The resulting total Hamiltonian conserves the photon number and can be diagonalized separately in each n-photon subspace. The general quantum state of such a system is

$$|n, k_n\rangle = |n\rangle \otimes \hat{D}(n\eta)|k\rangle, \tag{5}$$

where the integer k_n represents the vibrational excitations of the mechanical resonator in the corresponding n-photon subspace and

$$|k_n\rangle = \hat{D}(n\eta)|k\rangle \tag{6}$$

represents the displaced mechanical Fock state determined by the displacement operator $\hat{D}(n\eta)$, where

$$\eta \equiv g/\omega_m \tag{7}$$

is the normalized coupling strength. In the manifold with $n = 0$, the states $|0, k_0\rangle$, simply labeled $|0, k\rangle$, are the eigenstates of the harmonic oscillator decoupled from the cavity. When considering ultrahigh-frequency mechanical oscillators with resonance frequencies

$$\omega_m \simeq \omega_c, \tag{8}$$

the $\hat{V}_{\rm DCE}$ term cannot be neglected. In this case, the photon number is no longer conserved and there is no analytical solution for the system eigenstates. Moreover, it turns out that the introduction of the $\hat{V}_{\rm DCE}$ term increases the degree of anharmonicity, slightly modifying the levels structure but still preserving the quasiharmonic behavior. Consequently, the system dynamics has to be described using a generalized master equation developed without performing the usual secular approximation. A suitable approach, able to describe the time evolution of the density matrix operator $\hat{\rho}$ for any hybrid quantum system in the presence of dissipations and thermal-like noise, has been presented in Ref. [74].

In the interaction picture, this master equation can be written as

$$\dot{\hat{\rho}} = \kappa \mathcal{L}[\hat{A}]\hat{\rho} + \gamma \mathcal{L}[\hat{B}]\hat{\rho}, \tag{9}$$

with κ and γ the cavity and mirror damping rates, respectively. The dressed photon and phonon lowering operators $\hat{O} = \hat{A}, \hat{B}$ are defined in terms of their corresponding bare operators $\hat{o} = \hat{a}, \hat{b}$ by the relation [20,56]

$$\hat{O}(\omega) = \sum_{\epsilon - \epsilon' = \omega} \hat{\Pi}(\epsilon)(\hat{o} + \hat{o}^\dagger)\hat{\Pi}(\epsilon')e^{-i\omega t}, \tag{10}$$

where ϵ are the eigenvalues of $\hat{H}_S$ and $\hat{\Pi}(\epsilon) \equiv |\epsilon\rangle\langle\epsilon|$ indicate the projectors onto the respective eigenspaces. Furthermore, the Liouvillian superoperator $\mathcal{L}[\hat{O}]\hat{\rho}$ can be expressed in the general form

$$\begin{aligned}\mathcal{L}[\hat{O}]\hat{\rho} = \sum_{(\omega,\omega')>0} \frac{1}{2}\{&n(\omega', T)[\hat{O}^\dagger(\omega')\hat{\rho}\hat{O}(\omega) - \hat{O}(\omega)\hat{O}^\dagger(\omega')\hat{\rho}] \\ &+ [n(\omega, T) + 1][\hat{O}(\omega)\hat{\rho}\hat{O}^\dagger(\omega') - \hat{O}^\dagger(\omega')\hat{O}(\omega)\hat{\rho}] \\ &+ n(\omega, T)[\hat{O}^\dagger(\omega')\hat{\rho}\hat{O}(\omega) - \hat{\rho}\hat{O}(\omega)\hat{O}^\dagger(\omega')] \\ &+ [n(\omega', T) + 1][\hat{O}(\omega)\hat{\rho}\hat{O}^\dagger(\omega') - \hat{\rho}\hat{O}^\dagger(\omega')\hat{O}(\omega)]\},\end{aligned} \tag{11}$$

where ($k_B = 1$)

$$n(\omega, T) = [\exp(\omega/T) - 1]^{-1} \tag{12}$$

is the thermal noise occupation number of the system reservoir, at real or effective temperature T.

When counterrotating terms are taken into account in the interaction Hamiltonian, the introduction of master equations in the dressed basis is not sufficient. Indeed, a modification of input-output relationships, relating the intracavity field with the external fields [46,56,74–76], is also required. According to these modified relationships, the output fields are no longer determined by expectation values of the bare photon operators (see, e.g., [77–79]), but by the expectation values of the dressed operators in Eq. (10).

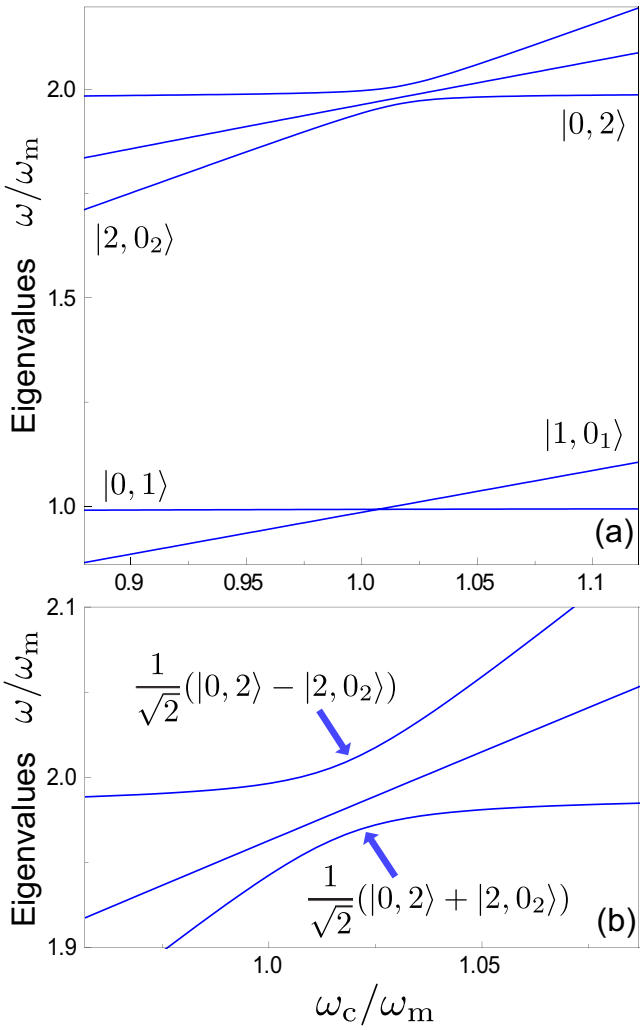

FIG. 2. (a) Lowest energy eigenvalues of the system as a function of ω_c/ω_m for a normalized optomechanical coupling strength $\eta = g/\omega_m = 0.1$. The ground state is not displayed. (b) Enlarged view of the avoided level crossing arising from the coherent coupling between the states $|0, 2\rangle$ and $|2, 0_2\rangle$. The energy splitting reaches its minimum at the resonant frequency $\omega_c \simeq \omega_m$.

III. VACUUM CASIMIR-RABI SPLITTINGS

In order to fully characterize our system, we numerically diagonalize the Hamiltonian $\hat{H}_S$ in Eq. (1). Figure 2(a) shows the lowest energy levels as a function of the cavity frequency ω_c/ω_m considering a normalized optomechanical coupling strength $\eta = 0.1$.

As reported in Ref. [46], when the resonant conditions

$$q\omega_m = 2\omega_c \tag{13}$$

are satisfied, the $\hat{V}_{\rm DCE}$ term induces a coherent resonant coupling between the bare states $|0, k\rangle$ (i.e., zero photons and k phonons) and $|2, (k - q)_2\rangle$ (i.e., two photons and $k - 1$ phonons), with $q \in \mathbb{N}^*$, having a different number of excitations. Figure 2(b) shows an enlarged view of the avoided level crossing arising for $\omega_m \simeq \omega_c$, involving the states $|0, 2\rangle$ and $|2, 0_2\rangle$. When the splitting is at its minimum, the two system eigenstates are essentially a symmetric and an antisymmetric

linear superposition of these bare states $|\psi_\pm\rangle \simeq \frac{1}{\sqrt{2}}(|0,2\rangle \pm |2,0_2\rangle)$. The size of this avoided level crossing (Casimir-Rabi splitting), analytically calculated using first-order perturbation theory, is given by

$$2\Omega_{0,2}^{2,0} = 2\langle 0,2|\hat{V}_{\rm DCE}|2,0_2\rangle = \sqrt{2}g[\sqrt{3}D_{3,0}(2\eta) + \sqrt{2}D_{1,0}(2\eta)], \quad (14)$$

where

$$D_{k',k}(2\eta) = \sqrt{k!/k'!}(2\eta)^{k'-k}e^{-|2\eta|^2/2}L_k^{k'-k}(|2\eta|^2) \quad (15)$$

represents the overlap between different displaced mechanical Fock states and $L_k^{k'-k}$ is an associated Laguerre polynomial. It is important to note that the quantity $2\Omega_{0,2}^{2,0}$ plays a fundamental role in the DCE, since it determines the rate at which a mechanical two-phonon state is able to generate photon pairs. Specifically, for a normalized optomechanical coupling $\eta = 0.1$ we obtain a matrix element $2\Omega_{0,2}^{2,0} \simeq 0.05$ that ensures that this avoided level crossing is able to produce a detectable rate of Casimir photon pairs.

IV. RESULTS

Here we present the system dynamics numerically evaluated taking into account a thermal-like pumping of the mechanical components and considering the photonic reservoir both at $T_\kappa = 0$ and at finite temperature. Specifically, we study the time evolution of the mean phonon (photon) number $\langle\hat{B}^\dagger\hat{B}\rangle$ ($\langle\hat{A}^\dagger\hat{A}\rangle$) and the zero-delay phononic (photonic) normalized second-order correlation function, defined as

$$g_{\rm O}^{(2)}(t,t) = \frac{\langle\hat{O}^\dagger(t)\hat{O}^\dagger(t)\hat{O}(t)\hat{O}(t)\rangle}{\langle\hat{O}^\dagger(t)\hat{O}(t)\rangle^2}, \quad (16)$$

with $\hat{O} \in [\hat{A}, \hat{B}]$.

A. System dynamics in the weak-coupling regime

We start by considering the system initially prepared in its ground state and in the weak-coupling regime, which corresponds to the case where the Casimir-Rabi splitting $2\Omega_{0,k}^{2,k-q}$ is smaller than the total decoherence rate of the system $\Gamma_{\rm tot} = \gamma + \kappa$. Specifically, we assume $\gamma/\omega_m = 0.05$ and $\kappa = \gamma/2$ with an optomechanical coupling $\eta = 0.1$, considering the resonant case $\omega_m \simeq \omega_c$ corresponding to the minimum splitting of the avoided level crossing arising between the states $|0,2\rangle$ and $|2,0_2\rangle$ [see Fig. 2(b)]. Figures 3(a) and 3(b) display the time evolution of the photonic $\langle\hat{A}^\dagger\hat{A}\rangle$ (red solid curve) and phononic $\langle\hat{B}^\dagger\hat{B}\rangle$ (blue dashed curve) populations, together with the time evolution of the respective two-photon and two-phonon correlation functions $g_{B(A)}^{(2)}(t,t)$. All these quantities have been evaluated taking into account the interaction with a zero-temperature ($T_\kappa = 0$) photonic reservoir and providing an incoherent thermal-like pumping of the mechanical component by means of a phononic reservoir with an effective temperature $T_\gamma/\omega_m = 0.9$. As shown in Fig. 3(a), the photonic and phononic populations start from zero and, due to the incoherent thermal-like pumping of the mechanical modes, reach a considerable stationary value. In particular, a steady-state intracavity mean photon number $\langle\hat{A}^\dagger\hat{A}\rangle_{\rm ss} \simeq 0.15$

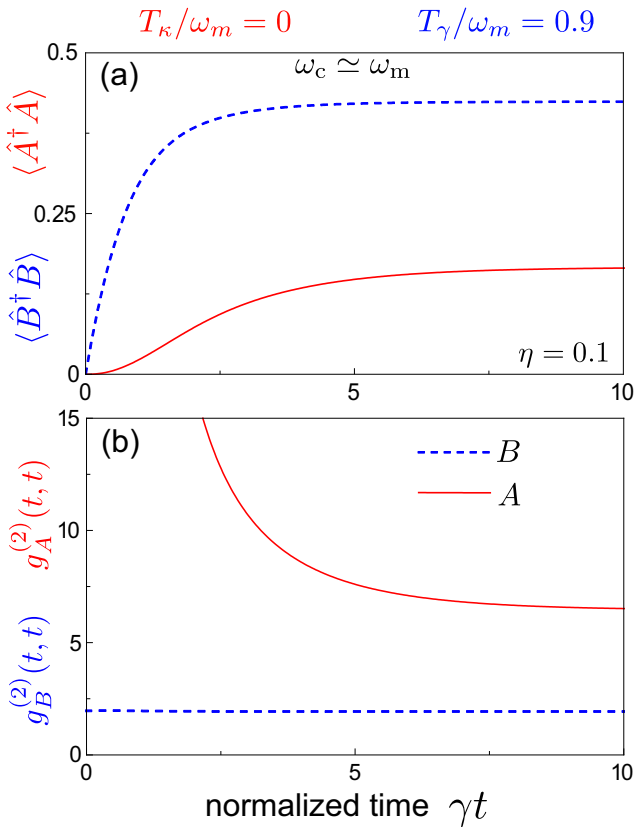

FIG. 3. System dynamics for the resonant case $\omega_c \simeq \omega_m$ considering a $T_\kappa = 0$ cavity reservoir and the mechanical oscillator coupled to a thermal-like noise source with an effective temperature $T_\gamma/\omega_m = 0.9$. (a) Time evolution of the mean phonon number $\langle\hat{B}^\dagger\hat{B}\rangle$ (blue dashed curve) and of the mean intracavity photon number $\langle\hat{A}^\dagger\hat{A}\rangle$ (red solid curve). Due to the thermal-like pumping, the populations reach stationary values. (b) Time evolution of the zero-delay normalized photon-photon $g_A^{(2)}(t,t)$ and phonon-phonon $g_B^{(2)}(t,t)$ correlation functions. At $t = 0$, the two-photon correlation function $g_A^{(2)}(t,t)$ displays values much higher than 2, showing that a considerable number of photon pairs are emitted. As the time goes on, this value decreases significantly due to the cavity losses and the corresponding increase of the mean photon number. In contrast, the mechanical correlation function sets on a constant value $g_B^{(2)}(t,t) \approx 2$, showing that the mechanical system is in an incoherent state produced by the thermal-like noise.

is obtained. For a cavity mode of frequency $\omega_c/2\pi \simeq 6$ GHz, this value corresponds to a steady-state output photon flux $\Phi = \kappa\langle\hat{A}^\dagger\hat{A}\rangle_{\rm ss} \sim 1.4 \times 10^8$ photons per second. This output photon flux is remarkable since it is much higher than the detection threshold of the state-of-the-art detectors, despite the quite-low-quality factor $Q_c = \omega_c/\kappa = 40$ of the cavity considered in the numerical calculations. Furthermore, also the mechanical loss rate γ corresponds to a quality factor Q_m one order of magnitude lower than the values which are experimentally measured in ultrahigh-frequency mechanical resonators [80,81]. Moreover, in Fig. 3(b) we observe that the photonic correlation function starts from a value much higher than 2, suggesting that a high number of photon pairs is produced. As time goes on, this value decreases significantly

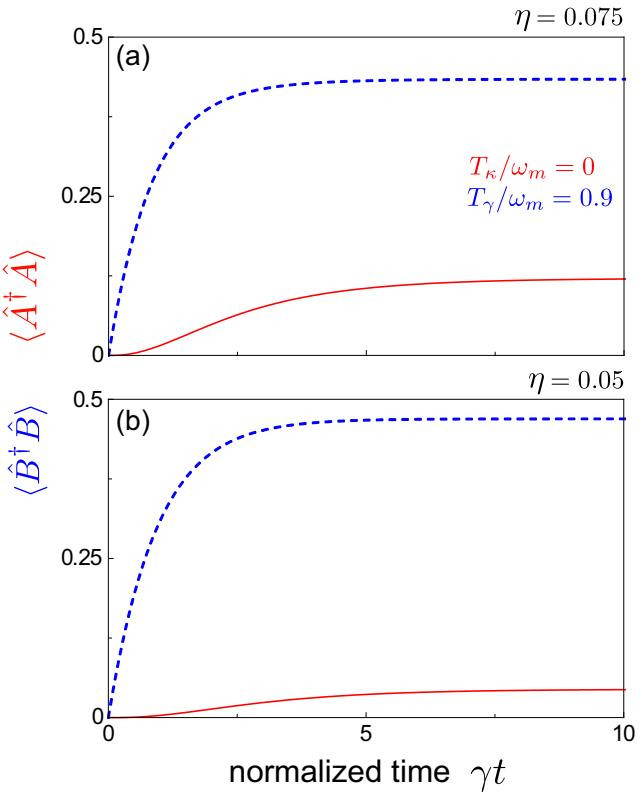

FIG. 4. Time evolution of the mean phonon number $\langle \hat{B}^\dagger \hat{B} \rangle$ (blue dashed curve) and of the mean intracavity photon number $\langle \hat{A}^\dagger \hat{A} \rangle$ (red solid curve) for (a) $\eta = 0.075$ and (b) $\eta = 0.05$, in the resonant case $\omega_c \simeq \omega_m$. We consider a $T_\kappa = 0$ cavity reservoir, while the mechanical oscillator is coupled to a thermal-like noise source with an effective temperature $T_\gamma/\omega_m = 0.9$. Since the coupling rate $\Omega_{0,2}^{2,0}$ between the states $|0, 2\rangle$ and $|2, 0_2\rangle$ becomes less effective for decreasing values of η, in both cases we observe a smaller production of Casimir photon pairs with respect to the case $\eta = 0.1$ displayed in Fig. 3.

due to the system losses and the corresponding increase of the mean photon number [note that $g_A^{(2)}(t, t)$ is inversely proportional to the square of the mean photon number]. In contrast, the mechanical correlation function is set to a constant value $g_B^{(2)}(t, t) \approx 2$, showing that the mechanical component is in an incoherent state produced by the thermal-like pumping. Note that the production of Casimir photon pairs is sensitive to the optomechanical coupling strength. Figure 4 displays the temporal evolution of the photonic $\langle \hat{A}^\dagger \hat{A} \rangle$ (red solid curve) and phononic $\langle \hat{B}^\dagger \hat{B} \rangle$ (blue dashed curve) populations for $\eta = 0.075$ [Fig. 4(a)] and $\eta = 0.05$ [Fig. 4(b)] using the same values for the reservoir temperatures $T_{\kappa(\gamma)}/\omega_m$ as in Fig. 3. We observe that the intracavity mean photon number $\langle \hat{A}^\dagger \hat{A} \rangle$ decreases for decreasing values of η, suggesting that a sufficiently high optomechanical coupling strength is required in order to obtain a detectable output flux of Casimir photon pairs. This effect can be explained by considering that lower values of η lead to smaller values of the two-phonon–two-photon effective coupling rate $\Omega_{0,2}^{2,0}$ and consequently to a lower conversion rate of phonons into Casimir photon pairs. These results are particularly interesting since they demonstrate that the DCE can also be experimentally observed exciting a movable mirror with an *incoherent thermal-like pump* such as, a white-noise generator (made by an ultrahigh-frequency resonator interacting with a microwave cavity). In real optomechanical systems ground-state cooling is never complete and the interaction with a finite-temperature reservoir has to be taken into account. The time evolution of the photonic and phononic populations together with the respective two-photon and two-phonon zero-delay correlation functions are displayed in Fig. 5. These functions are evaluated in more realistic conditions, taking into account a nonzero-temperature reservoir for both subsystems. In these conditions, both populations start from a nonzero value corresponding to the initial thermal equilibrium density matrix. As expected, a fraction of the observed photons are thermal and do not originate from the mechanical-to-optical energy conversion mechanism. This picture is confirmed by comparing the dynamics of the two correlation functions shown in Figs. 5(b) and 5(d). Specifically, when the cavity temperature increases, we observe a strong decrease of the $g_A^{(2)}(t, t)$ peak value, indicating that fewer photons are emitted in pairs. However, as expected, the phonon-phonon correlation functions remain constant at the thermal value $g_B^{(2)}(t, t) \simeq 2$. These results demonstrate that when the presence of a cavity thermal noise is taken into account, the number of Casimir photon pairs produced decreases. However, the output photon flux is still above the detection threshold of the photodetector and the peak value of the $g_A^{(2)}(t, t)$ indicates that photon pairs are produced.

B. Emission spectra in the weak- and strong-coupling regimes

In order to obtain more information on the ongoing physics, here we present the cavity emission spectra derived via a quantum regression approach. Considering a normalized optomechanical coupling $\eta = 0.1$, we present results for the system both in the weak- and in the strong-light-matter-coupling regimes for different values of ω_c/ω_m. We consider the cavity at $T_\kappa = 0$, while the mechanical oscillator is coupled to a reservoir with effective temperature $T_\gamma/\omega_m = 0.9$. For the sake of simplicity, we indicate the energy eigenvalues and eigenstates as ω_l and $|l\rangle$ ($l = 0, 1, \ldots$) and the transition frequencies as $\omega_{jk} \equiv \omega_j - \omega_k$, choosing the labeling of the states such that $\omega_j > \omega_k$ for $j > k$ [see Fig. 6(a)]. If the effective temperature of the mechanical reservoir is high enough to populate the state $|5\rangle$, the system decays toward the ground state via two different one-photon decay channels: $|5\rangle \to |2\rangle \to |0\rangle$ and $|3\rangle \to |2\rangle \to |0\rangle$. Since the states $|5\rangle$ and $|3\rangle$ do not couple with the state $|4\rangle$, the other possible one-photon transition $|4\rangle \to |0\rangle$ can occur only by decays from higher energy levels.

We start by considering the zero-detuning case $\Delta \equiv (\omega_c - \omega_r)/\omega_m = 0$, where $\omega_r \simeq 1.017\omega_m$ is the frequency corresponding to the minimum value of the splitting in Fig. 2(b). In this case the states $|3\rangle$ and $|5\rangle$ are well approximated, respectively, by the superpositions $|\psi_\pm\rangle = (|0, 2\rangle \pm |2, 0_2\rangle)/\sqrt{2}$.

Figure 6(b) displays the emission spectra for the system in the weak-coupling regime, e.g., $2\Omega_{0,2}^{2,0} < \Gamma_{\rm tot}$. Due to the high value of $\Gamma_{\rm tot}$, we observe a low-resolution emission spectrum that displays only a wide band composed of a single peak at

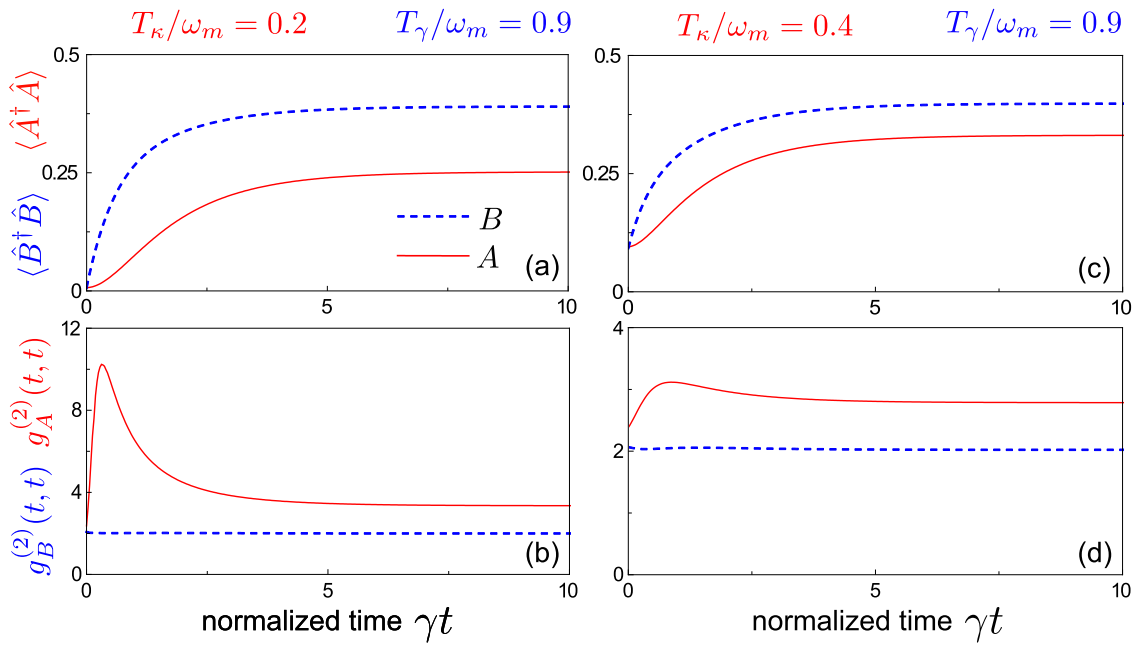

FIG. 5. System dynamics evaluated considering finite-temperature reservoirs and the system initially prepared in a thermal state at the same temperature T_κ of the photonic reservoir. Time evolutions of the cavity mean photon number $\langle \hat{A}^\dagger \hat{A} \rangle$ (red solid curves) and the mean phonon number $\langle \hat{B}^\dagger \hat{B} \rangle$ (blue dashed curves) are shown for $T_\gamma/\omega_m = 0.9$ and (a) $T_\kappa/\omega_m = 0.2$ and (c) $T_\kappa/\omega_m = 0.4$. Also shown are the time evolutions of the zero-delay two-photon (red solid curves) and two-phonon (blue dashed curves) correlation functions $g_A^{(2)}(t,t)$ and $g_B^{(2)}(t,t)$, respectively, for $T_\gamma/\omega_m = 0.9$ and (b) $T_\kappa/\omega_m = 0.2$ and (d) $T_\kappa/\omega_m = 0.4$.

frequency $\omega/\omega_m \simeq 0.98$. In contrast, when the system is in the strong-coupling regime ($2\Omega_{0,2}^{2,0} > \Gamma_{\rm tot}$), the spectrum becomes well resolved. As shown in Fig. 6(b), for $2\Omega_{0,2}^{2,0}/\Gamma_{\rm tot} \simeq 6.7$ the cavity emission spectrum displays two main peaks. Indeed, in the resonant case the accidentally quasidegenerate transitions $|5\rangle \to |2\rangle$ and $|2\rangle \to |0\rangle$ give rise to a single high-frequency peak at $\omega \simeq \omega_m$, whereas the lower-frequency peak at $\omega/\omega_m \simeq 0.98$ corresponds to the transition $|3\rangle \to |2\rangle$. It is important to note that, in the presence of a $T_\kappa = 0$ cavity reservoir, these peaks are observable only if the $V_{\rm DCE}$ term is included in the Hamiltonian. Indeed, without this term the states $|2, 0_2\rangle$ and $|0, 2\rangle$ are not coupled anymore and since the mechanical incoherent pumping only populates phononic states, the one-phonon decay peaks cannot be observed in the cavity emission spectra. We now turn to the numerical analysis of the detuning effects on the cavity emission spectra. Figure 7(a) displays the emission spectrum calculated for $\Delta = 0.028$. As the transitions $|5\rangle \to |2\rangle$ and $|2\rangle \to |0\rangle$ are no longer quasidegenerate, the peaks at frequencies ω_{52} and ω_{20} become well resolved, while the peak corresponding to $|3\rangle \to |2\rangle$ shifts towards a slightly lower frequency. As expected, if we reduce the detuning and approach the resonance point $\Delta = 0$, the spectrum essentially presents the same main features of Fig. 6(c). Specifically, Fig. 7(b) shows that for $\Delta = 0.014$ the two peaks at ω_{52} and ω_{20} merge and the emission spectrum presents only a main contribution at $\omega/\omega_m \simeq 1.015$, while the transition frequency ω_{32} does not change significantly. Finally, in Fig. 7(c) we study the emission spectrum in the presence of a negative detuning $\Delta = -0.028$. Also in this case, the spectrum displays three distinct peaks placed at lower frequencies with respect to Fig. 7(a). This shift arises from the energy-level crossing between the states $|1\rangle$ and $|2\rangle$ shown in Fig. 2(a). Although the highest peak still corresponds to the one-photon decay toward the ground state, the emission spectrum is not symmetric with respect to the one in Fig. 7(a). In particular, we observe that the intensity of the peak associated with the transition $|3\rangle \to |1\rangle$ increases, whereas the $|5\rangle \to |1\rangle$ transition peak displays a much lower intensity. This effect can be explained by considering that, differently from the positive-detuning cases studied above, for $\Delta < 0$ the state $|3\rangle \simeq |2, 0_2\rangle$ has more photonic character than $|5\rangle \simeq |0, 2\rangle$, which has more phononic character. Thus, while the photonic character of the polaron state $|3\rangle$ leads to an enhancement of the peak intensity at ω_{31} in the cavity emission spectrum, on the other hand, the phononic character of the state $|5\rangle$ is responsible for the intensity decrease of the peak at ω_{51}. This study provides useful information on the emission process. Moreover, the presence of these features in the experimental spectra would represent a signature of the production of DCE photons. A very promising experimental platform for the observation of the proposed effect is provided by circuit-optomechanical systems utilizing ultrahigh-frequency (∼4–6 GHz) dilatational resonators [80]. In these systems, it should be possible to easily achieve an optomechanical coupling strength $\eta = 0.02$, which is rather close to the lower value considered here [see Fig. 4(b)]. Finally, we notice that a higher-excitation noise would allow the observation of the DCE induced by an incoherent mechanical pumping, even for lower values of the optomechanical coupling strength.

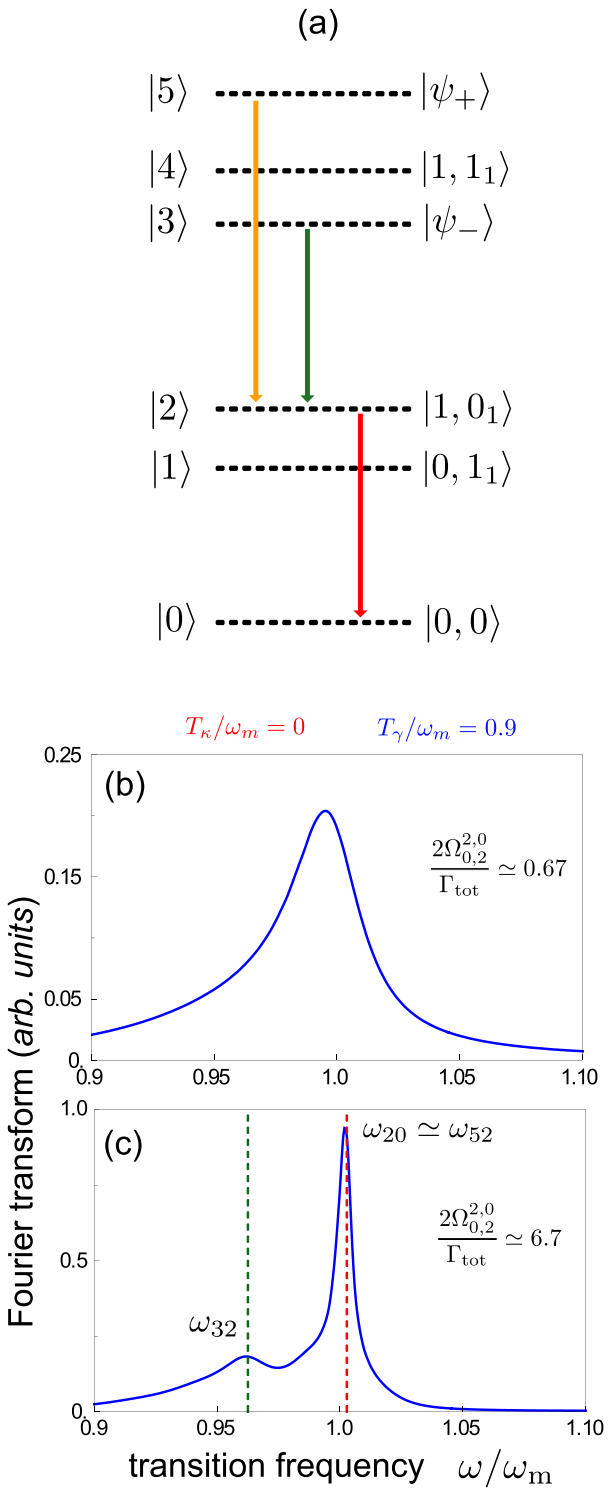

FIG. 6. (a) Schematics of the first energy levels of the optomechanical system. Solid arrows represent the possible one-photon decay channels when the effective temperature of the mechanical reservoir is high enough to populate the state $|5\rangle$. Also shown are the cavity emission spectra for the system in the (b) weak- and (c) strong-light-matter-coupling regime and at zero detuning. In both cases, the cavity reservoir is at $T_\kappa = 0$, while the mechanical oscillator is coupled to a reservoir with effective temperature $T_\gamma/\omega_m = 0.9$. The parameters are $\omega_m = 1$ and $\eta = 0.1$. The total loss rate $\Gamma_{\rm tot} = \kappa + \gamma$ of the system is (b) $7.5 \times 10^{-2}\omega_m$ and (c) $7.5 \times 10^{-3}\omega_m$.

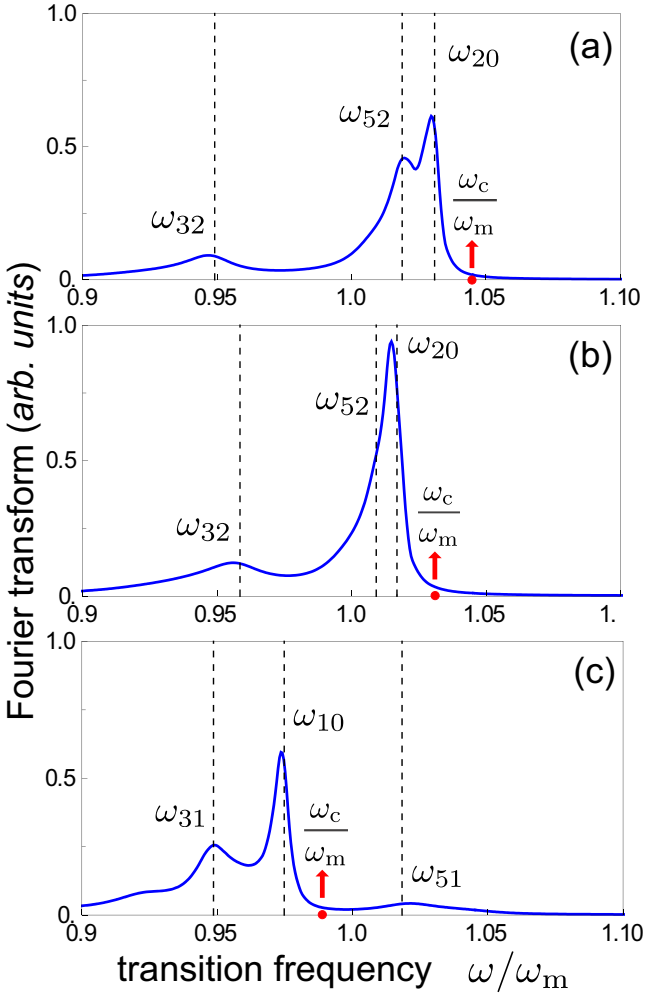

FIG. 7. Cavity emission spectra for the system in the strong-coupling regime for different values of the detuning $\Delta \equiv (\omega_c - \omega_r)/\omega_m$, where $\omega_r \simeq 1.017\,\omega_m$ is the frequency corresponding to the minimum value of the splitting in Fig. 2(b). Specifically, we considered the cases (a) $\Delta = 0.028$, (b) $\Delta = 0.01$, and (c) $\Delta = -0.028$. The main contributions are indicated by dashed lines. The parameters are the same as in Fig. 6(c).

V. CONCLUSION

We have studied the dynamical Casimir effect in cavity optomechanics achieved only under incoherent mechanical excitation. We employed a fully quantum-mechanical description of both the cavity field and the oscillating mirror. The system dynamics was evaluated under incoherent pumping of the mechanical component, provided by a thermal-like excitation. Using a master-equation approach [74] in order to take into account losses, thermal effects, and decoherence in the presence of a quasiharmonic spectrum, we showed that a measurable flux of Casimir photons can be obtained also without a coherent pumping, suggesting another way for experimental observation of the DCE. This master-equation approach could also be used to describe this effect in the presence of arbitrary colored-noise sources. The incoherent mechanical excitation mechanism described here is also expected to work in parametrically amplified optomechanical systems

in order to induce two-photon hyper-Raman scattering processes, where squeezed photons already present in an optical resonator are scattered into resonant cavity-photon pairs [82]. This method would allow the parametric conversion of mechanical energy into electromagnetic energy in optomechanical systems where the mechanical frequency is usually much lower than the cavity frequency, thus eliminating the need for extremely high mechanical oscillation frequencies and ultrastrong single-photon optomechanical coupling. In Ref. [46] it has been shown that a vibrating mirror is affected by spontaneous emission, in analogy with ordinary atoms. However, it decays emitting photon pairs. Here we showed that an incoherently excited vibrating mirror can emit light, in analogy to atomic fluorescence or electroluminescence in semiconductor devices.

By applying the quantum regression theorem, we have calculated numerically the steady-state cavity emission spectra under incoherent mechanical excitation, for different detunings and loss rates. When the loss rates were lower than the effective coupling rate, the emission spectra allowed us to identify the different emission channels.

ACKNOWLEDGMENTS

F.N. was supported in part by the: MURI Center for Dynamic Magneto-Optics via the Air Force Office of Scientific Research (AFOSR) (Grant No. FA9550-14-1-0040), Army Research Office (ARO) (Grant No. W911NF-18-1-0358), Asian Office of Aerospace Research and Development (AOARD) (Grant No. FA2386-18-1-4045), Japan Science and Technology Agency (JST) (via the Q-LEAP program, the ImPACT program, and CREST Grant No. JPMJCR1676), Japan Society for the Promotion of Science (JSPS) (JSPS-RFBR Grant No. 17-52-50023 and JSPS-FWO Grant No. VS.059.18N), RIKEN-AIST Challenge Research Fund, and the John Templeton Foundation. S.S. acknowledges the Army Research Office (Grant No. W911NF1910065).

[1] J. Schwinger, On gauge invariance and vacuum polarization, Phys. Rev. **82**, 664 (1951).
[2] G. T. Moore, Quantum theory of the electromagnetic field in a variable-length one-dimensional cavity, J. Math. Phys. **11**, 2679 (1970).
[3] S. A. Fulling and P. C. W. Davies, Radiation from a moving mirror in two dimensional space-time: Conformal anomaly, Proc. R. Soc. London Ser. A **348**, 393 (1976).
[4] E. Yablonovitch, Accelerating Reference Frame for Electromagnetic Waves in a Rapidly Growing Plasma: Unruh-Davies-Fulling-DeWitt Radiation and the Nonadiabatic Casimir Effect, Phys. Rev. Lett. **62**, 1742 (1989).
[5] J. Schwinger, Casimir light: The source, Proc. Natl. Acad. Sci. USA **90**, 2105 (1993).
[6] M. O. Scully and M. S. Zubairy, *Quantum Optics* (Cambridge University Press, Cambridge, 1997).
[7] W. Greiner and S. Schramm, Resource letter QEDV-1: The QED vacuum, Am. J. Phys. **76**, 509 (2008).
[8] V. V. Dodonov and A. B. Klimov, Long-time asymptotics of a quantized electromagnetic field in a resonator with oscillating boundary, Phys. Lett. A **167**, 309 (1992).
[9] V. V. Dodonov, A. B. Klimov, and D. E. Nikonov, Quantum phenomena in nonstationary media, Phys. Rev. A **47**, 4422 (1993).
[10] J.-Y. Ji, H.-H. Jung, J.-W. Park, and K.-S. Soh, Production of photons by the parametric resonance in the dynamical Casimir effect, Phys. Rev. A **56**, 4440 (1997).
[11] D. F. Mundarain and P. A. Maia Neto, Quantum radiation in a plane cavity with moving mirrors, Phys. Rev. A **57**, 1379 (1998).
[12] V. V. Dodonov and J. T. Mendonça, Dynamical Casimir effect in ultra-cold matter with a time-dependent effective charge, Phys. Scr. **2014**, 014008 (2014).
[13] N. Trautmann and P. Hauke, Quantum simulation of the dynamical Casimir effect with trapped ions, New J. Phys. **18**, 043029 (2016).
[14] A. Motazedifard, M. H. Naderi, and R. Roknizadeh, Dynamical Casimir effect of phonon excitation in the dispersive regime of cavity optomechanics, J. Opt. Soc. Am. B **34**, 642 (2017).
[15] I. Carusotto, R. Balbinot, A. Fabbri, and A. Recati, Density correlations and analog dynamical Casimir emission of Bogoliubov phonons in modulated atomic Bose-Einstein condensates, Eur. Phys. J. D **56**, 391 (2010).
[16] J.-C. Jaskula, G. B. Partridge, M. Bonneau, R. Lopes, J. Ruaudel, D. Boiron, and C. I. Westbrook, Acoustic Analog to the Dynamical Casimir Effect in a Bose-Einstein Condensate, Phys. Rev. Lett. **109**, 220401 (2012).
[17] S. De Liberato, C. Ciuti, and I. Carusotto, Quantum Vacuum Radiation Spectra from a Semiconductor Microcavity with a Time-Modulated Vacuum Rabi Frequency, Phys. Rev. Lett. **98**, 103602 (2007).
[18] A. A. Anappara, S. De Liberato, A. Tredicucci, C. Ciuti, G. Biasiol, L. Sorba, and F. Beltram, Signatures of the ultrastrong light-matter coupling regime, Phys. Rev. B **79**, 201303(R) (2009).
[19] S. De Liberato, D. Gerace, I. Carusotto, and C. Ciuti, Extracavity quantum vacuum radiation from a single qubit, Phys. Rev. A **80**, 053810 (2009).
[20] L. Garziano, A. Ridolfo, R. Stassi, O. Di Stefano, and S. Savasta, Switching on and off of ultrastrong light-matter interaction: Photon statistics of quantum vacuum radiation, Phys. Rev. A **88**, 063829 (2013).
[21] C. S. Muñoz, F. Nori, and S. De Liberato, Resolution of superluminal signaling in non-perturbative cavity quantum electrodynamics, Nat. Commun. **9**, 1924 (2018).
[22] A. Lambrecht, M.-T. Jaekel, and S. Reynaud, Motion Induced Radiation from a Vibrating Cavity, Phys. Rev. Lett. **77**, 615 (1996).
[23] L. H. Ford and A. Vilenkin, Quantum radiation by moving mirrors, Phys. Rev. D **25**, 2569 (1982).
[24] G. Barton and C. Eberlein, On quantum radiation from a moving body with finite refractive index, Ann. Phys. (NY) **227**, 222 (1993).

[25] E. Sassaroli, Y. N. Srivastava, and A. Widom, Photon production by the dynamical Casimir effect, Phys. Rev. A **50**, 1027 (1994).
[26] V. V. Dodonov and A. B. Klimov, Generation and detection of photons in a cavity with a resonantly oscillating boundary, Phys. Rev. A **53**, 2664 (1996).
[27] G. Schaller, R. Schützhold, G. Plunien, and G. Soff, Dynamical Casimir effect in a leaky cavity at finite temperature, Phys. Rev. A **66**, 023812 (2002).
[28] W.-J. Kim, J. H. Brownell, and R. Onofrio, Detectability of Dissipative Motion in Quantum Vacuum via Superradiance, Phys. Rev. Lett. **96**, 200402 (2006).
[29] V. V. Dodonov, Current status of the dynamical Casimir effect, Phys. Scr. **82**, 038105 (2010).
[30] Y. E. Lozovik, V. G. Tsvetus, and E. A. Vinogradov, Femtosecond parametric excitation of electromagnetic field in a cavity, JETP Lett. **61**, 723 (1995).
[31] M. Uhlmann, G. Plunien, R. Schützhold, and G. Soff, Resonant Cavity Photon Creation via the Dynamical Casimir Effect, Phys. Rev. Lett. **93**, 193601 (2004).
[32] M. Crocce, D. A. R. Dalvit, F. C. Lombardo, and F. D. Mazzitelli, Model for resonant photon creation in a cavity with time-dependent conductivity, Phys. Rev. A **70**, 033811 (2004).
[33] C. Braggio, G. Bressi, G. Carugno, C. Del Noce, G. Galeazzi, A. Lombardi, A. Palmieri, G. Ruoso, and D. Zanello, A novel experimental approach for the detection of the dynamical Casimir effect, Europhys. Lett. **70**, 754 (2005).
[34] E. Segev, B. Abdo, O. Shtempluck, E. Buks, and B. Yurke, Prospects of employing superconducting stripline resonators for studying the dynamical Casimir effect experimentally, Phys. Lett. A **370**, 202 (2007).
[35] R. de Melo e Souza, F. Impens, and P. A. Maia Neto, Microscopic dynamical Casimir effect, Phys. Rev. A **97**, 032514 (2018).
[36] J. R. Johansson, G. Johansson, C. M. Wilson, and F. Nori, Dynamical Casimir Effect in a Superconducting Coplanar Waveguide, Phys. Rev. Lett. **103**, 147003 (2009).
[37] J. R. Johansson, G. Johansson, C. M. Wilson, and F. Nori, Dynamical Casimir effect in superconducting microwave circuits, Phys. Rev. A **82**, 052509 (2010).
[38] C. M. Wilson, G. Johansson, A. Pourkabirian, M. Simoen, J. R. Johansson, T. Duty, F. Nori, and P. Delsing, Observation of the dynamical Casimir effect in a superconducting circuit, Nature (London) **479**, 376 (2011).
[39] J. R. Johansson, G. Johansson, C. M. Wilson, P. Delsing, and F. Nori, Nonclassical microwave radiation from the dynamical Casimir effect, Phys. Rev. A **87**, 043804 (2013).
[40] P. D. Nation, J. R. Johansson, M. P. Blencowe, and F. Nori, *Colloquium*: Stimulating uncertainty: Amplifying the quantum vacuum with superconducting circuits, Rev. Mod. Phys. **84**, 1 (2012).
[41] P. Lähteenmäki, G. S. Paraoanu, J. Hassel, and P. J. Hakonen, Dynamical Casimir effect in a Josephson metamaterial, Proc. Natl. Acad. Sci. USA **110**, 4234 (2013).
[42] M. Antezza, C. Braggio, G. Carugno, A. Noto, R. Passante, L. Rizzuto, G. Ruoso, and S. Spagnolo, Optomechanical Rydberg-Atom Excitation via Dynamic Casimir-Polder Coupling, Phys. Rev. Lett. **113**, 023601 (2014).
[43] I. Carusotto, M. Antezza, F. Bariani, S. De Liberato, and C. Ciuti, Optical properties of atomic Mott insulators: From slow light to dynamical Casimir effects, Phys. Rev. A **77**, 063621 (2008).
[44] C. K. Law, Interaction between a moving mirror and radiation pressure: A Hamiltonian formulation, Phys. Rev. A **51**, 2537 (1995).
[45] K. Sala and T. Tufarelli, Exploring corrections to the optomechanical Hamiltonian, Sci. Rep. **8**, 9157 (2018).
[46] V. Macrì, A. Ridolfo, O. Di Stefano, A. F. Kockum, F. Nori, and S. Savasta, Nonperturbative Dynamical Casimir Effect in Optomechanical Systems: Vacuum Casimir-Rabi Splittings, Phys. Rev. X **8**, 011031 (2018).
[47] O. Di Stefano, A. Settineri, V. Macrì, A. Ridolfo, R. Stassi, A. F. Kockum, S. Savasta, and F. Nori, Interaction of Mechanical Oscillators Mediated by the Exchange of Virtual Photon Pairs, Phys. Rev. Lett. **122**, 030402 (2019).
[48] H. M. Wang, M. P. Blencowe, C. M. Wilson, and A. J. Rimberg, Mechanically generating entangled photons from the vacuum: A microwave circuit-acoustic resonator analog of the Unruh effect, Phys. Rev. A **99**, 053833 (2019).
[49] T. J. Kippenberg and K. J. Vahala, Cavity optomechanics: Back-action at the mesoscale, Science **321**, 1172 (2008).
[50] A. Nunnenkamp, K. Børkje, and S. M. Girvin, Single-Photon Optomechanics, Phys. Rev. Lett. **107**, 063602 (2011).
[51] F. Marquardt and S. M. Girvin, Optomechanics, Physics **2**, 40 (2009).
[52] J. D. Teufel, D. Li, M. S. Allman, K. Cicak, A. J. Sirois, J. D. Whittaker, and R. W. Simmonds, Circuit cavity electromechanics in the strong-coupling regime, Nature (London) **471**, 204 (2011).
[53] J. Chan, T. P. M. Alegre, A. H. Safavi-Naeini, J. T. Hill, A. Krause, S. Gröblacher, M. Aspelmeyer, and O. Painter, Laser cooling of a nanomechanical oscillator into its quantum ground state, Nature (London) **478**, 89 (2011).
[54] A. J. Rimberg, M. P. Blencowe, A. D. Armour, and P. D. Nation, A cavity-Cooper pair transistor scheme for investigating quantum optomechanics in the ultra-strong coupling regime, New J. Phys. **16**, 055008 (2014).
[55] M. Aspelmeyer, T. J. Kippenberg, and F. Marquardt, Cavity optomechanics, Rev. Mod. Phys. **86**, 1391 (2014).
[56] A. Ridolfo, M. Leib, S. Savasta, and M. J. Hartmann, Photon Blockade in the Ultrastrong Coupling Regime, Phys. Rev. Lett. **109**, 193602 (2012).
[57] L. Garziano, R. Stassi, V. Macrì, A. F. Kockum, S. Savasta, and F. Nori, Multiphoton quantum Rabi oscillations in ultrastrong cavity QED, Phys. Rev. A **92**, 063830 (2015).
[58] L. Garziano, V. Macrì, R. Stassi, O. Di Stefano, F. Nori, and S. Savasta, One Photon Can Simultaneously Excite Two or More Atoms, Phys. Rev. Lett. **117**, 043601 (2016).
[59] L. Garziano, R. Stassi, V. Macrí, S. Savasta, and O. Di Stefano, Single-step arbitrary control of mechanical quantum states in ultrastrong optomechanics, Phys. Rev. A **91**, 023809 (2015).
[60] V. Macrí, L. Garziano, A. Ridolfo, O. Di Stefano, and S. Savasta, Deterministic synthesis of mechanical NOON states in ultrastrong optomechanics, Phys. Rev. A **94**, 013817 (2016).
[61] S. Butera and I. Carusotto, Mechanical back-reaction effect of the dynamical Casimir emission, Phys. Rev. A **99**, 053815 (2019).
[62] G. Plunien, B. Müller, and W. Greiner, Casimir energy at finite temperature, Physica A **145**, 202 (1987).

[63] R. Schützhold, G. Plunien, and G. Soff, Quantum radiation in external background fields, Phys. Rev. A **58**, 1783 (1998).

[64] G. Plunien, R. Schützhold, and G. Soff, Dynamical Casimir Effect at Finite Temperature, Phys. Rev. Lett. **84**, 1882 (2000).

[65] A. Motazedifard, A. Dalafi, M.H. Naderi, and R. Roknizadeh, Controllable generation of photons and phonons in a coupled Bose-Einstein condensate-optomechanical cavity via the parametric dynamical Casimir effect, Ann. Phys. (NY) **396**, 202 (2018).

[66] O. Di Stefano, R. Stassi, L. Garziano, A. F. Kockum, S. Savasta, and F. Nori, Feynman-diagrams approach to the quantum Rabi model for ultrastrong cavity QED: Stimulated emission and reabsorption of virtual particles dressing a physical excitation, New J. Phys. **19**, 053010 (2017).

[67] R. Stassi, V. Macrì, A. F. Kockum, O. Di Stefano, A. Miranowicz, S. Savasta, and F. Nori, Quantum nonlinear optics without photons, Phys. Rev. A **96**, 023818 (2017).

[68] A. F. Kockum, A. Miranowicz, V. Macrì, S. Savasta, and F. Nori, Deterministic quantum nonlinear optics with single atoms and virtual photons, Phys. Rev. A **95**, 063849 (2017).

[69] A. F. Kockum, A. Miranowicz, S. De Liberato, S. Savasta, and F. Nori, Ultrastrong coupling between light and matter, Nat. Rev. Phys. **1**, 19 (2019).

[70] P. Forn-Díaz, L. Lamata, E. Rico, J. Kono, and E. Solano, Ultrastrong coupling regimes of light-matter interaction, Rev. Mod. Phys. **91**, 025005 (2019).

[71] F. Beaudoin, J. M. Gambetta, and A. Blais, Dissipation and ultrastrong coupling in circuit QED, Phys. Rev. A **84**, 043832 (2011).

[72] D. Hu, S.-Y. Huang, J.-Q. Liao, L. Tian, and H.-S. Goan, Quantum coherence in ultrastrong optomechanics, Phys. Rev. A **91**, 013812 (2015).

[73] K. K. W. Ma and C. K. Law, Three-photon resonance and adiabatic passage in the large-detuning Rabi model, Phys. Rev. A **92**, 023842 (2015).

[74] A. Settineri, V. Macrí, A. Ridolfo, O. Di Stefano, A. F. Kockum, F. Nori, and S. Savasta, Dissipation and thermal noise in hybrid quantum systems in the ultrastrong-coupling regime, Phys. Rev. A **98**, 053834 (2018).

[75] S. Portolan, O. Di Stefano, S. Savasta, F. Rossi, and R. Girlanda, Nonequilibrium Langevin approach to quantum optics in semiconductor microcavities, Phys. Rev. B **77**, 035433 (2008).

[76] O. Di Stefano, S. Savasta, and R. Girlanda, Mode expansion and photon operators in dispersive and absorbing dielectrics, J. Mod. Opt. **48**, 67 (2001).

[77] C. W. Gardiner and M. J. Collett, Input and output in damped quantum systems: Quantum stochastic differential equations and the master equation, Phys. Rev. A **31**, 3761 (1985).

[78] S. Savasta, O. Di Stefano, and R. Girlanda, Light quantization for arbitrary scattering systems, Phys. Rev. A **65**, 043801 (2002).

[79] O. Di Stefano, A. F. Kockum, A. Ridolfo, S. Savasta, and F. Nori, Photodetection probability in quantum systems with arbitrarily strong light-matter interaction, Sci. Rep. **8**, 17825 (2018).

[80] A. D. O'Connell, M. Hofheinz, M. Ansmann, R. C. Bialczak, M. Lenander, E. Lucero, M. Neeley, D. Sank, H. Wang, M. Weides, J. Wenner, J. M. Martinis, and A. N. Cleland, Quantum ground state and single-phonon control of a mechanical resonator, Nature (London) **464**, 697 (2010).

[81] F. Rouxinol, Y. Hao, F. Brito, A. O. Caldeira, E. K. Irish, and M. D. La Haye, Measurements of nanoresonator-qubit interactions in a hybrid quantum electromechanical system, Nanotechnology **27**, 364003 (2016).

[82] W. Qin, V. Macrì, A. Miranowicz, S. Savasta, and F. Nori, Experimentally feasible dynamical Casimir effect in parametrically amplified cavity optomechanics, arXiv:1902.04216.

5.3 Interaction of mechanical oscillators mediated by the exchange of virtual photon pairs

Interaction of Mechanical Oscillators Mediated by the Exchange of Virtual Photon Pairs

Omar Di Stefano,[1] Alessio Settineri,[2] Vincenzo Macrì,[1] Alessandro Ridolfo,[3,1] Roberto Stassi,[1] Anton Frisk Kockum,[4,1] Salvatore Savasta,[2,1,*] and Franco Nori[1,5]

[1]*Theoretical Quantum Physics Laboratory, RIKEN Cluster for Pioneering Research, Wako-shi, Saitama 351-0198, Japan*
[2]*Dipartimento di Scienze Matematiche e Informatiche, Scienze Fisiche e Scienze della Terra, Università di Messina, I-98166 Messina, Italy*
[3]*Dipartimento di Fisica e Astronomia, Universitá di Catania, I-95123 Catania, Italy*
[4]*Wallenberg Centre for Quantum Technology, Department of Microtechnology and Nanoscience, Chalmers University of Technology, 412 96 Gothenburg, Sweden*
[5]*Physics Department, The University of Michigan, Ann Arbor, Michigan 48109-1040, USA*

(Received 1 December 2017; published 24 January 2019)

Two close parallel mirrors attract due to a small force (Casimir effect) originating from the quantum vacuum fluctuations of the electromagnetic field. These vacuum fluctuations can also induce motional forces exerted upon one mirror when the other one moves. Here, we consider an optomechanical system consisting of two vibrating mirrors constituting an optical resonator. We find that motional forces can determine noticeable coupling rates between the two spatially separated vibrating mirrors. We show that, by tuning the two mechanical oscillators into resonance, energy is exchanged between them at the quantum level. This coherent motional coupling is enabled by the exchange of virtual photon pairs, originating from the dynamical Casimir effect. The process proposed here shows that the electromagnetic quantum vacuum is able to transfer mechanical energy somewhat like an ordinary fluid. We show that this system can also operate as a mechanical parametric down-converter even at very weak excitations. These results demonstrate that vacuum-induced motional forces open up new possibilities for the development of optomechanical quantum technologies.

DOI: 10.1103/PhysRevLett.122.030402

Effective interactions able to coherently couple spatially separated qubits [1] are highly desirable for any quantum computer architecture. Efficient cavity-QED schemes, where the effective long-range interaction is mediated by the vacuum field, have been proposed [2–4] and realized [1,5,6]. In these schemes, the cavity is only virtually excited and thus the requirement on its quality factor is greatly loosened. Based on these interactions mediated by vacuum fluctuations, a two-qubit gate has been realized [7] and two-qubit entanglement has been demonstrated [1]. Creation of multiqubit entanglement [8] has also been demonstrated in circuit-QED systems. Very recently, it has been shown that the exchange of virtual photons between artificial atoms can give rise to effective interactions of multiple spatially separated atoms [9,10], opening the way to vacuum nonlinear optics. Moreover, it has been shown that systems where virtual photons can be created and annihilated can be used to realize many nonlinear optical processes with qubits [11,12]. Multiparticle entanglement and quantum logic gates, via virtual vibrational excitations in an ion trap, have also been implemented [13,14]. A recent proposal [15] suggests that classical driving fields can transfer quantum fluctuations between two suspended membranes in an optomechanical cavity system.

Given these results, one may wonder whether it is possible for spatially separated mesoscopic or macroscopic bodies to interact at a quantum level by means of the vacuum fluctuations of the electromagnetic field. It is known that, owing to quantum fluctuations, the electromagnetic vacuum is able, in principle, to affect the motion of objects through it, like a complex fluid [16]. For example, it can induce dissipation and decoherence effects on the motion of moving objects [17–19]. By using linear dispersion theory, it has also been shown that vacuum fluctuations can induce motional forces exerted upon one mirror when the other one moves [20]. Here, we show that two spatially separated moveable mirrors, constituting a cavity-optomechanical system, can exchange energy coherently and reversibly, by exchanging virtual photon pairs. The effects described here can be experimentally demonstrated with circuit-optomechanical systems, using ultra-high-frequency mechanical microresonators or nanoresonators in the GHz spectral range [21,22]. Coupling such a mechanical oscillator to a superconducting qubit, quantum control over a macroscopic mechanical system has been demonstrated [21]. Our results show that the electromagnetic quantum vacuum is able to transfer mechanical energy somewhat like an ordinary fluid. It would be as if the vibration of a string (mechanical

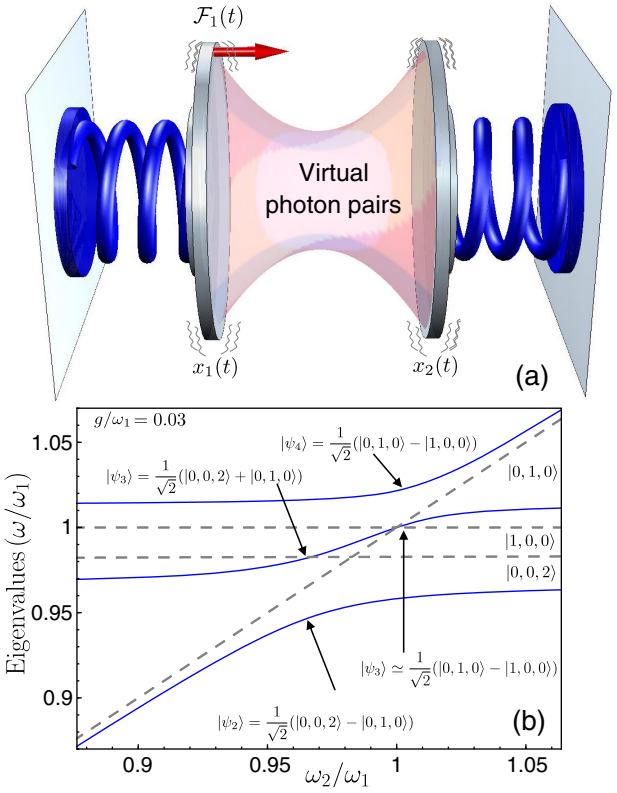

FIG. 1. (a) Schematic of an optomechanical system constituted by two vibrating mirrors. If one of the two vibrating mirrors is excited by an external drive $\mathcal{F}_1(t)$, its excitation can be transferred coherently and reversibly to the other mirror. The interaction is mediated by the exchange of virtual photon pairs. (b) Relevant energy levels of the system Hamiltonian $\hat{H}_s$ as a function of the ratio between the mechanical frequency of mirror 2 and that of mirror 1. An optomechanical coupling $g/\omega_1 = 0.03$ has been used; the cavity-mode resonance frequency is $\omega_c = 0.495\omega_1$. The lowest-energy anticrossing corresponds to the resonance condition for the DCE [26]. The higher energy one is the signature of the mirror-mirror interaction mediated by the virtual DCE photons.

oscillator 1) could be transferred to the membrane of a microphone (mechanical oscillator 2) in the absence of air (or any excited medium filling the gap).

We consider a system constituted by two vibrating mirrors interacting via radiation pressure [see Fig. 1(a)]. Very recently, entanglement between two mechanical oscillators has been demonstrated in a similar system, where, however, the two entangled mechanical oscillators have much lower resonance frequencies and the system is optically pumped [23]. This system can be described by a Hamiltonian that is a direct generalization to two mirrors of the Law Hamiltonian, describing the coupled mirror-field system [24–28]. It provides a unified description of cavity-optomechanics experiments [29] and of the dynamical Casimir effect (DCE) [30–34] in a cavity with a vibrating mirror [26]. It has been shown [32–38] that the photon pairs generated by the DCE can be used to produce entanglement. However, in the present case, the interaction and the entanglement between two mechanical oscillators is determined by virtual photon pairs. Both the cavity field and the position of the mirror are treated as dynamical variables and a canonical quantization procedure is adopted [24]. By considering only one mechanical mode for each mirror, with resonance frequency ω_i $(i = 1, 2)$ and bosonic operators $\hat{b}_i$ and $\hat{b}_i^\dagger$, the displacement operators can be expressed as $\hat{x}_i = X_{\rm zpf}^{(i)}(\hat{b}_i^\dagger + \hat{b}_i)$, where $X_{\rm zpf}^{(i)}$ is the zero-point-fluctuation amplitude of the ith mirror. The mirrors form a single-mode optical resonator with frequency ω_c and bosonic photon operators $\hat{a}$ and $\hat{a}^\dagger$. The system Hamiltonian can be written as $\hat{H}_s = \hat{H}_0 + \hat{H}_{\rm I}$, where $(\hbar = 1)$ $\hat{H}_0 = \omega_c \hat{a}^\dagger \hat{a} + \sum_i \omega_i \hat{b}_i^\dagger \hat{b}_i$ is the unperturbed Hamiltonian. The mirror-field interaction Hamiltonian can be written as $\hat{H}_{\rm I} = \hat{V}_{\rm om} + \hat{V}_{\rm DCE}$, where $\hat{V}_{\rm om} = \hat{a}^\dagger \hat{a} \sum_i g_i(\hat{b}_i + \hat{b}_i^\dagger)$ is the standard optomechanical interaction conserving the number of photons, $\hat{V}_{\rm DCE} = (1/2)(\hat{a}^2 + \hat{a}^{\dagger 2}) \sum_i g_i(\hat{b}_i + \hat{b}_i^\dagger)$ describes the creation and annihilation of photon pairs, and g_i is the optomechanical coupling rate for mirror i. The linear dependence of the interaction Hamiltonian on the mirror operators is a consequence of the usual small-displacement assumption [24]. This Hamiltonian can be directly generalized to include additional cavity modes. However, in most circuit-optomechanics experiments, the electromagnetic resonator is provided by a superconducting LC circuit, which only supports a *single* mode.

When describing most of the optomechanics experiments to date [29], $\hat{V}_{\rm DCE}$ is neglected. This is a very good approximation when $\omega_i \ll \omega_c$ (which is the most common experimental situation). However, when ω_i are of the order of ω_c, $\hat{V}_{\rm DCE}$ cannot be neglected. We are interested in studying this regime, which can be achieved using microwave resonators and ultra-high-frequency mechanical microresonators or nanoresonators [21,22]. The Hamiltonian $\hat{H}_s$ describes the interaction between two vibrating mirrors and the radiation pressure of a cavity field. However, the same radiation-pressure-type coupling is obtained for microwave optomechanical circuits (see, e.g., Ref. [39]).

In order to properly describe the system dynamics, including external driving and dissipation, the coupling to external degrees of freedom needs to be considered. A coherent external drive of the vibrating mirror i can be described by including the time-dependent Hamiltonian

$$\hat{V}_i(t) = \mathcal{F}_i(t)(\hat{b}_i + \hat{b}_i^\dagger), \tag{1}$$

where $\mathcal{F}_i(t)$ is equal to the external force applied to the mirror times the mechanical zero-point-fluctuation amplitude. Dissipation and decoherence effects are taken into

account by adopting a master-equation approach. For strongly coupled hybrid quantum systems, the description offered by the standard quantum-optical master equation breaks down [40,41]. Following Refs. [41–43], we express the system-bath interaction Hamiltonian in the basis formed by the energy eigenstates of $\hat{H}_s$ [26].

We begin our analysis by numerically diagonalizing the Hamiltonian $\hat{H}_s$ in a truncated finite-dimensional Hilbert space. The truncation is realized by only including eight Fock states for each of the three harmonic oscillators. The blue solid curves in Fig. 1(b) describe the eigenvalue differences $E_j - E_0$ (E_0 is the ground-state energy) of the total Hamiltonian $\hat{H}_s$ (including $\hat{V}_{\mathrm{DCE}}$) as a function of ω_2/ω_1. For the optomechanical couplings, we use $g_1 = g_2 = g = 0.03\omega_1$. Such a coupling strength is quite high, but nevertheless below the onset of the so-called ultrastrong optomechanical coupling regime [41,44–46]. The cavity-mode resonance frequency is fixed at $\omega_c = 0.495\omega_1$. This value is chosen close to the resonance condition for the DCE [26] in order to increase the effective coupling between the mirrors. For comparison, we also show in Fig. 1(b) (dashed gray lines) the lowest-energy levels $E_{n,k_1,k_2} = \omega_c n - \sum_i g_i^2 n^2/\omega_i + \sum_i \omega_i k_i$ of the standard optomechanics Hamiltonian $\hat{H}_0 + \hat{V}_{\mathrm{om}}$. This Hamiltonian has the eigenstates $|k_1, k_2, n\rangle \equiv D_1(n\beta_1)|k\rangle_1 \otimes D_2(n\beta_2)|k\rangle_2 \otimes |n\rangle_c$, where $|n\rangle_c$ are the cavity Fock states and $|k\rangle_i$ are the bare mechanical states for the ith mirror.

The bare mechanical states $|k\rangle_i$ are displaced by the optomechanical interaction, $\hat{D}_i(n\beta_i) = \exp[n\beta_i(\hat{b}_i^\dagger - \hat{b}_i)]$, with $\beta_i = g_i/\omega_i$ (see Sec. I of Supplemental Material [47]). The main differences between the blue solid and the gray dashed curves are the appearance of small energy shifts, and of level anticrossings in the region $\omega_2/\omega_1 \sim 1$. We indicate by $|\psi_n\rangle$ ($n = 0, 1, 2\ldots$) the eigenvectors of $\hat{H}_s$ and by E_n the corresponding eigenvalues, choosing the labeling of the states such that $E_j > E_k$ for $j > k$. The lowest-energy anticrossing corresponds to the resonance condition for the DCE [26]. The higher-energy splitting in Fig. 1(b) originates from the coherent coupling of the zero-photon states $|1,0,0\rangle$ and $|0,1,0\rangle$. At the minimum energy splitting $2\lambda_{10}^{01} \simeq 2.11 \times 10^{-2}\omega_1$, the resulting states are well approximated by $|\psi_{3,4}\rangle \simeq (1/\sqrt{2})(|1,0,0\rangle \pm |0,1,0\rangle)$. As we will show explicitly below by using perturbation theory, this mirror-mirror interaction is a result of virtual exchange of cavity photon pairs. When the mirrors have the same resonance frequency, an excitation in one mirror can be transferred to the other by virtually becoming a photon pair in the cavity, thanks to the DCE. The resulting minimum energy splitting provides a measure of the effective coupling strength between the two mirrors. At higher energy for $\omega_2 \simeq \omega_1$ a ladder of increasing level splittings, involving higher number phonon states, is present (see Sec. III in [47]).

The origin of the higher-energy avoided-level crossing shown in Fig. 1(b) can be understood by deriving an effective Hamiltonian, using second-order perturbation theory or, equivalently, the James' method [52,53] (see Sec. II in [47]). The resulting effective Hamiltonian, describing the coherent coupling of states $|1,0,0\rangle$ and $|0,1,0\rangle$, is

$$\hat{H}_{\mathrm{eff}} = \Omega_1|1,0,0\rangle\langle 1,0,0| + \Omega_2|0,1,0\rangle\langle 0,1,0| + (\lambda_{10}^{01}|1,0,0\rangle\langle 0,1,0| + \mathrm{H.c.}), \quad (2)$$

where $\Omega_1 = \omega_1 + \Delta_{10}$ and $\Omega_2 = \omega_2 + \Delta_{01}$ denote the Lamb-shifted levels [47]. The effective coupling strength is

$$\lambda_{10}^{01} = \sum_{k,q} \frac{\langle 0,1,0|\hat{V}_{\mathrm{DCE}}|k,q,2\rangle\langle k,q,2|\hat{V}_{\mathrm{DCE}}|1,0,0\rangle}{E_{0,1,0} - E_{k,q,2}}. \quad (3)$$

Equations (2) and (3) clearly show that the one-phonon state of mirror 1 can be transferred to mirror 2 through a virtual transition via the two-photon intermediate states $|k,q,2\rangle$. We notice that the largest contribution is provided by the zero-phonon intermediate state ($k = q = 0$). This perturbative calculation gives rise to an effective coupling strength λ and energy shifts Δ in good agreement with the numerical calculation shown in Fig. 1(b) (see Sec. II of [47]). Analogous effective Hamiltonians can be derived for the avoided-level crossings at higher energy (see Sec. II of [47]).

If the optomechanical couplings g_i are strong enough to ensure that the DCE-induced effective coupling (3) becomes larger than the relevant decoherence rates in the system, the transfer of one-phonon excitations between the two mirrors can be deterministic and reversible. Neglecting decoherence (calculations including losses can be found in Secs. V and VI of [47]), if the system is initially prepared in the state $|1,0,0\rangle$, it will evolve as

$$|\psi(t)\rangle = \cos(\lambda_{10}^{01}t)|1,0,0\rangle - i\sin(\lambda_{10}^{01}t)|0,1,0\rangle. \quad (4)$$

After a time $t = \pi/(2\lambda_{10}^{01})$, the excitation will be completely transferred to mirror 1. After a time $t = \pi/(4\lambda_{10}^{01})$, the two mirrors will be in a maximally entangled motional state.

We now investigate the system dynamics starting from a low-temperature thermal state and introducing the excitation of mirror 1 by a single-tone continuous-wave mechanical drive $\mathcal{F}_1(t) = \mathcal{A}\cos(\omega_d t)$. We numerically solve the master equation for hybrid quantum systems in a truncated Hilbert space [54]. Figure 2 shows the time evolution of the mean phonon numbers of the two mirrors $\langle \hat{B}_i^\dagger \hat{B}_i\rangle$ and the intracavity mean photon number $\langle \hat{A}^\dagger \hat{A}\rangle$. Here, $\hat{A}$, $\hat{B}_i$ are the *physical* photon and phonon operators. Such operators $\hat{O} = \hat{A}, \hat{B}_i$ can be defined in terms of their bare counterparts $\hat{o} = \hat{a}, \hat{b}_i$ as [55–58] $\hat{O} = \sum_{E_n > E_m} \langle \psi_m|(\hat{o} + \hat{o}^\dagger)|\psi_n\rangle|\psi_m\rangle\langle\psi_n|$. We

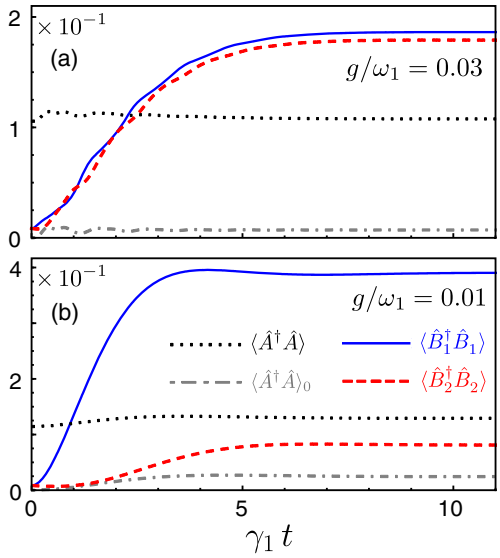

FIG. 2. System dynamics for $\omega_c \simeq 1.5\omega_1$ under continuous-wave drive of mirror 1. The blue solid and red dashed curves describe the mean phonon numbers $\langle \hat{B}_1^\dagger \hat{B}_1 \rangle$ and $\langle \hat{B}_2^\dagger \hat{B}_2 \rangle$, respectively, while the black dotted curve describes the mean intracavity photon number $\langle \hat{A}^\dagger \hat{A} \rangle$ and the gray dash-dotted curve shows the same photon number $\langle \hat{A}^\dagger \hat{A} \rangle_0$, calculated assuming zero temperature.

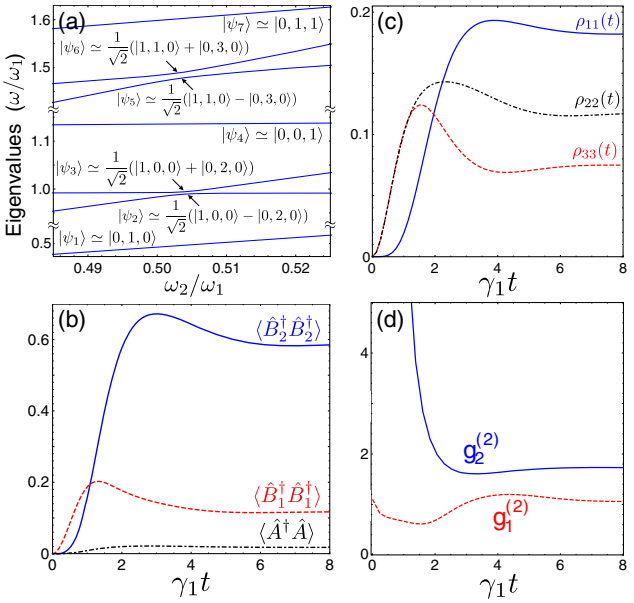

FIG. 3. Mechanical parametric down-conversion. (a) Lowest-energy levels of the system Hamiltonian as a function of the ratio between the mechanical frequency of mirror 2 and that of mirror 1. An optomechanical coupling $g/\omega_1 = 0.12$ has been used and the cavity-mode resonance frequency is $\omega_c = 1.2\omega_1$. Two avoided-level crossings are clearly visible. The one at lower energy corresponds to the resonant coupling of the one-phonon state of mirror 1 with the two-phonon state of mirror 2, whose resonance frequency is half that of mirror 1. The higher-energy anticrossing corresponds to the resonant coupling of the states $|1,1,0\rangle$ and $|0,3,0\rangle$. (b) Time evolution of the mean phonon and photon numbers. (c) Time evolution of the population of the first three energy states. (d) Equal-time phonon-phonon normalized correlation functions $g_i^{(2)}(t,t)$ for the two mirrors.

consider the system initially in a thermal state with a normalized thermal energy $k_B T/\omega_1 = 0.208$, corresponding to a temperature $T = 60$ mK for $\omega_1/2\pi = 6$ GHz. During its time evolution, the system interacts with thermal reservoirs all with the same temperature T. We use $\gamma_1 = \gamma_2 = \gamma = \omega_1/260$ and $\kappa = \gamma$ for the mechanical and photonic loss rates. We consider a weak ($\mathcal{A}/\gamma = 0.95$) resonant excitation of mirror 1 ($\omega_d = \omega_1$). We present results for two normalized coupling strengths ($g/\omega_1 = 0.01, 0.03$), and set $\omega_2 = \omega_1$. The results shown in Fig. 2(a) demonstrate that the excitation transfer mechanism via virtual DCE photon pairs, proposed here, works very well for $g/\omega_1 = 0.03$. In steady state, mirror 2 reaches almost the same excitation intensity as the driven mirror 1. The photon population differs only slightly from the thermal one at $t = 0$, showing that a negligible amount of DCE photon pairs are generated. We also observe that the influence of temperature on the mechanical expectation values is almost negligible (see Supplemental Material [47]). On the contrary, the cavity mode at lower frequency is much more affected by the temperature. We observe that for $g/\omega_1 = 0.01$, although the transfer is reduced, the effect is still measurable. The mean photon number obtained at $T = 0$ is also shown for comparison (dash-dotted curves) in both the panels. The mirror-mirror excitation transfer at $g/\omega_1 = 0.01$ can be significantly improved [47] by taking advantage of the DCE resonance condition $\omega_c = 2\omega_1$. However, in this case, a significant amount of real photon pairs are generated. This configuration can be used to probe the DCE effect in the presence of thermal photons.

In order to put forward the potentialities and the flexibility of this vacuum-field-mediated interaction between mechanical oscillators, we now show that this system also can operate as a mechanical parametric down-converter. For mechanical frequencies such that $\omega_1 \simeq 2\omega_2$, a ladder of avoided-level crossings manifests. Two of them are shown in Fig. 3(a). Also in this case, the avoided-level crossings originate from the exchange of virtual photon pairs, as can be understood by using second-order perturbation theory. For example, the dominant path for the lowest-energy level anticrossing goes through the intermediate state $|0,0,2\rangle$: $|1,0,0\rangle \leftrightarrow |0,0,2\rangle \leftrightarrow |0,2,0\rangle$ [47]. We note that these avoided-level crossings, in contrast to those shown in Fig. 1(b), do not conserve the excitation number. Analogous coherent coupling effects can be observed in the ultrastrong-coupling regime of cavity QED [9,11,43,59,60]. Using $\omega_c = 1.2\omega_1$ and $g/\omega_1 = 0.12$, we obtain a minimum energy splitting $\lambda_{10}^{02}/\omega_1 \simeq 4 \times 10^{-3}$. We fix the resonance frequency of mirror 2 at the value providing the minimum level splitting, and calculate the system dynamics considering a weak resonant excitation of

mirror 1, $\mathcal{F}_1(t)=\mathcal{A}\cos(\omega_d t)$, with $\omega_d=(E_3+E_2-2E_0)/2$, and $\mathcal{A}/\gamma=0.7$. We also used $\gamma=2\times10^{-3}\omega_1$ and $\kappa=\gamma/2$. The results shown in Fig. 3(b) demonstrate a very efficient excitation transfer between the two mechanical oscillators of different frequency. We also observe that the transfer occurs even in the presence of a very weak excitation of mirror 1 (peak mean phonon number of mirror 1: $\langle\hat{B}_1^\dagger\hat{B}_1\rangle\simeq0.2$). It may appear surprising that the steady-state mean phonon number of mirror 2 is significantly *larger* than that of mirror 1, even though it receives all the energy from the latter. This phenomenon can be partly understood by observing that a phonon of mirror 1 converts into two phonons (each at half energy) of mirror 2. In addition, once the system decays to the state $|\psi_1\rangle\simeq|0,1,0\rangle$, the remaining excitation in mirror 2 will not be exchanged back and forth with mirror 1, since the corresponding energy level is not resonantly coupled to other energy levels [see Fig. 3(a)]. Figure 3(c) displays the populations of the three lowest-energy levels, which are the levels that are most populated at this input power. This panel confirms that $|\psi_1\rangle$ has the higher population in steady state.

We also calculated the equal-time phonon-phonon normalized correlation functions

$$g_i^{(2)}(t,t)=\frac{\langle\hat{B}_i^\dagger(t)\hat{B}_i^\dagger(t)\hat{B}_i(t)\hat{B}_i(t)\rangle}{\langle\hat{B}_i^\dagger(t)\hat{B}_i(t)\rangle^2}. \tag{5}$$

The high value at early times obtained for mirror 2 [see Fig. 3(d)] confirms the *simultaneous* excitation of phonon pairs.

In conclusion, we demonstrated that mechanical quantum excitations can be coherently transferred among spatially separated mechanical oscillators, through a dissipationless quantum bus, due to the exchange of virtual photon pairs. The experimental demonstration of these processes would show that the electromagnetic quantum vacuum is able to transfer mechanical energy somewhat like an ordinary fluid [16]. The results presented here open up exciting possibilities of applying ideas from fluid dynamics in the study of the electromagnetic quantum vacuum. Furthermore, these results show that the DCE in high-frequency optomechanical systems can be a versatile and powerful new resource for the development of quantum-optomechanical technologies. If, in the future, it will be possible to control the interaction time (as currently realized in superconducting artificial atoms), e.g., changing rapidly the resonance frequencies of mechanical oscillators (see Sec. VI of [47]), the interaction scheme proposed here would represent an attractive architecture for quantum information processing with optomechanical systems [61]. The best platform to experimentally demonstrate these results is circuit optomechanics using ultra-high-frequency (ω_1 at 5–6 GHz) mechanical oscillators. Their quantum interaction with superconducting artificial atoms has been experimentally demonstrated [21,22]. Considering instead their interaction with a superconducting microwave resonator should allow the observation of the effects predicted here. Specifically, combining circuit-optomechanics schemes able to increase the coupling [39,62] with already demonstrated ultra-high-frequency mechanical resonators [21,22] represents a very promising setup for entangling spatially separated vibrations via virtual photon pairs (see Sec. VII of [47]).

F. N. is supported in part by the MURI Center for Dynamic Magneto-Optics via the Air Force Office of Scientific Research (AFOSR) (Grant No. FA9550-14-1-0040), Army Research Office (ARO) (Grant No. W911NF-18-1-0358), Asian Office of Aerospace Research and Development (AOARD) (Grant No. FA2386-18-1-4045), Japan Science and Technology Agency (JST) (Q-LEAP program, ImPACT program, and CREST Grant No. JPMJCR1676), Japan Society for the Promotion of Science (JSPS) (JSPS-RFBR Grant No. 17-52-50023, and JSPS-FWO Grant No. VS.059.18N), RIKEN-AIST Challenge Research Fund, and the John Templeton Foundation. S. S. acknowledges the Army Research Office (ARO) (Proposal No. 73511-PH-RFC).

*Corresponding author.
ssavasta@unime.it

[1] J. Majer, J. M. Chow, J. M. Gambetta, J. Koch, B. R. Johnson, J. A. Schreier, L. Frunzio, D. I. Schuster, A. A. Houck, A. Wallraff, A. Blais, M. H. Devoret, S. M. Girvin, and R. J. Schoelkopf, Coupling superconducting qubits via a cavity bus, Nature (London) **449**, 443 (2007).

[2] A. Sørensen and K. Mølmer, Quantum Computation with Ions in Thermal Motion, Phys. Rev. Lett. **82**, 1971 (1999).

[3] A. Imamoğlu, D. D. Awschalom, G. Burkard, D. P. DiVincenzo, D. Loss, M. Sherwin, and A. Small, Quantum Information Processing Using Quantum Dot Spins and Cavity QED, Phys. Rev. Lett. **83**, 4204 (1999).

[4] S.-B. Zheng and G.-C. Guo, Efficient Scheme for Two-Atom Entanglement and Quantum Information Processing in Cavity QED, Phys. Rev. Lett. **85**, 2392 (2000).

[5] S. Osnaghi, P. Bertet, A. Auffeves, P. Maioli, M. Brune, J.-M. Raimond, and S. Haroche, Coherent Control of an Atomic Collision in a Cavity, Phys. Rev. Lett. **87**, 037902 (2001).

[6] S. Filipp, M. Göppl, J. M. Fink, M. Baur, R. Bianchetti, L. Steffen, and A. Wallraff, Multimode mediated qubit-qubit coupling and dark-state symmetries in circuit quantum electrodynamics, Phys. Rev. A **83**, 063827 (2011).

[7] L. DiCarlo, J. M. Chow, J. M. Gambetta, L. S. Bishop, B. R. Johnson, D. I. Schuster, J. Majer, A. Blais, L. Frunzio, S. M. Girvin, and R. J. Schoelkopf, Demonstration of two-qubit algorithms with a superconducting quantum processor, Nature (London) **460**, 240 (2009).

[8] M. Neeley, R. C. Bialczak, M. Lenander, E. Lucero, M. Mariantoni, A. D. O'Connell, D. Sank, H. Wang, M. Weides, J. Wenner, Y. Yin, T. Yamamoto, A. N. Cleland,

and J. M. Martinis, Generation of three-qubit entangled states using superconducting phase qubits, Nature (London) **467**, 570 (2010).
[9] R. Stassi, V. Macrì, A. F. Kockum, O. Di Stefano, A. Miranowicz, S. Savasta, and F. Nori, Quantum nonlinear optics without photons, Phys. Rev. A **96**, 023818 (2017).
[10] P. Zhao, X. Tan, H. Yu, S.-L. Zhu, and Y. Yu, Circuit QED with qutrits: Coupling three or more atoms via virtual-photon exchange, Phys. Rev. A **96**, 043833 (2017).
[11] A. F. Kockum, A. Miranowicz, V. Macrì, S. Savasta, and F. Nori, Deterministic quantum nonlinear optics with single atoms and virtual photons, Phys. Rev. A **95**, 063849 (2017).
[12] A. F. Kockum, V. Macrì, L. Garziano, S. Savasta, and F. Nori, Frequency conversion in ultrastrong cavity QED, Sci. Rep. **7**, 5313 (2017).
[13] C. A. Sackett, D. Kielpinski, B. E. King, C. Langer, V. V. Meyer, C. J. Myatt, M. Rowe, Q. A. Turchette, W. M. Itano, D. J. Wineland, and C. Monroe, Experimental entanglement of four particles, Nature (London) **404**, 256 (2000).
[14] D. Leibfried, B. DeMarco, V. Meyer, D. Lucas, M. Barrett, J. Britton, W. M. Itano, B. Jelenković, C. Langer, T. Rosenband, and D. J. Wineland, Experimental demonstration of a robust, high-fidelity geometric two ion-qubit phase gate, Nature (London) **422**, 412 (2003).
[15] Y. H. Chen, Z.-C. Shi, J. Song, and Y. Xia, Invariant-based inverse engineering for fluctuation transfer between membranes in an optomechanical cavity system, Phys. Rev. A **97**, 023841 (2018).
[16] M. Kardar and R. Golestanian, The "friction" of vacuum, and other fluctuation-induced forces, Rev. Mod. Phys. **71**, 1233 (1999).
[17] D. A. R. Dalvit and P. A. Maia Neto, Decoherence via the Dynamical Casimir Effect, Phys. Rev. Lett. **84**, 798 (2000).
[18] M. T. Jackel and S. Reynaud, Fluctuations and dissipation for a mirror in vacuum, Quantum Opt. **4**, 39 (1992).
[19] S. Butera and I. Carusotto, Mechanical back-reaction effect of the dynamical Casimir emission, arXiv:1810.11281.
[20] M. T. Jaekel and S. Reynaud, Motional Casimir force, J. Phys. I **2**, 149 (1992).
[21] A. D. O'Connell, M. Hofheinz, M. Ansmann, R. C. Bialczak, M. Lenander, E. Lucero, M. Neeley, D. Sank, H. Wang, M. Weides *et al.*, Quantum ground state and single-phonon control of a mechanical resonator, Nature (London) **464**, 697 (2010).
[22] F. Rouxinol, Y. Hao, F. Brito, A. O. Caldeira, E. K. Irish, and M. D. LaHaye, Measurements of nanoresonator-qubit interactions in a hybrid quantum electromechanical system, Nanotechnology **27**, 364003 (2016).
[23] C. F. Ockeloen-Korppi, E. Damskägg, J.-M. Pirkkalainen, M. Asjad, A. A. Clerk, F. Massel, M. J. Woolley, and M. A. Sillanpää, Stabilized entanglement of massive mechanical oscillators, Nature (London) **556**, 478 (2018).
[24] C. K. Law, Interaction between a moving mirror and radiation pressure: A Hamiltonian formulation, Phys. Rev. A **51**, 2537 (1995).
[25] S. Butera and R. Passante, Field Fluctuations in a One-Dimensional Cavity with a Mobile Wall, Phys. Rev. Lett. **111**, 060403 (2013).
[26] V. Macrì, A. Ridolfo, O. Di Stefano, A. F. Kockum, F. Nori, and S. Savasta, Nonperturbative Dynamical Casimir Effect in Optomechanical Systems: Vacuum Casimir-Rabi Splittings, Phys. Rev. X **8**, 011031 (2018).
[27] K. Sala and T. Tufarelli, Exploring corrections to the optomechanical Hamiltonian, Sci. Rep. **8**, 9157 (2018).
[28] F. Armata, M. S. Kim, S. Butera, L. Rizzuto, and R. Passante, Nonequilibrium dressing in a cavity with a movable reflecting mirror, Phys. Rev. D **96**, 045007 (2017).
[29] M. Aspelmeyer, T. J. Kippenberg, and F. Marquardt, Cavity optomechanics, Rev. Mod. Phys. **86**, 1391 (2014).
[30] G. T. Moore, Quantum theory of the electromagnetic field in a variable-length one-dimensional cavity, J. Math. Phys. (N.Y.) **11**, 2679 (1970).
[31] P. D. Nation, J. R. Johansson, M. P. Blencowe, and Franco Nori, Colloquium: Stimulating uncertainty: Amplifying the quantum vacuum with superconducting circuits, Rev. Mod. Phys. **84**, 1 (2012).
[32] J. R. Johansson, G. Johansson, C. M. Wilson, and F. Nori, Dynamical Casimir Effect in a Superconducting Coplanar Waveguide, Phys. Rev. Lett. **103**, 147003 (2009).
[33] J. R. Johansson, G. Johansson, C. M. Wilson, and F. Nori, Dynamical Casimir effect in superconducting microwave circuits, Phys. Rev. A **82**, 052509 (2010).
[34] C. M. Wilson, G. Johansson, A. Pourkabirian, M. Simoen, J. R. Johansson, T. Duty, F. Nori, and P. Delsing, Observation of the dynamical Casimir effect in a superconducting circuit, Nature (London) **479**, 376 (2011).
[35] J. R. Johansson, G. Johansson, C. M. Wilson, P. Delsing, and F. Nori, Nonclassical microwave radiation from the dynamical Casimir effect, Phys. Rev. A **87**, 043804 (2013).
[36] S. Felicetti, M. Sanz, L. Lamata, G. Romero, G. Johansson, P. Delsing, and E. Solano, Dynamical Casimir Effect Entangles Artificial Atoms, Phys. Rev. Lett. **113**, 093602 (2014).
[37] R. Stassi, S. De Liberato, L. Garziano, B. Spagnolo, and S. Savasta, Quantum control and long-range quantum correlations in dynamical Casimir arrays, Phys. Rev. A **92**, 013830 (2015).
[38] D. Z. Rossatto, S. Felicetti, H. Eneriz, E. Rico, M. Sanz, and E. Solano, Entangling polaritons via dynamical Casimir effect in circuit quantum electrodynamics, Phys. Rev. B **93**, 094514 (2016).
[39] T. T. Heikkilä, F. Massel, J. Tuorila, R. Khan, and M. A. Sillanpää, Enhancing Optomechanical Coupling via the Josephson effect, Phys. Rev. Lett. **112**, 203603 (2014).
[40] F. Beaudoin, J. M. Gambetta, and A. Blais, Dissipation and ultrastrong coupling in circuit QED, Phys. Rev. A **84**, 043832 (2011).
[41] D. Hu, S.-Y. Huang, J.-Q. Liao, L. Tian, and H.-S. Goan, Quantum coherence in ultrastrong optomechanics, Phys. Rev. A **91**, 013812 (2015).
[42] H.-P. Breuer and F. Petruccione, *The Theory of Open Quantum Systems* (Oxford University Press, Oxford, 2002).
[43] K. K. W. Ma and C. K. Law, Three-photon resonance and adiabatic passage in the large-detuning Rabi model, Phys. Rev. A **92**, 023842 (2015).
[44] L. Garziano, R. Stassi, V. Macrí, S. Savasta, and O. Di Stefano, Single-step arbitrary control of mechanical quantum states in ultrastrong optomechanics, Phys. Rev. A **91**, 023809 (2015).

[45] V. Macrí, L. Garziano, A. Ridolfo, O. Di Stefano, and S. Savasta, Deterministic synthesis of mechanical NOON states in ultrastrong optomechanics, Phys. Rev. A **94**, 013817 (2016).
[46] A. F. Kockum, A. Miranowicz, S. De Liberato, S. Savasta, and F. Nori, Ultrastrong coupling between light and matter, Nat. Rev. Phys. **1**, 19 (2019).
[47] See Supplemental Material at http://link.aps.org/supplemental/10.1103/PhysRevLett.122.030402 for more details, including the additional Refs. [48–51].
[48] M. O. Scully and M. S. Zubairy, *Quantum Optics* (Cambridge University Press, Cambridge, England, 1997).
[49] A. N. Cleland and M. R. Geller, Superconducting Qubit Storage and Entanglement with Nanomechanical Resonators, Phys. Rev. Lett. **93**, 070501 (2004).
[50] D. Zueco, G. M. Reuther, S. Kohler, and P. Hänggi, Qubit-oscillator dynamics in the dispersive regime: Analytical theory beyond the rotating-wave approximation, Phys. Rev. A **80**, 033846 (2009).
[51] A. O'Connell and A. N. Cleland, Microwave-frequency mechanical resonators operated in the quantum limit, in *Cavity Optomechanics* (Springer, New York, 2014), pp. 253–281.
[52] O. Gamel and D. F. V. James, Time-averaged quantum dynamics and the validity of the effective Hamiltonian model, Phys. Rev. A **82**, 052106 (2010).
[53] W. Shao, C. Wu, and X.-L. Feng, Generalized James' effective Hamiltonian method, Phys. Rev. A **95**, 032124 (2017).
[54] A. Settineri, V. Macrì, A. Ridolfo, O. Di Stefano, A. F. Kockum, F. Nori, and S. Savasta, Dissipation and thermal noise in hybrid quantum systems in the ultrastrong-coupling regime, Phys. Rev. A **98**, 053834 (2018).
[55] A. Ridolfo, M. Leib, S. Savasta, and M. J. Hartmann, Photon Blockade in the Ultrastrong Coupling Regime, Phys. Rev. Lett. **109**, 193602 (2012).
[56] L. Garziano, R. Stassi, A. Ridolfo, O. Di Stefano, and S. Savasta, Vacuum-induced symmetry breaking in a superconducting quantum circuit, Phys. Rev. A **90**, 043817 (2014).
[57] O. Di Stefano, R. Stassi, L. Garziano, A. F. Kockum, S. Savasta, and F. Nori, Feynman-diagrams approach to the quantum Rabi model for ultrastrong cavity QED: Stimulated emission and reabsorption of virtual particles dressing a physical excitation, New J. Phys. **19**, 053010 (2017).
[58] O. Di Stefano, A. F. Kockum, A. Ridolfo, S. Savasta, and F. Nori, Photodetection probability in quantum systems with arbitrarily strong light-matter interaction, Sci. Rep. **8**, 17825 (2018).
[59] L. Garziano, R. Stassi, V. Macrì, A. F. Kockum, S. Savasta, and F. Nori, Multiphoton quantum Rabi oscillations in ultrastrong cavity QED, Phys. Rev. A **92**, 063830 (2015).
[60] L. Garziano, V. Macrì, R. Stassi, O. Di Stefano, F. Nori, and S. Savasta, One Photon Can Simultaneously Excite Two or More Atoms, Phys. Rev. Lett. **117**, 043601 (2016).
[61] K. Stannigel, P. Komar, S. J. M. Habraken, S. D. Bennett, M. D. Lukin, P. Zoller, and P. Rabl, Optomechanical Quantum Information Processing with Photons and Phonons, Phys. Rev. Lett. **109**, 013603 (2012).
[62] J.-M. Pirkkalainen, S. U. Cho, F. Massel, J. Tuorila, T. T. Heikkilä, P. J. Hakonen, and M. A. Sillanpää, Cavity optomechanics mediated by a quantum two-level system, Nat. Commun. **6**, 6981 (2015).

Supplemental Material for Interaction of Mechanical Oscillators Mediated by the Exchange of Virtual Photon Pairs

I. DIAGONALIZATION OF THE STANDARD OPTOMECHANICS HAMILTONIAN

We consider a system constituted by two vibrating mirrors interacting via radiation pressure [see Fig. 1(a) in the main paper]. Both the cavity field and the displacements of the mirrors are treated as dynamical variables and a canonical quantization procedure is adopted [1, 2].

By considering only one mechanical mode for each mirror, with resonance frequency ω_i ($i = 1, 2$) and bosonic operators $\hat{b}_i$ and $\hat{b}_i^\dagger$, the displacement operators can be expressed as $\hat{x}_i = X_{\rm zpf}^{(i)}(\hat{b}_i^\dagger + \hat{b}_i)$, where $X_{\rm zpf}^{(i)}$ is the zero-point-fluctuation amplitude of the ith mirror. We also consider a single-mode optical resonator with frequency $\omega_{\rm c}$ and bosonic photon operators $\hat{a}$ and $\hat{a}^\dagger$. The system Hamiltonian can be written as $\hat{H}_{\rm s} = \hat{H}_0 + \hat{H}_{\rm I}$, where

$$\hat{H}_0 = \omega_{\rm c}\hat{a}^\dagger\hat{a} + \omega_1\hat{b}_1^\dagger\hat{b}_1 + \omega_2\hat{b}_2^\dagger\hat{b}_2\,, \tag{S1}$$

is the unperturbed Hamiltonian. The Hamiltonian describing the mirror-field interaction is

$$\hat{H}_{\rm I} = (\hat{a} + \hat{a}^\dagger)^2 \sum_{i=1,2} \frac{g_i}{2}(\hat{b}_i + \hat{b}_i^\dagger)\,, \tag{S2}$$

where g_i are the coupling rates. Eq. (S2) is a direct generalization of the Law optomechanical Hamiltonian [1]. The linear dependence of the interaction Hamiltonian on the mirror operators is a consequence of the usual small-displacement assumption [1]. Once such linear dependence is assumed, the generalization (S2) to two mirrors, coupled to the same optical resonator, is straightforward. Equation (S2) has a clear physical meaning: the radiation pressure force acting on the mechanical resonators is proportional to the square modulus of the electric field.

By developing the photonic operators in normal order, and by defining new bosonic phonon and photon operators and a renormalized photon frequency, $\hat{H}_{\rm s}$ can be written as

$$\hat{H}_{\rm s} = \hat{H}_{\rm om} + \hat{V}_{\rm DCE}\,, \tag{S3}$$

where $\hat{V}_{\rm DCE}$ is the DCE interaction term:

$$\hat{V}_{\rm DCE} = (\hat{a}^2 + \hat{a}^{\dagger 2}) \sum_{i=1,2} \frac{g_i}{2} (\hat{b}_i + \hat{b}_i^\dagger) \,, \tag{S4}$$

and $\hat{H}_{\rm om}$ is the standard optomechanics Hamiltonian:

$$\hat{H}_{\rm om} = \hat{H}_0 + \hat{V}_{\rm om} \tag{S5}$$

with

$$\hat{V}_{\rm om} = \hat{a}^\dagger \hat{a} \sum_{i=1,2} g_i (\hat{b}_i + \hat{b}_i^\dagger) \,. \tag{S6}$$

$\hat{H}_{\rm om}$ can be easily diagonalized defining the displacement operators for the two mirrors. In particular, defining $(i = 1, 2)$

$$\hat{B}_i = \hat{b}_i + \beta_i \hat{a}^\dagger \hat{a} \tag{S7}$$

with $\beta_i = g_i/\omega_i$, we obtain

$$\hat{H}_{\rm om} = \omega_{\rm c} \left[1 - \left(\frac{\beta_1^2 \omega_1}{\omega_{\rm c}} + \frac{\beta_2^2 \omega_2}{\omega_{\rm c}} \right) \hat{a}^\dagger \hat{a} \right] \hat{a}^\dagger \hat{a} + \omega_1 \hat{B}_1^\dagger \hat{B}_1 + \omega_2 \hat{B}_2^\dagger \hat{B}_2 \,. \tag{S8}$$

It is possible to separate the Hilbert space spanned by the Hamiltonian eigenvectors into subspaces with a definite number of photons n. The eigenstates of $\hat{H}_{\rm om}$ can be labelled by three indexes: the first two labelling the mechanical occupation numbers (phonons) of the two mirrors, dressed by the presence of n cavity photons while the third label describes the number n of cavity photons. We use the following notation

$$|\psi_{k,q,n}\rangle = |k_n\rangle \otimes |q_n\rangle \otimes |n\rangle_c \equiv |k, q, n\rangle \,. \tag{S9}$$

In particular, the photon occupation number n determines the nth cavity-photon subspace, while the first two kets ($|k_n\rangle$ and $|q_n\rangle$) are the displaced mechanical Fock states, respectively, for the first and second mirror. The action of the dressed phonon operators on the eigenstates satisfy the relations

$$\begin{aligned}
&\hat{B}_1 |k_n, q_n, n\rangle = \sqrt{k}\, |(k-1)_n, q_n, n\rangle \,, && \hat{B}_2 |k_n, q_n, n\rangle = \sqrt{q}\, |k_n, (q-1)_n, n\rangle \,, \\
&\hat{B}_1^\dagger |k_n, q_n, n\rangle = \sqrt{(k+1)}\, |(k+1)_n, q_n, n\rangle, && \hat{B}_2^\dagger |k_n, q_n, n\rangle = \sqrt{(q+1)}\, |k_n, (q+1)_n, n\rangle.
\end{aligned} \tag{S10}$$

The explicit expression of the single displaced Fock state $|k_n\rangle_i$ for the ith mirror is (note that from Eq. (S7) and in the subspace with n cavity photons we have $\hat{B}_i^\dagger = \hat{b}_i^\dagger + n\beta_i \hat{I}_i$)

$$|k_n\rangle_i = \frac{1}{\sqrt{k!}} \hat{B}_i^{\dagger k} |0_n\rangle_i = \frac{1}{\sqrt{k!}} (\hat{b}_i^\dagger + n\beta_i \hat{I}_i)^k |0_n\rangle_i \,, \tag{S11}$$

where n-photons manifold and $|0_n\rangle_i$ is the coherent ground state for mirror i with n cavity photons, as is shown by the relation

$$\hat{b}_i |0_n\rangle_i = -n\beta_i |0_n\rangle_i \,, \tag{S12}$$

obtained using Eq. (S7) in $\hat{B}_i |0_n\rangle_i = 0$. Using the displacement operator $\hat{D}(n\beta_i) = \exp[n\beta_i(\hat{b}_i - \hat{b}_i^\dagger)]$, we have

$$|0_n\rangle_i = \hat{D}(n\beta_i)|0\rangle_i = \sum_j e^{-|n\beta_i|^2/2} \frac{(-n\beta_i)^j}{\sqrt{j!}} |j\rangle_i \,. \tag{S13}$$

In addition, from the relation $\hat{D}(n\beta)\hat{b}^\dagger \hat{D}^\dagger(n\beta) = b^\dagger + n\beta$ [3], using Eqs. (S11) and (S13), we obtain

$$|k_n\rangle_i = \frac{1}{\sqrt{k!}} (\hat{b}_i^\dagger + n\beta_i \hat{I}_i)^k |0_n\rangle_i = \frac{1}{\sqrt{k!}} (\hat{b}_i^\dagger + n\beta_i \hat{I}_i)^k \hat{D}(n\beta_i)|0\rangle = \hat{D}(n\beta_i) \frac{1}{\sqrt{k!}} \hat{b}_i^{\dagger k} |0\rangle = \hat{D}(n\beta_i)|k_0\rangle \tag{S14}$$

Finally, after a little bit of algebra, we have

$${}_i\langle k_0'|k_n\rangle_i = {}_i\langle k_0'|[\hat{D}(n\beta_i)]|k_0\rangle_i = D_{k',k}(n\beta_i) = \sqrt{k!/k'!}(n\beta_i)^{k'-k} e^{-|n\beta_i|^2/2} L_k^{k'-k}(|n\beta_i|^2) \,, \tag{S15}$$

where $L_k^p(x)$ are the associated Laguerre polynomials.

In conclusion, the standard optomecanical Hamiltonian can be diagonalized as shown above and we obtain

$$\hat{H}|k, q, n\rangle = E_{k,q,n}|k, q, n\rangle \,, \tag{S16}$$

where

$$E_{k,q,n} = \omega_c n \left[1 - \left(\frac{\beta_1^2 \omega_1}{\omega_c} + \frac{\beta_2^2 \omega_2}{\omega_c}\right) n\right] + \omega_1 k + \omega_2 q \,, \tag{S17}$$

or, in more compact form [replacing for clarity the phonon labels as $(k, q) \to (k_1, k_2)$]

$$E_{k_1,k_2,n} = \omega_c n - \sum_i g_i^2 n^2/\omega_i + \sum_i \omega_i k_i. \tag{S18}$$

II. THE DCE INTERACTION HAMILTONIAN AS A PERTURBATION

In this section, we introduce the DCE interaction term. We consider this additional contribution as a perturbation to the optomechanical Hamiltonian $\hat{H}_{\rm om}$. This additional term creates and destroys photon pairs. Here we consider processes at the lowest nonzero perturbation order. Thus we limit our calculations to the subspace containing zero and two cavity photons. The DCE interaction Hamiltonian $\hat{V}_{\rm DCE}$ is calculated using second-order perturbation theory. These perturbative calculations are carried out using the James' method [4]:

$$\hat{H}^{(2)}_{\rm eff} = \frac{1}{i}\hat{V}^{I(0,2)}_{\rm DCE}(t)\int_0^t \hat{V}^{I(0,2)}_{\rm DCE}(t')dt' \,, \tag{S19}$$

where

$$\hat{V}^{I(0,2)}_{\rm DCE}(t) = e^{i\hat{H}t}\hat{V}^{(0,2)}_{\rm DCE}e^{-i\hat{H}t}$$

is the projection operator $\hat{V}_{\rm DCE}$ acting in the subspace containing 0 and 2 photons expressed in the interaction picture. After some algebra, we obtain (we assume $g_1 = g_2 \equiv g$):

$$\hat{V}^{I(0,2)}_{\rm DCE}(t) = \frac{g}{2}\sum_{\substack{k\ q\\ k'\ q'}} A^{k'\ q'}_{k\ q}\,|k_2,q_2,2\rangle\langle k'_0,q'_0,0|\,e^{i\omega^{k'\ q'}_{k\ q}t} + (A^{k'\ q'}_{k\ q})^\dagger\,|k'_0,q'_0,0\rangle\langle k_2,q_2,2|\,e^{-i\omega^{k'\ q'}_{k\ q}t} \tag{S20}$$

where

$$\omega^{k'\ q'}_{k\ q} = 2\Omega_{\rm c} + (k'-k)\omega_1 + (q'-q)\omega_2; \tag{S21}$$

with $\Omega_{\rm c} = 1+\tilde{\beta}_1+\tilde{\beta}_2$, $\tilde{\beta}_i = g^2/(\omega_i\omega_{\rm c})$. We also have:

$$A^{k'\ q'}_{k\ q} = \left\langle k_2, q_2, 2\left|\hat{V}_{\rm DCE}\right|k'_0, q'_0, 0\right\rangle ;$$

that can be expressed in more explicit form as

$$\begin{aligned} A^{k'\ q'}_{k\ q} =& \sqrt{2}\left\{[\sqrt{k'}\langle k_2|(k'-1)_0\rangle + \sqrt{k'+1}\langle k_2|(k'+1)_0\rangle]\langle q_2|q'_0\rangle + \right.\\ & \left.[\sqrt{q'}\langle q_2|(q'-1)_0\rangle + \sqrt{q'+1}\langle q_2|(q'+1)_0\rangle]\langle k_2|k'_0\rangle\right\} . \end{aligned} \tag{S22}$$

Note that $A^{k'\ q'}_{k\ q} = A^{\dagger k\ q}_{k'\ q'}$. Using $D_{k',k}(2\beta_i) = \langle k'_2|k_0\rangle$, we have:

$$\begin{aligned} A^{k'\ q'}_{k\ q} =& \sqrt{2}[\sqrt{k'}D_{k,k'-1}(2\beta_1) + \sqrt{k'+1}D_{k,k'+1}(2\beta_1)]D_{q,q'}(2\beta_2) + \\ & \sqrt{2}[\sqrt{q'}D_{q,q'-1}(2\beta_2) + \sqrt{q'+1}D_{q,q'+1}(2\beta_2)]D_{k,k'}(2\beta_1)\,, \end{aligned} \tag{S23}$$

where the matrix elements of the displacement operators can be expressed in terms of associated Laguerre polynomials: $D_{k',k}(\alpha) = \sqrt{k!/k'!}\alpha^{k'-k}e^{-|\alpha|^2/2}L^{k'-k}_k(|\alpha|^2)$.

A. One phonon – zero photons subspace

The $(1+0)$ subspace containing zero photons and one phonon excitation is spanned by the eigenvectors $|1,0,0\rangle$ and $|0,1,0\rangle$. At $\omega_2 \sim \omega_1$, these states are degenerate in absence of the $\hat{V}_{\mathrm{DCE}}$ interaction. In presence of such interaction, degeneracy is removed and an avoided level crossing can be observed. This effect can be described by introducing an effective Hamiltonian. Specifically: a) we introduce Eq. (S20) into Eq. (S19); b) we perform the integration; c) we limit the calculations to matrix elements containing zero photons; d) we transform back to the Schrödinger picture; e) finally, we project the result into the $(1+0)$ subspace spanned by the vectors $|1,0,0\rangle$, $|0,1,0\rangle$. We obtain

$$\hat{H}_{\mathrm{eff}} = \hat{H}^0_{\mathrm{eff}} + [\lambda^{10}_{01}\,|0,1,0\rangle\langle 1,0,0| + \mathrm{H.c.}], \tag{S24}$$

where

$$\hat{H}^0_{\mathrm{eff}} = \Omega_1\,|1,0,0\rangle\langle 1,0,0| + \Omega_2\,|0,1,0\rangle\langle 0,1,0|\,, \tag{S25}$$

with $\Omega_1 = \omega_1 + \Delta_{10}$ and $\Omega_2 = \omega_2 + \Delta_{01}$, and with

$$\Delta_{10} = -\frac{g^2}{4}\sum_{k\,q}\frac{A^{1\,0\dagger}_{k\,q}A^{1\,0}_{k\,q}}{2\Omega_{\mathrm{c}} + (k-1)\omega_1 + q\omega_2}; \tag{S26}$$

$$\Delta_{01} = -\frac{g^2}{4}\sum_{k\,q}\frac{A^{0\,1\dagger}_{k\,q}A^{0\,1}_{k\,q}}{2\Omega_{\mathrm{c}} + k\omega_1 + (q-1)\omega_2}; \tag{S27}$$

$$\lambda^{10}_{01} = -\frac{g^2}{4}\sum_{k\,q}\frac{A^{0\,1\dagger}_{k\,q}A^{1\,0}_{k\,q}}{2\Omega_{\mathrm{c}} + (k-1)\omega_1 + q\omega_2}. \tag{S28}$$

In Fig. S1, we show a comparison between the numerically calculated normalized Rabi splitting $(2\lambda^{10}_{01}\omega_1)$ between the two one-phonon states $|1,0,0\rangle$ and $|0,1,0\rangle$ and the corresponding theoretical value calculated using second-order perturbation theory as a function of the normalized optomechanical coupling g/ω_1. The agreement is very good for g/ω_1 below 0.1.

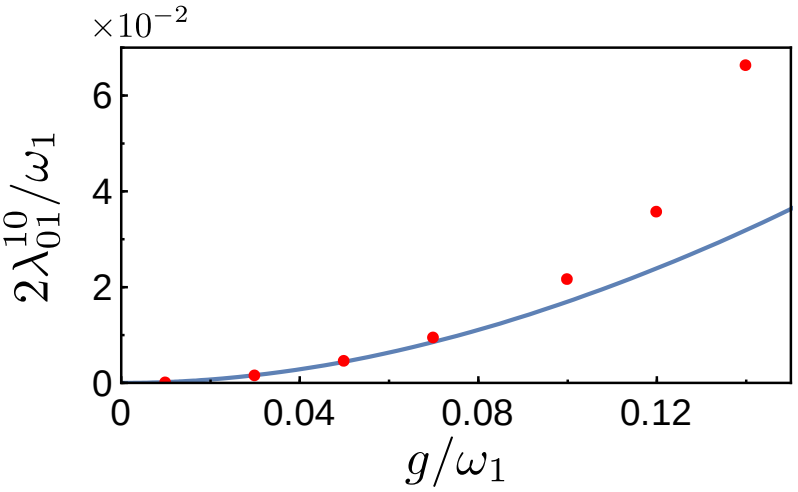

Figure S1. Comparison between the numerically calculated normalized Rabi splitting (red points) (corresponding to twice the effective coupling between the two one-phonon states $|1,0,0\rangle$ and $|0,1,0\rangle$) and the corresponding calculation using second-order perturbation theory (solid blue curve).

B. Two phonons – zero photons subspace

The $(2+0)$ subspace with zero photons in the cavity and containing two phonon excitations is spanned by the eigenvectors: $|2,0,0\rangle$, $|0,2,0\rangle$ and $|1,1,0\rangle$. Also in this case, at $\omega_2 \sim \omega_1$, these states are degenerate in the absence of the $\hat{V}_{\rm DCE}$ interaction. With the introduction of $\hat{V}_{\rm DCE}$, degeneracy is removed, and an avoided level crossing can be observed. Following the same procedure described in the previous subsection, this effect can be described by introducing an effective Hamiltonian acting on the $(2+0)$ subspace. We obtain:

$$\hat{H}_{\rm eff} = \hat{H}^0_{\rm eff} + [\lambda^{02}_{20}\,|2,0,0\rangle\langle 0,2,0| + \lambda^{11}_{20}\,|2,0,0\rangle\langle 1,1,0| + +\lambda^{11}_{02}\,|0,2,0\rangle\langle 1,1,0| + \text{H.c.}]; \quad \text{(S29)}$$

where

$$\hat{H}^0_{\rm eff} = \Omega_{20}\,|0,2,0\rangle\langle 0,2,0| + \Omega_{02}\,|2,0,0\rangle\langle 2,0,0| + \Omega_{11}\,|1,1,0\rangle\langle 1,1,0|\,; \quad \text{(S30)}$$

with $\Omega_{20} = 2\omega_1 + \Delta_{20}$, $\Omega_{11} = \omega_1 + \omega_2 + \Delta_{11}$ and $\Omega_{02} = 2\omega_2 + \Delta_{02}$, and

$$\lambda^{02}_{20} = -\frac{g^2}{4}\sum_{k\,q}\frac{A^{0\,2\dagger}_{k\,q}A^{2\,0}_{k\,q}}{2\Omega_{\rm c} + (k-2)\omega_1 + q\omega_2}, \quad \text{(S31)}$$

$$\lambda_{20}^{11} = -\frac{g^2}{4} \sum_{k\,q} \frac{A_{k\,q}^{1\,1\dagger} A_{k\,q}^{2\,0}}{2\Omega_{\rm c} + (k-2)\omega_1 + q\omega_2}, \tag{S32}$$

$$\lambda_{02}^{11} = -\frac{g^2}{4} \sum_{k\,q} \frac{A_{k\,q}^{1\,1\dagger} A_{k\,q}^{0\,2}}{2\Omega_{\rm c} + k\omega_1 + (q-2)\omega_2}, \tag{S33}$$

$$\Delta_{20} = -\frac{g^2}{4} \sum_{k\,q} \frac{A_{k\,q}^{2\,0\dagger} A_{k\,q}^{2\,0}}{2\Omega_{\rm c} + (k-2)\omega_1 + q\omega_2}, \tag{S34}$$

$$\Delta_{02} = -\frac{g^2}{4} \sum_{k\,q} \frac{A_{k\,q}^{0\,2\dagger} A_{k\,q}^{0\,2}}{2\Omega_{\rm c} + k\omega_1 + (q-2)\omega_2}, \tag{S35}$$

$$\Delta_{11} = -\frac{g^2}{4} \sum_{k\,q} \frac{A_{k\,q}^{1\,1\dagger} A_{k\,q}^{1\,1}}{2\Omega_{\rm c} + (k-1)\omega_1 + (q-1)\omega_2}. \tag{S36}$$

A comparison of these perturbative analytical results with the numerical result is provided in the Tables I and II. The discrepancies can be ascribed to higher-order terms that at a coupling strength $g/\omega_1 = 0.1$ provide non-negligible contributions.

	$2\lambda_{01}^{10}$	$2\lambda_{20}^{11}$	$2\lambda_{20}^{02}$	$2\lambda_{02}^{11}$
Numerical $\simeq$	0.0217	0.0217	0.0384	0.0167
Theoretical $\simeq$	0.0170	0.0171	0.0348	0.0177

Table I. Comparison between the effective splittings calculated both numerically (as difference between the eigenvalues) and analytically using the James' method [4]. In particular, the theoretical values corresponding to $2\lambda_{20}^{11}$, $2\lambda_{20}^{02}$ and $2\lambda_{02}^{11}$ are obtained by the diagonalization of a 3×3 matrix representing the effective Hamiltonian in the subspace with two phonon excitations and zero photons. The cavity-mode resonance frequency is $\omega_{\rm c} = 0.85\,\omega_1$ and $\omega_2 = \omega_1$.

	Δ_{10}	Δ_{01}	Δ_{11}	Δ_{02}	Δ_{20}
Numerical $\simeq$	-0.0131	-0.0159	-0.0221	-0.0239	-0.0217
Theoretical $\simeq$	-0.0120	-0.0121	-0.0207	-0.0199	-0.0207

Table II. Comparison between the numerically calculated energy shifts and the analytical calculations obtained using the James' method. The mechanical frequency of mirror 2 is $\omega_2 = 0.94\,\omega_1$. For this value the energy levels investigated do not interact significantly, and hence the energy shifts are not affected by the level-repulsion effect that occurs when the mirrors are on resonance with each other. The cavity-mode resonance frequency is $\omega_c = 0.85\,\omega_1$.

III. ENERGY LEVELS AND SPLITTINGS FOR DIFFERENT OPTOMECHANICAL COUPLINGS.

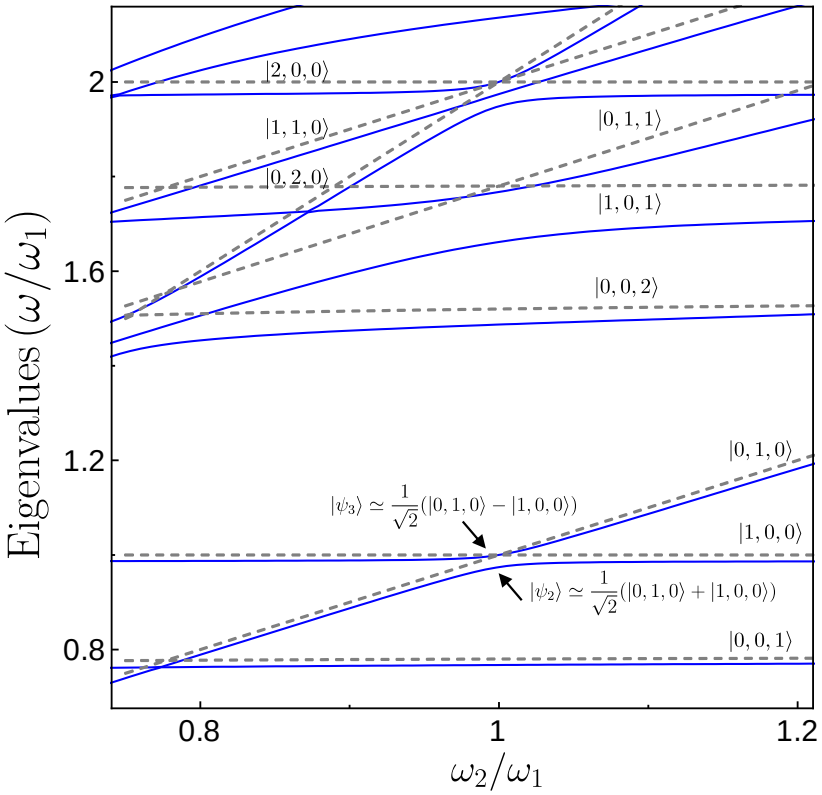

Figure S2. Lowest energy levels of the system Hamiltonian as a function of ω_2/ω_1. We used $g/\omega_1 = 0.1$ and $\omega_c/\omega_1 = 0.8$.

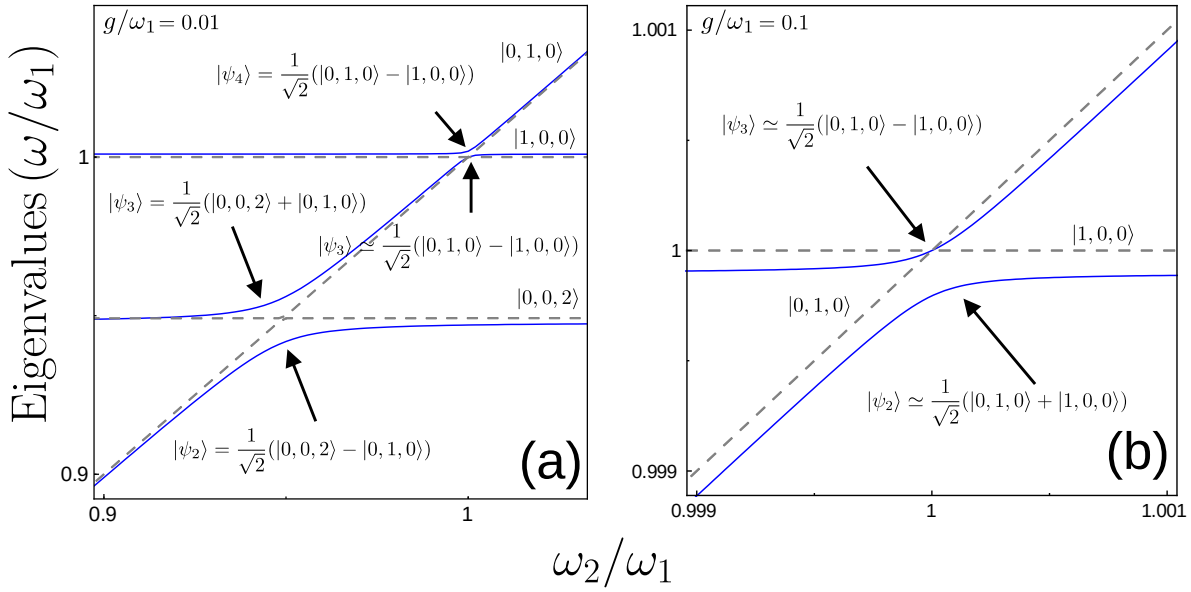

Figure S3. Relevant lowest energy levels of the system Hamiltonian as a function of ω_2/ω_1. Panel (a) has been obtained using $g/\omega_1 = 0.01$ and $\omega_c/\omega_1 = 0.475$. Panel (b) has been obtained with the same parameters of Fig. S2.

Figure S2 displays the lowest energy levels $E_j - E_0$ of the system Hamiltonian as a function of the ratio between the mechanical frequency of mirror 2 and that of mirror 1. An optomechanical coupling $g/\omega_1 = 0.1$ has been used, the cavity-mode resonance frequency is $\omega_c = 0.8\,\omega_1$. Starting from the lowest energy levels, we first avoided level crossing originates from the coherent coupling of the zero-photon states $|1,0,0\rangle$ and $|0,1,0\rangle$. At the minimum energy splitting, the resulting states are well approximated by $|\psi_{2,3}\rangle \simeq (1/\sqrt{2})(|1,0,0\rangle \pm |0,1,0\rangle)$. As shown in the main paper and in the previous section, this mirror-mirror interaction is a result of virtual exchange of cavity photon pairs. This coherent coupling is greatly enhanced by the presence of a cavity photon, resulting in the larger splitting $(E_6 - E_5)$, corresponding to the states $|\psi_{5,6}\rangle \simeq (1/\sqrt{2})(|1,0,1\rangle \pm |0,1,1\rangle)$. At higher energy, at $\omega_2/\omega_1 \sim 1$, $\hat{V}_{\rm DCE}$ removes the degeneracy between the three states $|2,0,0\rangle$, $|0,2,0\rangle$, and $|1,1,0\rangle$, determining a two-phonon coupling between the two mirrors.

Figure S3 shows the relevant energy levels of the system Hamiltonian $\hat{H}_s$ as a function of the ratio ω_2/ω_1. For the panel (a) an optomechanical coupling $g/\omega_1 = 0.01$ has been used and the cavity-mode resonance frequency is $\omega_c = 0.475\,\omega_1$. The lowest energy anticrossing corresponds to the resonance condition for the DCE. The higher energy one is the signature

of the mirror-mirror interaction mediated by the virtual DCE photons. At the minimum energy splitting $2\lambda_{10}^{01} \simeq 1,85 \times 10^{-2}\omega_1$, the resulting states are well approximated by $|\psi_{3,4}\rangle \simeq (1/\sqrt{2})(|1,0,0\rangle \pm |0,1,0\rangle)$. In panel (b) we use $g/\omega_1 = 0.1$. In this case the cavity-mode resonance frequency is $\omega_c = 0.8\,\omega_1$. Also in this case, the anticrossing is the signature of the mirror-mirror interaction mediated by the virtual DCE photons. At the minimum energy splitting $2\lambda_{10}^{01} \simeq 2,56 \times 10^{-2}\omega_1$, the resulting states are well approximated by $|\psi_{2,3}\rangle \simeq (1/\sqrt{2})(|1,0,0\rangle \pm |0,1,0\rangle)$.

IV. SYSTEM DYNAMICS UNDER A SINGLE-TONE CONTINUOUS-WAVE MECHANICAL DRIVE: ADDITIONAL RESULTS

We start investigating the system dynamics at $T = 0$, with the system starting from its ground state, and introducing the excitation of mirror 1 by a single-tone continuous-wave mechanical drive $\mathcal{F}_1(t) = \mathcal{A}\cos(\omega_{\rm d} t)$, with $\omega_d = \omega_1$. Figure S4 shows the time evolution of the mean phonon numbers of the two mirrors $\langle \hat{B}_i^\dagger \hat{B}_i \rangle$ and of the intracavity mean photon number $\langle \hat{A}^\dagger \hat{A} \rangle$. Here $\hat{A}, \hat{B}_i$ are the *physical* photon and phonon operators (see main paper). We assume a zero-temperature reservoir and use $\gamma_1 = \gamma_2 = \gamma = \omega_1/260$ and $\kappa = \gamma$ for the mechanical and photonic loss rates. We consider a weak ($\mathcal{A}/\gamma = 0.95$) resonant excitation of mirror 1. Panel (a) has been obtained using $g/\omega_1 = 0.1$ and $\omega_c/\omega_1 = 0.8$. Panel (b) using $g/\omega_1 = 0.03$ and $\omega_c/\omega_1 = 0.495$. Panel (c) using $g/\omega_1 = 0.01$ and $\omega_c/\omega_1 = 0.475$. We set $\omega_2 = \omega_1$. The results shown in Fig. S4 demonstrate that the excitation transfer mechanism via virtual DCE photon pairs, proposed here, works properly. In steady state, mirror 2 reaches almost the same excitation intensity as the driven mirror 1 at normalized couplings $g = 0.1$ and $g = 0.03$. The photon population remains very low throughout the considered time window. In Fig. S5, in order to obtain the maximum excitation transfer between the two mirrors (despite the small coupling strength $g/\omega_1 = 0.01$), we investigate the system dynamics using $\omega_c = 0.5\,\omega_1$. We also consider the system initially in a thermal state with a normalized thermal energy $kT/\omega_1 = 0.208$, corresponding to a temperature $T = 60$ mK for $\omega_1/2\pi = 6$ GHz. During, its time evolution, the system interacts with thermal baths with the same temperature T. The obtained results show that a good mechanical transfer is achieved. However, in this case, a significant amount of real photon pairs are generated. This configuration can be used to probe the DCE effect in the presence of thermal photons.

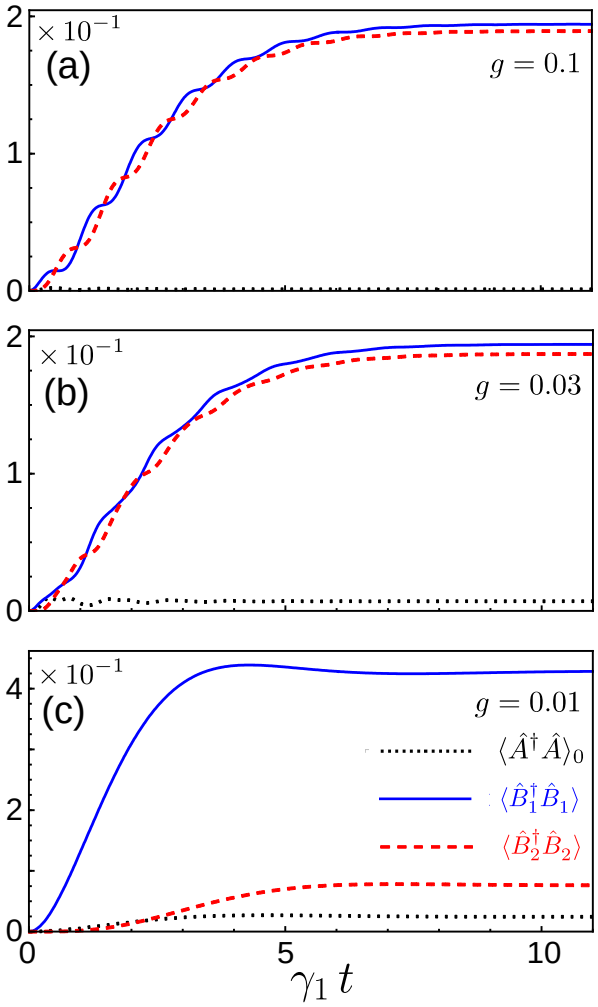

Figure S4. System dynamics under continuous-wave drive of mirror 1 for different optomechanical coupling strengths. The blue solid and red dashed curves describe the mean phonon numbers $\langle \hat{B}_1^\dagger \hat{B}_1 \rangle$ and $\langle \hat{B}_2^\dagger \hat{B}_2 \rangle$, respectively, while the black dotted curve describes the mean intracavity photon number $\langle \hat{A}^\dagger \hat{A} \rangle$. Parameters are given in the text.

V. MECHANICAL EXCITATION TRANSFER: PULSED EXCITATION

We now investigate the transfer of mechanical excitations mediated by virtual photon pairs by exciting mirror 1 with a resonant Gaussian pulse:

$$\mathcal{F}_1(t) = \mathcal{A}\,\mathcal{G}(t - t_0)\cos(\omega_\mathrm{d}\, t),$$

where $\omega_\mathrm{d} = \omega_1$, and $\mathcal{G}(t)$ is a normalized Gaussian function with standard deviation $\sigma = 1/(10\lambda_{10}^{01})$. We consider the case of the strong coupling regime, when the mirror-mirror

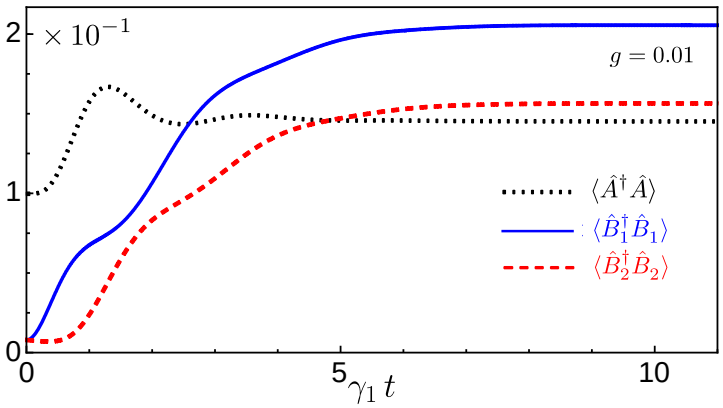

Figure S5. System dynamics for $\omega_c = 0.5\omega_1$ under continuous-wave drive of mirror 1, normalized coupling $g/\omega_1 = 0.01$ and T= 60 mK. The blue solid and red dashed curves describe the mean phonon numbers $\langle \hat{B}_1^\dagger \hat{B}_1 \rangle$ and $\langle \hat{B}_2^\dagger \hat{B}_2 \rangle$, respectively, while the black dotted curve describes the mean intracavity photon number $\langle \hat{A}^\dagger \hat{A} \rangle$ arising due to the DCE.

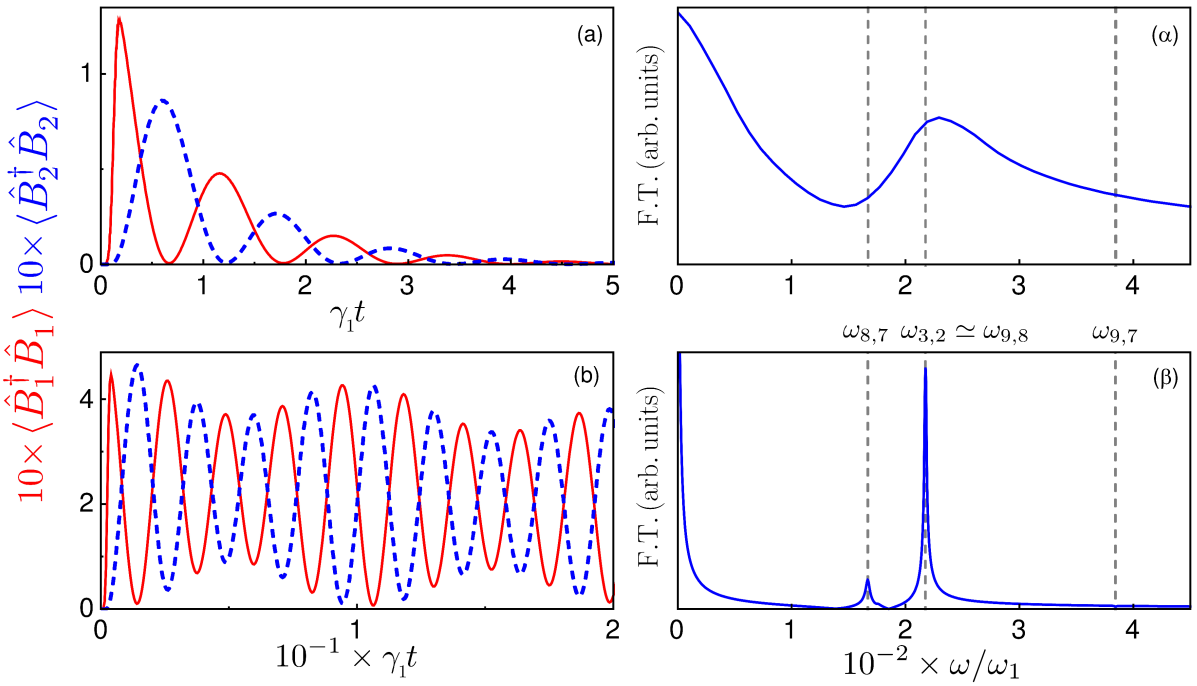

Figure S6. Time evolution of the mean phonon numbers of the two mirrors after the arrival of the pulse. We consider two different amplitudes which increase from top to bottom: $\mathcal{A} = 0.25\,\pi$ (a), 0.45π (b). Specifically, panels (a-b) display the mean phonon numbers $\langle \hat{B}_i^\dagger \hat{B}_i \rangle$. Panels ($\alpha$-$\beta$) display the Fourier transform of the mean phonon number shown in the corresponding panel on the left. Other parameters are given in the text.

coupling strength λ_{10}^{01} is larger than the total decoherence rate $\gamma_1+\gamma_2$. We set the resonance frequency of mirror 2 to $\omega_2 \simeq \omega_1$ providing the minimum level splitting $2\lambda_{10}^{01}$. The system starts in its ground state. Figure S6 displays the system dynamics after the pulse arrival and the Fourier transform of the mean phonon number of mirror 1 (no relevant changes occur for mirror 2), obtained for pulses with amplitudes increasing from top to bottom: $\mathcal{A} = 0.25\pi, 0.45\pi$. Panels S6(a) and S6($\alpha$) have been obtained using the loss rates $\gamma = 3.5\times10^{-3}\omega_1$ and $\kappa = 0.5\gamma$. Figure S6(a) displays coherent and reversible sinusoidal oscillations (with peak amplitudes decaying exponentially), showing that the mechanical state of the spatially separated mirrors is transferred from one to the other at a rate $\omega_{3,2} \equiv E_3 - E_2 = \lambda_{10}^{01}$, as confirmed by the peak in the Fourier transform in Fig. S6(α). We notice that the position and broadening of the peak at $\omega_{3,2}$ in Fig. S6(α) is influenced by the initial dynamics of $\langle \hat{B}_1^\dagger \hat{B}_1 \rangle$, which in turn is affected by the pulse shape (Fig. S7 displays the corresponding spectrum for mirror 2). The higher peak at $\omega = 0$ originates from the exponential decay of the signal. These results clearly show that, for the weaker excitation amplitude ($\mathcal{A} = 0.25\pi$), only the one-phonon states $|1,0,0\rangle$ and $|0,1,0\rangle$ are excited significantly and contribute to the dynamics.

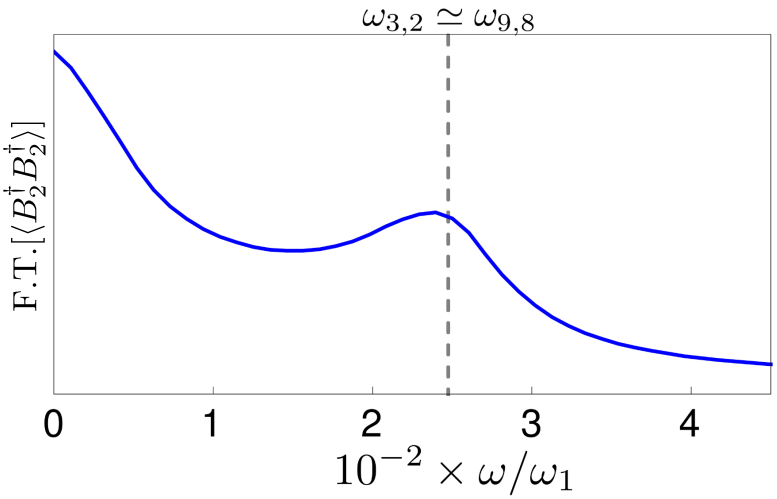

Figure S7. Fourier transform of the mean phonon number of mirror 2 obtained for a pulse with amplitude $\mathcal{A} = 0.25\pi$.

By increasing the pulse amplitude [Fig. S6(b)], the mean phonon numbers grow significantly and the signals are no more sinusoidal, owing to the additional excitation of the states $|2,0,0\rangle$, $|1,1,0\rangle$, and $|0,2,0\rangle$, whose DCE-induced coupling gives rise to the hybridized

energy eigenstates $|\psi_7\rangle$, $|\psi_8\rangle$, and $|\psi_9\rangle$. In order to better distinguish the nonsinusoidal behaviour, we used much lower loss rates: $\gamma = 8 \times 10^{-5}\omega$ and $\kappa = 0.5\gamma$. Figure S6(β) shows the appearence of an additional peak at $\omega = \omega_{8,7}$, confirming that higher-energy mechanical states get excited. We observe that the frequency splitting $\omega_{9,8}$ is very close to $\omega_{3,2}$, hence, it does not give rise to a new peak in Fig. S6(β). Moreover, the frequency splitting at $\omega_{9,7}$ does not contribute significantly to the dynamics as confirmed by the spectrum in Fig. S6(β). An analytic calculation based on three coupled levels confirms that the used parameters give rise to a negligible contribution at $\omega_{9,7}$.

VI. MECHANICAL EXCITATION TRANSFER: NONADIABATIC EFFECTIVE SWITCHING OF THE INTERACTION

As pointed out in the last paragraph of the main paper, if it is possible to control the interaction time (as currently realized in superconducting artificial atoms), e.g., by rapidly changing the resonance frequencies of the mechanical oscillators, the interaction scheme proposed here would represent an attractive architecture for quantum information processing with optomechanical systems. Here we provide some examples of quantum state transfer. In Fig. S8, we show the phonon population dynamics obtained preparing the system in three different initial states (a) $|1,0,0\rangle$, (b) $\frac{1}{\sqrt{2}}(|0,0,0\rangle + |1,0,0\rangle)$, (c) $|2,0,0\rangle$. Mirror 2 is initially set at a mechanical frequency $\omega_2^{\rm in}$. This value must be chosen sufficiently far from the value $\omega_2^{\rm min} \simeq 0.99\,\omega_1$ corresponding to the minimum splitting between states $|1,0,0\rangle$ and $|0,1,0\rangle$. In particular, we have fixed $\omega_2^{\rm in} = \omega_2^{\rm min} - \delta$ with $\delta = 0.069\,\omega_1$. This value is also sufficiently far from the region where the avoided three-level crossing between the states $|\psi_i\rangle$ with $i = 7, 8, 9$ appears. Subsequently, a time-dependent perturbation $H_{\rm na} = f(t)\hat{B}_2^\dagger \hat{B}_2$ [with $f(t) \approx \theta(t - t_0)$] is introduced in order to modify the resonance frequency of mirror 2 (θ is the Heaviside step function). More specifically $f(t) = \delta\,[\sin^2[\Omega(t-t_0)\theta(t-t_0) + \sin^2[\Omega(t-t_f)\theta(t-t_f)]]$ is a smoothed step function, where δ fixes the change in mechanical frequency of mirror 2, t_0 is the time when the frequency starts to change, $t_f = t_0 + \pi/(2A)$, and Ω is the frequency setting the smoothness.

This enables a non-adiabatic transition from the frequency region with $\omega_2 = \omega_2^{\rm in}$, where the states $|2,0,0\rangle$, $|1,0,0\rangle$ and $|0,1,0\rangle$ are eigenstates of the system, to the frequency region $\omega_2 = \omega_2^{\rm min}$ where the former states are no longer eigenstates of the system. As a consequence,

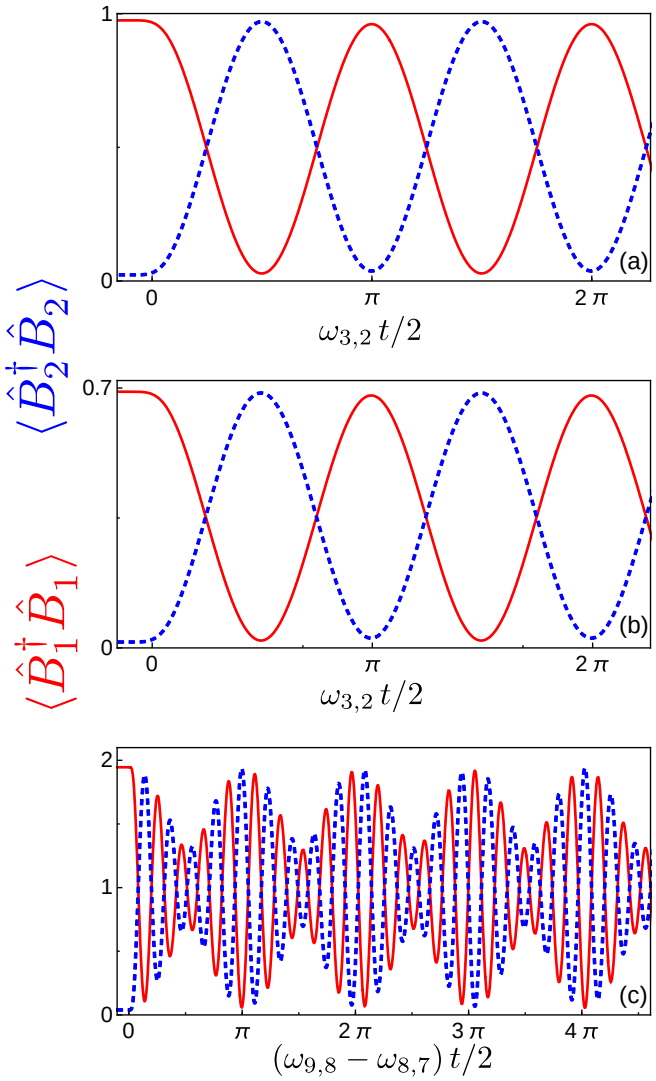

Figure S8. Time evolution of the mean phonon numbers of the two mirrors obtained preparing the system in an initial state (a) $|1,0,0\rangle$, (b) $\frac{1}{\sqrt{2}}(|1,0,0\rangle + |0,0,1\rangle)$, (c) $|2,0,0\rangle$. Mirror 2 is initially set at a mechanical frequency $\omega_2^{\rm in}$ (details are given in the text). We note that the dynamics display oscillations, (a) and (b), due to the avoided level crossing between the states $|\psi_3\rangle$ and $|\psi_2\rangle$ with frequency equal to $\omega_{3,2}$; (c) due to the splittings between the states $|\psi_9\rangle$, $|\psi_8\rangle$ and $|\psi_7\rangle$, whose transitions from higher to lower levels give rise to beats (the details are given in the text).

the dynamics of the phonon populations of the two mirrors display *quantum Rabi-like* oscillations [see Fig. S8(a) and (b)] due to the avoided level crossing between the states $|\psi_3\rangle$ and $|\psi_2\rangle$ (the eigenstates of the systems are, in this frequency region, the symmetric and

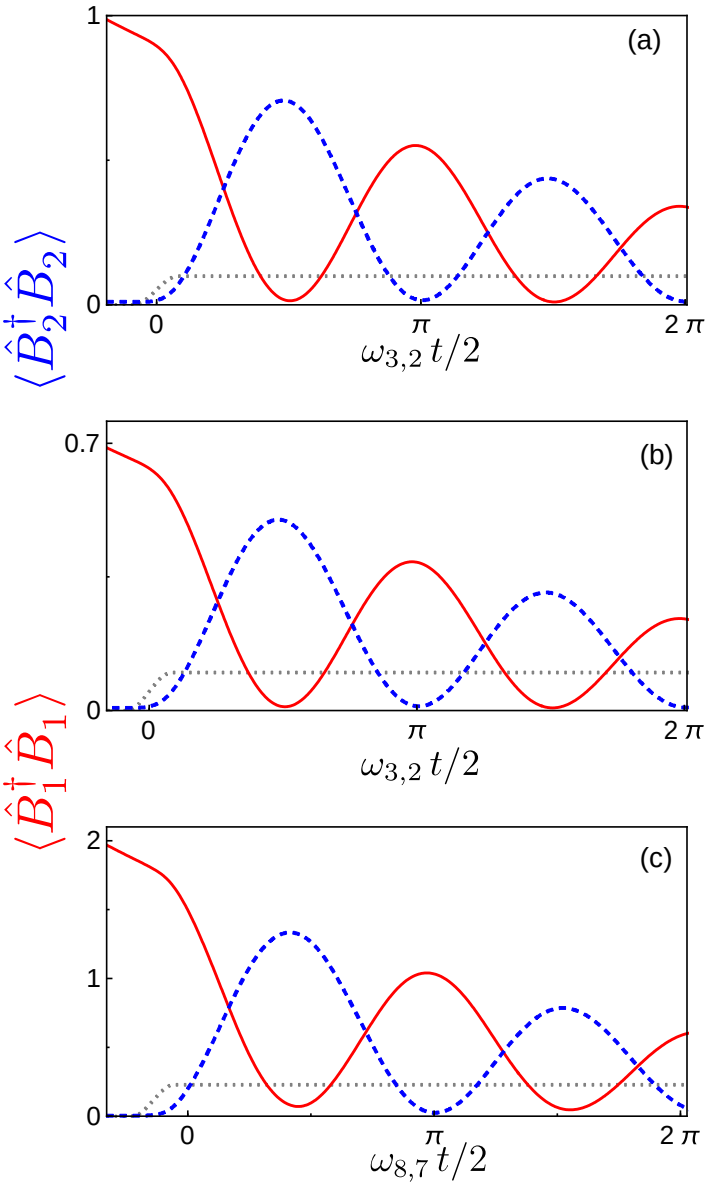

Figure S9. Time evolution of the mean phonon numbers of the two mirrors calculated after a non-adiabatic switching of the interaction, as explained in Fig. S8, but in the presence of losses both in mirrors and cavity. The parameters are the same as in Fig. S8; in addition we have $\gamma = \gamma_1 = \gamma_2 = \omega_1/650$ and $\kappa = 0.5\,\gamma$. The system is initially preparated in the states (a) $|1,0,0\rangle$, (b) $\frac{1}{\sqrt{2}}(|1,0,0\rangle + |0,0,1\rangle)$, (c) $|2,0,0\rangle$. As we can observe, the oscillations are damped and disappear after a few periods. In (c) the losses do not allow for observations of beats oscillations having a longer time period. The dotted gray lines show how the frequency of mirror 2 is tuned into resonance with mirror 1 (details are given in the text).

antisymmetric superpositions of $|1,0,0\rangle$ and $|0,1,0\rangle$; see Fig. 1b in the main paper). In Fig. S8(c), the avoided level crossing between the states $|\psi_9\rangle$, $|\psi_8\rangle$, and $|\psi_7\rangle$ gives rise to transitions from higher to lower levels. As a consequence, we observe beats between the two transition frequencies $\omega_{8,9}$ and $\omega_{8,7}$ (with the chosen parameters the other frequency transition $\omega_{9,7}$ does not contribute to the beats). Finally, in Fig. S9, we show the time evolution of the mean phonon numbers for the same cases discussed above, but in the presence of losses both in mirrors and cavity. We observe the damping of the population dynamics as expected in presence of losses.

VII. EXPERIMENTAL PLATFORM FOR THE OBSERVATION OF THE PROPOSED EFFECT

A platform to experimentally demonstrate these results is circuit optomechanics using ultra-high-frequency (ω_1 at 4-6 GHz) dilatational resonators [5]. These mechanical oscillators have a resonance frequency $f_m = v/2d$, where v is the average speed of sound and d is the resonator thickness. Their resonant quantum interaction with a superconducting phase qubit, described by the quantum Rabi (or also the Jaynes-Cummings) Hamiltonian, has been experimentally demonstrated [5, 6]. In the present case, we want to estimate the radiation-pressure interaction strength between the high-frequency mechanical resonator and an electromagnetic resonator. In order to estimate the achievable coupling strength, we begin by analyzing the coupling between a mechanical resonator and a flux qubit, experimentally realized in Ref. [5]. Then we use the experimentally achieved qubit-oscillator coupling strength to derive an accurate estimate of the presently achievable radiation-pressure coupling strength between this mechanical resonator and an electromagnetic resonator. Note that the mechanical oscillator considered in Ref. [5] has a quality factor equal to that used in our calculations: $Q = 260$. Moreover, it has been shown that lowering f_m can strongly increase the quality factor [7].

The mechanical resonator is coupled to a superconducting artificial atom through a capacitor [5]. An elastic strain in the vibrational resonator produces, through the piezoelectric effect, a charge on the capacitor enclosing it, which results in a charge Q on the coupling capacitor giving a current $\dot{Q}$. The coupling energy is $\hat{V}' = (\hbar/2e)\,\hat{\varphi}\,\dot{\hat{Q}}$, where $\hat{\varphi}$ is the phase-difference operator of the Josephson junction. Considering only the two lowest energy levels

(qubit) of the artificial atom, the phase operator can be expanded as $\hat{\phi} = (2E'_C/E'_J)^{1/4}\,\hat{\sigma}_x$, resulting in the Rabi-like interaction Hamiltonian

$$\hat{V}'_{qm} = \hbar\,(2E'_C/E'_J)^{1/4}\,\hat{\sigma}_x\,(\dot{\hat{Q}}/2e)\,, \tag{S37}$$

where E'_C and E'_J are the charging energy and the Josephson energy, respectively, of the phase qubit (with $E'_C \ll E'_J$), and $\dot{\hat{Q}}$ is proportional to the vibrational strain velocity $\dot{\hat{x}} = i\omega_1 X_{\rm zpf}\,(\hat{b}_1^\dagger - \hat{b}_1)$ ($X_{\rm zpf}$ is the zero-point fluctuation amplitude of the mechanical coordinate). Finally, this interaction Hamiltonian can also be expressed in the standard Rabi interaction form:

$$\hat{V}'_{qm} = -ig'_m(\hat{b} - \hat{b}^\dagger)\hat{\sigma}_x\,, \tag{S38}$$

where g'_m is the resulting coupling strength and $\hat{b}$ and $\hat{b}^\dagger$ are, respectively, the annihilation and creation operators for a generic mechanical oscillator.

For the observation of the effects described in this paper, optomechanical systems displaying a radiation-pressure interaction Hamiltonian are required. Moreover a strong optomechanical coupling (at least $g/\omega_1 \sim 0.01$) is needed. This kind of interaction with a reasonable coupling strength can be obtained by considering a tripartite system consisting of an electromagnetic resonator, an ultra-high-frequency mechanical resonator, and a superconducting charge qubit mediating the interaction between the former two parts [8, 9]. It has been shown that the presence of the qubit can strongly enhance the optomechanical coupling.

Without presenting a detailed circuit-optomechanical setup, which goes beyond the scope of the present work, we can provide an estimate of the resulting coupling strength which can be achieved within state-of-the-art technology. Specifically, considering one generic mechanical oscillator, coupled through a capacitor to a charge qubit, the qubit-mechanical oscillator interaction Hamiltonian can be written as $\hat{V}_{qm} = 8E_C\,\hat{n}\,(\hat{Q}/2e)$, where $\hat{n}$ is the number operator for the Cooper pairs transferred across the junction. In the full charge qubit limit, $E_J \ll E_C$, the bare qubit transition energy is $\omega_q \approx 4E_C$, and the mechanical coupling is longitudinal, i.e., in the two-state representation $\hat{n} \to \hat{\sigma}_z/2$. The resulting interaction Hamiltonian is

$$\hat{V}_{qm} = \hbar\omega_q\,\hat{\sigma}_z(Q/2e)\,, \tag{S39}$$

which can also be expressed as

$$\hat{V}_{qm} = g_m(\hat{b} + \hat{b}^\dagger)\hat{\sigma}_z\,. \tag{S40}$$

Assuming that the same mechanical oscillator is coupled through the same capacitor to the two different kinds of superconducting qubits, it is possible to compare the two qubit-mechanical oscillator coupling strengths. From Eqs (S37) and (S39), disregarding the phase difference, we obtain

$$\frac{g_m}{g'_m} = \left(\frac{E'_J}{2E'_C}\right)^{\frac{1}{4}} \frac{\omega_q}{\omega_1} \,. \tag{S41}$$

Below we will consider the case $2\omega_q \sim \omega_1$. Assuming the energies E'_J and E'_C for a typical phase qubit (see, e.g. Ref. [7]), we obtain $g_m/g'_m \gtrsim 12$.

Now, following Refs. [8] and [9], we consider the additional interaction of the charge qubit with an electromagnetic resonator, described by the Hamiltonian

$$\hat{V}_{\rm qc} = g_c(\hat{a} + \hat{a}^\dagger)\hat{\sigma}_x \,, \tag{S42}$$

where $\hat{a}$ is the destruction operator of the cavity mode. In the dispersive regime, the qubit-cavity interaction can be well approximated by [10]

$$\hat{V}_{\rm qc} = (g_c^2/2\Delta)\hat{\sigma}_z(\hat{a} + \hat{a}^\dagger)^2 \,, \tag{S43}$$

where $\Delta = \omega_q - \omega_c$. Corrections of the qubit energy not depending on photon operators have been disregarded. Equation (S40) shows that the coupling of the charge qubit with the mechanical oscillator induces a qubit energy shift depending on the mechanical displacement, so that $\omega_q \to \omega_q + 2g_m(\hat{b} + \hat{b}^\dagger)$. Replacing Δ with $\Delta(\hat{x}) = \omega_q + 2g_m(\hat{b} + \hat{b}^\dagger) - \omega_c$ in Eq. (S43), assuming small displacements, and considering the qubit in its ground state, from Eq. (S43) we obtain the following optomechanical interaction,

$$\hat{H}_I = \frac{g}{2}(\hat{a} + \hat{a}^\dagger)^2(\hat{b} + \hat{b}^\dagger) \,, \tag{S44}$$

with

$$g = \frac{2g_m g_c^2}{\Delta^2} \,. \tag{S45}$$

Using $g_m = 0.02\,\omega_1$, corresponding to the value of the electromechanical system employed for the demonstration of single-phonon control of a mechanical resonator [5], assuming $g_m/g'_m = 12$, and considering a detuning $\Delta = 5g_c$, we obtain $g \simeq 0.02\omega_1$. The achievable value could be even higher, noting that the electromechanical system used in Ref. [5] was designed to limit g_m in order to optimize the transfer process [7].

Beyond the direct observation of the energy transfer between the mechanical oscillators (see Fig. 1 in the main text), the effective coherent coupling between the two mirrors can also

be demonstrated by looking at the system response (e.g., $\langle \hat{B}_1^\dagger \hat{B}_1 \rangle$) under continuous-wave weak excitation as a function of the excitation frequency. For $\omega_1 = \omega_2$, if $\lambda > \gamma$, two peaks should be observed, corresponding, e.g., to the avoided level crossing at higher energy in Fig. 2(b) in the main text or to that in Fig. S3(a). In order to confirm that the two observed peaks originate from virtual DCE photons, it would be useful to perform measurements changing the optomechanical coupling. This coupling can be tuned by modifying the gate charge of the qubit mediating the interaction [9]. If the energy splitting originates from virtual DCE photons, as predicted by Eq. (3) in the main text, it should grow quadratically with the optomechanical coupling g (see Fig. S1). The anticrossing behaviour could also be probed, changing d of one of the two dilatational resonators and detecting, e.g., $\langle \hat{B}_1^\dagger \hat{B}_1 \rangle$ at steady state as a function of the thickness d (note that $\omega_2 = v/d$). Two peaks with a splitting determined by the thickness, following the avoided level crossing should be observed (see, e.g., Fig. S3). The detection of the mechanical excitations can be performed following the procedures used in Refs. [7, 11].

---

[1] C. K. Law, "Interaction between a moving mirror and radiation pressure: A Hamiltonian formulation," Phys. Rev. A **51**, 2537 (1995).

[2] V. Macrì, A. Ridolfo, O. Di Stefano, A. F. Kockum, F. Nori, and S. Savasta, "Nonperturbative dynamical casimir effect in optomechanical systems: Vacuum casimir-rabi splittings," Phys. Rev. X **8**, 011031 (2018).

[3] M. O. Scully and M. S. Zubairy, *Quantum Optics* (Cambridge University Press, 1997).

[4] W. Shao, C. Wu, and X.-L. Feng, "Generalized James' effective Hamiltonian method," Phys. Rev. A **95**, 032124 (2017).

[5] A. D. O'Connell, M. Hofheinz, M. Ansmann, R. C. Bialczak, M. Lenander, E. Lucero, M. Neeley, D. Sank, H. Wang, M. Weides, *et al.*, "Quantum ground state and single-phonon control of a mechanical resonator," Nature **464**, 697 (2010).

[6] F. Rouxinol, Y. Hao, F. Brito, A. O. Caldeira, E. K. Irish, and M. D. LaHaye, "Measurements of nanoresonator-qubit interactions in a hybrid quantum electromechanical system," Nanotechnology **27**, 364003 (2016).

[7] A. N. Cleland and M. R. Geller, "Superconducting qubit storage and entanglement with

nanomechanical resonators," Phys. Rev. Lett. **93**, 070501 (2004).

[8] T. T. Heikkilä, F. Massel, J. Tuorila, R. Khan, and M. A. Sillanpää, "Enhancing optomechanical coupling via the Josephson effect," Phys. Rev. Lett. **112**, 203603 (2014).

[9] J.-M. Pirkkalainen, S. U. Cho, F. Massel, J. Tuorila, T. T. Heikkilä, P. J. Hakonen, and M. A. Sillanpää, "Cavity optomechanics mediated by a quantum two-level system," Nat. Commun. **6**, 6981 (2015).

[10] D. Zueco, G. M. Reuther, S. Kohler, and P. Hänggi, "Qubit-oscillator dynamics in the dispersive regime: Analytical theory beyond the rotating-wave approximation," Phys. Rev. A **80**, 033846 (2009).

[11] A. O'Connell and A. N. Cleland, "Microwave-frequency mechanical resonators operated in the quantum limit," in *Cavity Optomechanics* (Springer, 2014) pp. 253–281.

Chapter 6

Resolution of Gauge ambiguities in the USC regime

6.1 Resolution of gauge ambiguities in ultrastrong-coupling cavity quantum electrodynamics

nature physics

ARTICLES

https://doi.org/10.1038/s41567-019-0534-4

Resolution of gauge ambiguities in ultrastrong-coupling cavity quantum electrodynamics

Omar Di Stefano[1], Alessio Settineri[2], Vincenzo Macrì[1], Luigi Garziano[1], Roberto Stassi[1], Salvatore Savasta[1,2*] and Franco Nori[1,3]

In quantum electrodynamics, the choice of gauge influences the form of light–matter interactions. However, gauge invariance implies that all physical results should be independent of this formal choice. The Rabi model, a widespread description for the dipolar coupling between a two-level atom and a quantized electromagnetic field, seemingly violates this principle in the presence of ultrastrong light–matter coupling, a regime that is now experimentally accessible in many physical systems. This failure is attributed to the finite-level truncation of the matter system, an approximation that enters the derivation of the Rabi model. Here, we identify the source of gauge violation and provide a general method for the derivation of light–matter Hamiltonians in truncated Hilbert spaces that produces gauge-invariant physical results, even for extreme light–matter interaction regimes. This is achieved by compensating the non-localities introduced in the construction of the effective Hamiltonians. The resulting quantum Rabi Hamiltonian in the Coulomb gauge differs significantly in form from the standard one, but provides the same physical results obtained by using the dipole gauge. These results shed light on gauge invariance in the non-perturbative and extreme-interaction regimes, and solve long-lasting controversies arising from gauge ambiguities in the quantum Rabi and Dicke models.

The ultrastrong coupling (USC) between an effective two-level system (TLS) and the electromagnetic field has been realized in several solid-state systems[1,2]. In this regime of quantum light–matter interaction, going beyond weak and strong coupling, the coupling strength becomes comparable to the transition frequencies of the system. Recently, light–matter coupling strengths larger than the system transition frequencies have been achieved in circuit quantum electrodynamics (QED) experiments involving a single *LC*-oscillator mode coupled to a flux qubit superconducting quantum circuit[3,4]. This extreme interaction regime has been denoted as deep strong coupling (DSC). In these regimes[1,2], several properties of coupled light–matter systems change drastically, opening the way to a wealth of new intriguing physical effects (see, for example, refs. [5–18]), which offer opportunities for the development of new quantum technologies[19–26].

The form of the electron–photon interaction is gauge dependent (see, for example, ref. [27]). However, all physical results must be independent of this choice. Gauge invariance is a general guiding principle in building the theory of fundamental interactions (see, for example, ref. [28]). Let us consider, for example, a particle field whose action is invariant under a global phase change [$U(1)$ invariance]. If this phase is allowed to depend on the space–time coordinate x, its action is not invariant. The symmetry can be restored, replacing the four-momentum derivatives in the action with covariant derivatives: $D_\mu = (\partial_\mu + iqA_\mu)$, where q is the charge parameter and A_μ is the gauge potential.

It has been shown[29–33] that approximate models for light–matter interactions derived in different gauges may lead to different predictions, or can display different convergence properties[34]. When the light–matter interaction becomes very strong, different gauges can lead to drastically different predictions, giving rise to controversies[35–43]. For example, in the case of several TLSs interacting with a single mode of an optical resonator[44], different gauges may even lead to very conflicting predictions, such as the presence or the absence of a quantum phase transition. One important conclusion that can be drawn from these controversies is that, once the light–matter coupling becomes non-perturbative, the validity of the two-level approximation for the atomic dipoles depends explicitly on the choice of gauge[45,46].

In all of these previous studies[35–43,45,46], it is clear that approximations in the description of the matter system (for example, a finite-level truncation) seem to ruin the gauge invariance of the theory. In 1971, it was pointed out[31] that gauge ambiguities in the calculation of atomic oscillator strengths can originate from the occurrence of non-local potentials determined by the approximation procedures. Because a non-local potential in the position representation is an integral operator, it does not commute with the position operator. Indeed, it is easy to show that it can be expressed as a local momentum-dependent operator $V(\mathbf{r}, \hat{\mathbf{p}})$. This affects the interaction of light with quantum systems described by approximate Hamiltonians. Specifically, to introduce the coupling of the matter system with the electromagnetic field, the minimal replacement rule $\hat{\mathbf{p}} \rightarrow \hat{\mathbf{p}} - \hat{\mathbf{A}}(\mathbf{r}, t)$ ($\hat{\mathbf{A}}$ is the vector potential) has to be applied not only to the kinetic energy terms, but also to the non-local potentials in the effective Hamiltonian of the particles in the system. By applying such a procedure, approximate matrix elements for electric dipole transitions[31] and two-photon transition rates, involving Wannier excitons in semiconductors[32], become gauge invariant. Also the microscopic quantum theory of excitonic polaritons is affected by the presence of non-local potentials[47,48].

Here we investigate whether this strategy can work in the maximally truncated Hilbert space provided by a TLS, and in the non-perturbative regimes of cavity QED. This investigation is relevant not only to remove gauge ambiguities in quantum optical systems,

[1]Theoretical Quantum Physics Laboratory, RIKEN Cluster for Pioneering Research, Wako-shi, Saitama, Japan. [2]Dipartimento di Scienze Matematiche e Informatiche, Scienze Fisiche e Scienze della Terra, Università di Messina, Messina, Italy. [3]Physics Department, The University of Michigan, Ann Arbor, MI, USA. *e-mail: ssavasta@unime.it

which are attracting great interest, but also to provide a general insight into gauge invariance in extreme interaction regimes. We find that the usual strategy, which consists of taking into account the non-locality of the atomic potential, performing the minimal coupling replacement and developing the resulting interaction Hamiltonian up to second order in the vector potential, fails when the coupling strength reaches a significant fraction of the resonance frequencies of the system. We demonstrate that these gauge ambiguities can be eliminated for arbitrary coupling strengths only by taking into account the approximation-induced non-locality and keeping the resulting interaction Hamiltonian to all orders in the vector potential $\hat{\mathbf{A}}$. The results presented here solve all the long-lasting controversies arising from gauge ambiguities in the quantum Rabi and Dicke models.

The minimal coupling replacement

We consider a non-relativistic quantum particle of mass m with Hamiltonian $\hat{H}_0 = \hat{\mathbf{p}}^2/(2m) + V(x)$, where $V(x)$ is a local potential. According to the gauge principle, the corresponding gauge-invariant Hamiltonian $\hat{H}_0$ can be expressed as

$$\hat{H}_0 = q\phi + \frac{1}{2m}(\hat{\mathbf{p}} - q\mathbf{A})^2 + V(x) \tag{1}$$

where q is the charge, and $\phi(\mathbf{x})$ and $\mathbf{A}(\mathbf{x})$ are the scalar and vector potentials of the electromagnetic field. Of course, the total energy also has to include the energy of the free field. We observe that, if the particle potential V is non-local, that is, momentum-dependent, the gauge principle, implying the replacement $\hat{\mathbf{p}} \rightarrow \hat{\mathbf{p}} - q\mathbf{A}$, should also be applied to it. In most cases, when dealing with the quantization of the electromagnetic field, it is useful to adopt the Coulomb gauge, where the particle momentum is coupled only to the transverse part of the vector potential. For an effective quantum particle, focusing on a single-cavity mode and considering the electric-dipole approximation, the Hamiltonian in the Coulomb gauge[27] is

$$\hat{H}_{\mathrm{C}} = \frac{1}{2m}(\hat{p} - q\hat{A})^2 + V(x) + \hat{H}_{\mathrm{ph}} \tag{2}$$

where $\hat{A} = A_0(\hat{a} + \hat{a}^\dagger)$ is the vector potential calculated at the particle position with a zero-point-fluctuation amplitude A_0, and $\hat{H}_{\mathrm{ph}} = \hbar\omega_{\mathrm{c}}\hat{a}^\dagger\hat{a}$ is the cavity-field Hamiltonian. For a multimode resonator: $\hat{A} = A_n(\hat{a}_n + \hat{a}_n^\dagger)$ and $\hat{H}_{\mathrm{ph}} = \sum_n \hbar\omega_n\hat{a}_n^\dagger\hat{a}_n$.

If the two lowest energy levels of the effective quantum particle are well separated from the higher energy levels, as in the case of flux qubits[3], and if the detuning $\Delta \equiv \omega_{\mathrm{c}} - \omega_{10}$ (where ω_{10} is the transition frequency of the two lowest energy levels) is much smaller than the detunings of other transitions, the truncation of the Hilbert space to the two lowest energy levels is expected to be a good approximation. Projecting $\hat{H}_{\mathrm{C}}$ in a two-level space, the standard quantum Rabi Hamiltonian in the Coulomb gauge is obtained

$$\hat{\mathcal{H}}'_{\mathrm{C}} = \hat{H}_{\mathrm{ph}} + \frac{\hbar\omega_{10}}{2}\hat{\sigma}_z + \hbar g_{\mathrm{C}}\hat{\sigma}_y(\hat{a}^\dagger + \hat{a}) + D(\hat{a}^\dagger + \hat{a})^2 \tag{3}$$

where $g_{\mathrm{C}} = \omega_{10}A_0 d_{10}/\hbar$, $D = q^2A_0^2/(2m)$, and $d_{10} \equiv q\langle 1|\hat{x}|0\rangle$ is the dipole matrix element. Throughout this Article we will use calligraphic symbols as, for example, $\hat{\mathcal{H}}'_{\mathrm{C}}$, to indicate quantum operators in truncated Hilbert spaces. The diamagnetic term $q^2\hat{A}^2/(2m)$ can be absorbed by using a Bogoliubov transformation involving only the photon operators[3,45]. In contrast to the interaction term of first order in the charge, the $\hat{A}^2$ term is not affected by the truncation of the particle Hilbert space. Hence, considering a few-level description of the matter part can result in an over-estimation of the diamagnetic term. Using the Thomas–Reiche–Kuhn sum rule, $\sum_k \hbar\omega_{kj}|d_{jk}|^2 = (\hbar q)^2/(2m)$, the coefficient of the diamagnetic term can be written as $D = A_0^2\sum_k \omega_{kj}|d_{jk}|^2/\hbar$. When a single transition is considered, this expression can be used to establish a lower bound: $D \geq \hbar g_{\mathrm{C}}^2/\omega_{10}$.

We observe that, in contrast to the Hamiltonian in equation (2), equation (3) violates the gauge principle, because its derivation does not take into account that, in the presence of a truncated Hilbert space, the particle potential loses its locality: $V(x) \rightarrow V'(x, \hat{p})$. We will discuss this problem below, showing the correct procedure for solving it.

The dipole gauge

The Hamiltonian in the dipole gauge, $\hat{H}_{\mathrm{D}}$, corresponds to the Power–Zienau–Woolley Hamiltonian after the dipole approximation[27]. It can be obtained directly from the Hamiltonian in the Coulomb gauge with the electric dipole approximation (2) by means of a gauge transformation, which is also a unitary trasformation: $\hat{H}_{\mathrm{D}} = \hat{U}_{\mathrm{I}}\hat{H}_{\mathrm{C}}\hat{U}_{\mathrm{I}}^\dagger$, where the unitary operator is $\hat{U}_{\mathrm{I}} = \exp[-iq\hat{x}\hat{A}/\hbar]$.

The resulting Hamiltonian in the dipole gauge is

$$\hat{H}_{\mathrm{D}} = \hat{H}_{\mathrm{ph}} + \hat{H}_0 + \frac{q^2A_0^2\omega_{\mathrm{c}}}{\hbar}x^2 + iq\omega_{\mathrm{c}}xA_0(\hat{a}^\dagger - \hat{a}) \tag{4}$$

Projecting $\hat{H}_{\mathrm{D}}$ to a two-level space, the quantum Rabi Hamiltonian in the dipole gauge is obtained:

$$\hat{\mathcal{H}}_{\mathrm{D}} = \hat{H}_{\mathrm{ph}} + \frac{\hbar\omega_{10}}{2}\hat{\sigma}_z + i\hbar g_{\mathrm{D}}(\hat{a}^\dagger - \hat{a})\hat{\sigma}_x \tag{5}$$

where $g_{\mathrm{D}} = \omega_{\mathrm{c}}A_0 d_{10}/\hbar = g_{\mathrm{C}}\omega_{\mathrm{c}}/\omega_{10}$, and $d_{10} \equiv q\langle 1|x|0\rangle$ is the dipole matrix element. In equation (5) we neglected the term $\hat{C} = (A_0^2d_{10}^2\omega_{\mathrm{c}}/\hbar)\hat{P}$, where $\hat{P} = |0\rangle\langle 0| + |1\rangle\langle 1|$ is the TLS identity operator. This term is obtained by projecting x^2 in the two-dimensional Hilbert space, $\hat{P}x^2\hat{P} = \hat{P}x\hat{P}x\hat{P}$, and using parity symmetry, which implies $\langle n|x|n\rangle = 0$. A more accurate derivation can be carried out including this term in the particle potential before the diagonalization[45] or using perturbation theory. However, we made the choice of considering the interaction terms only after the Hilbert space truncation. In ref. [45] it is shown that, if the two lowest energy levels are well separated from the higher ones ($\omega_{21} \gg g_{\mathrm{D}}$), the two-level approximation provides accurate results even for extreme coupling strengths ($g_{\mathrm{D}} \gg \omega_{10}$).

Revisiting the quantum Rabi model in the Coulomb gauge

As observed above, the derivation of equation (3) does not take into account that, in the presence of a truncated Hilbert space, the particle potential can lose its locality: $V(x) \rightarrow V'(x, \hat{p})$. Thus, to preserve gauge invariance, one has to also apply the substitution $\hat{p} \rightarrow \hat{p} - q\hat{A}$ to the potential. In principle, this procedure can give rise to additional terms in the interaction Hamiltonian to all orders in the vector potential. Although these higher-order terms are expected to be negligible for small normalized couplings $\eta \equiv g_{\mathrm{C}}/\omega_{\mathrm{c}}$, they can become important at higher coupling strengths.

As shown in detail in the Methods, by using some general operator theorems it is possible to apply the minimal coupling replacement to both the kinetic energy and the non-local potential of the effective Hamiltonian of a quantum particle by employing a unitary transformation[47]. In particular, applying equation (20) (see Methods), we obtain

$$\hat{H}_{\mathrm{C}} = \hat{U}\hat{H}_0\hat{U}^\dagger + \hat{H}_{\mathrm{ph}} \tag{6}$$

where the unitary operator is $\hat{U}=\hat{U}_1^{\dagger}$, with $\hat{U}_1$ as defined above.

This alternative, although equivalent, minimal-coupling method allows us to understand precisely why the standard quantum Rabi Hamiltonian in the Coulomb gauge $\hat{\mathcal{H}}_{\rm C}'$ violates the gauge principle. $\hat{\mathcal{H}}_{\rm C}'$ can be obtained by applying the minimal coupling replacement to the full matter Hamiltonian, $\hat{H}_0 \rightarrow \hat{U}\hat{H}_0\hat{U}^{\dagger}$, and then projecting in the truncated Hilbert space. Therefore

$$\hat{\mathcal{H}}_{\rm C}'=\hat{P}\hat{U}\hat{H}_0\hat{U}^{\dagger}\hat{P}+\hat{H}_{\rm ph}=\hat{P}\left[\hat{U}\frac{\hat{p}^2}{2m}\hat{U}^{\dagger}+\hat{V}\right]\hat{P}+\hat{H}_{\rm ph} \tag{7}$$

where $\hat{P}$ is the projection operator for the truncated Hilbert space, and we used the relation $\hat{U}\hat{V}\hat{U}^{\dagger}=\hat{V}$, valid when the potential $\hat{V}$ is local. Using Supplementary equation (6), it can easily be shown that equation (7) gives equation (3). Notice that equation (7) contains the non-local potential $\hat{P}\hat{V}\hat{P}$ to which the gauge principle has not been applied. Hence, we can conclude that $\hat{\mathcal{H}}_{\rm C}$ violates the gauge principle. This problem arises whenever the matter system is described within a truncated Hilbert space, and can be solved by first applying to the matter system Hamiltonian (in the absence of interaction) the projection operator, and then the unitary operator, $\hat{P}\hat{H}_0\hat{P}\rightarrow\hat{U}\hat{P}\hat{H}_0\hat{P}\hat{U}^{\dagger}$. Finally, if one desires the resulting Hamiltonian to be within the truncated Hilbert space, it can be done by projecting it at the end. Applying the projection operator and using $\hat{P}^2=\hat{P}$, we obtain

$$\hat{\mathcal{H}}_{\rm C}'=\hat{\mathcal{U}}\hat{\mathcal{H}}_0\hat{\mathcal{U}}^{\dagger}+\hat{H}_{\rm ph} \tag{8}$$

where the projected unitary operator is $\hat{\mathcal{U}}=\hat{P}\hat{U}\hat{P}$ and $\hat{\mathcal{H}}_0=\hat{P}\hat{H}_0\hat{P}$. Equation (8) describes the total light–matter interaction Hamiltonian in the Coulomb gauge and in the electric dipole approximation, satisfying the gauge principle despite the, often unavoidable, truncation of the Hilbert space. We note that $\hat{\mathcal{U}}$ is a unitary operator, in contrast to the operator $\hat{P}\hat{U}$ used in equation (7). This feature is very important because, as we will discuss below, it ensures gauge invariance in truncated Hilbert spaces.

When the matter system is described by a single transition (TLS), we have $\hat{\mathcal{H}}_0=\hbar\omega_{10}\hat{\sigma}_z/2$ and

$$\hat{\mathcal{U}}=\exp\left[i\eta\hat{\sigma}_x(\hat{a}+\hat{a}^{\dagger})\right] \tag{9}$$

where $\eta=g_{\rm D}/\omega_{\rm c}$ is the normalized coupling strength. Therefore, in the Coulomb gauge

$$\hat{\mathcal{H}}_{\rm C}=\hbar\omega_{\rm c}\hat{a}^{\dagger}\hat{a}+\frac{\hbar\omega_{10}}{2}\left\{\hat{\sigma}_z\cos\left[2\eta(\hat{a}+\hat{a}^{\dagger})\right]+\hat{\sigma}_y\sin\left[2\eta(\hat{a}+\hat{a}^{\dagger})\right]\right\} \tag{10}$$

is the correct quantum Rabi Hamiltonian. The price one has to pay for preserving the gauge principle in such a truncated space is that the resulting Hamiltonian will contain field operators at all orders. This result shows that the occurrence of a non-local potential, arising from the truncation of the matter system Hilbert space, does not simply modify the dipole moment[31], but profoundly changes the structure of the interaction Hamiltonian. In Supplementary Section I, we show (for the case of TLSs) that, in contrast to equation (3), $\hat{\mathcal{U}}\hat{\mathcal{H}}_0\hat{\mathcal{U}}^{\dagger}$ is able to restore the $U(1)$ symmetry that is broken by coordinate-dependent phase transformations of the matter system wavefunctions.

In addition to the two-level approximation for the matter system, the quantum Rabi model also relies on the single-mode approximation. This further assumption does not result in a breakdown of gauge invariance and it is also largely satisfied for very strong coupling strengths when the electromagnetic resonator is an LC circuit[3]. It may fail for other kinds of resonator displaying propagation effects[49–53]. Multimode calculations accounting for the infinite set of cavity modes can lead to divergences unless a cutoff is imposed (see, for example, refs. [50,51]). Recently, it has been shown[50] that finite expressions can be obtained when gauge invariance is respected. The generalization of equation (10) to multimode fields is straightforward. It can be directly obtained from equation (10) by replacing the normalized coupling $\eta(\hat{a}+\hat{a}^{\dagger})$ with $d_{10}\hat{A}/\hbar$, where $\hat{A}=\sum_n A_n(\hat{a}_n+\hat{a}_n^{\dagger})$ is the total vector potential operator at the atom position. Replacing the discrete index n with a proper continuous parameter, this generalization can also be applied to a matter quantum system strongly interacting with a continuum of electromagnetic modes[1,2].

The fulfilment of the gauge principle when considering a TLS interacting with a strong laser (classical) field[54–56] in the Coulomb gauge also requires us to take into account the effect of non-local potentials. In this case, the correct semiclassical Hamiltonian in the Coulomb gauge $\hat{\mathcal{H}}_{\rm C}^{\rm sc}$ is

$$\hat{\mathcal{H}}_{\rm C}^{\rm sc}=\frac{\hbar\omega_{10}}{2}\left\{\hat{\sigma}_z\cos\left[2\frac{d_{10}}{\hbar}A(t)\right]+\hat{\sigma}_y\sin\left[2\frac{d_{10}}{\hbar}A(t)\right]\right\} \tag{11}$$

where $A(t)$ is the classical time-dependent vector potential describing the applied field.

In Fig. 1, we plot the energy differences $((E-E_0)/\hbar\omega_{\rm c})$ for the lowest eigenstates of $H_{\rm D}$ (equation (5)), $\hat{\mathcal{H}}_{\rm C}'$ (equation (3)) and $\hat{\mathcal{H}}_{\rm C}$ (equation (10)), as a function of the normalized coupling $\eta=g_{\rm D}/\omega_{\rm c}$. For $\hat{\mathcal{H}}_{\rm C}'$ we used $D=g_{\rm C}^2/\omega_{10}$; however, the qualitative results do not

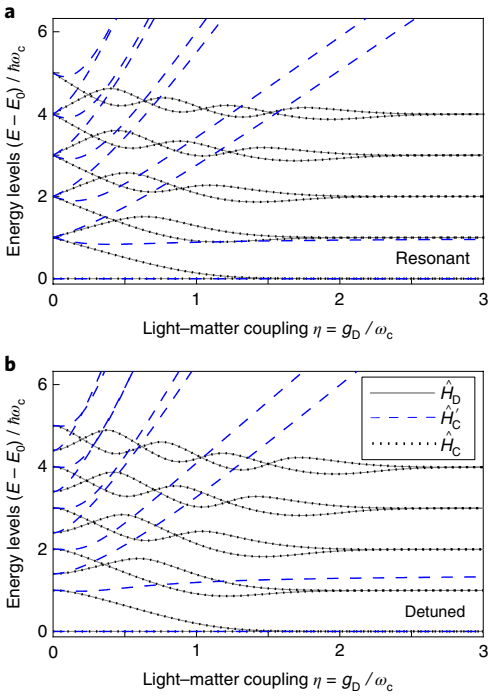

Fig. 1 | Numerical comparisons between different gauges. a,b, Comparison of the energy spectra as a function of the normalized coupling $\eta=g_{\rm D}/\omega_{\rm c}$, obtained from the quantum Rabi Hamiltonians in the dipole gauge ($\hat{\mathcal{H}}_{\rm D}$), in the standard Coulomb gauge ($\hat{\mathcal{H}}_{\rm D}'$) and in the Coulomb gauge taking into account the presence of non-local potentials ($\hat{\mathcal{H}}_{\rm C}$): plots for zero detuning ($\Delta=0$) (**a**) and $\Delta=2\omega_{\rm c}/3$ (**b**).

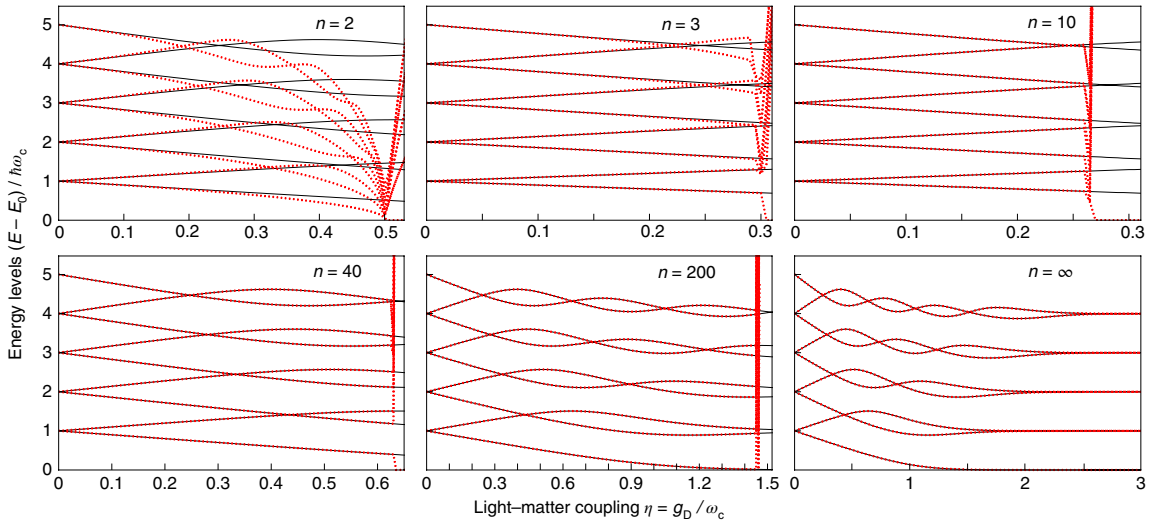

Fig. 2 | Breakdown of gauge invariance. Energy spectra versus normalized coupling η, obtained from the nth-order Taylor expansion $\hat{\mathcal{H}}_C^{(n)}$ of the quantum Rabi Hamiltonian $\hat{\mathcal{H}}_C$, taking into account the presence of non-local potentials. Each panel shows a comparison between the exact spectra, containing all terms (black continuous curves) and the approximated energy levels (red dotted curves) at different orders n of approximation. Note the breakdown of the $\hat{\mathcal{H}}_C^{(n)}$ spectra on the right-hand side of the panels.

change for higher values of D. The comparison in Fig. 1 shows that, for very small values of the coupling, the eigenvalues of the different Hamiltonians reproduce the expected behaviour. However, already at moderate coupling strengths, $\eta \sim 0.1$, there are significant deviations in the predicted energies. For $\eta \gtrsim 0.5$, these differences become drastic. In particular, while the eigenvalues of $\hat{\mathcal{H}}_D$ and $\hat{\mathcal{H}}_C$ do coincide for all the coupling strengths, $\hat{\mathcal{H}}_C'$ provides very different results. This anomalous behaviour of $\hat{\mathcal{H}}_C'$ is a direct consequence of its violation of the gauge principle, demonstrated here. If a Lagrangian or a Hamiltonian does not satisfy the gauge principle, a gauge transformation will produce different physical results. Recently, values of $\eta > 0.1$ have been obtained by several groups[1,2]. In 2017, the record value $\eta = 1.34$ was achieved[3]. The plots in Fig. 1 also enforce the validity of the quantum Rabi Hamiltonian in the dipole gauge (equation (5)), as they show that it provides the same energy levels as the corresponding Hamiltonian in the Coulomb gauge, obtained according to the gauge principle.

The strong differences between the energy levels of $\hat{\mathcal{H}}_C'$ and $\hat{\mathcal{H}}_D$ agree with the results in ref. [45] They also show that, when the matter system displays a strong anharmonicity, the energy levels of $\hat{\mathcal{H}}_D$ (in contrast to those of $\hat{\mathcal{H}}_C$) agree very well with those obtained from the numerically calculated energy levels of the full light–matter Hamiltonian $\hat{H}_D$ for a large range of coupling strengths. Indeed, the two-level approximation is expected to be robust for $\mu \gg \eta$, where $\mu \equiv (\omega_{21} - \omega_{10})/\omega_{10}$ is the anharmonicity. The results of ref. [45] confirm this robustness only for the dipole gauge. Surprisingly, this conclusion seems to be in contrast with the results of ref. [46], where they concluded that the flux gauge (analogous to the dipole gauge for a superconducting artificial atom) provides completely incorrect predictions in most cases. These contradictory results are discussed in Supplementary Section V. Here, we only observe that the degree of anharmonicity of the matter system considered in ref. [46] ($\mu \sim \eta$) is not enough to ensure the validity of the two-level approximation. However, a common feature of refs. [45,46] is that the energy levels of the quantum Rabi model are strongly gauge dependent. In contrast, our derivation of the Rabi Hamiltonian in the Coulomb gauge and the results in Fig. 1 clearly show that, as highly desired, the predictions of the quantum Rabi model are gauge invariant if the gauge principle is correctly applied.

To understand how many powers of the photon operators have to be included in $\hat{\mathcal{H}}_C$ to obtain the correct spectra, in Fig. 2 we compare the approximate spectra, calculated from different n-order Taylor expansions $\hat{\mathcal{H}}_C^{(n)}$ of $\hat{\mathcal{H}}_C$, with the exact ones (the eigenvalues of $\hat{\mathcal{H}}_C$). The results are interesting. For $n = 3$ there is already a significant improvement (with respect to $n = 2$), up to $\eta \lesssim 0.25$. However, the spectra become completely wrong at $\eta \lesssim 0.3$. Accuracy improves for $n = 10$, but only up to $\eta \lesssim 0.25$. For $n = 200$, there is an excellent agreement, but only for $\eta \lesssim 1.3$. These results show that for values of η larger than 1 (DSC), a very large n is needed to obtain the correct spectra. However, further increasing η requires the inclusion of more and more terms in the expansion. This shows that the procedure of taking into account the non-locality of the atomic potential and modifying the interaction Hamiltonian only up to second order in the vector potential[31,32,47,48] completely fails in the USC regime. Figure 2 clearly displays that, for arbitrary coupling strengths, the breakdown of gauge invariance can be avoided only by taking into account the approximation-induced non-locality and keeping the resulting interaction Hamiltonian to all orders in the vector potential. This confirms the non-perturbative spatial non-locality that occurs when heavily truncating the particle's Hilbert space. The results obtained here for a single two-level dipole (Rabi) can be extended to the multi-dipole case (Dicke) [35,43]. Supplementary Section III shows how to obtain the correct Dicke model in the Coulomb gauge. As addressed in ref. [46], gauge ambiguities also arise in circuit-QED systems. For example, the full Hamiltonian of a fluxonium capacitively coupled to an LC oscillator circuit[57] (corresponding to the charge gauge) can be obtained through an analogous minimal coupling replacement. As shown in Supplementary Section IV, the resulting correct total Hamiltonian for the two-level model in the charge gauge is very similar to equation (10).

Resolution of gauge ambiguities

Note that $\hat{H}_D$ and $\hat{H}_C$ are related by a gauge transformation[27,45], which can be expressed by $\hat{H}_D = \hat{U}_1 \hat{H}_C \hat{U}_1^\dagger$. As discussed above, $\hat{\mathcal{H}}_C'$ (the standard two-level approximation of $\hat{H}_C$) gives rise to wrong spectra, thus ruining gauge invariance. Instead, we have demonstrated that $\hat{\mathcal{H}}_C$ in equation (10) is the correct quantum Rabi Hamiltonian in the Coulomb gauge. The numerical results in Fig. 1 show that $\hat{\mathcal{H}}_C$

gives the same spectra as $\hat{\mathcal{H}}_{\rm D}$, thus providing clear evidence that the procedure developed here restores gauge invariance in TLSs.

We now present an analytical demonstration of the gauge invariance of a TLS coupled to the electromagnetic field. We start from $\hat{\mathcal{H}}_{\rm D}$, which, according to ref. [45], provides a very good approximation of the full Hamiltonian $\hat{H}_{\rm D}$, and apply the gauge transformation projecting $\hat{U}_1^{\dagger}=\hat{U}$ in the two-level space, $\hat{\mathcal{U}}_1^{\dagger}\hat{\mathcal{H}}_{\rm D}\hat{\mathcal{U}}_1$, where $\hat{\mathcal{U}}_1^{\dagger}=\hat{\mathcal{U}}$. The result of this unitary transformation should be $\hat{\mathcal{H}}_{\rm D}\rightarrow\hat{\mathcal{H}}_{\rm C}$. Noticing that $\hat{\mathcal{U}}$ corresponds to a spin rotation along the x axis, and using the Baker–Campbell–Hausdorff lemma, it is easy to obtain

$$\begin{aligned}\hat{\mathcal{U}}_1^{\dagger}\hat{\mathcal{H}}_{\rm D}\hat{\mathcal{U}}_1 &= \hbar\omega_{\rm c}\hat{a}^{\dagger}\hat{a}+\frac{\hbar\omega_0}{2}\{\hat{\sigma}_z\cos[2\eta(\hat{a}+\hat{a}^{\dagger})]\\ &\quad+\hat{\sigma}_y\sin[2\eta(\hat{a}+\hat{a}^{\dagger})]\}=\hat{\mathcal{H}}_{\rm C}\end{aligned}\tag{12}$$

This result demonstrates that, if we use $\hat{\mathcal{H}}_{\rm C}$ instead of $\hat{\mathcal{H}}_{\rm C}'$ and apply the gauge transformation consistently, gauge invariance is preserved in a two-level truncated space.

Following ref. [46], it is possible to employ a formulation in which the gauge freedom is contained within a single real continuous parameter α, which determines the gauge through a function operator $\hat{X}_{\alpha}$. The general gauge transformation in the dipole approximation is generated by a unitary transformation determined by $\hat{U}_{\alpha}=\exp[-i\hat{X}_{\alpha}]$, where $\hat{X}_{\alpha}=\alpha qx\hat{A}/\hbar$. The values $\alpha=\{0,1\}$ specify the Coulomb and the dipole gauge, respectively. According to the standard procedure (violating the gauge principle), the α-gauge quantum Rabi Hamiltonians can be expressed as[46] $\hat{\mathcal{H}}'^{(\alpha)}=\hat{P}\hat{U}_{\alpha}\hat{H}_{\rm C}\hat{U}_{\alpha}^{\dagger}\hat{P}$. Indeed, following the procedure described above, one finds that the corresponding correct two-level projected unitary operator is $\hat{\mathcal{U}}_{\alpha}=\exp[-i\hat{\chi}_{\alpha}]$, where $\hat{\chi}_{\alpha}=\alpha\eta(\hat{a}+\hat{a}^{\dagger})\hat{\sigma}_x$ and the correct α-gauge Hamiltonian for a TLS is thus

$$\hat{\mathcal{H}}^{(\alpha)}=\hat{\mathcal{U}}_{\alpha}\hat{\mathcal{H}}_{\rm C}\hat{\mathcal{U}}_{\alpha}^{\dagger}\tag{13}$$

We obtain

$$\begin{aligned}\hat{\mathcal{H}}^{(\alpha)} &= \hbar\omega_{\rm c}\hat{a}^{\dagger}\hat{a}-i\alpha g_{\rm D}(\hat{a}-\hat{a}^{\dagger})\hat{\sigma}_x\\ &\quad+\frac{\hbar\omega_0}{2}\{\hat{\sigma}_z\cos[2\eta(1-\alpha)(\hat{a}+\hat{a}^{\dagger})]\\ &\quad+\hat{\sigma}_y\sin[2\eta(1-\alpha)(\hat{a}+\hat{a}^{\dagger})]\}\end{aligned}\tag{14}$$

Because $\hat{\mathcal{U}}_{\alpha}$ is unitary, the Hamiltonians (14) will have the same energy spectra of $\hat{\mathcal{H}}_{\rm C}=\hat{\mathcal{H}}^{(\alpha=0)}$ and of $\hat{\mathcal{H}}_{\rm D}=\hat{\mathcal{H}}^{(\alpha=1)}$ for any value of α. This eliminates the gauge ambiguities of the quantum Rabi model.

We conclude this subsection with two remarks. First, when calculating expectation values in the various gauges, the unitary transformation in equation (13) also applies to the operators. For example, the photon destruction operator transforms as $\hat{a}_{\alpha}=\hat{\mathcal{U}}_{\alpha}\hat{a}_0\hat{\mathcal{U}}_{\alpha}^{\dagger}=\hat{a}_0+i\alpha\eta\hat{\sigma}_x$, where $\hat{a}_0$ is the photon operator in the Coulomb gauge. Second, different gauges give rise to different eigenstates (all related by unitary transformations), even when using the correct gauge transformations. This feature can lead to some apparent gauge ambiguities when considering time-dependent coupling strengths. In USC systems, the virtual photons in the ground state can be released if the interaction is suddenly switched off [16,53]. Because the different gauges give rise to different eigenstates, the number of emitted photons (proportional to the virtual photon population in the ground state) seems to be gauge dependent. We observe that, during and after the switch off of the interaction, only the $\alpha=0$ (Coulomb) gauge is well defined. Indeed, in the $\alpha\neq0$ gauges the field momenta depend on the interaction strength. According to this reasoning, the vacuum emission after the switch-off can be safely described only in the Coulomb gauge. This points out the relevance of obtaining the correct quantum Rabi Hamiltonian in the Coulomb gauge (14) for the design and analysis of these experiments.

Discussion

The method developed here is not limited to TLSs but can be applied to derive gauge-invariant Hamiltonians in arbitrary light–matter quantum systems. These results are also relevant for the study of systems with non-adiabatic time-dependent coupling strength[1,2], as the Coulomb gauge ($\alpha=0$) is the only one where the field canonical operators are independent of the interaction.

Our results are also relevant for the study of open quantum systems. For example, it turns out that when the interaction of the light and matter components of a quantum system is very strong (USC), the correct gauge dependence of the subsystem operators appearing in the master equation cannot be neglected as usual. Moreover, if the coupling between a subsystem (for example, the matter system) and the environment is described by a gauge interaction and the system–bath coupling strength is not weak, the preservation of the gauge principle should be ensured despite any truncation procedure.

Finally, our investigation also applies to quantum matter systems under the effect of strong laser fields[56] and can be extended to study ultrastrong and deep strong light–matter interactions beyond the dipole approximation[33], where the multipolar gauge[27] is also affected by the presence of non-local potentials.

Online content

Any methods, additional references, Nature Research reporting summaries, source data, statements of code and data availability and associated accession codes are available at https://doi.org/10.1038/s41567-019-0534-4.

Received: 12 October 2018; Accepted: 12 April 2019;
Published online: 3 June 2019

References

1. Kockum, A. F., Miranowicz, A., Liberato, S. D., Savasta, S. & Nori, F. Ultrastrong coupling between light and matter. *Nat. Rev. Phys.* **1**, 19–40 (2019).
2. Forn-Díaz, P., Lamata, L., Rico, E., Kono, J. & Solano, E. Ultrastrong coupling regimes of light–matter interaction. Preprint at https://arxiv.org/abs/1804.09275 (2018).
3. Yoshihara, F. et al. Superconducting qubit–oscillator circuit beyond the ultrastrong-coupling regime. *Nat. Phys.* **13**, 44–47 (2017).
4. Yoshihara, F. et al. Inversion of qubit energy levels in qubit-oscillator circuits in the deep-strong-coupling regime. *Phys. Rev. Lett.* **120**, 183601 (2018).
5. Ashhab, S. & Nori, F. Qubit-oscillator systems in the ultrastrong-coupling regime and their potential for preparing nonclassical states. *Phys. Rev. A* **81**, 042311 (2010).
6. Casanova, J., Romero, G., Lizuain, I., García-Ripoll, J. J. & Solano, E. Deep strong coupling regime of the Jaynes–Cummings model. *Phys. Rev. Lett.* **105**, 263603 (2010).
7. Niemczyk, T. et al. Circuit quantum electrodynamics in the ultrastrong-coupling regime. *Nat. Phys.* **6**, 772–776 (2010).
8. Zaks, B. et al. THz-driven quantum wells: coulomb interactions and Stark shifts in the ultrastrong coupling regime. *New J. Phys.* **13**, 083009 (2011).
9. Stassi, R., Ridolfo, A., Di Stefano, O., Hartmann, M. J. & Savasta, S. Spontaneous conversion from virtual to real photons in the ultrastrong-coupling regime. *Phys. Rev. Lett.* **110**, 243601 (2013).
10. Cirio, M., De Liberato, S., Lambert, N. & Nori, F. Ground state electroluminescence. *Phys. Rev. Lett.* **116**, 113601 (2016).
11. De Liberato, S., Gerace, D., Carusotto, I. & Ciuti, C. Extracavity quantum vacuum radiation from a single qubit. *Phys. Rev. A* **80**, 053810 (2009).
12. De Liberato, S. Light–matter decoupling in the deep strong coupling regime: the breakdown of the Purcell effect. *Phys. Rev. Lett.* **112**, 016401 (2014).
13. Garziano, L. et al. Multiphoton quantum Rabi oscillations in ultrastrong cavity QED. *Phys. Rev. A* **92**, 063830 (2015).

14. Garziano, L. et al. One photon can simultaneously excite two or more atoms. *Phys. Rev. Lett.* **117**, 043601 (2016).
15. Garziano, L., Ridolfo, A., De Liberato, S. & Savasta, S. Cavity QED in the ultrastrong coupling regime: photon bunching from the emission of individual dressed qubits. *ACS Photon.* **4**, 2345–2351 (2017).
16. Di Stefano, O. et al. Feynman-diagrams approach to the quantum Rabi model for ultrastrong cavity QED: stimulated emission and reabsorption of virtual particles dressing a physical excitation. *New J. Phys.* **19**, 053010 (2017).
17. Kockum, A. F., Miranowicz, A., Macrì, V., Savasta, S. & Nori, F. Deterministic quantum nonlinear optics with single atoms and virtual photons. *Phys. Rev. A* **95**, 063849 (2017).
18. Felicetti, S., Rossatto, D. Z., Rico, E., Solano, E. & Forn-Daz, P. Two-photon quantum Rabi model with superconducting circuits. *Phys. Rev. A* **97**, 013851 (2018).
19. Nataf, P. & Ciuti, C. Vacuum degeneracy of a circuit QED system in the ultrastrong coupling regime. *Phys. Rev. Lett.* **104**, 023601 (2010).
20. Nataf, P. & Ciuti, C. Protected quantum computation with multiple resonators in ultrastrong coupling circuit QED. *Phys. Rev. Lett.* **107**, 190402 (2011).
21. Romero, G., Ballester, D., Wang, Y. M., Scarani, V. & Solano, E. Ultrafast quantum gates in circuit QED. *Phys. Rev. Lett.* **108**, 120501 (2012).
22. Kyaw, T. H., Felicetti, S., Romero, G., Solano, E. & Kwek, L.-C. Scalable quantum memory in the ultrastrong coupling regime. *Sci. Rep.* **5**, 8621 (2015).
23. Wang, Y., Zhang, J., Wu, C., You, J. Q. & Romero, G. Holonomic quantum computation in the ultrastrong-coupling regime of circuit QED. *Phys. Rev. A* **94**, 012328 (2016).
24. Stassi, R. et al. Quantum nonlinear optics without photons. *Phys. Rev. A* **96**, 023818 (2017).
25. Kockum, A. F., Macrì, V., Garziano, L., Savasta, S. & Nori, F. Frequency conversion in ultrastrong cavity QED. *Sci. Rep.* **7**, 5313 (2017).
26. Armata, F., Calajo, G., Jaako, T., Kim, M. S. & Rabl, P. Harvesting multiqubit entanglement from ultrastrong interactions in circuit quantum electrodynamics. *Phys. Rev. Lett.* **119**, 183602 (2017).
27. Babiker, M. & Loudon, R. Derivation of the Power–Zienau–Woolley Hamiltonian in quantum electrodynamics by gauge transformation. *Proc. R. Soc. Lond. A* **385**, 439–460 (1983).
28. Maggiore, M. *A Modern Introduction to Quantum Field Theory* (Oxford Series in Physics no. 12, Oxford University Press, 2005).
29. Lamb, W. E. Fine structure of the hydrogen atom. III. *Phys. Rev.* **85**, 259–276 (1952).
30. Lamb, W. E., Schlicher, R. R. & Scully, M. O. Matter–field interaction in atomic physics and quantum optics. *Phys. Rev. A* **36**, 2763–2772 (1987).
31. Starace, A. F. Length and velocity formulas in approximate oscillator-strength calculations. *Phys. Rev. A* **3**, 1242–1245 (1971).
32. Girlanda, R., Quattropani, A. & Schwendimann, P. Two-photon transitions to exciton states in semiconductors. Application to CuCl. *Phys. Rev. B* **24**, 2009–2017 (1981).
33. Ismail-Beigi, S., Chang, E. K. & Louie, S. G. Coupling of nonlocal potentials to electromagnetic fields. *Phys. Rev. Lett.* **87**, 087402 (2001).
34. Bassani, F., Forney, J. J. & Quattropani, A. Choice of gauge in two-photon transitions: 1*s*–2*s* transition in atomic hydrogen. *Phys. Rev. Lett.* **39**, 1070–1073 (1977).
35. Hepp, K. & Lieb, E. H. On the superradiant phase transition for molecules in a quantized radiation field: the Dicke maser model. *Ann. Phys.* **76**, 360–404 (1973).
36. Wang, Y. K. & Hioe, F. T. Phase transition in the Dicke model of superradiance. *Phys. Rev. A* **7**, 831–836 (1973).
37. Rzażewski, K., Wódkiewicz, K. & Żakowicz, W. Phase transitions, two-level atoms, and the A^2 term. *Phys. Rev. Lett.* **35**, 432–434 (1975).
38. Lambert, N., Emary, C. & Brandes, T. Entanglement and the phase transition in single-mode superradiance. *Phys. Rev. Lett.* **92**, 073602 (2004).
39. Keeling, J. Coulomb interactions, gauge invariance and phase transitions of the Dicke model. *J. Phys. Condens. Matter* **19**, 295213 (2007).
40. Nataf, P. & Ciuti, C. No-go theorem for superradiant quantum phase transitions in cavity QED and counter-example in circuit QED. *Nat. Commun.* **1**, 72 (2010).
41. Vukics, A., Grießer, T. & Domokos, P. Elimination of the *a*-square problem from cavity QED. *Phys. Rev. Lett.* **112**, 073601 (2014).
42. Grießer, T., Vukics, A. & Domokos, P. Depolarization shift of the superradiant phase transition. *Phys. Rev. A* **94**, 033815 (2016).
43. De Bernardis, D., Jaako, T. & Rabl, P. Cavity quantum electrodynamics in the nonperturbative regime. *Phys. Rev. A* **97**, 043820 (2018).
44. Dicke, R. H. Coherence in spontaneous radiation processes. *Phys. Rev.* **93**, 99–110 (1954).
45. De Bernardis, D., Pilar, P., Jaako, T., De Liberato, S. & Rabl, P. Breakdown of gauge invariance in ultrastrong-coupling cavity QED. *Phys. Rev. A* **98**, 053819 (2018).
46. Stokes, A. & Nazir, A. Gauge ambiguities imply Jaynes–Cummings physics remains valid in ultrastrong coupling QED. *Nat. Commun.* **10**, 499 (2019).
47. Savasta, S. & Girlanda, R. The particle–photon interaction in systems described by model Hamiltonians in second quantization. *Solid State Commun.* **96**, 517–522 (1995).
48. Savasta, S. & Girlanda, R. Quantum description of the input and output electromagnetic fields in a polarizable confined system. *Phys. Rev. A* **53**, 2716–2726 (1996).
49. Sundaresan, N. M. et al. Beyond strong coupling in a multimode cavity. *Phys. Rev. X* **5**, 021035 (2015).
50. Malekakhlagh, M., Petrescu, A. & Türeci, H. E. Cutoff-free circuit quantum electrodynamics. *Phys. Rev. Lett.* **119**, 073601 (2017).
51. Gely, M. F. et al. Convergence of the multimode quantum Rabi model of circuit quantum electrodynamics. *Phys. Rev. B* **95**, 245115 (2017).
52. Bosman, S. J. et al. Multi-mode ultra-strong coupling in circuit quantum electrodynamics. *npj Quantum Inf.* **3**, 46 (2017).
53. Muñoz, C. S., Nori, F. & De Liberato, S. Resolution of superluminal signalling in non-perturbative cavity quantum electrodynamics. *Nat. Commun.* **9**, 1924 (2018).
54. Hughes, S. Breakdown of the area theorem: carrier-wave Rabi flopping of femtosecond optical pulses. *Phys. Rev. Lett.* **81**, 3363–3366 (1998).
55. Ciappina, M. F. et al. Carrier-wave Rabi-flopping signatures in high-order harmonic generation for alkali atoms. *Phys. Rev. Lett.* **114**, 143902 (2015).
56. Brabec, T. & Krausz, F. Intense few-cycle laser fields: frontiers of nonlinear optics. *Rev. Mod. Phys.* **72**, 545–591 (2000).
57. Manucharyan, V. E., Koch, J., Glazman, L. I. & Devoret, M. H. Fluxonium: single Cooper-pair circuit free of charge offsets. *Science* **326**, 113–116 (2009).

Acknowledgements

The authors acknowledge discussions with S. De Liberato, A. Nazir and P. Rabl. F.N. is supported in part by the MURI Center for Dynamic Magneto-Optics via the Air Force Office of Scientific Research (AFOSR) (FA9550-14-1-0040), the Army Research Office (ARO) (grant no. W911NF-18-1-0358), the Asian Office of Aerospace Research and Development (AOARD) (grant no. FA2386-18-1-4045), the Japan Science and Technology Agency (JST) (via the Q-LEAP programme and CREST grant no. JPMJCR1676), the Japan Society for the Promotion of Science (JSPS) (JSPS-RFBR grant no. 17-52-50023 and JSPSFWO grant no. VS.059.18N), the RIKEN-AIST Challenge Research Fund and the John Templeton Foundation. S.S. acknowledges support from the Army Research Office (ARO) (grant no. W911NF1910065).

Author contributions

S.S. conceived the main idea and F.N. supervised the work. S.S., O.D. and F.N. designed the study. O.D. and L.G. performed analytical calculations. O.D. and A.S. performed numerical calculations. V.M. and R.S. numerically studied the full Rabi model and the Dicke model. O.D., S.S., L.G. and F.N. contributed to writing the manuscript. All authors were involved in the preparation and discussion of the manuscript.

Competing interests

The authors declare no competing interests.

Additional information

Supplementary information is available for this paper at https://doi.org/10.1038/s41567-019-0534-4.

Reprints and permissions information is available at www.nature.com/reprints.

Correspondence and requests for materials should be addressed to S.S.

Publisher's note: Springer Nature remains neutral with regard to jurisdictional claims in published maps and institutional affiliations.

Methods

Non-local potentials. To understand why local potentials become non-local when the Hilbert space is truncated, let us consider a 1D potential $\hat{V}$. In the coordinate basis, it can be written as

$$\hat{V} = \iint_{-\infty} \mathrm{d}x\mathrm{d}x' \langle x|\hat{V}|x'\rangle |x\rangle\langle x'| \tag{15}$$

If the potential is local, its matrix elements can be written as $\langle x|\hat{V}|x'\rangle \equiv V(x,x') = W(x)\delta(x-x')$. Considering a complete orthonormal basis $\{|n\rangle\}$, these matrix elements can be expressed as $V(x,x') = W(x)\delta(x-x') = \sum_{n,n'} W_{n,n'}\psi_n^*(x')\psi_{n'}(x)$, where we define $\psi_n(x) \equiv \langle x|n\rangle$. Notice that the Dirac delta function can be reconstructed only by keeping all the infinite vectors of the basis. Hence, any truncation of the complete basis can transform a local potential into a non-local one. If only two states are included, for example, the two lowest energy levels, we obtain

$$V(x,x') = W_{1,0}\left[\psi_0^*(x')\psi_1(x) + \psi_1^*(x')\psi_0(x)\right] \tag{16}$$

where, for simplicity, we assume parity symmetry (which implies that the diagonal matrix elements $W_{n,n}$ are zero) and real matrix elements. It is evident that the sum of the two terms in equation (16), which are products of two smooth wavefunctions, cannot reproduce the Dirac-delta function, and this will result in a potential with a high degree of spatial non-locality. It has been shown by several authors[31–33] that a non-local potential can be expressed as a momentum-dependent operator $V(r,\hat{p})$. Indeed, by using the translation operator $\psi(x') = \exp[i(x'-x)\hat{p}]\psi(x)$, where $\hat{p}$ is the momentum operator, we obtain

$$\int V(x,x')\psi(x')\mathrm{d}x' = V(x,\hat{p})\psi(x) \tag{17}$$

Generalized minimal coupling replacement. In this section, using some general operator theorems[58], we show how to implement the minimal coupling replacement on a generic operator $O(x,\hat{p})$ by performing a unitary transformation[47]. Given two non-commuting operators $\hat{\alpha}$ and $\hat{\beta}$ and a parameter μ we want to calculate $\mathrm{e}^{\mu\hat{\beta}}O(\hat{\alpha})\mathrm{e}^{-\mu\hat{\beta}}$. The function $O(\hat{\alpha})$ can be expanded in a power series:

$$O(\hat{\alpha}) = \sum_n c_n\hat{\alpha}^n \tag{18}$$

Using equation (18), we have

$$\mathrm{e}^{\mu\hat{\beta}}O(\hat{\alpha})\mathrm{e}^{-\mu\hat{\beta}} = \sum_n c_n\mathrm{e}^{\mu\hat{\beta}}\hat{\alpha}^n\mathrm{e}^{-\mu\hat{\beta}} \tag{19}$$

Observing that

$$\mathrm{e}^{\mu\hat{\beta}}\hat{\alpha}^n\mathrm{e}^{-\mu\hat{\beta}} = \mathrm{e}^{\mu\hat{\beta}}\hat{\alpha}\mathrm{e}^{-\mu\hat{\beta}}\mathrm{e}^{\mu\hat{\beta}}\hat{\alpha}\mathrm{e}^{-\mu\hat{\beta}}\cdots\mathrm{e}^{\mu\hat{\beta}}\hat{\alpha}\mathrm{e}^{-\mu\hat{\beta}} = \left(\mathrm{e}^{\mu\hat{\beta}}\hat{\alpha}\mathrm{e}^{-\mu\hat{\beta}}\right)^n$$

we have

$$\mathrm{e}^{\mu\hat{\beta}}O(\hat{\alpha})\mathrm{e}^{-\mu\hat{\beta}} = \sum_n c_n\left(\mathrm{e}^{\mu\hat{\beta}}\hat{\alpha}\mathrm{e}^{-\mu\hat{\beta}}\right)^n = O(\mathrm{e}^{\mu\hat{\beta}}\hat{\alpha}\mathrm{e}^{-\mu\hat{\beta}}) \tag{20}$$

We now apply equation (20) to $\mathrm{e}^{i\hat{\chi}(x)/\hbar}O(x,\hat{p})\mathrm{e}^{-i\hat{\chi}(x)/\hbar}$. For the sake of simplicity, here we consider the 1D case. The generalization to 3D is straightforward. We obtain

$$\mathrm{e}^{i\hat{\chi}(x)/\hbar}O(x,\hat{p})\mathrm{e}^{-i\hat{\chi}(x)/\hbar} = O(x,\mathrm{e}^{i\hat{\chi}(x)/\hbar}\hat{p}\,\mathrm{e}^{-i\hat{\chi}(x)/\hbar}) \tag{21}$$

Then, by using the Baker–Campbell–Hausdorff formula, we obtain

$$\mathrm{e}^{i\hat{\chi}(x)/\hbar}\hat{p}\,\mathrm{e}^{-i\hat{\chi}(x)/\hbar} = \hat{p} + \frac{i}{\hbar}[\hat{\chi}(x),\hat{p}] + \frac{1}{2}\left(\frac{i}{\hbar}\right)^2[\hat{\chi}(x),[\hat{\chi}(x),\hat{p}]] + \cdots = \hat{p} - \partial_x\hat{\chi}(x) \tag{22}$$

where we used the result $[\hat{\chi}(x),\hat{p}] = i\hbar\partial_x\hat{\chi}(x)$. In conclusion, using equations (21) and (22), this becomes

$$\mathrm{e}^{i\hat{\chi}(x)/\hbar}O(x,\hat{p})\mathrm{e}^{-i\hat{\chi}(x)/\hbar} = O[x,\hat{p} - \partial_x\hat{\chi}(x)] \tag{23}$$

Considering now the special function

$$\hat{\chi}(x) = q\,x\hat{A}_0 \tag{24}$$

with $\hat{A}_0 \equiv \hat{A}(x_0)$ being the field potential calculated at atom position x_0, we obtain

$$\partial_x\hat{\chi}(x) = q\hat{A}_0 \tag{25}$$

If we plug this result into equation (23), we obtain

$$\mathrm{e}^{i\hat{\chi}(x)/\hbar}O(x,\hat{p})\mathrm{e}^{-i\hat{\chi}(x)/\hbar} = O(x,\hat{p} - q\hat{A}_0) \tag{26}$$

demonstrating that the unitary transformation in equation (23) corresponds to the application of the minimal coupling replacement in the dipole approximation.

Data availability

The data that support the plots within this paper and other findings of this study are available from the corresponding author upon reasonable request.

References

58. Louisell, W. H. *Quantum Statistical Properties of Radiation* (Wiley, 1990).

Supplementary Information for

Resolution of Gauge Ambiguities in Ultrastrong-Coupling Cavity QED

S-I. LOCAL $U(1)$ INVARIANCE IN TWO-LEVEL HILBERT SPACES.

We consider a local (position dependent) phase transformation $[U(1)]$ of the wavefunctions:

$$\psi(x) \to \exp[iq\,\theta(x)]\psi(x) \equiv \psi'(x)\,. \tag{S1}$$

We perform a Taylor expansion of the function $\theta(x)$ and project the resulting terms in a 2D Hilbert space, considering as basis, e.g., the two lowest-energy eigenstates of the system. We assume parity symmetry, so the system eigenfunctions have definite parity. Recalling that $\hat{P}x\hat{P} = x_{10}\sigma_x \equiv \hat{x}_p$ (here x_{10} is the matrix element of the position operator between the two-level system (TLS) orthonormal states) and $(\hat{\sigma}_x)^{2n} = 1$, we obtain

$$q\hat{\theta}_p \equiv \hat{P}\theta(x)\hat{P} = \beta_0\hat{I} + \Lambda d_{10}\hat{\sigma}_x\,, \tag{S2}$$

where β_0 and Λ are constants which depend on the coefficients of the Taylor expansion. Therefore, besides the trivial constant phase factor $\exp[i\beta_0]$, the local $U(1)$ transformation, after the two-level projection, can be implemented as

$$|\psi\rangle \to \exp[i\Lambda d_{10}\hat{\sigma}_x]|\psi\rangle\,. \tag{S3}$$

We now observe that the system energy is not invariant under this local phase transformation:

$$\langle\psi'|\hat{\mathcal{H}}_0|\psi'\rangle \neq \langle\psi|\hat{\mathcal{H}}_0|\psi\rangle\,. \tag{S4}$$

On the other hand, it is well known that the action of the free electromagnetic field is invariant under the transformation

$$A \to A + \partial_x\theta(x) \equiv A'\,. \tag{S5}$$

We try to exploit gauge invariance in order to search for a *covariant* Hamiltonian $\hat{\mathcal{H}}^{(c)}$, depending on the field A, such that

$$\langle\psi'|\hat{\mathcal{H}}_0^{\prime(c)}|\psi'\rangle = \langle\psi|\hat{\mathcal{H}}_0^{(c)}|\psi\rangle\,. \tag{S6}$$

Note that, if the field transforms as

$$A' = A + \Lambda\,, \tag{S7}$$

we can define the Hamiltonian

$$\hat{\mathcal{H}}_0^{(c)} = e^{idA\hat{\sigma}_x}\hat{\mathcal{H}}_0 e^{-idA\hat{\sigma}_x} = \hat{\mathcal{U}}\hat{\mathcal{H}}_0\hat{\mathcal{U}}^\dagger\,, \tag{S8}$$

which satisfies Eq. (S6). We observe that, consistently, Eq. (S7) corresponds to a gauge transformation of the field with the coordinate projected in a TLS:

$$A \to A + \partial_{\hat{x}_p}\hat{\theta}_p = A + \Lambda = A'\,. \tag{S9}$$

We can conclude that the Hamiltonian given by $\hat{\mathcal{H}}_0^{(c)} = e^{id\hat{A}\hat{\sigma}_x}\hat{\mathcal{H}}_0 e^{-id\hat{A}\hat{\sigma}_x} = \hat{\mathcal{U}}\hat{\mathcal{H}}_0\hat{\mathcal{U}}^\dagger$ ensures the invariance of the expectation values for a local position-dependent phase transformation implemented in TLSs. However, it is now evident that the Hamiltonian in Eq. (3) of the main text is not able to ensure the invariance of the mean value of the Hamiltonian under the gauge transformation (S3).

S-II. SECOND-ORDER EXPANSION OF THE QUANTUM RABI HAMILTONIAN IN THE COULOMB GAUGE

Using the generalized minimal coupling replacement, in the main text we derived the correct Coulomb gauge Hamiltonian of the quantum Rabi model [Eq. (18) in the main text]

$$\hat{\mathcal{H}}_C = \hbar\omega_c\hat{a}^\dagger\hat{a} + \frac{\hbar\omega_{10}}{2}\times\left\{\hat{\sigma}_z\cos\left[2\eta(\hat{a}+\hat{a}^\dagger)\right] + \hat{\sigma}_y\sin\left[2\eta(\hat{a}+\hat{a}^\dagger)\right]\right\}\,. \tag{S10}$$

When the normalized interaction strength $\eta \equiv g_D/\omega_c$ is sufficiently weak, it is possible to expand the trigonometric functions in Eq. (S10) up to the linear or quadratic terms. However, when g_D becomes comparable with ω_c (i.e., the USC regime), such expansion is not sufficient. When approaching, or reaching, the deep strong coupling regime ($\eta \gtrsim 1$), the field terms have to be included to all orders (see Fig. 2 in the main text). Expanding Eq. (S10) up to second order in the potential, we obtain

$$\hat{\mathcal{H}}_C^{(2)} = \hbar\omega_c\hat{a}^\dagger\hat{a} + \frac{\hbar\omega_{10}}{2}\hat{\sigma}_z + \hbar g_C\hat{\sigma}_y(\hat{a}+\hat{a}^\dagger) - \frac{\hbar g_C^2}{\omega_{10}}\hat{\sigma}_z(\hat{a}+\hat{a}^\dagger)^2\,. \tag{S11}$$

This equation differs from the standard quantum Rabi Hamiltonian in the Coulomb gauge $\hat{\mathcal{H}}'_C$ for the diamagnetic term, which now displays a different coefficient and depends on

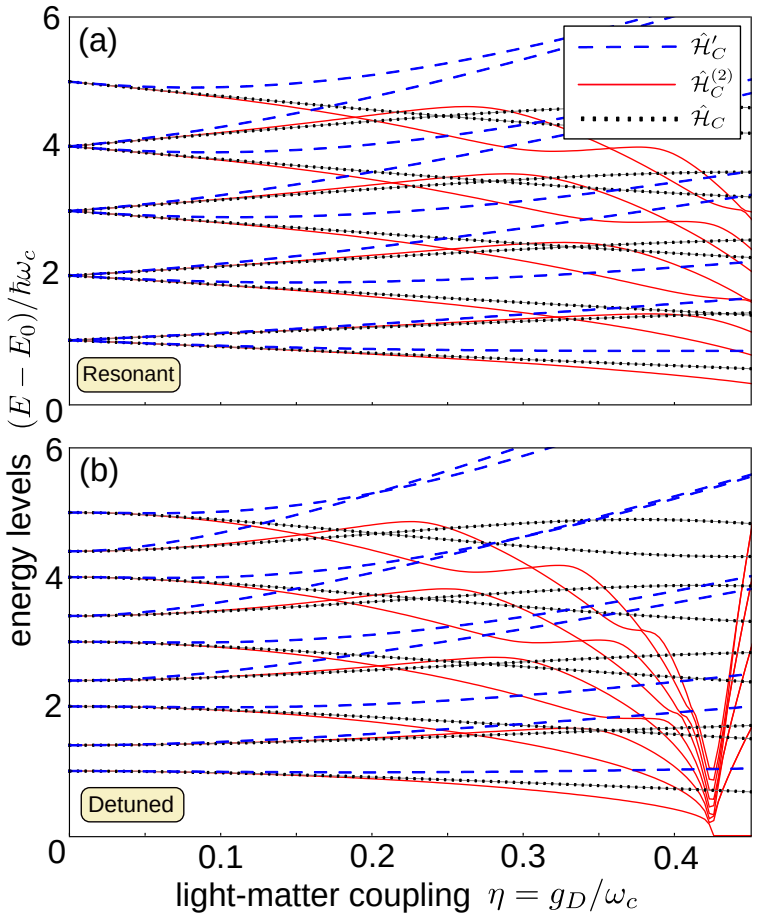

Figure S1. Comparison of the energy spectra as a function of the normalized coupling $\eta = g_D/\omega_c$, obtained from the quantum Rabi Hamiltonians: in the dipole gauge ($\hat{\mathcal{H}}_D$), in the standard Coulomb gauge; ($\hat{\mathcal{H}}'_C$), and in the Coulomb gauge; taking into account the presence of nonlocal potentials up to second order ($\hat{\mathcal{H}}^{(2)}_C$). The plots in (a) have been obtained at zero detuning ($\Delta = 0$); the plots in (b) using $\Delta/\omega_c = 2/3$.

$\hat{\sigma}_z$. By introducing the Thomas-Reiche-Kuhn sum rule in the diamagnetic term of $\hat{\mathcal{H}}'_C$ and applying the two-level truncation [S1], $\hat{\mathcal{H}}'_C$ turns into $\hat{\mathcal{H}}^{(2)}_C$. However, in contrast to the derivation of Eq. (S11), this procedure is quite arbitrary. Figure S1 compares the energy spectra of $\hat{\mathcal{H}}'_C$, $\hat{\mathcal{H}}^{(2)}_C$, and $\hat{\mathcal{H}}_C$. In particular, we observe that for $\eta < 0.1$ the spectra of both $\hat{\mathcal{H}}^{(2)}_C$ (red curves) and $\hat{\mathcal{H}}'_C$ (blue dashed curves) are in quite good agreement with the exact results (expecially those of $\hat{\mathcal{H}}^{(2)}_C$) given by $\hat{\mathcal{H}}_C$ (black dotted curves). Increasing the coupling, $\hat{\mathcal{H}}'_C$ gives spectra which rapidly become very different from the exact energy levels. The spectra of $\hat{\mathcal{H}}^{(2)}_C$ provide an improved approximation which, for the lowest few levels, is

acceptable for $\eta \lesssim 0.2$. The range of values of η where the approximate models provide acceptable spectra reduces when detuning is nonzero [Fig. S1(b)]. A critical behaviour, where all the plotted energy levels of $\hat{\mathcal{H}}_C^{(2)}$ tend to collapse towards the ground state energy, can be observed at $\eta \simeq 0.42$. However, as shown in Fig. 2 of the main text, this effect is removed by increasing the order n of the Taylor expansion.

S-III. DERIVATION OF THE DICKE MODEL IN THE COULOMB GAUGE

We now extend the results obtained in the subsection *Resolution of gauge ambiguities* of the main text for a single two-level dipole (Rabi) to the multi-dipole case (Dicke) [S2–S4]. The standard Dicke Hamiltonian in the Coulomb gauge can be written as

$$\begin{aligned}\hat{\mathcal{H}}_C'^N &= \hbar\omega_c \hat{a}^\dagger \hat{a} + \hbar\omega_{10} \hat{J}_z \\ &\quad + 2\hbar g_C \left(\hat{a}^\dagger + \hat{a}\right) \hat{J}_y + j \frac{q^2 A_0^2}{m} \left(\hat{a}^\dagger + \hat{a}\right)^2 ,\end{aligned} \tag{S12}$$

where the number N of dipoles determines the effective main angular momentum quantum number $j = N/2$, and $2\hat{J}_i = \sum_{k=1}^{N} \hat{\sigma}_i^{(k)}$.

Similarly to the quantum Rabi Hamiltonian, it is possible to introduce the coupling between the matter Hamiltonian (in this case $\hat{\mathcal{H}}_0^N = \hbar\omega_{10}\hat{J}_z$) and the electromagnetic field, by using the minimal coupling replacement. In the presence of nonlocal potentials, this can be done by applying the unitary transformation

$$\hat{\mathcal{H}}_C^N = \hat{\mathcal{U}}_N \hat{\mathcal{H}}_0^N \hat{\mathcal{U}}_N^\dagger + \hat{H}_{\rm ph} \,, \tag{S13}$$

where

$$\hat{\mathcal{U}}_N = \exp\left[i2\eta(\hat{a}^\dagger + \hat{a})\hat{J}_x\right] \tag{S14}$$

is the projection of $\hat{U}_N = \exp\left[iq\sum_k \hat{x}_k \hat{A}/\hbar\right]$ in a reduced Hilbert space, which is the tensor product of N two-dimensional Hilbert spaces. We, then, obtain

$$\boxed{\hat{\mathcal{H}}_C^N = \hbar\omega_c \hat{a}^\dagger \hat{a} + \hbar\omega_{10} \left\{ \hat{J}_z \cos\left[2\eta(\hat{a}^\dagger + \hat{a})\right] + \hat{J}_y \sin\left[2\eta(\hat{a}^\dagger + \hat{a})\right] \right\} .} \tag{S15}$$

This is the correct Hamiltonian in the Coulomb gauge for the Dicke model. Its gauge invariance can be easily proved following the same procedure shown in the subsection *Resolution of gauge ambiguities* of the main text. For example, applying the proper unitary gauge

transformation, we obtain from Eq. (S13) the dipole-gauge Dicke Hamiltonian [S4]:

$$\begin{aligned}\hat{\mathcal{H}}_D^N &= \hat{\mathcal{U}}_N^\dagger \hat{\mathcal{H}}_C^N \hat{\mathcal{U}}_N = \hat{\mathcal{H}}_0^N + \hat{\mathcal{U}}_N^\dagger \hat{H}_{\rm ph} \hat{\mathcal{U}}_N = \hbar\omega_c \hat{\mathcal{U}}_N^\dagger \hat{a}^\dagger \hat{a} \hat{\mathcal{U}}_N + \hbar\omega_{10} \hat{J}_z \\ &= \hbar\omega_c \hat{a}^\dagger \hat{a} + \hbar\omega_{10} \hat{J}_z + 2i\hbar\omega_c \eta (\hat{a}^\dagger - \hat{a}) \hat{J}_x + 4\hbar\omega_c \eta^2 \hat{J}_x^2 \,. \end{aligned} \tag{S16}$$

This result eliminates any gauge ambiguity [S4–S6] *of the Dicke model.*

The Hamiltonian in Eq. (S15) is equivalent to the one in Eq. 45 of Ref. [S4] (if direct dipole-dipole interactions are not included). The latter has been obtained applying a polaron transformation to the Dicke Hamiltonian in the dipole gauge. As observed in [S4], this unitary transformation is equivalent to a gauge transformation and hence gives rise to the Dicke Hamiltonian in the Coulomb gauge. However, as pointed out in [S4], it does not solve the gauge ambiguities of the Rabi and Dicke models (see also Ref. [S7]). Indeed, their direct derivation of the Dicke Hamiltonian in the Coulomb gauge was obtained employing the standard minimal coupling substitution, instead of the correct generalized one proposed here [Eq. (S13)].

S-IV. FLUXONIUM QUBIT-*LC* OSCILLATOR HAMILTONIAN IN THE CHARGE GAUGE

Here we derive the total Hamiltonian describing a fluxonium qubit (TLS) interacting with a superconducting LC oscillator [S1, S8]. Considering for simplicity the case of a zero-flux offset, the fluxonium Hamiltonian is:

$$\hat{H}_{\rm flux} = 4\tilde{E}_C \hat{N}^2 + \frac{\tilde{E}_L}{2} \hat{\phi}^2 - E_J \cos\hat{\phi} \,. \tag{S17}$$

where $\hat{\phi} = \hat{\Phi}_f/\Phi_0$, with $\Phi_0 = h/2e$ the flux quantum, is the reduced flux operator with conjugate momentum $\hat{N} = \hat{Q}_f/2e$ (the reduced charge) such that $[\hat{\phi}, \hat{N}] = i$. In Eq. (S17), $\tilde{E}_C$, $\tilde{E}_L$, and E_J are, respectively, the capacitive, inductive, and Josephson energies.

The LC oscillator is characterized by a capacitance C and an inductance L. Its resonance frequency is $\Omega = 1/\sqrt{LC}$ and its characteristic impedance is $Z = \sqrt{L/C}$. The Hamiltonian of the LC oscillator is

$$\hat{H}_{\rm osc} = \frac{\hat{Q}^2}{2C} + \frac{\hat{\Phi}^2}{2L} \,, \tag{S18}$$

where $\hat{Q}$ and $\hat{\Phi}$ are the charge and the flux operator, respectively.

We now introduce the reduced flux operator $\hat{\varphi} = 2\pi\,\hat{\Phi}/\Phi_0$ and the reduced charge operator $\hat{\chi} = \hat{Q}/(2e)$, whose commutator is $[\hat{\varphi}, \hat{\chi}] = i$. These can be expanded in terms of the creation and annihilation operators:

$$\hat{\varphi} = \varphi_0(\hat{a} + \hat{a}^\dagger)\,,$$

$$\hat{\chi} = -i\chi_0(\hat{a} - \hat{a}^\dagger)\,,$$

where $\varphi_0 = \sqrt{2e^2 L\hbar\Omega} = \sqrt{2\hbar e^2 Z}$, and $\chi_0 = \sqrt{C\hbar\Omega/(8e^2)} = \sqrt{\hbar/8e^2 Z}$.

The Hamiltonian of the LC oscillator can be expressed as

$$\hat{H}_{\rm osc} = 4E_C\,\hat{\chi}^2 + \frac{E_L}{2}\hat{\varphi}^2\,, \tag{S19}$$

where $E_C = e^2/(2C)$ and $E_L = (\Phi_0/2\pi)^2/L$.

The capacitive coupling (charge gauge) between the fluxonium and the LC oscillator can be described by making the substitution $\hat{N} \to \hat{N} + \hat{\chi}$ in the fluxonium Hamiltonian in Eq. (S17). The total Hamiltonian then becomes:

$$\hat{H}_{\rm charge} = 4\tilde{E}_C(\hat{N} + \hat{\chi})^2 - E_J\cos(\hat{\phi}) + \frac{\tilde{E}_L}{2}\hat{\phi}^2 + 4E_C\hat{\chi}^2 + E_L\frac{\hat{\varphi}^2}{2}\,. \tag{S20}$$

This replacement is different from the standard *minimal coupling replacement*, since it involves two conjugate momenta instead of a conjugate momentum and a field coordinate. This minimal coupling replacement can also be obtained by applying a unitary transformation to the fluxonium Hamiltonian $\hat{H}_{\rm flux}$:

$$\hat{H}_{\rm charge} = \hat{H}_{\rm osc} + \hat{R}\,\hat{H}_{\rm flux}\hat{R}^\dagger\,, \tag{S21}$$

where $\hat{R} = \exp[i\hat{\phi}\hat{\chi}]$. This can be proved by following the procedure described in the next section.

Diagonalizing $\hat{H}_{\rm flux}$ and then projecting Eq. (S20) in a two-level space spanned by the eigenstates $|0\rangle$ (ground state) and $|1\rangle$ (excited state), we obtain

$$\hat{\mathcal{H}}'_{\rm charge} = \hat{\mathcal{H}}_{\rm flux} + \hbar\omega_c\hat{a}^\dagger\hat{a} + i\hbar g_C\hat{\sigma}_y(\hat{a} - \hat{a}^\dagger) - 4\tilde{E}_C\chi_0^2(\hat{a} - \hat{a}^\dagger)^2\,, \tag{S22}$$

where the reduced flux operator in the two-level approximation becomes $\hat{\phi} = \Phi_{10}\hat{\sigma}_x$ ($\Phi_{10} \equiv \langle e|\hat{\phi}|g\rangle$ is assumed to be real), and $g_C = \omega_{10}\phi_{10}\chi_0$. We also have:

$$\hat{\mathcal{H}}_{\rm flux} = \frac{\hbar\omega_{10}}{2}\hat{\sigma}_z\,, \tag{S23}$$

with $\hat{\sigma}_z = |1\rangle\langle 1| - |0\rangle\langle 0|$.

It can be shown that the total Hamiltonian in Eq. (S22) is not gauge invariant because its derivation does not take into account the presence of an effective nonlocal potential which originates from the two-level truncation. In analogy with the procedure employed in the main text, *the correct gauge invariant total Hamiltonian* can be obtained applying the following unitary transformation to $\hat{\mathcal{H}}_{\rm flux}$:

$$\hat{\mathcal{H}}_{\rm charge} = \hbar\omega_c\, \hat{a}^\dagger \hat{a} + \hat{\mathcal{R}}\, \hat{\mathcal{H}}_{\rm flux} \hat{\mathcal{R}}^\dagger\,, \tag{S24}$$

where

$$\hat{\mathcal{R}} = \exp\left[\frac{g_C}{\omega_{10}} \hat{\sigma}_x (\hat{a} - \hat{a}^\dagger)\right] \tag{S25}$$

is the unitary operator resulting from the truncation in the two-level space of the unitary operator $\hat{R}$. The minimal coupling replacement in the truncated space Eq. (S24) gives

$$\boxed{\hat{\mathcal{H}}_{\rm charge} = \hbar\omega_c \hat{a}^\dagger \hat{a} + \frac{\hbar\omega_{10}}{2}\left\{\cosh\left[\frac{2g_C}{\omega_{10}}(\hat{a} - \hat{a}^\dagger)\right]\hat{\sigma}_z + i\sinh\left[\frac{2g_C}{\omega_{10}}(\hat{a} - \hat{a}^\dagger)\hat{\sigma}_y\right]\right\}.}$$

This equation describes the correct (gauge invariant) total Hamiltonian for a fluxonium qubit interacting with an LC circuit in the charge gauge.

S-V. COMPARISON WITH RECENT RESULTS ON GAUGE AMBIGUITIES IN CAVITY QED AND COMPARISON BETWEEN TWO-LEVEL MODELS AND THE FULL MODEL

As pointed out in the main text, the results in [S1] are in conflict with those in [S7] and with our gauge-preserving formulation of the quantum Rabi model. Indeed, [S1] claims that the flux-gauge (the analog of the dipole gauge for a superconducting artificial atom) provides in most cases very inaccurate predictions in the USC regime.

Here we analyse the main findings of these papers, discussing them in view of our results. Reference [S7] numerically shows that the energy levels of $\hat{\mathcal{H}}'_C$ become very different from those of $\hat{\mathcal{H}}_D$ in the USC regime. It also shows that the energy levels of $\hat{\mathcal{H}}_D$ (in contrast to those of $\hat{\mathcal{H}}'_C$) agree very well with those of $\hat{H}_D$ for a large range of coupling strengths. These numerical calculations [S7] were performed at zero detuning and considering an atomic

potential providing a strong anharmonicity ($\mu \approx 100$), corresponding to the condition where the two-level approximation is expected to be very robust.

Our results demonstrate that: (i) the breakdown of gauge invariance is a direct consequence of the fact that $\hat{\mathcal{H}}'_C$ violates the gauge principle; (ii) if one derives a quantum Rabi Hamiltonian in the Coulomb gauge ($\hat{\mathcal{H}}_C$) fully obeying the gauge principle, then its energy levels do coincide with those of $\hat{\mathcal{H}}_D$ independently from the detuning. We also demonstrate that, if the gauge principle is applied correctly, the whole class of quantum Rabi Hamiltonians $\hat{\mathcal{H}}_\alpha$ all provide the same energy spectrum. Hence, contrary to the claims of [S1, S7], we have demonstrated that it *is* possible to develop a gauge theory in the presence of a finite-level truncation of the matter system.

One question, however, remains open: is such a gauge theory for TLSs a good approximation of the corresponding exact theory for high values of the light-matter coupling strength? Since we have demonstrated that $\hat{\mathcal{H}}_D$ is related by unitary transformations to all the α-gauge Hamiltonians satisfying the gauge principle, and since De Bernardis *et al.* [S7] have shown that the energy levels of $\hat{\mathcal{H}}_D$ agree very well with those of the full light-matter Hamiltonian $\hat{H}_D$ for a large range of coupling strengths, the answer is affirmative: *if the gauge principle is obeyed, light-matter theories for TLSs provide a very good approximation of the exact corresponding theory, at least when the two-level approximation is expected to work.* Specifically, this occurs when the anharmonicity of the effective quantum particle is high compared to the coupling strength.

All this coherent and consistent picture, however, conflicts with [S1], which seems to contradict the results in [S7]. Indeed, [S1] claims that the flux-gauge (the analog of the dipole gauge for a superconducting artificial atom) provides in most cases very inaccurate predictions in the USC regime. Ref. [S1] presents a formulation in which the gauge freedom is contained within a single real continuous parameter α, which leads to α-dependent predictions. Ref. [S1] claims that the specific value of $\alpha = \alpha_{\rm JC}$, determining a model without rotating-wave terms (named JC-gauge), provides the most accurate results. However, in contrast to the results of [S7], no α-gauge in [S1] is able to produce overall accurate results, not even for all the three lowest-energy states. In summary, the numerical results of [S1], more than the validity of the JC-gauge, would suggest that the quantum Rabi model provides inaccurate overall results in the USC regime.

A first observation about the results in [S1] is that $\alpha_{\rm JC}$ does not represent a fixed op-

timal parameter, since its value depends on both the coupling strength and the resonance frequency ω_c of the cavity mode. Hence, every change of the detuning would require a gauge adjustment in order to obtain the more accurate quantum Rabi model. Moreover, looking at the numerical results [S1], the agreement between the JC-gauge and the exact model strongly depends on the detuning as well as on the specific energy level of the total system. For example, at zero detuning ($\delta \equiv \omega_c/\omega_{10} = 1$), they find that the flux gauge accurately predicts the third energy level (also the levels $n = 5$ and 8), in contrast to the JC-gauge which provides completely wrong results for the same levels [S1]. In addition, while the ground state fidelity in the JC-gauge is the closest to 1, the fidelity of the first excited state in the flux-gauge outperforms the one in the JC-gauge, despite its energy level being less accurate. Even more contradictory results [S1] are obtained for $\delta = 1/5$. In this case, the flux-gauge produces a ladder of energy levels in good agreement with the exact calculation, while the JC-gauge at most works only for the first two energy levels. For large detuning ($\delta = 5$), except for the first two energy levels, all the gauges provide very inaccurate energy levels [S1].

These results show that the JC-gauge works quite well only for the description of the ground state and sometimes of the first excited state. In contrast to the results of Ref. [S7], in most cases no gauge is able to produce overall accurate results [S1]. Finally, we observe that it is generally possible to find a specific value of $\alpha \neq \alpha_{\rm JC}$ where the ground state energy coincides with the exact value. In summary, the numerical results of Ref. [S1] would suggest that the quantum Rabi model provides inaccurate overall results in the USC regime.

We find that this breakdown of the quantum Rabi model originates from the degree of anharmonicity of the matter system studied in Ref. [S1], which is comparable to the considered light-matter coupling strengths. Using the parameters of the artificial atom (fluxonium) considered in [S1], and numerically solving the corresponding time-independent Schrödinger equation, an energy spectrum of the matter system with a quite low degree of anharmonicity is produced. Specifically, using $\tilde{E}_C = E_J = 10\tilde{E}_L$, where $\tilde{E}_C$, $\tilde{E}_L$, and E_J are, respectively, the capacitive, inductive and Josephson energies of the fluxonium, we obtain an anharmonicity $\mu \simeq 2.2$.

In view of the above described gauge ambiguities [S1, S7], and as a further check, we have performed additional numerical calculations considering our matter system constituted by an effective quantum particle in a double-well potential. In particular, we consider a dipole

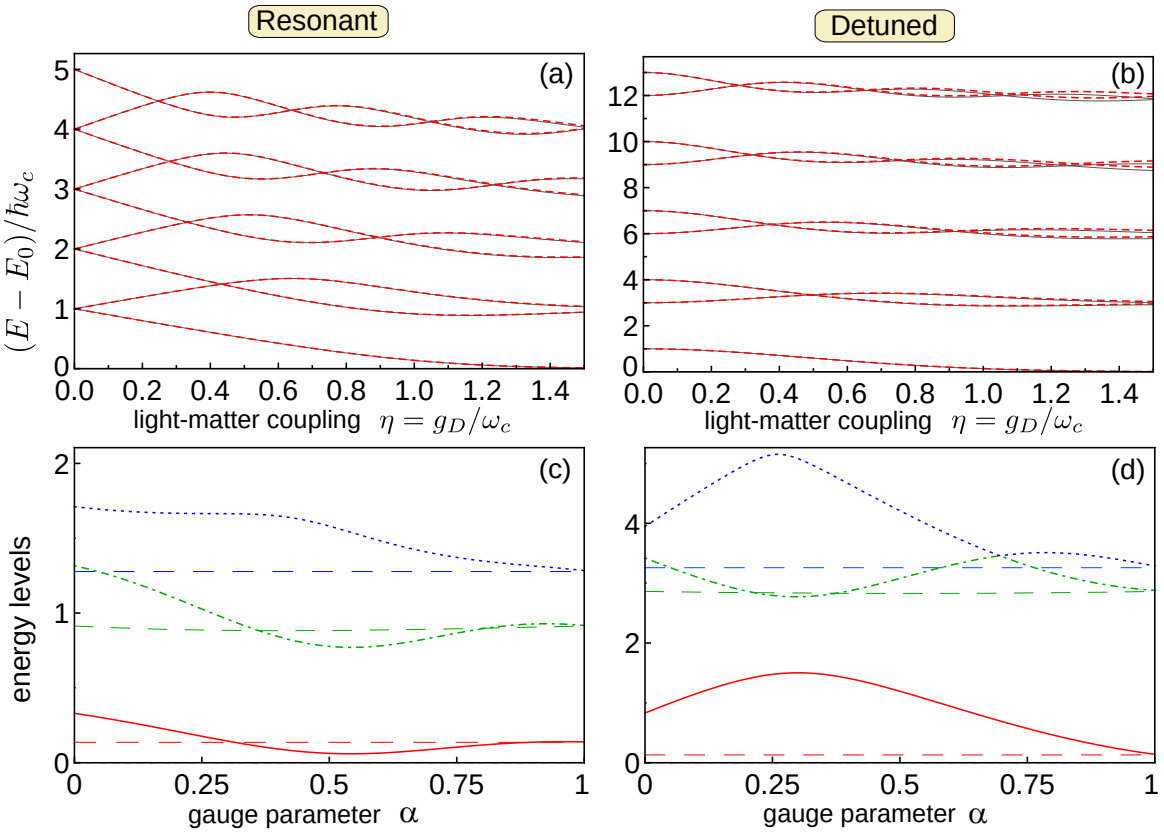

Figure S2. Comparison between exact and approximate energy spectra. (a) Energy differences $(E - E_0)/\hbar\omega_c$ versus the normalized coupling η, obtained diagonalizing numerically the exact Hamiltonian $\hat{H}_D$ (solid grey curves) and the quantum Rabi Hamiltonian $\hat{\mathcal{H}}_D$ at zero detuning (dashed red curves). (b) As in (a), but with a detuning $\delta = 3$. (c) Normalized energy differences versus α for the three lowest excited levels calculated at $\eta = 1$, obtained by diagonalizing the standard α-gauge quantum Rabi Hamiltonians $\hat{\mathcal{H}}'^{(\alpha)}$ (violating the gauge principle except for $\alpha = 1$). Dashed straight lines describe the corresponding energy levels obtained diagonalizing the exact Hamiltonian $\hat{H}_D$. (d) As in (c), but with a detuning $\delta = 3$.

represented by a charged particle of mass m moving in the potential

$$V(x) = -\frac{\kappa}{2}x^2 + \frac{\lambda}{4}x^4\,, \tag{S26}$$

where the two parameters $\kappa, \lambda > 0$ specify the shape of the double well. The Hamiltonian for the effective particle is given by

$$\hat{H}_0 = -\frac{\hbar^2}{2m}\frac{\partial^2}{\partial x^2} + V(x)\,. \tag{S27}$$

Analogously to Ref. [S4], we introduce the energy scale $E_d = \hbar^2/(mx_0^2)$ and the rescaled variable $\xi = x/x_0$, where $x_0 = [\gamma\hbar^2/(m\lambda)]^{1/6}$ with $\gamma > 0$. In terms of these quantities, Eq. (S27) can be written as

$$\hat{H}_0 = E_d \left[\frac{p_\xi^2}{2} + \frac{\beta}{2}\xi^2 + \frac{\gamma}{4}\xi^4 \right], \tag{S28}$$

where $\beta = m\kappa x_0^4/(\hbar^2)$ and $p_\xi = -i\partial/(\partial\xi)$.

We now start considering a system with a high degree of anharmonicity. Specifically, we used the parameters $\beta = 2.27$ and $\gamma = 0.5$. Within this model, the degree of anharmonicity can be controlled by changing the value of γ. The value of E_d is fixed by the choice of the detuning $\delta \equiv \omega_c/\omega_{10}$. Notice that these parameters determine an anharmonicity: $\mu \equiv (\omega_{21} - \omega_{10})/\omega_{10} \approx 70$.

Figure S2(a) shows a comparison between the energy spectra (for $\delta = 1$) versus the normalized coupling strength η of $\hat{\mathcal{H}}_D$ (red-dashed curves) and those of $\hat{H}_D$ (black continuous curves). We verified that the energy eigenvalues of the full Hamiltonian $\hat{H}_D$ are gauge invariant. The agreement is excellent. Figure S2(b) shows that a very good agreement is also obtained in the presence of some detuning ($\delta = 3$), although some small discrepancy for the highest energy levels arises at the highest coupling strengths. Panels S2(c)-(d) display the energy differences versus the gauge parameter α for the three lowest excited levels of $\hat{\mathcal{H}}'^{(\alpha)}$ calculated at $\eta = 1$. The dashed straight lines describe the corresponding energy levels obtained diagonalizing $\hat{H}_D$. The exact energy levels are all very well approximated only for $\alpha = 1$, although some *accidental* agreements can occur for some level at some values of $\alpha \neq 1$. Of course, the energy levels of $\hat{\mathcal{H}}_D$ all coincide with those of $\hat{\mathcal{H}}_D = \hat{\mathcal{H}}'^{(1)} = \hat{\mathcal{H}}^{(1)}$.

In order to test how well the approximated quantum Rabi models reproduce the exact results, it is useful to also consider the energy eigenstates in addition to energy-level calculations. The accuracy of the approximated eigenstates can be tested by calculating the fidelities. It turns out that, in contrast to the energy levels, the eigenstates change according to the gauge (even in the absence of approximations). Hence, we compare the exact numerically calculated eigenstates $|\Psi_i^\alpha\rangle$ of the full α-gauge Hamiltonian $\hat{H}^{(\alpha)}$ with the eigenstates $|\psi_i'^\alpha\rangle$ of the α-gauge quantum Rabi Hamiltonian $\hat{\mathcal{H}}'^{(\alpha)}$ (the one which violates the gauge principle [S1]), and also with the eigenstates $|\psi_i^\alpha\rangle$ of the Hamiltonian $\hat{\mathcal{H}}^{(\alpha)}$ (preserving the gauge principle). Here the subscript $i = 0, 1, 2, \ldots$ labels the energy eigenstates. For this

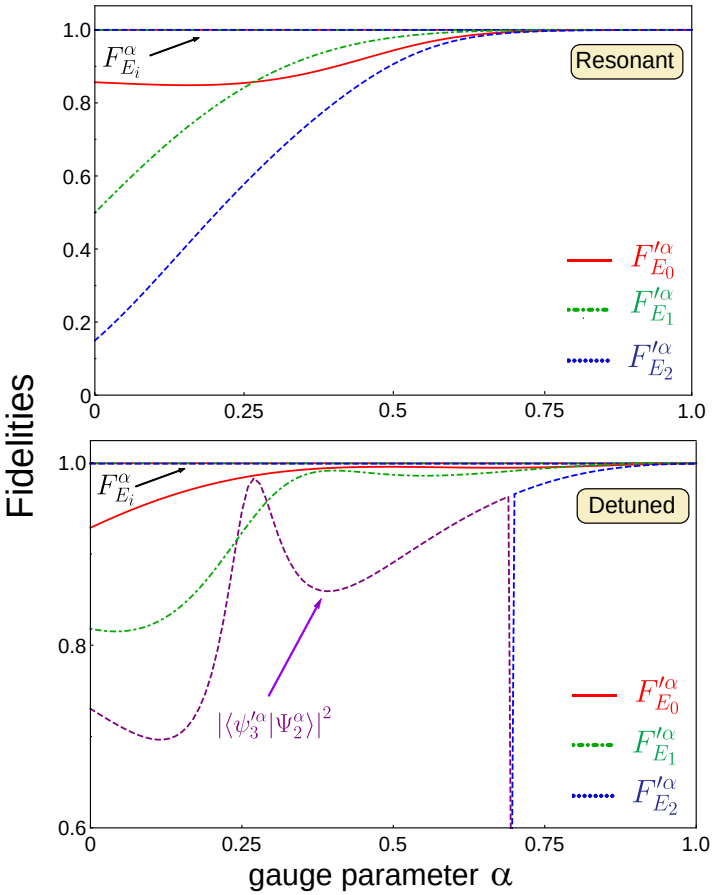

Figure S3. Fidelity for the three lowest energy levels at $\eta = 1$. The matter system is a charged particle in a double well potential (and the parameters are given in the text). The anharmonicity for this system is $\mu \approx 70$.

purpose, we define two fidelities:

$$F'^{\alpha}_{E_i} = |\langle\psi'^{\alpha}_i|\Psi^{\alpha}_i\rangle|^2 , \tag{S29}$$

and

$$F^{\alpha}_{E_i} = |\langle\psi^{\alpha}_i|\Psi^{\alpha}_i\rangle|^2 . \tag{S30}$$

Figure S3 displays the fidelities $F'^{\alpha}_{E_i}$ and $F^{\alpha}_{E_i}$ calculated for the three lowest energy levels for a normalized light-matter coupling strength $\eta = 1$. We used the same parameters specified above, and considered two cases: $\delta = 1$ (resonant case), and $\delta = 3$ (detuned case). In particular, we observe that $F^{\alpha}_{E_i}$ are very close to 1 for any α and for all the three states considered (horizontal lines). This behaviour is the one expected for quantum Rabi Hamiltonians $\hat{\mathcal{H}}^{(\alpha)}$

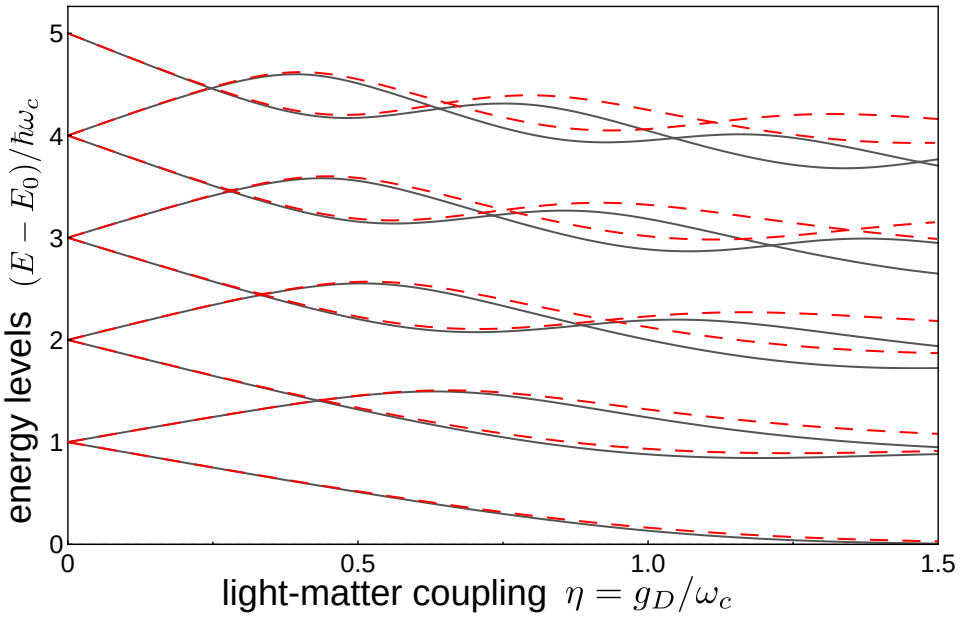

Figure S4. Energy levels of $\hat{\mathcal{H}}^{(\alpha=1)}$ (red-dashed curves) and $\hat{H}^{(\alpha=1)}$ (grey continuous curves) as a function of the normalized light-matter coupling η. The anharmonicity of the matter system is $\mu \approx 8$.

well approximating the full Hamiltonians $\hat{H}^{(\alpha)}$. On the contrary, moving away from $\alpha = 1$ (notice that $\hat{\mathcal{H}}'^{(\alpha=1)} = \hat{\mathcal{H}}^{(\alpha=1)}$), the fidelities $F'^{\alpha}_{E_i}$, obtained using the eigenstates $|\psi'^{\alpha}_i\rangle$ of $\hat{\mathcal{H}}'^{(\alpha)}$, are significantly lower. We notice that, lowering α, in panel S3(b) the fidelity $F'^{\alpha}_{E_2}$ suddenly drops to zero at $\alpha \approx 0.7$. This is due to a degeneracy point in the energy levels of $\hat{\mathcal{H}}'^{(\alpha)}$, so that the state $|\psi'^{\alpha}_3\rangle$ becomes, for $\alpha \lesssim 0.7$, a better approximation of the state $|\Psi^{\alpha}_2\rangle$. We can conclude that quantum Rabi Hamiltonians based on the standard minimal coupling replacement and violating the gauge principle provide worse approximations of the full model with respect to the gauge-preserving ones $\hat{\mathcal{H}}^{(\alpha)}$.

Finally, we compare the energy levels of $\hat{\mathcal{H}}^{(\alpha=1)}$ (red-dashed curves) and $\hat{H}^{(\alpha=1)}$ (grey continuous curves) considering a matter system with a lower degree of anharmonicity. We used $\beta = 1.7$ and $\gamma = 0.5$. These values determine a lower anharmonicity $\mu \approx 8$. Figure S4 displays the energy spectra at zero detuning as a function of the normalized coupling η. The agreement is very good for all the displayed energy levels when $\eta \lesssim 0.7$ (η is one order of magnitude lower than μ). For the two lowest energy excited levels, the agreement remains good for the whole range displayed. For $\eta \gtrsim 1$, the agreement becomes less accurate, as

expected when the coupling strength becomes comparable to the anharmonicity. We have also calculated the fidelities for the three lowest energy levels. They remain very high ($F^{\alpha}_{E_i} > 0.989$), although they are slightly lower than those obtained for the system with a higher degree of anharmonicity.

In summary, if the anharmonicity μ is much higher than the normalized coupling strength η, the gauge quantum Rabi model developed in this work provides accurate, gauge-independent results. The breakdown of the quantum Rabi model shown in Ref [S1] can be attributed to the inadequate degree of anharmonicity of the considered matter system. Indeed, a well-known result for light-matter systems is that the influence of an atomic transition with frequency ω_{jk} can be neglected only if $g_{jk}/|\omega_{jk} - \omega_c| \ll 1$, where g_{jk} is the transition coupling strength [S9]. Hence, if we desire to include only the two lowest energy states ($|0\rangle$ and $|1\rangle$) of the matter system, neglecting the influence of the higher state $|2\rangle$, the following inequality has to be satisfied: $|\omega_{21} - \omega_c| \gg g_{21}$. Assuming $g_{21} \sim g_{10} \equiv g$ and dividing by ω_{10}, the above inequality can be rewritten as

$$|\mu - \delta + 1| \gg \eta\delta\,, \tag{S31}$$

where $\delta \equiv \omega_c/\omega_{10}$. For the resonant case ($\delta = 1$), we have $\mu \gg \eta$. Using the parameters of the artificial atom (fluxonium) in [S1], we obtain an anharmonicity $\mu \simeq 2.2$ for which the condition of Eq. (S31) is not adequately satisfied. It is worth noticing that, when $\delta \ll 1$, the inequality is easier to satisfy for a given value of μ. This could explain the improved accuracy of the flux-gauge energy levels obtained for $\delta = 1/5$ in Ref. [S1].

In conclusion, we can state that the degree of anharmonicity of the matter system considered in [S1] is not enough to guarantee the validity of the two-level approximation. Of course, depending on the degree of anharmonicity of each matter system, there will always be a light-matter coupling strength beyond which the two-level approximation fails. In these cases, if additional levels of the matter system are included, the gauge theory in truncated Hilbert spaces presented here is still expected to work.

[S1] A. Stokes and A. Nazir, "Gauge ambiguities imply Jaynes-Cummings physics remains valid in ultrastrong coupling QED," Nat. Commun. **10** (2019).

[S2] K. Hepp and E. H. Lieb, "On the superradiant phase transition for molecules in a quantized radiation field: the Dicke maser model," Ann. Physics **76**, 360–404 (1973).

[S3] N. Shammah, N. Lambert, F. Nori, and S. De Liberato, "Superradiance with local phase-breaking effects," Phys. Rev. A **96**, 023863 (2017).

[S4] D. De Bernardis, T. Jaako, and P. Rabl, "Cavity quantum electrodynamics in the nonperturbative regime," Phys. Rev. A **97**, 043820 (2018).

[S5] J. Keeling, "Coulomb interactions, gauge invariance, and phase transitions of the Dicke model," J. Phys.: Condens. Matter **19**, 295213 (2007).

[S6] P. Nataf and C. Ciuti, "No-go theorem for superradiant quantum phase transitions in cavity QED and counter-example in circuit QED," Nat. Commun. **1**, 72 (2010).

[S7] D. De Bernardis, P. Pilar, T. Jaako, S. De Liberato, and P. Rabl, "Breakdown of gauge invariance in ultrastrong-coupling cavity QED," Phys. Rev. A **98**, 053819 (2018).

[S8] V. E. Manucharyan, J. Koch, L. I. Glazman, and M. H. Devoret, "Fluxonium: single Cooper-pair circuit free of charge offsets," Science **326**, 113–116 (2009).

[S9] L. Allen and J. H. Eberly, *Optical resonance and two-level atoms*, Vol. 28 (Courier Corporation, 1987).

6.2 Gauge freedom, quantum measurements, and time-dependent interactions in cavity and circuit QED

Gauge freedom, quantum measurements, and time-dependent interactions in cavity and circuit QED

Alessio Settineri,[1] Omar Di Stefano,[2] David Zueco,[3,4]
Stephen Hughes,[5] Salvatore Savasta,[1,*] and Franco Nori[2,6]

[1] *Dipartimento di Scienze Matematiche e Informatiche, Scienze Fisiche e Scienze della Terra, Università di Messina, I-98166 Messina, Italy*

[2] *Theoretical Quantum Physics Laboratory, RIKEN Cluster for Pioneering Research, Wako-shi, Saitama 351-0198, Japan*

[3] *Instituto de Ciencia de Materiales de Aragón and Departamento de Física de la Materia Condensada , CSIC-Universidad de Zaragoza, Pedro Cerbuna 12, 50009 Zaragoza, Spain*

[4] *Fundación ARAID, Campus Río Ebro, 50018 Zaragoza, Spain*

[5] *Department of Physics, Engineering Physics, and Astronomy, Queen's University, Kingston, Ontario K7L 3N6, Canada*

[6] *Physics Department, The University of Michigan, Ann Arbor, Michigan 48109-1040, USA*

Abstract

The interaction between the electromagnetic field inside a cavity and natural or artificial atoms has played a crucial role in developing our understanding of light-matter interaction, and is central to various quantum technologies. Recently, new regimes beyond the weak and strong light-matter coupling have been explored in several settings. These regimes, where the interaction strength is comparable (ultrastrong) or even higher (deep-strong) than the transition frequencies in the system, can give rise to new physical effects and applications. At the same time, they challenge our understanding of cavity QED. When the interaction strength is so high, fundamental issues like the proper definition of subsystems and of their quantum measurements, the structure of light-matter ground states, or the analysis of time-dependent interactions are subject to ambiguities leading to even qualitatively distinct predictions. The resolution of these ambiguities is also important for understanding and designing next-generation quantum devices that will exploit the ultrastrong coupling regime. Here we discuss and provide solutions to these issues.

* corresponding author: ssavasta@unime.it

I. INTRODUCTION

Light-matter ultrastrong coupling (USC) [1, 2] can be achieved by coupling many dipoles (collectively) to light, or by using matter systems like superconducting artificial atoms whose coupling is not bound by the small size of the fine-structure constant. The largest light-matter coupling strengths have been measured in experiments with Landau polaritons in semiconductor systems [3] and in setups with superconducting quantum circuits [4]. Another potentially promising route to realize USC with natural atoms and molecules is using metal resonators, since the coupling rates are not bound by diffraction. Single molecules in plasmonic cavities are starting to enter the USC regime [5], and two-dimensional transition metal dichalcogenides (TMDs) coupled to metal particles have already reached the USC regime [6], even at room temperature. Ultrastrong plasmon exciton interactions has also been reported with crystallized films of carbon nanotubes [7]. The physics of the USC regime can also be accessed by using quantum simulation approaches (see, e.g., [8]).

These very strong interaction regimes also turned out to be a test bed for gauge invariance [9–11]. The issue of gauge invariance, first pointed out by Lamb in 1952 [12], has constantly affected the theoretical predictions in atomic physics and in non-relativistic quantum electrodynamics (QED) (see, e.g., [13–16]). Recently, it has been shown that the standard quantum Rabi model, describing the coupling between a two-level system (TLS) and a single-mode quantized electromagnetic field, heavily violates this principle in the presence of ultrastrong light-matter coupling [9, 10]. This issue has been recently solved by introducing a generalized minimal-coupling replacement [11].

A distinguishing feature of USC systems is the presence of entangled light and matter excitations in the ground state, determined by the counter-rotating terms in the interaction Hamiltonian [17–19]. Actually, all excited states are also dressed by multiple virtual excitations [20]. Much research on these systems has dealt with understanding whether these dressing excitations are real or virtual and how they can be probed or extracted [1, 2]. These vacuum excitations can be converted into real detectable ones (see, e.g., [20–26]). However, the analysis of these effects is affected by possible ambiguities arising from the gauge dependence of the system eigenstates [10, 11, 27]. Specifically, the unitary gauge transformation does not conserve virtual excitations, nor light-matter entanglement [27]. Hence, the definition of these key features of the USC regime is subject to ambiguities, so that, as we show

here, a maximally entangled ground state can become separable in a different gauge.

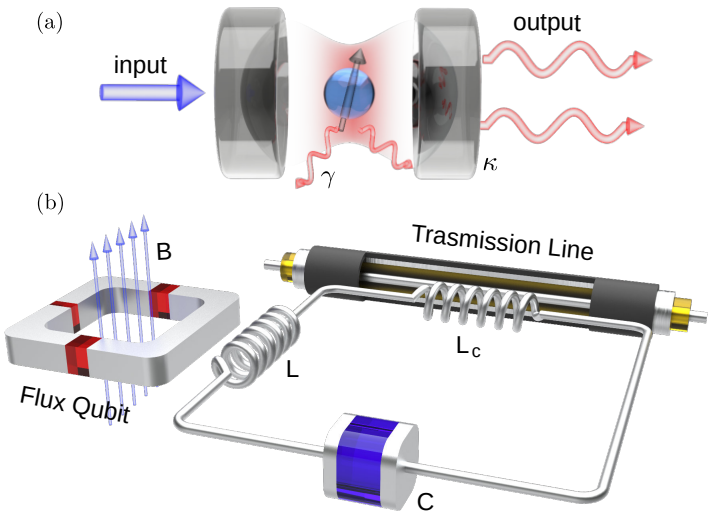

Figure 1. Cavity and circuit QED setups. (a) Schematic view of a typical cavity QED system constituted by an atom (depicted as an effective spin) embedded in an optical cavity. (b) Circuit QED: schematic view of a superconducting flux qubit and a superconducting LC oscillator inductively coupled to each other. The LC oscillator is also inductively coupled to a transmission line.

Ambiguities are not limited to those properties dependent on virtual excitations, but also affect physical detectable photons. This issue originates from the gauge dependence of the field canonical momentum (see, e.g., Refs. [13, 14, 16]). According to the Glauber's photodetection theory [28], the detection rate for photons polarized along a direction i is proportional to $\langle\psi|\hat{E}_i^{(-)}\hat{E}_i^{(+)}|\psi\rangle$, where $\hat{\mathbf{E}}^{(\pm)}$ are the positive and negative frequency components of the electric-field operator. In the Coulomb gauge, $\hat{\mathbf{E}}$ is proportional to the field canonical momentum and can be expanded in terms of photon operators. On the contrary, in the multipolar gauge, the canonical momentum that can be expanded in terms of photon operators is not $\hat{\mathbf{E}}$ but the displacement operator $\hat{\mathbf{D}}$. This subtlety is generally disregarded, and the usual procedure is to obtain the system states in the dipole gauge (the multipolar gauge after the electric-dipole approximation) $|\psi_D\rangle$, and to calculate the photodetection rate ignoring that in this gauge the electric field operator is not a canonical momentum. As we show here, this procedure, when applied to the quantum Rabi model, can lead to strongly incorrect predictions. In this article, we face and solve all these issues by adopting an ap-

proach based on operational procedures involving measurements on the individual light and matter components of the interacting system.

The exploration of fundamental quantum physics in the strong coupling [29] and USC regimes [1, 2] has greatly evolved thanks to circuit QED systems based on superconducting artificial atoms coupled to on-chip cavities [30]. We show that these systems are not free from gauge ambiguities and, despite displaying energy spectra very similar to traditional cavity QED systems, have drastically distinct measurable ground-state properties, like the photon number and the entanglement.

II. QUANTUM RABI HAMILTONIANS

Let us consider a simple cavity QED system represented by a single atom (dipole) coupled to an optical resonator. We start adopting the Coulomb gauge, where the particle momentum is coupled only to the transverse part of the vector potential $\hat{\mathbf{A}}$. It represents the field coordinate, while its conjugate momentum is proportional to the transverse electric field operator. The latter (as well as the vector potential) can be expanded in terms of photon creation and destruction operators: $\hat{\mathbf{E}}_C(\mathbf{r},t) = \sum_k \mathbf{E}_k(\mathbf{r})\hat{a}_k e^{-i\omega_k t} + \text{h.c.}$, where $\mathbf{E}_k(\mathbf{r}) = \sqrt{\hbar\omega_k/2\varepsilon_0}\,\mathbf{f}_k(\mathbf{r})$ are the effective mode amplitudes, and h.c. represents hermitian conjugate. Here, $\mathbf{f}_k(\mathbf{r})$ are any general "normal modes" with real eigenfrequencies, ω_k, obtained from Maxwell's equations for a particular medium. They are normalized and complete (including also the longitudinal modes, $\omega_k = 0$), so that $\sum_k \epsilon_b(\mathbf{r}')\mathbf{f}_k^*(\mathbf{r})\mathbf{f}_k(\mathbf{r}') = \mathbf{1}\delta(\mathbf{r}-\mathbf{r}')$, where ϵ_b is the relative dielectric function of a background dielectric medium. The system Hamiltonian is

$$\hat{H}_C = \frac{1}{2m}[\hat{\mathbf{p}}_C - q\hat{\mathbf{A}}(\mathbf{r})]^2 + V(\mathbf{r}) + \sum_k \hbar\omega_k \hat{a}_k^\dagger \hat{a}_k \,, \tag{1}$$

where $\hat{\mathbf{p}}_C$ and $V(\mathbf{r})$ are the particle's canonical momentum and potential.

The quantum Rabi Hamiltonian, can be obtained considering a single two-level system (TLS) at position $\mathbf{r}_0$, with (real) dipole moment $\boldsymbol{\mu} = q\langle e|\mathbf{x}|g\rangle$, interacting with a single cavity mode $[(\hat{a}_k, \mathbf{f}_k, \omega_k) \to (\hat{a}, \mathbf{f}_c, \omega_c)]$. The correct (namely, satisfying the gauge principle) quantum Rabi Hamiltonian [11], strongly differs from the standard quantum Rabi model:

$$\hat{\mathcal{H}}_C = \hbar\omega_c \hat{a}^\dagger\hat{a} + \frac{\hbar\omega_0}{2}\left\{\hat{\sigma}_z \cos\left[2\eta(\hat{a}+\hat{a}^\dagger)\right] + \hat{\sigma}_y \sin\left[2\eta(\hat{a}+\hat{a}^\dagger)\right]\right\} \,, \tag{2}$$

where $\omega_c\eta \equiv g = \sqrt{\omega_c/2\hbar\epsilon_0}\,\boldsymbol{\mu}\cdot\mathbf{f}_c(\mathbf{r}_0)$, and $\hat{\sigma}_j$ are the usual Pauli operators.

In cavity QED, the multipolar gauge after the dipole approximation (dipole gauge) represents a convenient and widely used choice. A generic system operator in the multipolar gauge $\hat{O}_M$ is related to the corresponding operator in the Coulomb gauge $\hat{O}_C$ by a suitable unitary Power-Zienau-Woolley (PZW) transformation [16, 31] $\hat{O}_{\rm M} = \hat{T}\hat{O}_{\rm C}\hat{T}^\dagger$ (see Appendix A). It turns out that in the multipolar gauge, while the field coordinate remains unchanged, its conjugate momentum is $\hat{\mathbf{\Pi}}_M = -\epsilon_0\epsilon_b(\mathbf{r})\hat{\mathbf{E}}_M - \hat{\mathbf{P}} = -\hat{\mathbf{D}}_M$, where $\hat{\mathbf{P}}$ is the electric polarization and $\hat{\mathbf{D}}_M$ is the displacement field [13, 32, 33], which can be directly expanded in terms of photon operators:

$$\hat{\mathbf{F}}_M(\mathbf{r},t) \equiv \frac{\hat{\mathbf{D}}_M(\mathbf{r},t)}{\epsilon_0\epsilon_{\rm b}(\mathbf{r})} = i\sum_k \sqrt{\frac{\hbar\omega_k}{2\epsilon_0}}\mathbf{f}_k(\mathbf{r})\hat{a}_k(t) + \text{h.c.}, \tag{3}$$

where $\hat{\mathbf{F}}_M$ is the effective electric field that atomic dipoles couple to [33]. For a single dipole at position $\mathbf{r}_0$, the interaction Hamiltonian is $H_I = -q\boldsymbol{x}\cdot\hat{\mathbf{F}}(\mathbf{r}_0) + (qx)^2/\epsilon_0\epsilon_b(\mathbf{r}_0)$. Considering a single TLS, we obtain

$$\hat{\mathbf{F}}_D(\mathbf{r}) = \hat{\mathbf{E}}_D(\mathbf{r}) + \frac{\boldsymbol{\mu}}{\epsilon_0\epsilon_b(\mathbf{r}_0)}\delta(\mathbf{r}-\mathbf{r}_0)\,\hat{\sigma}_x, \tag{4}$$

where $\hat{\mathbf{E}}_D(\mathbf{r})$ is the electric field operator in the dipole gauge. We note that for spatial locations away from the dipole ($\mathbf{r} \neq \mathbf{r}_0$), then $\hat{\mathbf{F}}_D$ and $\hat{\mathbf{E}}_D$ are equivalent. Next, we rewrite $\hat{\mathbf{E}}_D(\mathbf{r})$ in a way that makes each mode contribution clear:

$$\hat{\mathbf{E}}_D(\mathbf{r},t) = i\sum_k \sqrt{\frac{\hbar\omega_k}{2\epsilon_0}}\mathbf{f}_k(\mathbf{r})\hat{a}_k(t) + \text{h.c.} - \frac{1}{2\epsilon_0}\left[\sum_k \mathbf{f}_k^*(\mathbf{r})\mathbf{f}_k(\mathbf{r}_0) + \mathbf{f}_k^*(\mathbf{r}_0)\mathbf{f}_k(\mathbf{r})\right]\cdot\boldsymbol{\mu}\,\hat{\sigma}_x. \tag{5}$$

We now consider the single-mode limit, which is typically assumed in models such as the quantum Rabi model, where a single-mode cavity is the dominant mode of interest (see Appendix A):

$$\hat{\mathbf{E}}_D(\mathbf{r},t) = i\sqrt{\frac{\hbar\omega_c}{2\epsilon_0}}\mathbf{f}_c(\mathbf{r})\hat{a}'(t) + \text{h.c.}, \tag{6}$$

where $\hat{a}'(t) = \hat{a}(t) + i\eta\hat{\sigma}_x(t)$. We observe that the operators $\hat{a}'$ and $\hat{a}'^\dagger$ obey the same commutation relations of the bosonic operators $\hat{a}$ and $\hat{a}^\dagger$. The total Hamiltonian (throughout the article we use the calligraphic font for operators projected in a two level space) in the dipole gauge is

$$\hat{\mathcal{H}}_D = \hat{\mathcal{H}}_{\rm free} + \hat{\mathcal{V}}_D\,, \tag{7}$$

where $\hat{\mathcal{H}}_{\rm free} = \hbar\omega_c \hat{a}^\dagger \hat{a} + \frac{\hbar\omega_0}{2}\hat{\sigma}_z$, ω_0 is the transition frequency of the TLS, and the interaction Hamiltonian is

$$\hat{\mathcal{V}}_D = i\eta\hbar\omega_c(\hat{a}^\dagger - \hat{a})\hat{\sigma}_x \,. \tag{8}$$

The two gauges are related by the transformation $\hat{\mathcal{H}}_D = \hat{\mathcal{T}}\hat{\mathcal{H}}_C\hat{\mathcal{T}}^\dagger$, where $\hat{\mathcal{T}} = \exp(i\hat{\mathcal{F}})$ with $\hat{\mathcal{F}} = -\eta\hat{\sigma}_x(\hat{a} + \hat{a}^\dagger)$ (see Appendix A).

III. PHOTODETECTION

The photon rate that can be measured placing a point-like detector in the resonator at the position $\mathbf{r}$ and at a given time t is proportional to [28]

$$\langle \hat{\mathbf{E}}^{(-)}(\mathbf{r},t) \cdot \hat{\mathbf{E}}^{(+)}(\mathbf{r},t) \rangle \,, \tag{9}$$

where $\hat{\mathbf{E}}^{(+)}$ and $\hat{\mathbf{E}}^{(-)}$ are the positive and negative frequency components of the electric-field operator, with $\hat{\mathbf{E}}^{(-)} = [\hat{\mathbf{E}}^{(+)}]^\dagger$ (see Appendix B). Note that, in the absence of the interactions, or when the rotating-wave approximation can be applied to the interaction Hamiltonian, the positive-frequency operator only contains destruction photon operators. However, when the rotating-wave approximation cannot be applied, this direct correspondence does not hold [34]. By using the input-output theory (see Appendix J), analogous results for the rate of emitted photons can be obtained for a detector placed outside the cavity [35].

Considering a single-mode resonator coupled to a TLS (quantum Rabi model), assuming that the system is prepared initially in a specific energy eigenstate $|j_C\rangle$, and using Eq. (9), then the resulting detection rate in the Coulomb gauge is proportional to

$$W = \sum_{k<j} |\langle k_C|\hat{\mathcal{P}}|j_C\rangle|^2 \,, \tag{10}$$

where

$$\hat{\mathcal{P}} = i(\hat{a} - \hat{a}^\dagger) \,, \tag{11}$$

and we ordered the eigenstates so that $j > k$ for eigenfrequencies $\omega_j > \omega_k$. If a tunable narrow-band detector is employed, a single transition can be selected, so that the detection rate for a frequency $\omega = \omega_{j,k} \equiv \omega_j - \omega_k$ is proportional to

$$W_{j,k} = |\langle k_C|\hat{\mathcal{P}}|j_C\rangle|^2 \,. \tag{12}$$

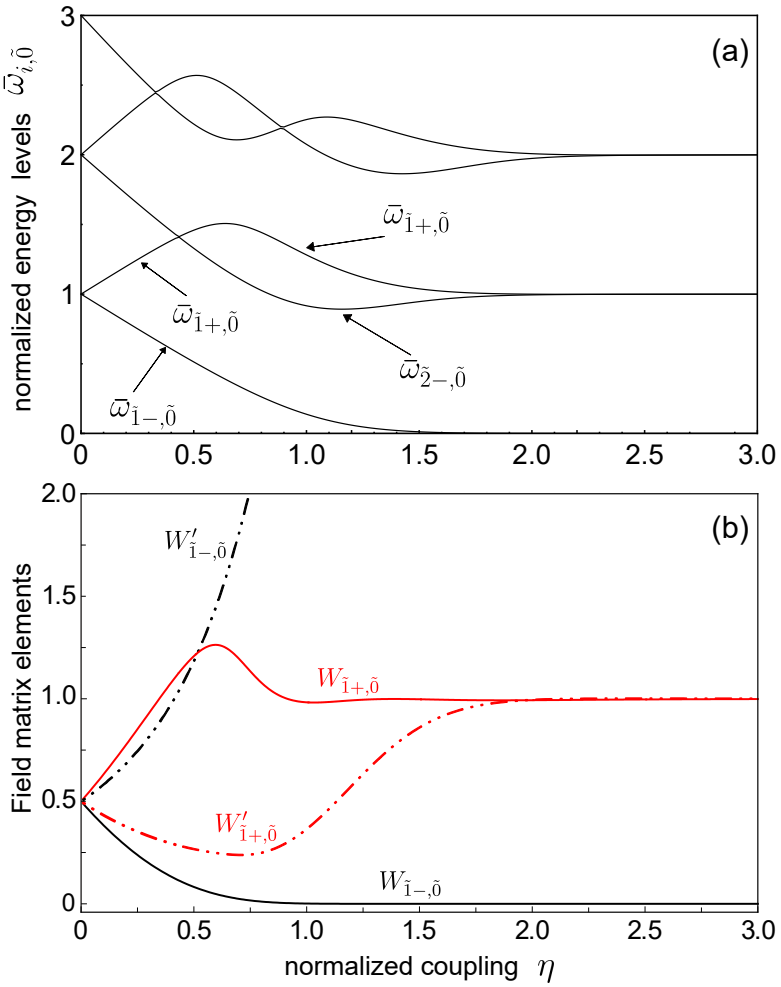

Figure 2. Quantum Rabi model. (a) Normalized energy levels differences between the lowest excited levels and the ground energy level of the quantum Rabi Hamiltonian $\hat{\mathcal{H}}_C$ for the case of zero detuning ($\omega_c = \omega_0$) as a function of the normalized coupling strength η; (b) Square moduli of the transition matrix elements of the electric-field operator, $W_{\tilde{1}\pm,\tilde{0}}$, accounting for the transitions between the two lowest excited levels and the ground state of the quantum Rabi Hamiltonian, versus η. For comparison, the panel also reports the wrong matrix elements $W'_{\tilde{1}\pm,\tilde{0}}$ (see text).

In the dipole gauge, we obtain

$$W_{j,k} = |\langle k_D|i(\hat{a} - \hat{a}^\dagger) - 2\eta\hat{\sigma}_x|j_D\rangle|^2 \,. \tag{13}$$

The gauge principle, as well as the theory of unitary transformations, ensure that Eqs. (12) and (13) provide the same result [11]. On the contrary, the usual procedure, consisting in using the dipole gauge without changing accordingly the field operator (see, e.g., [1,

2]): $W'_{j,k} = |\langle k_D|i(\hat{a} - \hat{a}^\dagger)|j_D\rangle|^2$, provides wrong results. When the normalized coupling strength $\eta \ll 1$, the error can be small. However, when η is non-negliglible, W and W' can provide very different predictions, as shown in Fig. 2. Panel 2(a) displays the energy differences between the lowest excited levels and the ground energy level of the quantum Rabi Hamiltonian $\hat{\mathcal{H}}_C$ (or $\hat{\mathcal{H}}_D$) for the case of zero cavity-atom detuning ($\omega_c = \omega_0$). Here we indicate the dressed ground state as $|\tilde{0}\rangle$, and the excited states as $|\tilde{n}\pm\rangle$ on the basis of the usual notation for the Jaynes-Cummings (JC) eigenstates $|n\pm\rangle$ (see, e.g., [36]). Panel 2(b) shows that, except for negligible couplings (where $W_{\tilde{1}\pm,\tilde{0}} = W'_{\tilde{1}\pm,\tilde{0}} = 0.5$), $W_{\tilde{1}\pm,\tilde{0}}$ and $W'_{\tilde{1}\pm,\tilde{0}}$ display different results. The differences are evident already for $\eta \sim 0.1$.

It is interesting to point out some noteworthy features of this comparison. First, we observe that $W_{\tilde{1}+,\tilde{0}} > W_{\tilde{1}-,\tilde{0}}$ for all the values of η, and finally, increasing η, $W_{\tilde{1}-,\tilde{0}} \to 0$. These results originate from the dependence on η of the corresponding transition frequencies $\omega_{\tilde{1}\pm,\tilde{0}}$. Specifically, photodetection is an energy absorbing process, whose rate is proportional to the intensity, which in turn is proportional to the energy of the absorbed photons. Hence, $\omega_{\tilde{1}+,\tilde{0}} > \omega_{\tilde{1}-,\tilde{0}}$ implies $W_{\tilde{1}+,\tilde{0}} > W_{\tilde{1}-,\tilde{0}}$. For the same reason, when $\omega_{\tilde{1}-,\tilde{0}} \to 0$, there is no energy to be absorbed, and $W_{\tilde{1}-,\tilde{0}} \to 0$. On the contrary, $W'_{\tilde{1}\pm,\tilde{0}}$ displays the opposite (*unphysical*) behaviour.

IV. READOUT OF A STRONGLY COUPLED QUBIT

While in the Coulomb gauge, the atom momentum is affected by the coupling with the field [16] [$m\dot{\mathbf{x}} = \hat{\mathbf{p}}_C - q\hat{\mathbf{A}}(\mathbf{x})$], in the dipole gauge it is interaction-independent: $m\dot{\mathbf{x}} = \hat{\mathbf{p}}_D$. This feature can give rise to ambiguities in the definition of the physical properties of an atom interacting with a field [15]. Moreover, an unambiguous separation between light and matter systems becomes problematic with increasing coupling strength. Again, we face this problem by adopting an operational approach based on what is actually measured. In cavity and circuit QED quantum-non-demolition measurements are widely used [37–42]. Specifically, a quantum-non-demolition-like readout of the qubit can be realized by coupling it, with a moderate coupling strength, to a resonator mode b with resonance frequency ω_b. The readout can be accomplished by detecting the dispersive qubit state-dependent shift of the resonator frequency: $\omega_b \to \omega_b + \chi\langle\hat{\sigma}_z\rangle$, where $\chi = \omega_b^2\eta_b^2/(\omega_0 - \omega)$ [29, 40, 43, 44]. If the qubit is coupled very strongly to a second field-mode a, this readout scheme can provide

interesting information on how the qubit state is affected by the USC regime. However, the expectation value $\langle\hat{\sigma}_z\rangle$ for a qubit in the USC regime is ambiguous when the coupling becomes strong. Specifically, since $\langle\psi_C|\hat{\sigma}_z|\psi_C\rangle \neq \langle\psi_D|\hat{\sigma}_z|\psi_D\rangle$, the question arises which of these two quantities is actually detected?

We start from the Hamiltonian in the Coulomb gauge Eq. (1), limited to include only two quantized normal modes (a and b). We then project the atomic system in order to consider two levels only, and assume for the resulting coupling strengths that $\eta_b \ll \eta_a$. If the USC system is in the state $|\psi_C\rangle$, applying the standard procedure for obtaining dispersive shifts [44], we find for the readout mode b: $\chi\langle\psi_C|\hat{\mathcal{T}}_a^\dagger\hat{\sigma}_z\,\hat{\mathcal{T}}_a|\psi_C\rangle = \chi\langle\psi_D|\hat{\sigma}_z|\psi_D\rangle$, where $\hat{\mathcal{T}}_a^\dagger\hat{\sigma}_z\,\hat{\mathcal{T}}_a = \hat{\sigma}_z\cos\left[2\eta(\hat{a}+\hat{a}^\dagger)\right] - \hat{\sigma}_y\sin\left[2\eta(\hat{a}+\hat{a}^\dagger)\right]$ (see Appendix C). Hence, we can conclude that *the readout shift provides a measurement of the expectation value of the* bare *qubit population difference, as defined in the dipole gauge*. Interestingly, this measurement is able to provide direct information on the ground state qubit excitations induced by the interaction with resonator a.

The dot-dashed curves in Fig. 3 display the qubit excitation probabilities that can be measured by dispersive readout: $\langle i_C|\hat{\mathcal{T}}_a^\dagger\hat{\sigma}_+\hat{\sigma}_-\hat{\mathcal{T}}_a|i_C\rangle = \langle i_D|\hat{\sigma}_+\hat{\sigma}_-|i_D\rangle$, together with $\langle i_C|\hat{\sigma}_+\hat{\sigma}_-|i_C\rangle$, for the two lowest energy levels of the quantum Rabi model (notice that $2\hat{\sigma}_+\hat{\sigma}_- = \hat{\sigma}_z + \hat{\mathcal{I}}$ where $\hat{\mathcal{I}}$, is the identity operator in the TLS space) . As shown in Fig. 3, $\langle i_D|\hat{\sigma}_+\hat{\sigma}_-|i_D\rangle$ strongly differs from $\langle i_C|\hat{\sigma}_+\hat{\sigma}_-|i_C\rangle$. An analytical description of these results in the large-coupling limit is provided in Appendix D.

V. LIGHT-MATTER ENTANGLEMENT AND NON-ADIABATIC TUNABLE COUPLING

One of the most interesting features of USC systems is the presence of entangled ground states with virtual excitations [1, 2]. However, since the ground state of a cavity QED system is gauge dependent (e.g., $|\psi_D\rangle = \hat{\mathcal{T}}|\psi_C\rangle$), the mean numbers of excitations in the ground state are gauge dependent. Moreover, the unitary operator $\hat{\mathcal{T}}$ does not preserve the atom-field entanglement. Since physical observable quantities cannot be gauge dependent, the question arises if these ground state properties have any physical meaning. Actually, it is known that these excitations, e.g., the photons in the ground state, are unable to leave the cavity and can be regarded as virtual (see, e.g., Refs. [20, 45]). However, if the interaction

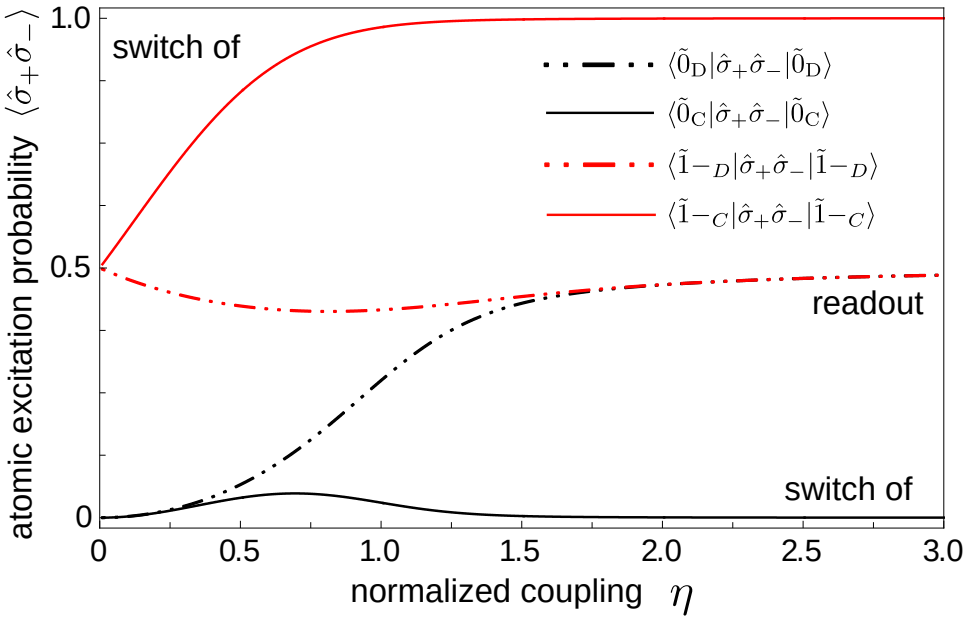

Figure 3. Readout of a strongly coupled qubit. Qubit's excitation probabilities for the system in its ground states (black curves) and in the first excited state (red curves) calculated in both the Coulomb (solid curves) and the dipole (dotted-dashed) gauges as a function of the normalized coupling strength η. Note that $\langle\hat{\sigma}_+\hat{\sigma}_-\rangle_D$ corresponds to what is measured via dispersive readout of the qubit (see text). On the contrary, the photon rate released by the qubit after a sudden switch off of the light-matter interaction is proportional to $\langle\hat{\sigma}_+\hat{\sigma}_-\rangle_C$ (see Sect. V).

is suddenly switched off (with switching time T going to zero), the system quantum state remains unchanged for regular Hamiltonians [46], and the excitations in the ground state, can then evolve according to the free Hamiltonian and can thus be released and detected (see, e.g., [23]). Of course *detectable* subsystem excitations and correlations have to be gauge invariant, since the results of experiments cannot depend on the gauge. On this basis *we can define gauge invariant excitations and qubit-field entanglement.*

It is instructive to analyse these quantities by using both the Coulomb gauge and the dipole gauge. We start with the Coulomb gauge. We consider the system initially prepared in its ground state $|\psi_C(t_0)\rangle = |\tilde{0}_C\rangle$. At $t = t_0$, the interaction is abruptly switched off within a time $T \to 0$. This non-adiabatic switch does not alter the quantum state [46], which at $t \geq t_1 = t_0 + T$ evolves as $|\psi_C(t)\rangle = \exp\left[-i\hat{\mathcal{H}}_{\rm free}(t - t_0)\right]|\psi_C(t_0)\rangle$. We can use this state to calculate, e.g., the observable mean photon number: $\langle\psi_C(t)|\hat{a}^\dagger\hat{a}|\psi_C(t)\rangle$, which can be

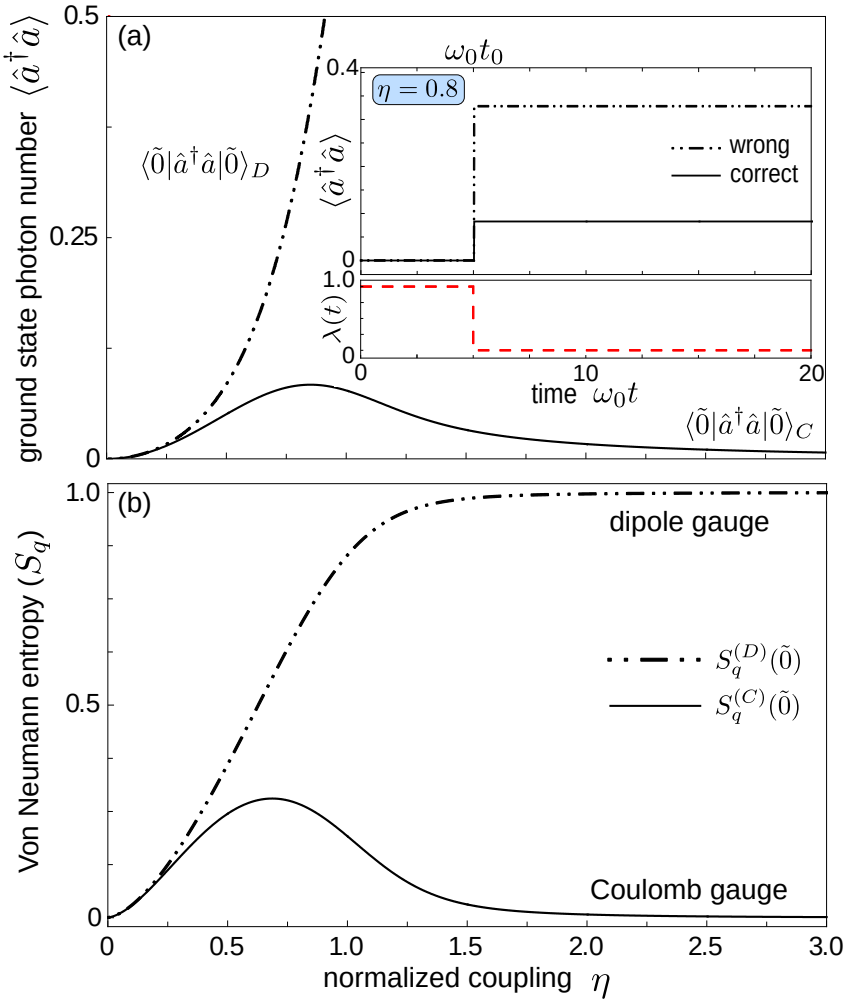

Figure 4. Vacuum emission. (a) Mean photon number calculated in the Coulomb (solid curve) and in the wrong dipole (dot-dashed curve) gauges as a function of η for the system prepared in the ground state of the quantum Rabi model. (inset) Vacuum emission (mean photon number) after the switch off evaluated for $\eta = 0.8$. (b) Qubit's entropies (which quantifies the qubit-oscillator entanglement) for the ground states (black curves) calculated in both the Coulomb (solid curves) and the wrong dipole (dotted-dashed) gauges as a function of the normalized coupling strength η.

measured by detecting the output photon flux from the resonator. It is worth noting that this expectation value can also be calculated by using the dipole gauge, by applying the unitary transformation to both the operator and the quantum states: $\langle \psi_C(t)|\hat{a}^\dagger \hat{a}|\psi_C(t)\rangle = \langle \psi_D(t)|\hat{a}'^\dagger \hat{a}'|\psi_D(t)\rangle$.

The Hamiltonian in the dipole gauge can be obtained from that in the Coulomb gauge via

a unitary transformation which, in this case becomes time-dependent. It can also be obtained by considering the corresponding gauge transformation of the fields potentials, taking into account that, during the switch, the transformation depends explicitly on time. Carrying out the calculations in the dipole gauge (see also Appendix F), it can be shown that, even in the presence of a non-adiabatic switch off of the interaction, there are no gauge ambiguities if the explicit time-dependence of the transformation (or of the generating function for the gauge transformation) is properly taken into account.

In order to test explicitly gauge invariance in the presence of ultrastrong interactions and non-adiabatic tunable couplings, we calculate the quantum state after a sudden switch off of the interaction, by using the dipole gauge. During the switch, the transformation is time-dependent and can be expressed as $\hat{\mathcal{T}}(t) = \exp\left[i\lambda(t)\hat{\mathcal{F}}\right]$, where $\lambda(t)$ is the switching function [with $\lambda(t) = 1$ for $t \leq t_0$, and $\lambda(t) = 0$ for $t \geq t_1$]. The resulting correct Hamiltonian in the dipole gauge is

$$\hat{\mathcal{H}}_D(t) = \hat{\mathcal{H}}_{\rm free} + \hat{\mathcal{V}}_D(t) - \dot{\lambda}\hat{\mathcal{F}}\,. \tag{14}$$

For very fast switches, the last term in $\hat{\mathcal{H}}_D(t)$ dominates during the switching and goes to infinity for switching times $T \to 0$. Hence its contribution to the time evolution during the switching time cannot be neglected. Let us consider the system at $t = t_0$ (before the switch off) to be in the state $|\psi_D(t_0)\rangle$. Assuming $T \to 0$, just after the switch off ($t_1 = t_0 + T$), the resulting state is

$$|\psi_D(t_1)\rangle = \exp\left(i\hat{\mathcal{F}}\int_{t_0}^{t_1} dt\dot{\lambda}\right)|\psi_D(t_0)\rangle. \tag{15}$$

Since the integral is equal to -1, and $|\psi_D\rangle = \hat{\mathcal{T}}|\psi_C\rangle$, we obtain

$$|\psi_D(t_1)\rangle = \hat{\mathcal{T}}^\dagger|\psi_D(t_0)\rangle = |\psi_C(t_0)\rangle\,. \tag{16}$$

This result shows that, even in the presence of a non-adiabatic switch off of the interaction, there are no gauge ambiguities, since the final state (after the interaction has been switched off) does coincide with the corresponding state in the Coulomb gauge. The case where the system is prepared in the absence of interaction, which is then switched on and finally switched off before measurements, is analyzed in Appendix F.

In Ref. [27], it has been shown that the standard practice of promoting the coupling to a time-dependent function gives rise, for sufficiently strong and non-adiabatic time-dependent interactions, to gauge-dependent predictions on final subsystem properties, such as the qubit-field entanglement or the number of emitted photons. This problem persists also when the

system is prepared in the absence of interaction, and measurements are carried out after switching off the coupling. Our analysis of gauge transformations in the presence of time-dependent interactions eliminates these ambiguities (see Appendix E).

Figure 4(a) displays the mean photon numbers $\langle\tilde{0}_C|\hat{a}^\dagger\hat{a}|\tilde{0}_C\rangle$ and $\langle\tilde{0}_D|\hat{a}^\dagger\hat{a}|\tilde{0}_D\rangle$. The first quantity is the correct one, calculated using the time evolution induced by $\hat{\mathcal{H}}_C(t)$. The latter is the wrong one, obtained considering the wrong dipole-gauge Hamiltonian $\hat{\mathcal{H}}_D(t) = \hat{\mathcal{T}}(t)\hat{\mathcal{H}}_C(t)\hat{\mathcal{T}}^\dagger(t)$ (see Appendix F). As shown in Fig. 4(b), the two mean values provide very different predictions for the observable mean photon number after the switch off. Very different predictions are also obtained for the qubit excitation probabilities (see Fig. 3). Figure 4(c) displays the Von Neumann entropy S_q (which quantifies the qubit-oscillator entanglement for the system ground state (black curves) of the quantum Rabi model. This quantity [17] is obtained by calculating the ground state of the combined system $|\tilde{0}\rangle$, using it to obtain the qubit's reduced density matrix in the ground state $\rho_q = \mathrm{Tr}_{\mathrm{osc}}\{|\tilde{0}\rangle\langle\tilde{0}|\}$, and then evaluating the entropy of that state $S_q = -\mathrm{Tr}_{\mathrm{osc}}\{\rho_q \log_2 \rho_q\}$. The continuous curves have been obtained using the Coulomb gauge, while the dotted-dashed ones, within the wrong dipole gauge (using $\hat{\mathcal{H}}_D(t)$). It is interesting to observe that, for $\eta \gtrsim 0.2$, the degree of entanglement strongly differs in the two cases. In particular, while in the wrong dipole gauge both states become entangled cat states [47] displaying maximum entanglement above $\eta = 2$, S_q goes to zero in the Coulomb gauge, after reaching a maximum at $\eta \simeq 0.6$. These significant differences for large values of η can be understood by using an analytical approximation which works well for $\eta \gg 1$ (see Appendix D).

In summary, the main result of this section consists of an operational *definition of ground state entanglement in cavity-QED systems which is independent on gauge transformation*

VI. CIRCUIT QED

An ideal platform for exploring atomic physics and quantum optics [48] is circuit QED (see Fig. 1(b)). The main reasons for that are, their flexibility in design, the possibility of parameter tunability *in situ* [49] and their capability to reach the USC and even the so-called deep strong coupling (DSC) (when $\eta > 1$) regimes at the single photon – single atom level [1, 2, 4, 50, 51].

Here, we start considering a well known architecture constituted by a superconducting

flux qubit and a LC oscillator inductively coupled to each other by sharing an inductance [4] (Galvanic coupling). An important feature of the flux qubit is its strong anharmonicity, so that the two lowest energy levels are well isolated from the higher levels [4]. The system Hamiltonian can be written in the flux gauge as (see Appendix G)

$$\hat{\mathcal{H}}_{\rm fg} = \frac{\hbar\omega_0}{2}\hat{\sigma}_z + \hbar\omega_c\hat{a}^\dagger\hat{a} + \hbar\omega_c\eta(\hat{a}+\hat{a}^\dagger)(\cos\theta\,\hat{\sigma}_x - \sin\theta\,\hat{\sigma}_z)\,, \tag{17}$$

where $\hbar\omega_c\eta = L_c I_p I_{\rm zpf}$. Here, L_c is the qubit-oscillator coupling inductance, I_p is the persistent current in the qubit loop, and $I_{\rm zpf}$ is the zero-point-fluctuation amplitude of the LC resonator. The flux dependence in encoded in $\theta = \arcsin(\varepsilon/\omega_0)$, where ε is the flux bias. Here $\omega_0 = \sqrt{\Delta^2+\varepsilon^2}$, where $\hbar\Delta$ is the tunnel energy splitting. For $\theta = 0$, the qubit parity is conserved, and the Hamiltonian in Eq. (17) resembles the quantum Rabi Hamiltonian in the dipole gauge for natural atoms $\hat{\mathcal{H}}_D$. However, it is worth noticing that, while the interaction term in $\hat{\mathcal{H}}_D$ is of the coordinate-momentum kind, in $\hat{\mathcal{H}}_{\rm fg}$ it is coordinate-coordinate. As we will show, this difference, despite not affecting the energy levels of the total system, affects eigenstates and physical observables, and hence quantum measurements.

The LC oscillator can be probed by measuring the voltage at the end of a coplanar transmission line that is inductively coupled to the inductor L of the LC oscillator (see Fig. 1(b) and Appendix J). Such voltage is proportional to the voltage across L. In the flux gauge, the canonical coordinate for the resonator corresponds to the flux across the capacitor [$\hat{\Phi}_C = (I_{\rm zpf}/Z)(\hat{a}+\hat{a}^\dagger)$] ($Z = \sqrt{L/C}$ is the oscillator characteristic impedance), and not that across the inductor. As a result, in analogy with the electric field in the dipole gauge, the voltage across the inductor also contains qubit operators: $\hat{V}_L^{\rm fg} = L_0 I_{\rm zpf}[i\omega_c(\hat{a}-\hat{a}^\dagger) + 2\eta\omega_0\hat{\sigma}_y]$ (see Appendix J). If the system is prepared (e.g., by a pulse with central frequency $\omega \simeq \omega_{\tilde{1}\pm,\tilde{0}}$) in one of the two lowest excited states $|\tilde{1}\pm\rangle$, the output signal emitted into the transmission line is proportional to $\mathcal{V}^{\rm L}_{\tilde{1}\pm,\tilde{0}} = |\langle\tilde{1}\pm|\hat{V}_L|\tilde{0}\rangle|^2/(\omega_c L_0 I_{\rm zpf})^2$. This quantity differs from what can be obtained measuring the voltage across the capacitor, $\mathcal{V}^{\rm C}_{\tilde{1}\pm,\tilde{0}} = |\langle\tilde{1}\pm|\hat{a}-\hat{a}^\dagger|\tilde{0}\rangle|^2$. Figure 5(a) displays $\mathcal{V}^{\rm L}_{\tilde{1}\pm,\tilde{0}}$ and $\mathcal{V}^{\rm C}_{\tilde{1}\pm,\tilde{0}}$ as a function of the normalized coupling η. The significant differences between these two quantities indicate that, in the USC and DSC regimes, similar observables can lead to very different results, as recently observed in the context of quantum phase transitions [52]. Comparing these results with the corresponding ones ($W_{\tilde{1}\pm,\tilde{0}}$) obtained in Fig. 2 for the cavity QED system, significant differences can be found, although the results share some qualitative features.

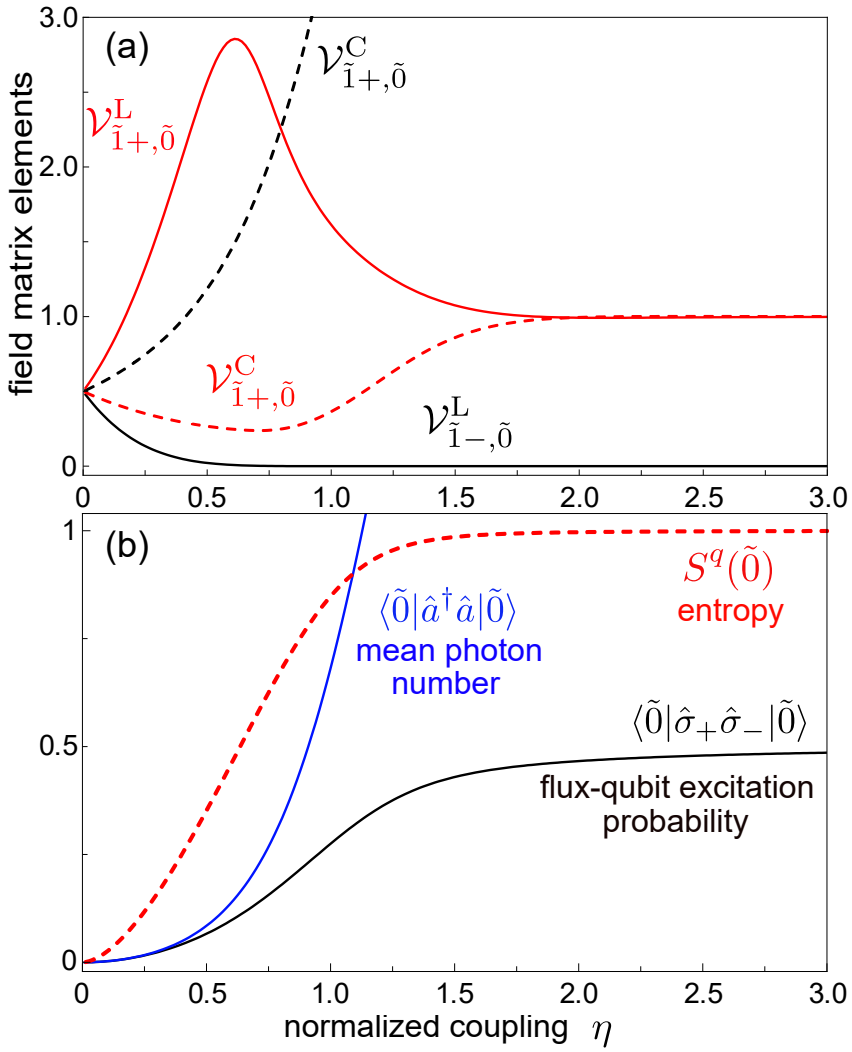

Figure 5. Circuit QED. (a) Emitted signal $\mathcal{V}^{\rm L}_{\tilde{1}\pm,\tilde{0}}$ as a function of the normalized coupling η. This quantity is proportional to the power emitted from the system prepared in the initial states $|\tilde{1}\pm\rangle$ into a transmission line inductively (and weakly) coupled to the inductor of the LC oscillator. For comparison, the panel also displays $\mathcal{V}^{\rm C}_{\tilde{1}\pm,\tilde{0}}$. (b) Mean photon number (blue solid curve), flux-qubit excitation probability (black solid curve), and Von Neumann entropy (red dashed curve) (quantifying the qubit-field entanglement) in the system ground state as a function of the normalized coupling η. All the displayed curves have been calculated using $\theta = 0$, which corresponds to a flux offset $\varepsilon = 0$.

The Hamiltonian in Eq. (17) can also be obtained (in full analogy with the dipole and Coulomb gauges), in the so-called charge-gauge, performing a unitary transformation [10, 11, 53] (see Appendix G). After such transformation, the voltage across the oscillator inductor corresponds to the oscillator canonical momentum: $\hat{V}_L^{\rm cg} = L_0 I_{\rm zpf}[i\omega_c(\hat{a} - \hat{a}^\dagger)]$. However, its matrix elements are gauge invariant (of course using the system states in the charge gauge). Interestingly this gauge transformation corresponds to a different choice of the grounded node in the circuit (see Appendix G).

The switch off of the interaction in Galvanically coupled systems also quenches the qubit coordinate. Hence, these systems are not suitable to study qubit properties after the sudden switch off. We consider instead a mutual-inductance coupling [see Fig. 1(b)]. The system Hamiltonian is still described by Eq. (17); however in this case, after the switch off, the qubit and oscillator signals can be independently measured (see Appendix H), as in cavity QED systems (see Sect. V).

Results on *measurable* vacuum expectation values are shown in Fig. 5(b). Specifically, it displays the mean photon number, the qubit excitation probability, and the Von Neumann entropy (quantifying the qubit-field entanglement) in the system ground state. It is interesting to observe that these results strongly differ from the corresponding ones in Figs. 2 and 3. In particular, in the circuit QED system, the mean photon number strongly increases for increasing coupling strengths. In addition, in the limit of very strong coupling strengths, the qubit-field entanglement reaches its maximum in contrast to the correct calculation in Fig. 3(a). It is very surprising that two platforms (cavity and circuit QED) displaying the same energy spectra give rise to very different ground state properties. This behaviour arises from the different fundamental origin of the coupling in the two systems, namely coordinate-momentum versus coordinate-coordinate interaction forms (see last paragraph in Appendix H).

Also for the case of mutual inductance coupling, it is possible to apply a unitary (gauge) transformation giving rise to a momentum-momentum coupling (charge gauge, see Appendix H). Such transformation is time-dependent if the mutual inductance is tuned, like the unitary transformation $\hat{\mathcal{T}}$ introduced to obtain the dipole gauge. Analogously, it can be shown that after the switch off $|\psi_{\rm cg}\rangle = |\psi_{\rm fg}\rangle$ and no gauge ambiguity arises. Hence, also *in circuit QED, it is possible to define gauge-invariant ground state properties.*

VII. DISCUSSION

By adopting an approach based on operational procedures involving measurements, we have highlighted and solved a number of qualitative ambiguities in the theoretical description of cavity and circuit QED systems. Broadly, these results deepen our understanding of subtle, although highly relevant, quantum aspects of the interaction between light and matter, and are also relevant for the design and development of new technological photonic applications exploiting the unprecedented possibilities offered by the USC and DSC regimes (see, e.g., [54]).

Here, we focused on the quantum Rabi model. However, our results can be extended to matter systems including a collection of quantum emitters, or collective excitations (see, e.g., [52, 55]). The conceptual issues discussed and solved here also apply to light-matter systems involving multi-mode resonators [45, 56–58], or to atoms (natural or artificial) coupled to a continuum of light modes [59], or even in cavity quantum optomechanics [60, 61].

Appendix A: Derivation of the photon operators in the dipole gauge

We start by considering the simplest case of a two-level system coupled to a single-mode resonator, where $\hat{a}$ is the photon destruction operator in the Coulomb gauge. Following Ref. [11] (see also Sect. II), the corresponding operator in the dipole gauge is $\hat{a}' = \hat{\mathcal{T}}\hat{a}\hat{\mathcal{T}}^\dagger$, where $\hat{\mathcal{T}} = \exp(i\hat{\mathcal{F}})$ with $\hat{\mathcal{F}} = -\eta\hat{\sigma}_x(\hat{a} + \hat{a}^\dagger)$. We obtain $\hat{a}' = \hat{a} + i\eta\hat{\sigma}_x$, where $\eta = g/\omega_c$ (g is assumed real).

We now check the consistency of this result by deriving the general case using an alternative approach not based on unitary transformations. Specifically, we consider a single two-level system interacting with a collection of complete electromagnetic modes, and then generalize the result to a strict single-mode coupling regime.

It is well known [13, 32, 62] that the dipole interaction Hamiltonian between an atom and the radiation field, should involve the transverse displacement field, $\hat{\mathbf{D}}$, rather than the electric field, $\hat{\mathbf{E}}$, so that (we neglect a μ^2 term that is trivially proportional to the identity operator in a two-level approximation):

$$\hat{\mathcal{H}}_I = -\frac{\boldsymbol{\mu}\cdot\hat{\mathbf{D}}(\mathbf{r})}{\epsilon_0\epsilon_b(\mathbf{r})}, \tag{A1}$$

where $\epsilon_b(\mathbf{r})$ is the background dielectric constant of the medium where the two-level system is embedded. The point is that in the dipole gauge the electric field operator is not a canonical operator and thus the energy has to be expressed in terms of $\hat{\mathbf{D}}(\mathbf{r})$ (which is a canonical operator), in order to obtain the interaction Hamiltonian. Given the displacement field's fundamental importance [33], we introduce a new field operator through

$$\hat{\mathbf{F}}(\mathbf{r}) = \frac{\hat{\mathbf{D}}(\mathbf{r})}{\epsilon_0\epsilon_b(\mathbf{r})}, \tag{A2}$$

and carry out field quantization with respect to this quantum field operator. Thus, for a single dipole at position $\mathbf{r}_0$,

$$\hat{\mathcal{H}}_I = -\boldsymbol{\mu}\cdot\hat{\mathbf{F}}(\mathbf{r}_0), \tag{A3}$$

and below we assume $\boldsymbol{\mu}$ is real (though this is not necessary). This procedure can be generalized for multiple dipoles, however, in this case the field-induced dipole-dipole interaction terms have to be also included (see Appendix B). In this Section, we only consider a single dipole (two-level system) at $\mathbf{r}_0$. The field operator, obtained from the Power-Zienau-Woolley

(PZW) transformation, can be expanded in terms of photon field operators (that also couple to matter degrees of freedom), $\hat{a}_k$, so that

$$\hat{\mathbf{F}}(\mathbf{r},t) = \hat{\mathbf{F}}^{+}(\mathbf{r},t) + \hat{\mathbf{F}}^{-}(\mathbf{r},t) = i\sum_k \sqrt{\frac{\hbar\omega_k}{2\epsilon_0}}\mathbf{f}_k(\mathbf{r})\hat{a}_k(t) + \text{h.c.}, \tag{A4}$$

where $\mathbf{f}_k(\mathbf{r})$ are "normal modes" with real eigenfrequencies, ω_k, obtained from Maxwell's equations for a particular medium. The normalization of these normal modes is obtained from $\int d\mathbf{r}\epsilon_b(\mathbf{r})\mathbf{f}_k^*(\mathbf{r})\cdot\mathbf{f}_{k'}(\mathbf{r}) = \delta_{kk'}$. These modes are complete, so that $\sum_k \epsilon_b(\mathbf{r})\mathbf{f}_k^*(\mathbf{r})\mathbf{f}_k(\mathbf{r}') = \mathbf{1}\delta(\mathbf{r}-\mathbf{r}')$, and note that the sum includes both quasi-transverse and quasi-longitudinal modes ($\omega_k = 0$). For convenience, one can also write this as

$$\mathbf{1}\delta(\mathbf{r}-\mathbf{r}_0) = \frac{1}{2}\epsilon_b(\mathbf{r})\left[\sum_k \mathbf{f}_k(\mathbf{r})\mathbf{f}_k^*(\mathbf{r}_0) + \mathbf{f}_k^*(\mathbf{r}_0)\mathbf{f}_k(\mathbf{r})\right]. \tag{A5}$$

We can also introduce the usual TLS-mode coupling rate from

$$g_k \equiv \sqrt{\frac{\omega_k}{2\hbar\epsilon_0}}\boldsymbol{\mu}\cdot\mathbf{f}_k(\mathbf{r}_0), \tag{A6}$$

which is only finite for transverse modes (which is due to the choice of gauge).

Next, it is useful to recall the relation between $\hat{\mathbf{E}}$ and $\hat{\mathbf{F}}$:

$$\hat{\mathbf{F}}(\mathbf{r}) = \hat{\mathbf{E}}(\mathbf{r}) + \frac{\delta(\mathbf{r}-\mathbf{r}_0)}{\epsilon_0\epsilon_b(\mathbf{r})}\hat{\mathbf{P}}_d(\mathbf{r}_0), \tag{A7}$$

where we consider a single dipole. Treating the dipole as a quantized TLS, then

$$\hat{\mathbf{F}}(\mathbf{r}) = \hat{\mathbf{E}}(\mathbf{r}) + \frac{\boldsymbol{\mu}}{\epsilon_0\epsilon_b(\mathbf{r})}\delta(\mathbf{r}-\mathbf{r}_0)(\hat{\sigma}_+ + \hat{\sigma}_-), \tag{A8}$$

where $\hat{\sigma}_+ + \hat{\sigma}_- = \hat{\sigma}_x$ are the usual Pauli operators. Thus, defining $\hat{\mathbf{E}}_D(\mathbf{r})$ as the electric field operator in the dipole gauge, we have

$$\begin{aligned}\hat{\mathbf{E}}_D(\mathbf{r},t) = {}& i\sum_k \sqrt{\frac{\hbar\omega_k}{2\epsilon_0}}\mathbf{f}_k(\mathbf{r})\hat{a}_k(t) + \text{h.c.} \\ & - \frac{1}{2\epsilon_0}\left[\sum_k \mathbf{f}_k(\mathbf{r})\mathbf{f}_k^*(\mathbf{r}_0) + \mathbf{f}_k^*(\mathbf{r}_0)\mathbf{f}_k(\mathbf{r})\right]\cdot\boldsymbol{\mu}(\hat{\sigma}_+ + \hat{\sigma}_-),\end{aligned} \tag{A9}$$

with the understanding that the last term is formally zero for $\mathbf{r} \neq \mathbf{r}_0$. For positions away from the dipole location, then

$$\hat{\mathbf{E}}_D(\mathbf{r} \neq \mathbf{r}_0, t) = i\sum_k \sqrt{\frac{\hbar\omega_k}{2\epsilon_0}}\mathbf{f}_k(\mathbf{r})\hat{a}_k(t) + \text{h.c.}, \tag{A10}$$

while for positions at the dipole location,

$$\hat{\mathbf{E}}_D(\mathbf{r}_0,t) = i\sum_k \sqrt{\frac{\hbar\omega_k}{2\epsilon_0}}\mathbf{f}_k(\mathbf{r}_0)\hat{a}_k(t) + \text{h.c.} - \frac{1}{\epsilon_0}\left[\sum_k \mathbf{f}_k^*(\mathbf{r}_0)\mathbf{f}_k(\mathbf{r}_0)\right]\cdot\boldsymbol{\mu}(\hat{\sigma}_+ + \hat{\sigma}_-). \tag{A11}$$

Also note, that since $\hat{\mathbf{E}}_D(\mathbf{r}\neq\mathbf{r}_0,t) = \hat{\mathbf{F}}(\mathbf{r},t)$, then one can use either operator for field detection analysis (away from the two-level system), which is a result of including a sum over all modes. It is also important to note that the general solution of $\hat{a}_k(t)$ also includes coupling to the two-level system, which can be obtained, e.g., from the appropriate Heisenberg equations of motion. It is worth noticing that Eq. (A9) can be rewritten in a way that makes each mode contribution more clear:

$$\hat{\mathbf{E}}_D(\mathbf{r},t) = i\sum_k \sqrt{\frac{\hbar\omega_k}{2\epsilon_0}}\mathbf{f}_k(\mathbf{r})\hat{a}'_k(t) + \text{h.c.}\,, \tag{A12}$$

where

$$\hat{a}'_k(t) = \hat{a}_k(t) + i\eta_k\hat{\sigma}_x\,, \tag{A13}$$

with $\omega_k\eta_k = \sqrt{\omega_k/2\hbar\epsilon_0}\,\boldsymbol{\mu}\cdot\mathbf{f}_k(\mathbf{r}_0)$. Comparing Eq. (A12) and Eq. (A4), it is clear that, although $\hat{\mathbf{E}}_D(\mathbf{r}\neq\mathbf{r}_0,t) = \hat{\mathbf{F}}(\mathbf{r},t)$, the electric field operator $\hat{\mathbf{E}}_D(\mathbf{r},t)$ and the field $\hat{\mathbf{F}}_D(\mathbf{r},t)$ correspond to two different modal expansions.

Single-mode limit

Next, we focus on a single-mode solution ($k = c, \hat{a}\equiv\hat{a}_c, \eta\equiv\eta_c$) as this is typically the most interesting case for cavity QED regimes, and is one of the key models considered in the main text (the quantum Rabi model). Of course, treating a single-field mode as a normal mode is not a rigorous model for open cavities, as we cannot include the cavity mode loss rigorously, but similar result can be obtained using a quantized quasinormal mode approach [63] (which are the correct resonant modes in the presence of dissipative output losses). Nevertheless, for high-Q resonators, it is an excellent approximation. Exploiting Eq. (A12), we obtain:

$$\hat{\mathbf{E}}_D(\mathbf{r},t) \approx i\sqrt{\frac{\hbar\omega_c}{2\epsilon_0}}\mathbf{f}_c(\mathbf{r})\hat{a}'(t) + \text{h.c.}\,, \tag{A14}$$

where

$$\hat{a}'(t) = \hat{a}(t) + i\eta\hat{\sigma}_x\,, \tag{A15}$$

with $\omega_c\eta = \sqrt{\omega_c/2\hbar\epsilon_0}\,\boldsymbol{\mu}\cdot\mathbf{f}_c(\mathbf{r}_0)$. Again assuming that g is real, then $g = \omega_c\eta$, and $\hat{\mathcal{H}}_I = i\hbar g(\hat{a}^\dagger - \hat{a})\hat{\sigma}_x \equiv \hat{\mathcal{V}}_D$, as used in the main text.

It is worth highlighting a rather striking difference between the single-mode model and the multi-mode model. The latter case causes the two field operators $\hat{\mathbf{F}}_D(\mathbf{r})$ and $\hat{\mathbf{E}}_D(\mathbf{r})$ to be identical, *unless* $\mathbf{r}$ *at the dipole location* ($\mathbf{r}_0$). This multi-mode result also enforces some fundamental results in electromagnetism, e.g., it recovers well known limits such as the local field problem (requiring the self-consistent polarization), and ensures causality. The need to enforce causality in quantum optics has been pointed out in other contexts [45]. We also observe that, as shown explicitly by the unitary transformation $\hat{a}' = \hat{\mathcal{T}}\hat{a}\hat{\mathcal{T}}^\dagger$ at the beginning of this section (see also [11]), by only using the primed operators in the dipole gauge, gauge invariance of the expectation values is ensured. Generalizing this approach to the multimode-interaction case, it can also be shown that $\hat{a}'_k = \hat{T}\hat{a}_k\hat{T}^\dagger$, where $\hat{T}$ is the appropriate unitary gauge operator [16]. Consequently, $\langle\psi_D|\hat{a}_k^{'\dagger}\,\hat{a}'_k|\psi_D\rangle = \langle\psi_C|\hat{a}_k^\dagger\,\hat{a}_k|\psi_C\rangle$, where $|\psi_D\rangle = \hat{T}|\psi_C\rangle$.

Appendix B: Two-level sensors

It has been shown that normal-order correlation functions, which describe the detection of photons according to Glauber's theory, can be calculated considering frequency-tunable two-level sensors in the limit of their vanishing coupling with the field [64]. The rate at which the sensor population growth corresponds to the photodetection rate. If two or more sensors are included, their joint excitation rates provides information on normal-order multi-photon correlations.

This procedure can also be applied when the electromagnetic field interacts strongly with a matter system so that the counter-rotating terms in the interaction Hamiltonians cannot be neglected. Let us consider a simple USC system constituted by an electromagnetic single-mode resonator strongly interacting with a two-level system with normalized coupling strength η. Then we also consider a two-level sensor interacting with the resonator with vanishing coupling $\eta_s \ll \eta$. The standard cavity-sensor interaction Hamiltonian in the dipole gauge is written as [64]

$$\hat{V}'_{\rm dg} = -i\hbar\omega_c\eta_s(\hat{a} - \hat{a}^\dagger)\hat{\sigma}_x^s\,. \tag{B1}$$

If the USC system is prepared in a state $|j\rangle$ and the sensor has a resonance frequency

$\omega_s = \omega_{jl}$ $(l < j)$, by applying the Fermi golden rule, it results that the excitation rate of the sensor is proportional to

$$|\langle l_D|\hat{\mathcal{P}}|j_D\rangle|^2\,, \tag{B2}$$

where $|j_D\rangle$ is a system eigenstate in the dipole gauge and $\hat{\mathcal{P}} = i(\hat{a}-\hat{a}^\dagger)$. This result, however is different from what can be obtained within the Coulomb gauge: $W_{lj} = |\langle l_C|\hat{\mathcal{P}}|j_C\rangle|^2$.

It is instructive to find the origin of such gauge ambiguity and to solve it. Actually, in the dipole gauge, the interaction energy between the field and the sensor is $-\int d^3r\,\hat{\mathbf{E}}\cdot\hat{\mathbf{P}}_s$, where $\hat{\mathbf{P}}_s = \boldsymbol{\mu}\hat{\sigma}_x^s$ is the sensor polarization. Using the relation $\hat{\mathbf{E}} = (\hat{\mathbf{D}} - \hat{\mathbf{P}})/\epsilon_0$ (we here assume $\epsilon_b(\mathbf{r}) = 1$), the total Hamiltonian in the dipole gauge can be written as

$$\hat{\mathcal{H}}_{\rm dg} = \hat{\mathcal{H}}_{\rm dg}^{\rm USC} + \hat{\mathcal{H}}_s + \hat{\mathcal{V}}_{\rm dg}^s\,, \tag{B3}$$

where $\hat{\mathcal{H}}_{\rm dg}^{\rm USC}$ is the system Hamiltonian in the absence of the sensor, $\hat{\mathcal{H}}_s = (\hbar\omega_s/2)\hat{\sigma}_z^s$, and

$$\hat{\mathcal{V}}_{\rm dg}^s = -\frac{1}{\epsilon_0}\int d^3r\hat{\mathbf{D}}\cdot\boldsymbol{\mu}\,\hat{\sigma}_x^s + \frac{1}{\epsilon_0}\int d^3r\hat{P}^2\,, \tag{B4}$$

where

$$\hat{\mathbf{P}} = \boldsymbol{\mu}\hat{\sigma}_x + \boldsymbol{\mu}_s\hat{\sigma}_x^s\,, \tag{B5}$$

is the total polarization. By expanding $\hat{\mathbf{D}}$ in terms of the photon operators, and using the relationship

$$\frac{1}{2}\sum_k\left[\mathbf{f}_k^*(\mathbf{r})\mathbf{f}_k(\mathbf{r}') + \mathbf{f}_k^*(\mathbf{r}')\mathbf{f}_k(\mathbf{r})\right] = \mathbf{1}\delta(\mathbf{r}-\mathbf{r}')\,, \tag{B6}$$

and after neglecting the terms proportional to the qubits identities, we obtain

$$\hat{\mathcal{V}}_{\rm dg}^s = \sum_k \hbar\omega_k\eta_k^s\left[i(\hat{a}_k^\dagger - \hat{a}_k) + 2\eta_k\hat{\sigma}_x\right]\hat{\sigma}_x^s\,. \tag{B7}$$

In the single-mode limit, this simplifies to

$$\hat{\mathcal{V}}_{\rm dg}^s = \hbar\omega_c\eta^s\left[i(\hat{a}^\dagger - \hat{a}) + 2\eta\hat{\sigma}_x\right]\hat{\sigma}_x^s\,. \tag{B8}$$

Equation (B8) differs from Eq. (B1) only for the field-induced qubit-sensor interaction term, arising from the self-polarization terms in the dipole-gauge light-matter interaction Hamiltonian [65]. However, *it is precisely this term that ensures gauge invariance*: applying the Fermi golden rule, by using Eq. (B8), instead of Eq. (B1), we obtain the gauge invariant result

$$|\langle l_D|\hat{\mathcal{P}} - 2\eta\hat{\sigma}_x|j_D\rangle|^2 = |\langle l_C|\hat{\mathcal{P}}|j_C\rangle|^2 \equiv W_{lj}\,. \tag{B9}$$

Appendix C: Dispersive readout of a qubit strongly coupled to a cavity mode

Let us consider a two-level system ultrastrongly coupled to a cavity mode of frequency ω_a and weakly coupled to a second mode (e.g., a readout cavity) of frequency ω_b acting as a sensor for the matter system. The resulting Hamiltonian in the Coulomb gauge can be written as [11]

$$\begin{aligned}\hat{\mathcal{H}}_C &= \hbar\omega_a\hat{a}^\dagger\hat{a} + \hbar\omega_b\hat{b}^\dagger\hat{b} \\ &+ \frac{\hbar\omega_0}{2}\left\{\hat{\sigma}_z\cos\left[2\eta_a(\hat{a}^\dagger+\hat{a}) + 2\eta_b(\hat{b}^\dagger+\hat{b})\right] + \hat{\sigma}_y\sin\left[2\eta_a(\hat{a}^\dagger+\hat{a}) + 2\eta_b(\hat{b}^\dagger+\hat{b})\right]\right\},\end{aligned} \tag{C1}$$

with $\eta_a = g_a/\omega_0$ and $\eta_b = g_b/\omega_0$. By using the angle transformation formulae, Eq. (C1) becomes

$$\begin{aligned}\hat{\mathcal{H}}_C &= \hbar\omega_a\hat{a}^\dagger\hat{a} + \hbar\omega_b\hat{b}^\dagger\hat{b} \\ &+ \frac{\hbar\omega_0}{2}\hat{\sigma}_z\left\{\cos\left[2\eta_a(\hat{a}^\dagger+\hat{a})\right]\cos\left[2\eta_b(\hat{b}^\dagger+\hat{b})\right] - \sin\left[2\eta_a(\hat{a}^\dagger+\hat{a})\right]\sin\left[2\eta_b(\hat{b}^\dagger+\hat{b})\right]\right\} \\ &+ \frac{\hbar\omega_0}{2}\hat{\sigma}_y\left\{\sin\left[2\eta_a(\hat{a}^\dagger+\hat{a})\right]\cos\left[2\eta_b(\hat{b}^\dagger+\hat{b})\right] + \cos\left[2\eta_a(\hat{a}^\dagger+\hat{a})\right]\sin\left[2\eta_b(\hat{b}^\dagger+\hat{b})\right]\right\}.\end{aligned} \tag{C2}$$

Furthermore, since $2\eta_b(\hat{b}^\dagger+\hat{b})$ is small, we can also apply the small-angle approximation $\cos(x)\simeq 1$, $\sin(x)\simeq x$, thus obtaining

$$\begin{aligned}\hat{\mathcal{H}}_C \simeq \hbar\omega_a\hat{a}^\dagger\hat{a} + \hbar\omega_b\hat{b}^\dagger\hat{b} + \frac{\hbar\omega_0}{2}\left\{\hat{\sigma}_z\cos\left[2\eta_a(\hat{a}^\dagger+\hat{a})\right] + \hat{\sigma}_y\sin\left[2\eta_a(\hat{a}^\dagger+\hat{a})\right]\right\} \\ +\hbar\omega_0\eta_b(\hat{b}^\dagger+\hat{b})\left\{\hat{\sigma}_y\cos\left[2\eta_a(\hat{a}^\dagger+\hat{a})\right] - \hat{\sigma}_z\sin\left[2\eta_a(\hat{a}^\dagger+\hat{a})\right]\right\}.\end{aligned} \tag{C3}$$

Introducing the Pauli operators in the Coulomb gauge:

$$\begin{aligned}\hat{\sigma}'_y &= \hat{\mathcal{T}}_a^\dagger\hat{\sigma}_y\hat{\mathcal{T}}_a = \hat{\sigma}_y\cos\left[2\eta_a(\hat{a}^\dagger+\hat{a})\right] - \hat{\sigma}_z\sin\left[2\eta_a(\hat{a}^\dagger+\hat{a})\right], \\ \hat{\sigma}'_z &= \hat{\mathcal{T}}_a^\dagger\hat{\sigma}_z\hat{\mathcal{T}}_a = \hat{\sigma}_z\cos\left[2\eta_a(\hat{a}^\dagger+\hat{a})\right] + \hat{\sigma}_y\sin\left[2\eta_a(\hat{a}^\dagger+\hat{a})\right], \\ \hat{\sigma}'_x &= \hat{\mathcal{T}}_a^\dagger\hat{\sigma}_x\hat{\mathcal{T}}_a = \hat{\sigma}_x,\end{aligned} \tag{C4}$$

with $\hat{\mathcal{T}}_a = \exp[-i\eta_a\hat{\sigma}_x(\hat{a}+\hat{a}^\dagger)]$, Eq. (C3) can be written in a more compact form as

$$\hat{\mathcal{H}}_C = \hbar\omega_a\hat{a}^\dagger\hat{a} + \hbar\omega_b\hat{b}^\dagger\hat{b} + \frac{\hbar\omega_0}{2}\hat{\sigma}'_z + \eta_b\hbar\omega_0(\hat{b}^\dagger+\hat{b})\hat{\sigma}'_y. \tag{C5}$$

It is important to note that, despite the $\hat{\sigma}'_i$ operators also containing photon operators, their commutation rules remain unchanged: $[\hat{\sigma}'_i,\hat{\sigma}'_j] = 2i\epsilon_{ijk}\hat{\sigma}'_k$. Moreover, we define

$$\hat{\mathcal{X}}'_\pm = (\hat{b}^\dagger\hat{\sigma}'_- \pm \hat{b}\hat{\sigma}'_+),$$

$$\hat{\mathcal{Y}}'_{\pm} = (\hat{b}\hat{\sigma}'_{-} \pm \hat{b}^{\dagger}\hat{\sigma}'_{+})\,. \tag{C6}$$

Subsequently, Eq. (C5) can be rewritten in a more convenient form as

$$\hat{\mathcal{H}}_C = \hbar\omega_a \hat{a}^{\dagger}\hat{a} + \hbar\omega_b \hat{b}^{\dagger}\hat{b} + \frac{\hbar\omega_0}{2}\hat{\sigma}'_z + i\eta_b\hbar\omega_0(\hat{\mathcal{X}}'_{-} + \hat{\mathcal{Y}}'_{-})\,. \tag{C7}$$

In order to investigate the effect of the readout cavity on the TLS, we can always perform a canonical (unitary) transformation (see, e.g., [44]):

$$\hat{\mathcal{H}}_C \to \tilde{H}_C \equiv e^{-\hat{S}}\hat{\mathcal{H}}_C e^{\hat{S}} = \hat{\mathcal{H}}_C + [\hat{\mathcal{H}}_C, \hat{S}] + \frac{1}{2!}[\hat{S}, [\hat{S}, \hat{\mathcal{H}}_C]] + \ldots\,., \tag{C8}$$

where we defined $\tilde{H}_C$ to indicate the corresponding dispersive Hamiltonian in the Coulomb gauge. In the usual way, we search for an anti-Hermitian operator $\hat{S}$ which satisfies the relation

$$\hat{\mathcal{H}}_I + [\hat{\mathcal{H}}_0, \hat{S}] = 0\,, \tag{C9}$$

where

$$\hat{\mathcal{H}}_I = i\eta_b\hbar\omega_0(\hat{\mathcal{X}}'_{-} + \hat{\mathcal{Y}}'_{-}), \tag{C10}$$

and

$$\hat{\mathcal{H}}_0 = \hbar\omega_b \hat{b}^{\dagger}\hat{b} + \frac{\hbar\omega_0}{2}\hat{\sigma}'_z\,. \tag{C11}$$

Equation (C9) is satisfied using

$$\hat{S} = \lambda\hat{\mathcal{X}}'_{+} + \bar{\lambda}\hat{\mathcal{Y}}'_{+}\,, \tag{C12}$$

with

$$\lambda = -i\frac{g_b}{\Delta}, \tag{C13}$$

and

$$\bar{\lambda} = -i\frac{g_b}{\Sigma}\,, \tag{C14}$$

where $\Delta = \omega_0 - \omega_b$ and $\Sigma = \omega_0 + \omega_b$. With such a choice, we obtain

$$\tilde{\mathcal{H}}_C = \hbar\omega_a \hat{a}^{\dagger}\hat{a} + \hat{\mathcal{H}}_0 + [\hat{\mathcal{H}}_I, \hat{S}] + \frac{1}{2!}[\hat{S}, [\hat{S}, \hat{\mathcal{H}}_C]] + \ldots \tag{C15}$$

Developing the calculations up to the second order in g_b, we obtain

$$\tilde{\mathcal{H}}_C = \hat{\mathcal{H}}_0^C + \frac{\hbar\chi}{2}(\hat{b}^{\dagger} + \hat{b})^2\,\hat{\sigma}'_z\,, \tag{C16}$$

where

$$\chi = \frac{g_b^2}{\Delta} + \frac{g_b^2}{\Sigma}\,, \tag{C17}$$

and

$$\hat{\mathcal{H}}_0^C = \hbar\omega_a \hat{a}^\dagger \hat{a} + \hbar\omega_b \hat{b}^\dagger \hat{b} + \frac{\hbar\omega_0}{2}\hat{\sigma}'_z \,. \tag{C18}$$

Neglecting the counter-rotating terms proportional to $\hat{b}^{\dagger 2}$ and $\hat{b}^2$, Eq. (C16) becomes

$$\tilde{\mathcal{H}}_C = \hbar\omega_a \hat{a}^\dagger \hat{a} + \left(\frac{\hbar\omega_0}{2} - \frac{\hbar\chi}{2}\right)\hat{\sigma}'_z + \hbar\left(\omega_b + \chi\hat{\sigma}'_z\right)\hat{b}^\dagger \hat{b} \,. \tag{C19}$$

As it is clear from this expression, the last term in Eq. (C19) can be interpreted as a dispersive shift of the cavity transition by $\chi\hat{\sigma}'_z$, depending on the state of the qubit [66]. Sending a frequency-tunable probe signal into the resonator b, transmission spectroscopy can provide direct information on the expectation value $\langle\hat{\sigma}'_z\rangle_C$ which coincides with $\langle\hat{\sigma}_z\rangle_D$. Hence, we can conclude that this kind of readout spectroscopy provides direct information on the expectation value of the qubit population difference, as defined in the dipole gauge.

Appendix D: Large-coupling limit

Here we discuss the large-coupling limit ($\eta \gg 1$) by using an analytical perturbative method. Notice that for $\eta \gg 1$ the system enters in the so-called deep strong coupling regime (DSC). We start from the quantum Rabi Hamiltonian in the dipole gauge:

$$\hat{\mathcal{H}}_D = \hat{\mathcal{H}}_{\rm free} + \hat{\mathcal{V}}_D \,, \tag{D1}$$

where

$$\hat{\mathcal{H}}_{\rm free} = \hbar\omega_c \hat{a}^\dagger \hat{a} + \frac{\hbar\omega_0}{2}\hat{\sigma}_z, \tag{D2}$$

and the interaction Hamiltonian is

$$\hat{\mathcal{V}}_D = i\eta\hbar\omega_c(\hat{a}^\dagger - \hat{a})\hat{\sigma}_x \,. \tag{D3}$$

When $\eta\omega_c \gg \omega_0$, the last term in Eq. (D1) can be regarded as a perturbation. Equation (D2) can be rewritten as $\hat{\mathcal{H}}_D = \hat{\mathcal{H}}'_0 + \hat{\mathcal{V}}'_D$, where

$$\hat{\mathcal{H}}'_0 = \hbar\omega_c \hat{a}^\dagger \hat{a} + i\eta\hbar\omega_c(\hat{a}^\dagger - \hat{a})\hat{\sigma}_x \,, \tag{D4}$$

and

$$\hat{\mathcal{V}}'_D = \frac{\hbar\omega_0}{2}\hat{\sigma}_z \,. \tag{D5}$$

In the limit $\eta \gg 1$, $\hat{\mathcal{V}}'_D$ can be regarded as a small perturbation; neglecting it, the resulting Hamiltonian can be analytically diagonalized. The two resulting lowest-energy degenerate

eigenstates can be written as $|\mp i\eta\rangle|\pm_x\rangle$, where the first ket indicates photonic coherent states with amplitude $\mp i\eta$, such that: $\hat{a}|\mp i\eta\rangle = \mp i\eta|\mp i\eta\rangle$; while the second ket indicates the two-qubit eigenstates of $\hat{\sigma}_x$. The perturbation $(\hbar\omega_0/2)\hat{\sigma}_z$ removes the degeneracy and mixes the two states, so that the two eigenstates become entangled:

$$|\psi_D^{\pm}\rangle = \frac{1}{\sqrt{2}}\Big[|-i\eta\rangle|+_x\rangle \pm |+i\eta\rangle|-_x\rangle\Big]. \tag{D6}$$

The corresponding eigenstates in the Coulomb gauge are $|\psi_C^{\pm}\rangle = \hat{\mathcal{T}}^\dagger|\psi_D^{\pm}\rangle$, where

$$\hat{\mathcal{T}} = \exp\left[-i\eta\left(\hat{a}+\hat{a}^\dagger\right)\hat{\sigma}_x\right], \tag{D7}$$

is the unitary operator determining the gauge transformation of the qubit-oscillator system: $\hat{\mathcal{H}}_D = \hat{\mathcal{T}}\hat{\mathcal{H}}_C\hat{\mathcal{T}}^\dagger$. By applying the operator $\hat{\mathcal{T}}^\dagger$ to both members of Eq. (D6), and using the properties of the displacement operator, we obtain the separable states

$$|\psi_C^{\pm}\rangle = |0\rangle|\pm_z\rangle\,. \tag{D8}$$

Equations (D6) and (D8), describing the lowest two energy states in the dipole and Coulomb gauge respectively (for $\eta \gg 1$), explain the results in Figs 3 and 4 for very large values of η. In particular, it is easy to obtain: $\langle\psi_C^-|\hat{\sigma}_+\hat{\sigma}_-|\psi_C^-\rangle = 0$, $\langle\psi_C^+|\hat{\sigma}_+\hat{\sigma}_-|\psi_C^+\rangle = 1$, $\langle\psi_D^{\pm}|\hat{\sigma}_+\hat{\sigma}_-|\psi_D^{\pm}\rangle = 0.5$, $\langle\psi_C^-|\hat{a}^\dagger\hat{a}|\psi_C^-\rangle = 0$, $\langle\psi_C^+|\hat{a}^\dagger\hat{a}|\psi_C^+\rangle = \eta^2$. Moreover, Eq. (D6) describes two light-matter maximally entangled cat sates providing a qubit entropy $S_D^q = 1$, while Eq. (D8) describes two separable states ($S_C^q = 0$), see Fig. 4. This analysis can be easily extended to understand the results in Fig. 5 obtained for a circuit QED system for $\eta \gg 1$. Applying the same procedure used to derive Eq. (D6), starting from the Hamiltonian in Eq. (17), we obtain

$$|\psi_D^{\pm}\rangle = \frac{1}{\sqrt{2}}\Big[|-\eta\rangle|+_x\rangle \pm |+\eta\rangle|-_x\rangle\Big]. \tag{D9}$$

Appendix E: Gauge transformations in the presence of time-dependent coupling

We start by summarizing some well-known results on equivalent descriptions of the dynamics of a physical system (see, e.g., Ref. [16]). We consider a simple 1D dynamical system described by the Lagrangian $L(x,\dot{x})$, where x is the coordinate and $\dot{x}$ the velocity. The momentum conjugate with x is $p = \partial L/\partial x$. By adding to the lagrangiaan $L(x,\dot{x})$ the total time derivative of a function $F(x,t)$, one obtains a new Lagrangian

$$L'(x,\dot{x}) = L(x,\dot{x}) + \frac{d}{dt}F(x,t) = L(x,\dot{x}) + \dot{x}\frac{\partial F}{\partial x} + \frac{\partial F}{\partial t}, \tag{E1}$$

which is equivalent to L in the sense that it gives the same equation of motion for the coordinate x . Considering the new Lagrangian, the momentum conjugate with x becomes

$$p' = \frac{\partial L'}{\partial \dot{x}} = p + \frac{\partial F}{\partial x} \,. \tag{E2}$$

When one applies the standard canonical quantization procedure, starting with L on the one hand and L' on the other, one derives two equivalent quantum descriptions for the system, related by a unitary transformation, described by the operator (we use $\hbar = 1$)

$$\hat{T} = \exp[i\hat{F}(t)] \,, \tag{E3}$$

where $\hat{F}(t) \equiv F(\hat{x}, t)$ is the quantum operator corresponding to the classical function $F(x, t)$, with the hat " $\hat{}$ " indicating the promotion of classical variables to quantum operators. Considering a generic operator $\hat{O} = O(\hat{x}, \hat{p})$, it transforms as $\hat{O}' = \hat{T}\hat{O}\hat{T}^\dagger$, while the state vectors transform as $|\psi'\rangle = \hat{T}|\psi\rangle$, so that the generic matrix elements of the operators remain unchanged. If the function $F(x, t)$ depends explicitly on time, the system Hamiltonain transforms differently:

$$\hat{H}' = \hat{T}\hat{H}\hat{T}^\dagger + i\dot{\hat{T}}\hat{T}^\dagger = \hat{T}\hat{H}\hat{T}^\dagger - \frac{\partial \hat{F}}{\partial t} \,. \tag{E4}$$

The function F introduced by PZW [31, 62] is

$$F = -\int d^3r \, \mathbf{P}(\mathbf{r}) \cdot \mathbf{A}_\perp(\mathbf{r}) \,, \tag{E5}$$

where, considering a single charge centered on a single reference point $\mathbf{R}$, the polarization operator can be expressed as

$$\mathbf{P}(\mathbf{r}) = q \int_0^1 du (\mathbf{r} - \mathbf{R}) \delta[(1-u)(\mathbf{r} - \mathbf{R})] \,. \tag{E6}$$

Hence, the PZW Lagrangian can be derived by that in the Coulomb gauge by the transformation

$$L' = L + \frac{d}{dt} F \tag{E7}$$

where F is given by Eq. (E5).

In a gauge transformation, defined by a function $\chi(\mathbf{r}, t)$, the potentials become

$$\mathbf{A}'(\mathbf{r}, t) = \mathbf{A}(\mathbf{r}, t) + \boldsymbol{\nabla}\chi(\mathbf{r}, t) \tag{E8a}$$

$$U'(\mathbf{r}, t) = U(\mathbf{r}, t) - \frac{\partial}{\partial t}\chi(\mathbf{r}, t) \,. \tag{E8b}$$

Introducing Eqs. (E8a) and (E8b) in the Lagrangian L in the Coulomb gauge, the following relationship between the two Lagrangians holds (see, e.g., p. 267 of Ref. [16]):

$$L' = L + \frac{d}{dt}\chi(\mathbf{r}, t)\,. \tag{E9}$$

If the function $\chi(\mathbf{r}, t)$ is chosen equal to the function $F(\mathbf{r}, t)$, then:

$$\chi(\mathbf{r}, t) = \int d^3r\, \mathbf{P}(\mathbf{r}) \cdot \mathbf{A}_\perp(\mathbf{r})\,. \tag{E10}$$

Equations (E7) and (E9) shows that the PZW transformation and the multipolar gauge transformation are equivalent.

This equivalence still holds in the presence of a time-dependent interaction strength. As discussed in the main text, a time-dependent coupling can be properly described assuming an atom moving in and out a Fabry-Pérot Gaussian cavity mode, like in experiments with Rydberg atoms [67], so that the coupling strength becomes time dependent. In this case, the charge is localized around a time-dependent position $\mathbf{R}(t)$. This will give rise to additional terms when taking the time derivative of F. However, Eq. (E7) and Eq. (E9) do still coincide, as well as the conjugate momenta. Both approaches give rise to the same Hamiltonian in Eq. (E4). Notice that the resulting Hamiltonian after the gauge transformation is different from

$$\hat{H}_D(t) = \hat{T}(t)\hat{H}_C(t)\hat{T}^\dagger(t)\,. \tag{E11}$$

This explains precisely why the Hamiltonian in Eq. (E11) does not describe a dynamics which is equivalent to that of the Hamiltonian in the Coulomb gauge [27]. In short, Eq. (E11) is not a correct Hamiltonian to describe the correct light-matter interaction dynamics. Specifically, considering the time dependent unitary transformation, Eq. (E11) is not correct because it misses the explicit time dependence on the transformation, see last term in Eq. (E4). Considering the gauge transformation, Eq. (E11) is not correct because it is obtained neglecting the explicit time dependence of $\chi(\mathbf{r}, t)$ in Eq. (E8b), arising from the time dependence of $\mathbf{R}$ in Eq. (E6). The correct Hamiltonian in the dipole gauge, in the presence of time-dependent interactions, is $\hat{H}'_D = \hat{T}(t)\hat{H}_C(t)\hat{T}^\dagger(t) + i\dot{\hat{T}}\hat{T}^\dagger$.

In summary, in the absence of time-dependent interactions, the Coulomb gauge Hamiltonian $\hat{H}_C$ and the standard multipolar gauge Hamiltonain $\hat{H}_D = \hat{H}'_D$ provide equivalent dynamics. In the presence of time-dependent interactions, only $\hat{H}'_D$ provides a dynamics

which is equivalent to the one determined by $\hat{H}_C$, and the standard multipolar Hamiltonian $\hat{H}_D$ has to be disregarded. Consequently, we can consider $\hat{H}_C$ more fundamental than $\hat{H}_D$. The first ($\hat{H}_C$) originates directly from the minimal coupling replacement enforcing the gauge principle, while the latter ($\hat{H}_D$) results from the first, after a transformation which can be time-dependent. A different point of view could be to consider, independently on the historical derivation, $\hat{H}_D$ as the fundamental Hamiltonian and deriving $\hat{H}_C$ from it after a unitary transformation. In this case the correct Hamiltonian in the Coulomb gauge, providing a dynamics equivalent to that of $\hat{H}_D(t)$, would be $\hat{H}'_C(t) = \hat{T}^\dagger(t)\hat{H}_D(t)\hat{T}(t) + i\dot{\hat{T}}(t)^\dagger\hat{T}(t)$. This Hamiltonain, owing to the second term on the right-hand side of the above equation, does not correspond to a minimal coupling replacement as prescribed by the gauge principle. On the contrary, $\hat{H}_C$ is directly obtained by the minimal coupling replacement (which implements the gauge principle) after setting to zero the longitudinal component of the vector potential (which has no dynamical relevance) [16].

Analogous considerations apply to the case of switchable circuit QED systems (see Appendix H). In this case the more fundamental gauge is the so-called *flux* gauge, which is somewhat analogous to the dipole gauge. Also in this case, it is possible to apply a unitary transformation, in order to obtain an equivalent representation, called the charge gauge.

Appendix F: Non-adiabatic tunable coupling: Switch-on and switch-off dynamics

Following Ref. [27], we consider the treatment of tuneable light-matter interactions through the promotion of the coupling to a time-dependent function. In Ref. [27] it is shown that applying the standard widespread procedure, for sufficiently strong light-matter interactions, the final subsystem properties, such as entanglement and subsystem energies, depend significantly on the definitions (gauges) of light and matter adopted during their interaction. This occurs even if the interaction is not present at the initial and final stages of the protocol, at which times the subsystems are uniquely defined and can be individually addressed. Such an ambiguity is surprising and poses serious doubts on the predictability of the system dynamics in the presence of ultrastrong time-dependent light-matter interactions.

Here we address this apparent problem by considering a light-atom system initially in the absence of interaction and starting, e.g., in its ground state $|\psi(t_{\rm in})\rangle = |g, 0\rangle$. A different choice of the initial state does not change the conclusions. This situation can be visualized

considering a system constituted by an optical cavity (initially prepared in the zero-photon state) and an atom initially external to the cavity and in its ground state. At $t = t_1$, the atom enters the cavity and flies out of it at $t = t_2$. We consider the case of a TLS (the generalization to multilevel systems is straightforward). In addition, for the sake of simplicity, we assume that for $t_1 < t < t_2$ the normalized interaction strength η is constant. *We demonstrate that, after the switch off of the interaction, the same quantum state is obtained independently of the adopted gauge.*

We start our analysis considering the Coulomb gauge. The initial state (actually independent on the gauge) is $|\psi_C(t_{\rm in})\rangle = |g,0\rangle_C$. At $t = t_1$, the interaction is non-adiabatically switched on within a time $T \to 0$. This sudden switch has no effect on the quantum state [46], hence, at $t = t_1^+ = t_1 + T$, $|\psi_C(t_1^+)\rangle = |g,0\rangle$. For $t > t_1^+$, the quantum state evolves as $|\psi_C(t)\rangle = \exp\left[-i\hat{\mathcal{H}}_C(t-t_1)\right]|g,0\rangle_C$. Then, at $t = t_2$, the interaction is suddenly switched off. At $t = t_2^+ = t_2 + T$, the system state is $|\psi_C(t_2^+)\rangle = \exp\left[-i\hat{\mathcal{H}}_C(t_2-t_1)\right]|g,0\rangle_C$. For $t > t_2$, the quantum state evolves according to the Hamiltonian for the noninteracting system ($\eta = 0$): $|\psi_C(t)\rangle = \exp\left[-i\hat{\mathcal{H}}_{\rm free}(t-t_2)\right]|\psi_C(t_2^+)\rangle$, where $\mathcal{H}_{\rm free}$ is the system Hamiltonian in the absence of interaction. We can use these quantum states to calculate any system expectation value at any time. For example, the mean photon number can be calculated as

$$\langle\psi_C(t)|\hat{Y}^{(-)}\,\hat{Y}^{(+)}|\psi_C(t)\rangle\,, \tag{F1}$$

where $\hat{Y}^{(+)}$ and $\hat{Y}^{(-)}$ are the positive and negative-frequency components of the operator $\hat{Y} = i(\hat{a} - \hat{a}^\dagger)$ [with $\hat{Y}^{(-)} = (\hat{Y}^{(+)})^\dagger$]. Notice that, for $t < t_1$ and $t > t_2$, $\hat{Y}^{(+)} = i\hat{a}$.

Now we describe the same dynamics in the dipole gauge. Before switching on the interaction, the state is simply $|\psi_D(t_1^-)\rangle = |g,0\rangle$. As shown in Appendix E, the system Hamiltonian in the dipole gauge is

$$\begin{aligned}\hat{\mathcal{H}}_D(t) &= \hat{\mathcal{T}}(t)\hat{\mathcal{H}}_C\hat{\mathcal{T}}^\dagger(t) + i\dot{\hat{\mathcal{T}}}(t)\hat{\mathcal{T}}^\dagger(t)\\ &= \hat{\mathcal{H}}_{\rm free} + \hat{\mathcal{V}}_D(t) - \dot{\lambda}\hat{\mathcal{F}}\,,\end{aligned} \tag{F2}$$

where $\lambda(t)$ is the switching function (see Fig. 6). Notice that, when the interaction strength is time independent, the last term in Eq. (F2) goes to zero. On the contrary, during non-adiabatic switches or modulations, this term can become the dominant one. Owing to the presence of the last term in Eq. (F2), the state after the switch-on of the interaction becomes

$$|\psi_D(t_1^+)\rangle = \exp\left(i\hat{\mathcal{F}}\int_{t_1^-}^{t_1^+} dt\dot{\lambda}\right)|\psi_D(t_1^-)\rangle = \hat{\mathcal{T}}|g,0\rangle\,. \tag{F3}$$

For $t > t_1^+$, the quantum state evolves as $|\psi_D(t)\rangle = \exp\left(-i\hat{\mathcal{H}}_D(t-t_1)\hat{\mathcal{T}}|g,0\rangle\right.$. Then, at $t = t_2$, the interaction is suddenly switched off. At $t = t_2^+ = t_2 + T$ the system state becomes $|\psi_D(t_2^+)\rangle = \hat{\mathcal{T}}^\dagger \exp\left[-i\hat{\mathcal{H}}_D(t_2-t_1)\right]\hat{\mathcal{T}}|g,0\rangle$. Since $\hat{\mathcal{H}}_C = \hat{\mathcal{T}}^\dagger\hat{\mathcal{H}}_D\hat{\mathcal{T}}$, it implies that

$$|\psi_D(t_2^+)\rangle = |\psi_C(t_2^+)\rangle\,. \tag{F4}$$

As an example, we reported in Fig. (6) the gauge-invariant emission,

$$\langle\psi_C(t)|\hat{Y}^{(-)}\,\hat{Y}^{(+)}|\psi_C(t)\rangle\,,$$

from a two-level system coupled to a single-mode resonator (quantum Rabi Hamiltonian) induced by sudden switches of the light-matter interaction, calculated for three normalized coupling strengths.

As a final remark, we observe that the procedure described here can be directly extended to show that gauge invariance is also preserved for intermediate gauge transformations dependent on a continuous parameter α [10]. Indeed, it is sufficient to replace $\hat{\mathcal{F}}$ with $\alpha\hat{\mathcal{F}}$ in the demonstration.

Appendix G: Circuit QED: Galvanic Coupling

A qubit-resonator system is said to be Galvanically coupled when the two components share a portion of their respective circuits [2]. With circuits, this strategy has been used to reach both the USC and the deep strong coupling regimes. Besides, the generic lumped circuit analysis is formally equivalent to the description of the fluxonium-resonator system. Moreover, these architectures seem to be optimal test-beds for performing experiments on the gauge issues discussed in this work.

To analyse the different architectures in a unified way, we consider the qubit as a "black-box", while the coupler is the part shared with the resonator. The lumped circuit is drawn in Fig. 7. The coupler can be an effective inductance and the dashed region can describe, e.g., the three junctions forming the flux qubit as in the experiments [4, 50] or one of the qubit-junctions as in this other experiment [59].

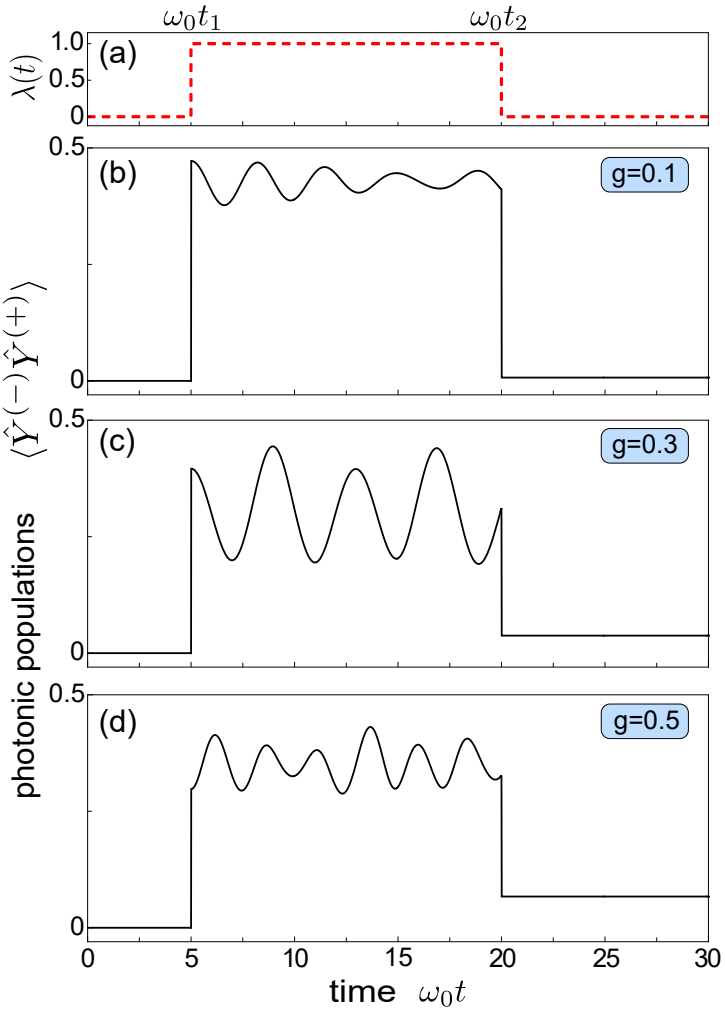

Figure 6. Gauge-invariant emission of a two-level atom coupled to a single-mode resonator (quantum Rabi Hamiltonian) induced by sudden switches of the light-matter interaction, calculated for three normalized coupling strengths. (a) Displays the switching function $\lambda(t)$. The system is initially prepared in its ground state: $|\psi_C(t_{in})\rangle = |g, 0\rangle$. At $t = t_1$ the interaction is suddenly switched on, and it is finally switched off at $t = t_2$.

1. Flux gauge

In the flux gauge, the Lagrangian can be written as [68],

$$\mathcal{L}_{\rm fg} = \mathcal{L}^0_{\rm qubit} + \frac{1}{2}C\dot{\Phi}^2 - \frac{1}{2L}(\Phi - \Phi_q)^2 \,. \tag{G1}$$

Here, $\mathcal{L}^0_{\rm qubit}$ describes the qubit part, which depends on the specific artificial atom considered and $\frac{1}{2L}(\Phi - \Phi_q)^2$ provides the coupling term. Recall that here Φ is the flux through the

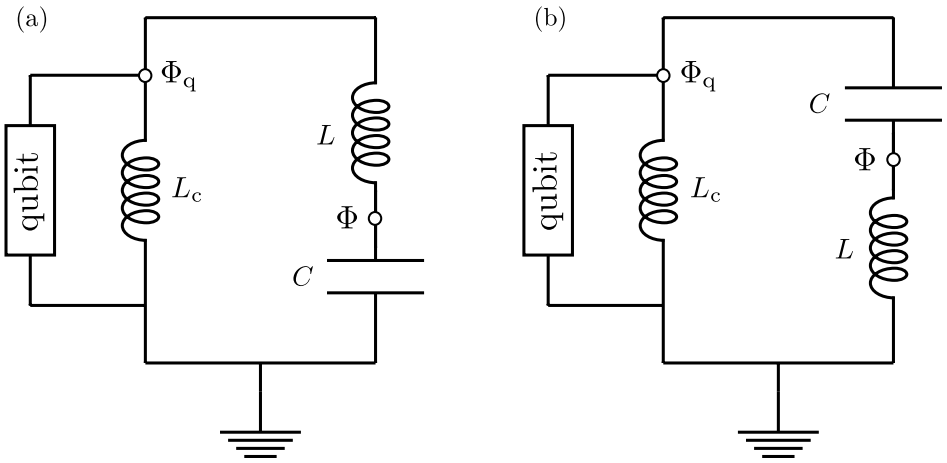

Figure 7. Circuit QED systems with Galvanic coupling. (a) In the *flux* gauge the chosen coordinates correspond to the flux across the qubit Φ_q and the flux across the ocillator capacitor Φ. (b) In the charge gauge the chosen coordinates correspond to the flux across the qubit Φ_q and the flux across the oscillator inductor Φ.

resonator *c*apactitor and Φ_q is the flux through the coupler, as specified in figure Fig. 7(a). It is convenient to rewrite Eq. (G1) as a sum of three contributions: the qubit, the LC-resonator, and their interaction:

$$\mathcal{L}_{\rm fg} = \mathcal{L}_{\rm LC} + \mathcal{L}_{\rm qubit} + \frac{1}{L}\Phi\,\Phi_q\,, \tag{G2}$$

where $\mathcal{L}_{\rm LC} = \frac{1}{2}C\dot{\Phi}^2 - \Phi^2/(2L)$, and $\mathcal{L}_{\rm qubit} = \mathcal{L}^0_{\rm qubit} - \Phi_q^2/(2L)$. Notice that $\mathcal{L}_{\rm LC}$ describes an oscillator with resonant frequency $\omega_c = 1/\sqrt{LC}$.

In order to deal with an explicit qubit Lagrangian, we consider a fluxonium-type qubit, such that:

$$\mathcal{L}_{\rm qubit} = \frac{1}{2}C_q\dot{\Phi}_q^2 - \Phi_q^2/(2L_\parallel) + E_j\cos\left(2\pi\frac{\Phi_q - \Phi_{\rm ext}}{\Phi_0}\right)\,, \tag{G3}$$

where C_q is the qubit capacitance, $L_\parallel \simeq L_cL/(L_c+L)$, $\Phi_0 = h/2e$ is the flux quantum, and $\Phi_{\rm ext}$ is the external flux. The superconducting loop is maximally frustrated at a specific value of the external flux $\Phi_{\rm ext} = \Phi_0/2$. In this case [53], the atom's effective potential has a symmetric double-well shape consisting of two lowest degenerate local minima separated by approximately the flux quantum Φ_0. This configuration can give rise to artificial atoms with a high degree of anharmonicity, with the two lowest energy levels well separated by the higher energy ones. An analogous energy spectrum can also be obtained considering a flux

qubit [4].

The momenta conjugate to Φ and Φ_q can be easily obtained starting from Eq. (G2) by using the canonical relations

$$Q = \frac{\partial \mathcal{L}}{\partial \dot{\Phi}} = C\dot{\Phi}\,, \tag{G4a}$$

$$Q_q = \frac{\partial \mathcal{L}}{\partial \dot{\Phi}_q} = C_q\dot{\Phi}_q\,. \tag{G4b}$$

In this case, Q and Q_q represent the charge across the capacitor C of the oscillator, and the charge across the coupler, respectively.

By performing the Legendre transformation $H_{\rm fg} = Q\dot{\Phi} + Q_q\dot{\Phi}_q - \mathcal{L}_{\rm fg}$, the flux gauge Hamiltonian can be written as

$$H_{\rm fg} = H^0_{\rm qubit} + \frac{Q^2}{2C} + \frac{(\Phi_q - \Phi)^2}{2L}\,, \tag{G5}$$

where

$$H^0_{\rm qubit} = \frac{Q_q^2}{2C_q} + \frac{\Phi_q^2}{2L_c} - E_j\cos\left(2\pi\frac{\Phi_q - \Phi_{\rm ext}}{\Phi_0}\right)\,. \tag{G6}$$

The system Hamiltonian can also be written as

$$H_{\rm fg} = H_{\rm LC} + H_{\rm qubit} - \frac{\Phi_q\Phi}{L}\,, \tag{G7}$$

where

$$H_{\rm LC} = \frac{Q^2}{2C} + \frac{\Phi^2}{2L}\,, \tag{G8}$$

and

$$H_{\rm qubit} = \frac{Q_q^2}{2C_q} + \frac{\Phi_q^2}{2L_{\|}} - E_j\cos\left(2\pi\frac{\Phi_q - \Phi_{\rm ext}}{\Phi_0}\right)\,. \tag{G9}$$

The quantization procedure of Eq. (G7) is straightforward. In our case, the resonator operators can be expressed in terms of the creation and annihilation operators as

$$\hat{\Phi} = \Phi_{\rm zpf}(\hat{a} + \hat{a}^\dagger)\,,$$

$$\hat{Q} = -iQ_{\rm zpf}(\hat{a} - \hat{a}^\dagger)\,,$$

where $\Phi_{\rm zpf} = \sqrt{L\hbar\omega_c/2}$, and $Q_{\rm zpf} = \sqrt{C\hbar\omega_c/2}$ with $\omega_c = 1/\sqrt{LC}$.

It is important to note that in Eq. (G9) we implicitly considered all the fluxonium levels. However, when the energy-level spectrum of the system displays a high degree of anharmonicity, such that the higher energy levels are well spaced with respect to the first two,

Eq. (G9) can be projected in a two-level space spanned by the flux-qubit eigenstates $|g\rangle$ (ground state) and $|e\rangle$ (excited state) using the operator $\hat{P} = |e\rangle\langle e| + |g\rangle\langle g|$.

The flux across the coupling inductor can be treated as a constant operator with off-diagonal matrix elements which are directly calculated in the qubit energy eigenbasis as $\langle g|\Phi_q|e\rangle \simeq L_c I_p$, where I_p is the persistent current in the qubit loop. Performing this projection, the two-level flux gauge Hamiltonian becomes

$$\hat{\mathcal{H}}_{\rm fg} = \hbar\omega_c \hat{a}^\dagger \hat{a} + \frac{\hbar\omega_0}{2}\hat{\sigma}_z + \hbar\omega_c \eta(\hat{a}^\dagger + \hat{a})\hat{\sigma}_x \,, \tag{G10}$$

where $\hbar\omega_0$ is the qubit transition energy and $\hbar\omega_c\eta = L_c I_p I_{\rm zpf}$, where $I_{\rm zpf} = \Phi_{\rm zpf}/L$ is the zero-point current fluctuation of the oscillator.

In the flux gauge, the flux across the oscillator inductor is $\hat{\Phi}_L = \hat{\Phi} - \hat{\Phi}_q$. Projecting the artificial-atom flux $\hat{\Phi}_q$ in the two-level space, we obtain $\hat{\Phi}_L = \Phi_{\rm zpf}(\hat{a} + \hat{a}^\dagger - 2\eta\hat{\sigma}_x)$. The voltage across the oscillator inductor is

$$\hat{V} = \dot{\hat{\Phi}} = [\hat{\Phi}_L, \hat{\mathcal{H}}_{\rm fg}]/(i\hbar) = \omega_c \Phi_{\rm zpf}\left[i(\hat{a}^\dagger - \hat{a}) + 2\eta\omega_0\hat{\sigma}_y\right] . \tag{G11}$$

2. Charge gauge

In order to derive the charge gauge Hamiltonian of the system (see Fig. 7(b), we consider as canonical coordinates the node flux Φ_q and the flux Φ across the resonator inductance L. Following the same procedure of the previous subsection, the system Lagrangian can be written as

$$\mathcal{L}_{\rm cg} = \frac{1}{2}C_q\dot{\Phi}_q^2 + \frac{1}{2}C\left(\dot{\Phi}_q - \dot{\Phi}\right)^2 - \frac{1}{2L_c}\Phi_q^2 - \frac{1}{2L}\Phi^2 + E_J\cos\left[2\pi(\Phi_q - \Phi_{\rm ext})/\Phi_0\right] \,, \tag{G12}$$

with the canonical momenta defined as

$$Q_q = (C_q + C)\dot{\Phi}_q + C\dot{\Phi} \,, \tag{G13a}$$

$$Q = C(\dot{\Phi} - \dot{\Phi}_q) \,. \tag{G13b}$$

Performing the Legendre transformation (see Subsection G 1), and promoting the canonical variables to operators, the system Hamiltonian in the charge gauge results in

$$\hat{H}_{\rm cg} = \frac{1}{2C_q}(\hat{Q}_q + \hat{Q})^2 + \frac{1}{2C}\hat{Q}^2 + \frac{1}{2L_c}\hat{\Phi}_q^2 + \frac{1}{2L}\hat{\Phi}^2 - E_J\cos\left[2\pi(\hat{\Phi}_q - \Phi_{\rm ext})/\Phi_0\right] . \tag{G14}$$

Also in this case, if the system displays a high degree of anharmonicity, we can project the system Hamiltonian in the two-level subspace $\{|g\rangle, |e\rangle\}$. However, it has been shown that this truncation ruins gauge invariance [11]. The coupling described in Eq. (G14) is analogous to the minimal coupling replacement used to introduce the particle-field interaction in quantum field theory and atomic physics. According to this procedure, the particle momentum is replaced by the sum of the particle momentum and the product of the charge and the field coordinate. In the present case, the coupling is introduced by replacing the momentum of the artificial atom: $\hat{Q}_q \to \hat{Q}_q + \hat{Q}$. It has been shown that, when the atom Hilbert space is truncated, unavoidably some degree of spatial nonlocality is introduced in the atomic potential [11]. As a consequence, the truncated potential will depend also on the momentum $\hat{Q}$ and gauge invariance is preserved only by also applying the minimal coupling replacement to it. To solve this problem, we introduce the minimal coupling replacement by applying a unitary transformation to the atomic Hamiltonian:

$$\hat{H}_{\rm cg} = \hat{H}_{\rm LC} + \hat{R}^\dagger \hat{H}_{\rm qubit} \hat{R}\,, \tag{G15}$$

where $\hat{R} = \exp(i\hat{\Phi}_q \hat{Q}/\hbar)$. It is worth noticing that Eq. (G15) is equivalent to Eq. (G14). After truncating the atomic space to only two states, the bare qubit Hamiltonian reduces to $\hat{\mathcal{H}}_{\rm qubit} = \hbar(\omega_0/2)\hat{\sigma}_z$, The resulting unitary operator in the reduced space is

$$\hat{\mathcal{R}} = \exp\left[\eta \hat{\sigma}_x (\hat{a} - \hat{a}^\dagger)\right], \tag{G16}$$

and Eq. (G15) becomes

$$\hat{\mathcal{H}}_{\rm cg} = \hat{H}_{\rm LC} + \hat{\mathcal{R}}^\dagger \hat{\mathcal{H}}_{\rm qubit} \hat{\mathcal{R}}\,. \tag{G17}$$

We finally obtain

$$\begin{aligned} \hat{\mathcal{H}}_{\rm cg} &= \hbar\omega_c \hat{a}^\dagger \hat{a} + \frac{\hbar\omega_{\rm eg}}{2}\left\{\hat{\sigma}_z \cosh\left[2\eta(\hat{a} - \hat{a}^\dagger)\right] + i\hat{\sigma}_y \sinh\left[2\eta(\hat{a} - \hat{a}^\dagger)\right]\right\} \\ &= \hbar\omega_c \hat{a}^\dagger \hat{a} + \frac{\hbar\omega_{\rm eg}}{2}\hat{\sigma}'_z\,, \end{aligned} \tag{G18}$$

where, in the last line, we indicated with the primed symbol the transformed Pauli operator:

$$\hat{\sigma}'_z = \hat{\mathcal{R}}^\dagger \hat{\sigma}_z \hat{\mathcal{R}}\,. \tag{G19}$$

3. Gauge invariance

The Hamiltonians derived in the previous sections are connected (in full analogy with the dipole to Coulomb transformation), by a unitary transformation. It results that such

unitary operator coincides with $\hat{R}$ that we used in the previous subsection to implement the minimal coupling replacement (charge gauge). For example, the flux gauge Hamiltonian can be obtained starting from $\hat{H}_{\rm cg}$ by performing the unitary transformation [11]

$$\hat{H}_{\rm fg} = \hat{R}\hat{H}_{\rm cg}\hat{R}^\dagger = \hat{H}_{\rm qubit} + \hat{R}\hat{H}_{\rm LC}\hat{R}^\dagger \,. \tag{G20}$$

By using the generalized minimal coupling replacement, described in the previous subsection, gauge invariance holds even after the reduction of the atomic degrees of freedom to only two levels. Specifically, it results [11]

$$\hat{\mathcal{H}}_{\rm fg} = \hat{\mathcal{R}}\hat{\mathcal{H}}_{\rm cg}\hat{\mathcal{R}}^\dagger = \hat{\mathcal{H}}_{\rm qubit} + \hat{\mathcal{R}}\hat{\mathcal{H}}_{\rm LC}\hat{\mathcal{R}}^\dagger \,. \tag{G21}$$

The inverse transformation from the charge to the flux gauge is straightforward. The unitary transformation procedure also allows to derive the relationship between the operators in the different gauges. For example, we can derive the charge gauge operators (labelled with the 'prime' superscript):

$$\hat{\sigma}_x' = \hat{\mathcal{R}}^\dagger\hat{\sigma}_x\hat{\mathcal{R}} = \hat{\sigma}_x \tag{G22a}$$

$$\hat{\sigma}_z' = \cosh\left[2\eta(\hat{a}-\hat{a}^\dagger)\right]\hat{\sigma}_z + i\sinh\left[2\eta(\hat{a}-\hat{a}^\dagger)\right]\hat{\sigma}_y \tag{G22b}$$

$$\hat{\sigma}_y' = \cosh\left[2\eta(\hat{a}-\hat{a}^\dagger)\right]\hat{\sigma}_y - i\sinh\left[2\eta(\hat{a}-\hat{a}^\dagger)\right]\hat{\sigma}_z \tag{G22c}$$

$$\hat{a}' = \hat{a} - \eta\hat{\sigma}_x \,. \tag{G22d}$$

It turns out that, in the above equations, the only gauge invariant qubit operator is $\hat{\sigma}_x$ while the others have to be transformed accordingly to the considered gauge. Finally, we notice that the oscillator momentum $\hat{Q} = iQ_{\rm zpf}(\hat{a}^\dagger - \hat{a})$ is also invariant under the unitary transformation.

Appendix H: Qubit-oscillator coupling by mutual inductance

We now discuss the qubit-resonator system which is *inductively* coupled to a LC resonator via mutual inductance (see Figure 8). In the *flux gauge*, the Kirchoff equations yield the Hamiltonian:

$$\hat{H}_{\rm fg} = \hat{H}_{\rm qubit} + \hat{H}_{\rm LC} - \frac{1}{\widetilde{M}}\hat{\Phi}\,\hat{\Phi}_q \,, \tag{H1}$$

where the qubit Hamiltonian is

$$\hat{H}_{\rm qubit} = \frac{1}{2C_q}\hat{Q}_q^2 + \frac{1}{2\widetilde{L}_q}\hat{\Phi}_q^2 - E_J \cos\left[2\pi(\hat{\Phi}_q - \Phi_{\rm ext})/\Phi_0)\right] \,,$$

and the oscillator Hamiltonian is

$$\hat{H}_{\rm LC} = \frac{1}{2C}\hat{Q}^2 + \frac{1}{2\widetilde{L}}\hat{\Phi}^2 \,.$$

Assuming for symplicity $L \gg M$, we obtain for the renormalized inductances: $\widetilde{L} = (L_q L - M^2)/L_q \approx L$; $\widetilde{L}_q = (L_q L - M^2)/L \approx L_q$ where L_q is the qubit inductance. The relevant dynamical variables are the flux Φ at the node between the inductor and the capacitor of the oscillator (see Figure 8), Q the corresponding charge (the canonical momentum conjugate to Φ), Φ_q corresponding to the flux through the qubit and the qubit charge Q_q (the canonical momentum conjugate to Φ_q). The last term in the right-hand side of Eq. (H1) describes the coupling of the LC-resonator with the superconducting artificial atom via the effective mutual inductance $\widetilde{M} = (LL_q - M^2)/M \approx LL_q/M$ (see also Appendix I). Hence, Eq. (H1) can be written as

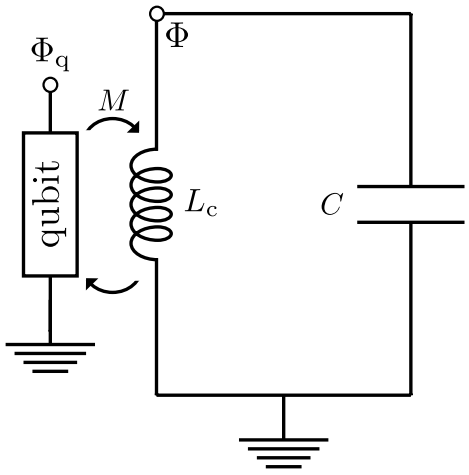

Figure 8. The fluxonium-LC circuit inductively coupled to a LC resonator.

$$\hat{H}_{\rm fg} = \frac{\hat{Q}^2}{2C} + \frac{\hat{\Phi}^2}{2L} + \frac{\hat{Q}_q^2}{2C_q} + \frac{\hat{\Phi}_q^2}{2L_q} - E_J \cos\left[2\pi(\hat{\Phi}_q - \Phi_{\rm ext})/\Phi_0)\right] - \frac{M}{LL_q}\hat{\Phi}\hat{\Phi}_q \,. \qquad \text{(H2)}$$

The coupling strength in Eq. (H2) is proportional to the mutual inductance M. When the energy level spectrum of the superconducting artificial atom displays a high degree of anharmonicity, such that the higher-energy levels are well spaced with respect to the first two,

as in Appendix G10, Eq. (H2) can be projected in a two-level space spanned by the flux-qubit eigenstates $|g\rangle$ (ground state) and $|e\rangle$ (excited state) using the operator $\hat{P} = |e\rangle\langle e| + |g\rangle\langle g|$. The resulting qubit-oscillator Hamiltonian coincides with Eq. (G10).

It is possible to define a unitary operator in order to perform a transformation from flux to *charge* gauge:

$$\hat{H}_{\rm cg} = \hat{R}\hat{H}_{\rm fg}\hat{R}^\dagger \qquad \text{with} \qquad \hat{R} = \exp\left[i\frac{M}{L_q}\hat{Q}\,\hat{\Phi}_q\right] . \tag{H3}$$

We obtain

$$\hat{H}_{\rm cg} = \frac{\hat{Q}^2}{2C} + \frac{\hat{\Phi}^2}{2L} + \frac{1}{2C_q}\left[\hat{Q}_q - \frac{M}{L_q}\hat{Q}\right]^2 + \frac{\hat{\Phi}_q^2}{2L_q} - E_J\cos\left[2\hat{\pi}(\Phi_q - \Phi_{\rm ext})/\Phi_0)\right] . \tag{H4}$$

In this case we observe that the interaction term is transformed and, instead of involving the product of the two coordinates, it involves the product of the two momenta. *The charge gauge interaction closely resembles the minimal coupling replacement for natural atoms.* However, it is worth pointing out that in the case of time-dependent interactions $[M \to M(t)]$, also $\hat{R}(t)$ becomes time dependent. As a result, the correct Hamiltonian in the charge gauge is no more $\hat{H}_{\rm cg} = \hat{R}\hat{H}_{\rm fg}\hat{R}^\dagger$, but it becomes:

$$\hat{H}_{\rm cg}(t) = \hat{R}(t)\hat{H}_{\rm fg}(t)\hat{R}^\dagger(t) + i\dot{\hat{R}}\hat{R}^\dagger , \tag{H5}$$

which contains additiona terms with respect to Eq. (H4).

It is interesting to compare this result with the corresponding one for natural atoms in Appendix E (see in particular the discussion in the last paragraph). For natural atoms, the Hamiltonian resulting from the minimal coupling replacement is the fundamental one (especially in the presence of time-dependent interactions). However, in the present case, $\hat{H}_{\rm cg}$ (which describes the minimal coupling replacement for superconducting circuits) is not the fundamental Hamiltonian. Here we can adopt an operative definition: the fundamental gauge is the one where the Hamiltonian does not change its structure in the presence of time-dependent interactions, which actually is $\hat{H}_{\rm fg}$ (the analogous of the dipole gauge Hamiltonian).

This difference between circuit QED and cavity QED systems arises from the different origin of interactions. For natural atoms, the specific form of the interaction is given by the minimal coupling replacement (the interaction Hamiltonian can be obtained from the gauge principle applied to the Dirac equation and then taking the nonrelativistic limit).

On the other hand, in circuit QED we do not have such a fundamental theory, it is an effective one which can be derived from the Kirchoff equations. We also notice that these differences result into a coordinate-momentum interaction Hamiltonian for natural atoms and into a coordinate-coordinate interaction (which becomes momentum-momentum in the charge gauge) for superconducting artificial atoms inductively coupled to an oscillator. The different kind of behaviour of cavity and circuit QED systems after switching off the interaction, shown in the main text [cf. Fig. 4 and Fig. 5], originates from these differences.

Appendix I: Coupling to a transmission line

We now discuss the qubit-resonator system that it is *inductively* coupled to a transmission line [cf. Fig. 1(b) in main text]. After discretization, the equivalent circuit for the transmission line (TL) is a set of coupled resonators, each of size Δx. The properties of the line are given by the effective impedance. Here, we assume it homogeneous, thus $L_T = l_T \Delta x$ and $C_T = c_T \Delta_x$ are the inductance and capacitance at each site, while l_T and c_T are those per unit of length. The mutual inductance is M. See Fig. 9 for a representation of the circuit.

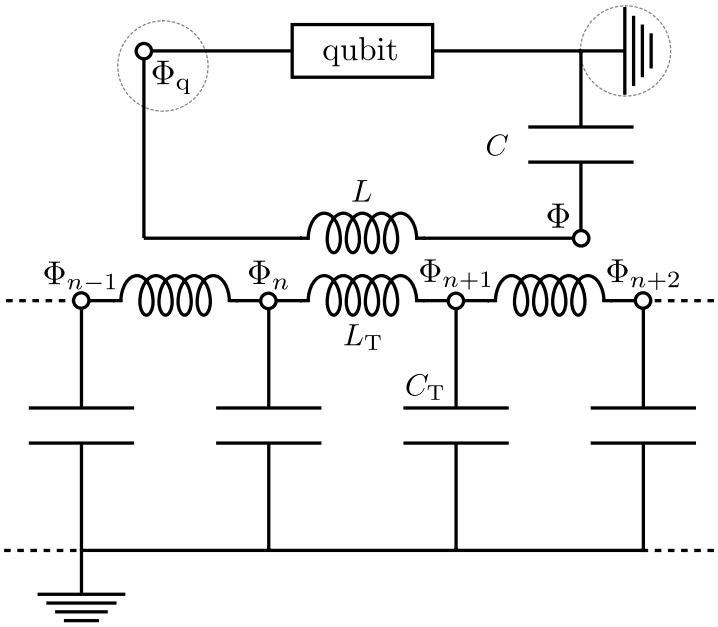

Figure 9. The fluxonium-LC circuit coupled to a transmission line (TL) in the flux gauge.

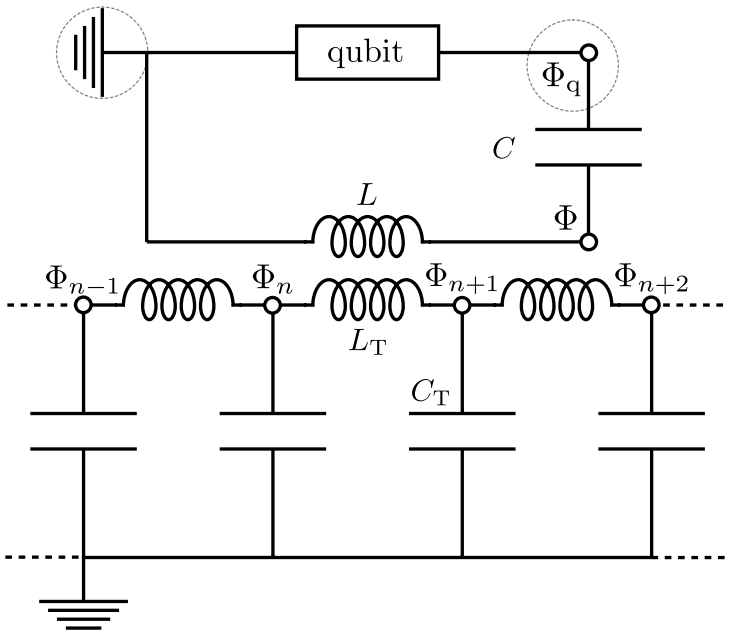

Figure 10. The fluxonium-LC circuit coupled to a transmission line (TL) in the charge gauge.

In the *flux gauge*, the Kirchoff equations yield the Hamiltonian:

$$\begin{aligned} H_{\rm fg} = H_{\rm qubit} &+ \frac{1}{2C}Q^2 + \frac{1}{2\widetilde{L}}\Phi^2 + \frac{1}{2L}(\Phi-\Phi_q)^2 \\ &+ \frac{1}{C_T}\sum_{j=1} Q_j^2 + \frac{1}{2\widetilde{L}_T}(\Phi_{n+1}-\Phi_n)^2 + \frac{1}{2L_T}\sum_{j\neq n}(\Phi_{j+1}-\Phi_j)^2 \\ &+ \frac{1}{2\widetilde{M}}(\Phi-\Phi_q)(\Phi_{n+1}-\Phi_n)\ . \end{aligned} \tag{I1}$$

The terms in the first line include the qubit and the resonator Hamiltonians and the resonantor-qubit coupling with a renormalized inductance $\widetilde{L} = (L_T L - M^2)/L_T$. The second line includes the Hamiltonian of the linear chain, i.e., the transmission line. Notice that in the inductor coupled to the oscillator the inductance is also renormalized: $\widetilde{L}_T = (L_T L - M^2)/L$. The term in the last line describes the coupling of the LC-resonator with the transmission line via the effective mutual inductance $\widetilde{M} = (LL_T - M^2)/M$. We are interested in the situation where the TL is used for readout, thus the circuit is designed to have $M \ll L$. Consequently, we can safely approximate the renormalized terms by its bare values $\widetilde{L}_T = L_T + \mathcal{O}(M^2) \cong L_T$ and $\widetilde{L} = L + \mathcal{O}(M^2) \cong L$. Notice that, in Eq. (I1) the dynamical variables are Φ_j, the node fluxes in each capacitor (Q_j their canonical charges). Φ is the flux through the capacitor of the oscillator, and Q the conjugate canonical charge. Finally, Φ_q is the flux through the qubit. Notice that this Hamiltonian is written in the flux gauge.

Finally, introducing the position-dependent flux $\phi(x)$ for the open transmission line, and the charge density $\hat{\rho}(x) = \hat{Q}_j/\Delta x$, the Hamiltonian in the continuum ($\Delta x \to 0$) reads

$$\begin{aligned} H_{\rm fg} &= H_{\rm LC} + H_{\rm qubit} - \frac{\Phi_q \Phi}{2} \\ &+ \int dx \left\{ \frac{1}{2c_T}\rho^2(x) + \frac{1}{2l_T}\left[\partial_x \phi(x)\right]^2 \right\} \\ &+ \frac{M}{2Ll_T}(\Phi - \Phi_q) \int dx\, \partial_x \phi(x)\,. \end{aligned} \tag{I2}$$

This Hamiltonian can be quantized promoting the canonical coordinates to operator and introducing the commutation relations $[\hat{\Phi}_q, \hat{Q}_q] = i\hbar$, and $[\hat{\Phi}, \hat{Q}] = i\hbar$, and $[\hat{\phi}, \hat{\rho}] = i\hbar\delta(x - x')$.

Performing then the projection on the two-level subspace for the qubit, we end up with

$$\hat{\mathcal{H}}^{\rm tot}_{\rm fg} = \hat{\mathcal{H}}_{\rm fg} + \hat{H}_{\rm tl} + \hat{\mathcal{V}}_{\rm fg}\,, \tag{I3}$$

where

$$\hat{H}_{\rm tl} = \int dx \left\{ \frac{1}{2c_T}\rho^2(x) + \frac{1}{2l_T}\left[\partial_x \phi(x)\right]^2 \right\}\,, \tag{I4}$$

and

$$\hat{\mathcal{V}}_{\rm fg} = \alpha \Phi_{\rm zpf}(\hat{a} + \hat{a}^\dagger - 2\eta\hat{\sigma}_x) \int dx\, \partial_x \hat{\phi}(x)\,, \tag{I5}$$

with $\alpha = M/(Ll_T)$. It is important to notice that the coupling operator to the two-level system is $(\hat{a} + \hat{a}^\dagger - 2\eta\hat{\sigma}_x)$. We emphasize that this is a consequence of the chosen dynamical variables, which define the gauge, in this case the flux one.

We can also work in the charge gauge (See fig. 10):

$$\hat{\mathcal{H}}^{\rm tot}_{\rm cg} = \mathcal{R}^\dagger \hat{\mathcal{H}}^{\rm tot}_{\rm fg} \mathcal{R} = \hat{\mathcal{H}}_{\rm cg} + \hat{H}_{\rm tl} + \hat{\mathcal{V}}_{\rm cg}\,, \tag{I6}$$

where

$$\hat{\mathcal{V}}_{\rm cg} = \alpha \Phi_{\rm zpf}(\hat{a} + \hat{a}^\dagger) \int dx\, \partial_x \hat{\phi}(x)\,. \tag{I7}$$

In this case, the coupling to the transmission depends only on the oscillator operators.

The position-dependent flux of the transmission line can be expanded in terms of photon operators as

$$\hat{\phi}(x) = \Lambda \int \frac{d\omega}{\sqrt{\omega}} \left(\hat{b}_\omega e^{ik_\omega x} + \text{h.c.} \right)\,, \tag{I8}$$

where $\Lambda = \sqrt{\hbar Z_0/4\pi}$, with Z_0 the impedance of the transmission line, $k_\omega = \omega/v$ is the wavenumber ($v = 1/\sqrt{l_T c_T}$ is the phase velocity of the transmission line), and the photon

operators obey the commutation rules $\left[\hat{b}_\omega, \hat{b}^\dagger_{\omega'}\right] = \delta(\omega - \omega')$. By using this expansion, the oscillator-line interaction Hamiltonian can be written as

$$\mathcal{V} = i\hbar \frac{\hat{\Phi}_L}{\Phi_{\rm zpf}} \int d\omega g(\omega)(\hat{b}_\omega - \hat{b}^\dagger_\omega)\,, \tag{I9}$$

where $\hat{\Phi}_L$ is the flux across the oscillator inductor, and $\hbar g(\omega) = \alpha \Phi_{\rm zpf} \Lambda \sqrt{\omega}/v$. Note that this expression describes the interaction potential in both the flux and charge gauges. In the first case $\hat{\Phi}^{\rm fg}_L = \Phi_{\rm zpf}(\hat{a} + \hat{a}^\dagger)$, in the latter $\hat{\Phi}^{\rm cg}_L = \Phi_{\rm zpf}(\hat{a} + \hat{a}^\dagger - 2\eta\hat{\sigma}_x)$. Equation (I9) is the starting point for the derivation of the input-output relationship for an LC oscillator inductively (weakly) coupled to an open transmission line. An analogous interaction term can be derived for an optical cavity [69].

Appendix J: Input-output theory in the USC regime: LC oscillator coupled to a transmission line

In the following we assume that $g(\omega)$ (with $g(\omega) = 0$ for $\omega < 0$) is a slowly varying function of frequency, as compared to the line-widths of the system resonances. We also define $\hat{\varphi} = \hat{\Phi}_L/\Phi_{\rm zpf}$. Using Eq. (I9), the Heisenberg equation of motion for $\hat{b}_\omega$ becomes

$$\dot{\hat{b}}_\omega = -i\omega\hat{b}_\omega - g(\omega)\,\hat{\varphi}\,. \tag{J1}$$

By expanding the operator $\hat{\varphi}$, using the eigenstates of the interacting system $\{|i\rangle\}$ and defining $\hat{P}_{ij} = |i\rangle\langle j|$, we obtain:

$$\hat{\varphi} = \sum_{i,j} \varphi_{ij} \hat{P}_{ij}(t)\,.$$

The solution of Eq. (J1) can be expressed in two different ways; depending if we choose to integrate using the input initial conditions at $t = t_0$ or the input initial conditions at $t = t_1$, with $t_0 \ll t_1$, and $t_0 < t < t_1$. By integrating Eq. (J1), the two solutions are, respectively,

$$\hat{b}_\omega(t) = e^{-i\omega(t-t_0)}\hat{b}_\omega(t_0) - \sum_{i,j} g(\omega_{ji})\,\varphi_{ij} \int_{t_0}^{t} dt' e^{-i\omega(t-t')}\hat{P}_{ij}(t')\,, \tag{J2a}$$

$$\hat{b}_\omega(t) = e^{-i\omega(t-t_1)}\hat{b}_\omega(t_1) + \sum_{i,j} g(\omega_{ji})\,\varphi_{ij} \int_{t}^{t_1} dt' e^{-i\omega(t-t')}\hat{P}_{ij}(t')\,. \tag{J2b}$$

Subtracting the solution given by Eq. (J2b) from that given by Eq. (J2a), after some algebra we obtain

$$\hat{b}^{\rm out}_\omega(t) = \hat{b}^{\rm in}_\omega(t) - \sum_{i,j} g(\omega_{ji})\,\varphi_{ij} \int_{t_0}^{t_1} dt' e^{-i\omega(t-t')}\hat{P}_{ij}(t')\,. \tag{J3}$$

In Eq. (J3) we defined the output operator as $\hat{b}^{\rm out}_\omega(t) = \exp\left[-i\omega(t-t_1)\right]\hat{b}_\omega(t_1)$ and the input operator as $\hat{b}^{\rm in}_\omega(t) = \exp\left[-i\omega(t-t_0)\right]\hat{b}_\omega(t_0)$. The positive frequency component of the output (input) vector potential operator is defined as

$$\hat{\phi}^+_{\rm out(in)}(t) = \Lambda \int_0^\infty \frac{d\omega}{\sqrt{\omega}}\ \hat{b}^{\rm out(in)}_\omega(t)\,, \tag{J4}$$

where, for the sake of simplicity, we disregarded the spatial dependence. From Eq. (J3) we obtain

$$\hat{\phi}^+_{\rm out}(t) = \hat{\phi}^+_{\rm in}(t) - \Lambda \sum_{i,j} \varphi_{ij} \int_0^\infty d\omega\, \frac{g(\omega)}{\sqrt{\omega}} \int_{t_0}^{t_1} dt' e^{-i\omega(t-t')}\hat{P}_{ij}(t')\,. \tag{J5}$$

Let us assume that $\hat{P}_{ij}(t) \approx \exp\left[-i\omega_{ji}t\right]\hat{P}_{ij}(0)$, perform the limits $t_0 \to -\infty$ and $t_1 \to \infty$, consider $g(\omega)$ and $A(\omega)$ slowly varying functions of ω around the value ω_{ji} (i.e., approximately constant respect to the linewidth), and use the relation

$$\int_{-\infty}^{\infty} dt' e^{-i(\omega_{ji}-\omega)t'} = 2\pi\delta(\omega-\omega_{ji})\,.$$

Observing that only those terms oscillating with frequency $\omega_{ji} > 0$ can give a nonzero contribution (owing to the factor $\delta(\omega-\omega_{ji})$ with $\omega > 0$) and extending the integration in ω, we have for $i < j$:

$$\begin{aligned}\int_0^\infty d\omega \frac{g(\omega)}{\sqrt{\omega}} \int_{t_0}^{t_1} dt' e^{-i\omega(t-t')}\hat{P}_{ij}(t') &\to \frac{g(\omega_{ji})}{\sqrt{\omega_{ji}}} \int_{-\infty}^{\infty} dt'\, \hat{P}_{ij}(t') \int_{-\infty}^{\infty} d\omega e^{-i\omega(t-t')} \\ &= 2\pi \frac{g(\omega_{ji})}{\sqrt{\omega_{ji}}} \hat{P}_{ij}(t)\,.\end{aligned} \tag{J6}$$

Using Eq. (J6) and inserting the result in Eq. (J5), we obtain

$$\hat{\phi}^+_{\rm out}(t) = \hat{\phi}^+_{\rm in}(t) - 2\pi\Lambda \sum_{i<j} \frac{g(\omega_{ji})}{\sqrt{\omega_{ji}}} \varphi_{ij}\hat{P}_{ij}(t)\,. \tag{J7}$$

Note that $g(\omega_{ji})$ is different from zero only for $\omega_{ji} > 0$ (hence for $i < j$). We now also calculate the output voltage operator using the relation $\hat{V}^+_{\rm out}(t) = \dot{\hat{\phi}}^+_{\rm out}(t)$. From Eq. (J7),

$$\hat{V}^+_{\rm out}(t) = \hat{V}^+_{\rm in}(t) - 2\pi\Lambda \sum_{i<j} \frac{g(\omega_{ji})}{\sqrt{\omega_{ji}}} \varphi_{ij}\dot{\hat{P}}_{ij}(t)\,, \tag{J8}$$

which can be expressed as

$$\hat{V}^+_{\rm out}(t) = \hat{V}^+_{\rm in}(t) - K\,\hat{V}^+_L(t)\,, \tag{J9}$$

where $K = 2\pi\alpha\Lambda^2/(\hbar v)$, and

$$\hat{V}_L^+ = \Phi_{\rm zpf} \sum_{i<j} \varphi_{ij} \dot{\hat{P}}_{ij}(t)\,.$$

Notice that when the oscillator interacts in the USC regime with a qubit, $\hat{V}_L^+$ cannot be expanded in terms of the destruction photon operator only, independently on the chosen gauge. It also contains contributions from the photon creation operator $\hat{a}^\dagger$.

We observe that an analogous input-output theory can be developed for optical cavities interacting with a matter system in the USC regime [35, 69]. In the presence of systems interacting quite strongly with thermal reservoirs, this approach can be improved using ab-initio approaches [70] or introducing quasinormal modes [63].

Acknowledgments

A.S., D.Z., and S.H. acknowledge RIKEN for its hospitality, O.D. acknowledges the University of Messina for its hospitality, D.Z. acknowledges the support by the Spanish Ministerio de Ciencia, Innovaciòn y Universidades within project MAT2017-88358-C3-1-R, the Aragòn Government project Q-MAD, EU-QUANTERA project SUMO and the Fundaciòn BBVA. S.H. acknowledges funding from the Natural Sciences and Engineering Research Council of Canada and the Canadian Foundation for Innovation. F.N. is supported in part by the: MURI Center for Dynamic Magneto-Optics via the Air Force Office of Scientific Research (AFOSR) (FA9550-14-1-0040), Army Research Office (ARO) (Grant No. Grant No. W911NF-18-1-0358), Asian Office of Aerospace Research and Development (AOARD) (Grant No. FA2386-18-1-4045), Japan Science and Technology Agency (JST) (via the Q-LEAP program, and the CREST Grant No. JPMJCR1676), Japan Society for the Promotion of Science (JSPS) (JSPS-RFBR Grant No. 17-52-50023, and JSPS-FWO Grant No. VS.059.18N), the RIKEN-AIST Challenge Research Fund, the Foundational Questions Institute (FQXi), and the NTT PHI Laboratory.

[1] A. F. Kockum, A. Miranowicz, S. De Liberato, S. Savasta, and F. Nori, "Ultrastrong coupling between light and matter," Nat. Rev. Phys. **1**, 19–40 (2019).

[2] P. Forn-Díaz, L. Lamata, E. Rico, J. Kono, and E. Solano, "Ultrastrong coupling regimes of light-matter interaction," Rev. Mod. Phys. **91**, 025005 (2019).

[3] A. Bayer, M. Pozimski, S. Schambeck, D. Schuh, R. Huber, D. Bougeard, and C. Lange, "Terahertz light-matter interaction beyond unity coupling strength," Nano Lett. **17**, 6340 (2017).

[4] F. Yoshihara, T. Fuse, S. Ashhab, K. Kakuyanagi, S. Saito, and K. Semba, "Superconducting qubit-oscillator circuit beyond the ultrastrong-coupling regime," Nat. Phys. **13**, 44–47 (2017).

[5] R. Chikkaraddy, B. de Nijs, F. Benz, S. J. Barrow, O. A. Scherman, E. Rosta, A. Demetriadou, P. Fox, O. Hess, and J. J. Baumberg, "Single-molecule strong coupling at room temperature in plasmonic nanocavities," Nature **535**, 127–130 (2016).

[6] A. Bisht, J. Cuadra, M. Wersäll, A. Canales, T. J. Antosiewicz, and T. Shegai, "Collective strong light-matter coupling in hierarchical microcavity-plasmon-exciton systems," Nano Lett. **19**, 189–196 (2018).

[7] P.-H. Ho, D. B. Farmer, G. S. Tulevski, S.-J. Han, D. M. Bishop, L. M. Gignac, J. Bucchignano, P. Avouris, and A. L. Falk, "Intrinsically ultrastrong plasmon–exciton interactions in crystallized films of carbon nanotubes," Proc. Natl. Acad. Sci. **115**, 12662–12667 (2018).

[8] D. Ballester, G. Romero, J. J. García-Ripoll, F. Deppe, and E. Solano, "Quantum simulation of the ultrastrong-coupling dynamics in circuit quantum electrodynamics," Phys. Rev. X **2**, 021007 (2012).

[9] D. De Bernardis, P. Pilar, T. Jaako, S. De Liberato, and P. Rabl, "Breakdown of gauge invariance in ultrastrong-coupling cavity QED," Phys. Rev. A **98**, 053819 (2018).

[10] A. Stokes and A. Nazir, "Gauge ambiguities imply Jaynes-Cummings physics remains valid in ultrastrong coupling QED," Nat. Commun. **10**, 499 (2019).

[11] O. Di Stefano, A. Settineri, V. Macrì, L. Garziano, R. Stassi, S. Savasta, and F. Nori, "Resolution of gauge ambiguities in ultrastrong-coupling cavity QED," Nat. Phys. **15**, 803 (2019).

[12] W. E. Lamb, "Fine structure of the hydrogen atom. III," Phys. Rev. **85**, 259–276 (1952).

[13] W. P. Healy, "Comment onelectric dipole interaction in quantum optics," Phys. Rev. A **22**, 2891–2893 (1980).

[14] E. A. Power and T. Thirunamachandran, "Comment on electric dipole interaction in quantum optics," Phys. Rev. A **22**, 2894–2895 (1980).

[15] W. E. Lamb, R. R. Schlicher, and M. O. Scully, "Matter-field interaction in atomic physics and quantum optics," Phys. Rev. A **36**, 2763–2772 (1987).

[16] C. Cohen-Tannoudji, J. Dupont-Roc, and G. Grynberg, "Photons and atoms-introduction to quantum electrodynamics," Wiley-VCH (1997).

[17] S. Ashhab and F. Nori, "Qubit-oscillator systems in the ultrastrong-coupling regime and their potential for preparing nonclassical states," Phys. Rev. A **81**, 042311 (2010).

[18] R. Stassi, A. Ridolfo, O. Di Stefano, M. J. Hartmann, and S. Savasta, "Spontaneous conversion from virtual to real photons in the ultrastrong-coupling regime," Phys. Rev. Lett. **110**, 243601 (2013).

[19] S. De Liberato, "Virtual photons in the ground state of a dissipative system," Nat. Commun. **8**, 1465 (2017).

[20] O. Di Stefano, R. Stassi, L. Garziano, A. F. Kockum, S. Savasta, and F. Nori, "Feynman-diagrams approach to the quantum Rabi model for ultrastrong cavity QED: stimulated emission and reabsorption of virtual particles dressing a physical excitation," New J. Phys. **19**, 053010 (2017).

[21] C. Ciuti, G. Bastard, and I. Carusotto, "Quantum vacuum properties of the intersubband cavity polariton field," Phys. Rev. B **72**, 115303 (2005).

[22] S. De Liberato, C. Ciuti, and I. Carusotto, "Quantum vacuum radiation spectra from a semiconductor microcavity with a time-modulated vacuum Rabi frequency," Phys. Rev. Lett. **98**, 103602 (2007).

[23] L. Garziano, A. Ridolfo, R. Stassi, O. Di Stefano, and S. Savasta, "Switching on and off of ultrastrong light-matter interaction: Photon statistics of quantum vacuum radiation," Phys. Rev. A **88**, 063829 (2013).

[24] L. Garziano, R. Stassi, V. Macrì, A. F. Kockum, S. Savasta, and F. Nori, "Multiphoton quantum Rabi oscillations in ultrastrong cavity QED," Phys. Rev. A **92**, 063830 (2015).

[25] G. Falci, A. Ridolfo, P. G. Di Stefano, and E. Paladino, "Ultrastrong coupling probed by coherent population transfer," Sci. Rep. **9**, 9249 (2019).

[26] E. Sánchez-Burillo, L. Martín-Moreno, J. J. García-Ripoll, and D. Zueco, "Single photons by quenching the vacuum," Phys. Rev. Lett. **123** (2019).

[27] A. Stokes and A. Nazir, "Ultrastrong time-dependent light-matter interactions are gauge-relative," arXiv:1902.05160 (2019).

[28] R. J. Glauber, "The quantum theory of optical coherence," Phys. Rev. **130**, 2529–2539 (1963).

[29] S. Haroche and J.-M. Raimond, *Exploring the Quantum* (Oxford University Press, 2006).

[30] X. Gu, A. F. Kockum, A. Miranowicz, Y.-X. Liu, and F. Nori, "Microwave photonics with superconducting quantum circuits," Phys. Rep. **718-719**, 1–102 (2017).

[31] M. Babiker and R. Loudon, "Derivation of the Power-Zienau-Woolley Hamiltonian in quantum electrodynamics by gauge transformation," Proc. R. Soc. Lond. A **385**, 439–460 (1983).

[32] J. M. Wylie and J. E. Sipe, "Quantum electrodynamics near an interface," Phys. Rev. A **30**, 1185–1193 (1984).

[33] M. Wubs, L. G. Suttorp, and A. Lagendijk, "Multiple-scattering approach to interatomic interactions and superradiance in inhomogeneous dielectrics," Phys. Rev. A **70**, 053823 (2004).

[34] O. Di Stefano, A. F. Kockum, A. Ridolfo, S. Savasta, and F. Nori, "Photodetection probability in quantum systems with arbitrarily strong light-matter interaction," Sci. Rep. **8**, 17825 (2018).

[35] A. Ridolfo, M. Leib, S. Savasta, and M. J. Hartmann, "Photon blockade in the ultrastrong coupling regime," Phys. Rev. Lett. **109**, 193602 (2012).

[36] L. Garziano, A. Ridolfo, S. De Liberato, and S. Savasta, "Cavity QED in the ultrastrong coupling regime: Photon bunching from the emission of individual dressed qubits," ACS Photonics **4**, 2345 (2017).

[37] M. Brune, S. Haroche, V. Lefevre, J. M. Raimond, and N. Zagury, "Quantum nondemolition measurement of small photon numbers by rydberg-atom phase-sensitive detection," Phys. Rev. Lett. **65**, 976–979 (1990).

[38] M. Brune, S. Haroche, J. M. Raimond, L. Davidovich, and N. Zagury, "Manipulation of photons in a cavity by dispersive atom-field coupling: Quantum-nondemolition measurements and generation of "schrödinger cat" states," Phys. Rev. A **45**, 5193–5214 (1992).

[39] J. A. Grangier, P.and Levenson and J.-P. Poizat, "Quantum non-demolition measurements in optics," Nature **396**, 537 (1998).

[40] M. Boissonneault, J. M. Gambetta, and A. Blais, "Dispersive regime of circuit QED: Photon-dependent qubit dephasing and relaxation rates," Phys. Rev. A **79**, 013819 (2009).

[41] F. Helmer, M. Mariantoni, E. Solano, and F. Marquardt, "Quantum nondemolition photon detection in circuit qed and the quantum zeno effect," Phys. Rev. A **79**, 052115 (2009).

[42] B. Peaudecerf, T. Rybarczyk, S. Gerlich, S. Gleyzes, J. M. Raimond, S. Haroche, I. Dotsenko, and M. Brune, "Adaptive quantum nondemolition measurement of a photon number," Phys. Rev. Lett. **112**, 080401 (2014).

[43] A. Blais, R.-S. Huang, A. Wallraff, S. M. Girvin, and R. J. Schoelkopf, "Cavity quantum electrodynamics for superconducting electrical circuits: An architecture for quantum computation," Phys. Rev. A **69**, 062320 (2004).

[44] D. Zueco, G. M. Reuther, S. Kohler, and P. Hänggi, "Qubit-oscillator dynamics in the dispersive regime: Analytical theory beyond the rotating-wave approximation," Phys. Rev. A **80**, 033846 (2009).

[45] C. S. Muñoz, F. Nori, and S. De Liberato, "Resolution of superluminal signalling in non-perturbative cavity quantum electrodynamics," Nat. Commun. **9**, 1924 (2018).

[46] A. Messiah, *Quantum Mechanics*, Dover books on physics (Dover Publications, 1999).

[47] F. Assemat, D. Grosso, A. Signoles, A. Facon, I. Dotsenko, S. Haroche, J. M. Raimond, M. Brune, and S. Gleyzes, "Quantum rabi oscillations in coherent and in mesoscopic cat field states," Phys. Rev. Lett. **123**, 143605 (2019).

[48] J. Q. You and Franco Nori, "Atomic physics and quantum optics using superconducting circuits," Nature **474**, 589–597 (2011).

[49] G. Wendin, "Quantum information processing with superconducting circuits: a review," Rep. Prog. Phys. **80**, 106001 (2017).

[50] T. Niemczyk, F. Deppe, H. Huebl, E. P. Menzel, F. Hocke, M. J. Schwarz, J. J. Garcia-Ripoll, D. Zueco, T. Hümmer, E. Solano, A. Marx, and R. Gross, "Circuit quantum electrodynamics in the ultrastrong-coupling regime," Nat. Phys. **6**, 772–776 (2010).

[51] P. Forn-Díaz, J. Lisenfeld, D. Marcos, J. J. García-Ripoll, E. Solano, C. J. P. M. Harmans, and J. E. Mooij, "Observation of the Bloch-Siegert shift in a qubit-oscillator system in the ultrastrong coupling regime," Phys. Rev. Lett. **105**, 237001 (2010).

[52] D. De Bernardis, T. Jaako, and P. Rabl, "Cavity quantum electrodynamics in the nonperturbative regime," Phys. Rev. A **97**, 043820 (2018).

[53] V. E. Manucharyan, A. Baksic, and C. Ciuti, "Resilience of the quantum Rabi model in circuit QED," J. Phys. A: Math. Theor. **50**, 294001 (2017).

[54] R. Stassi and F. Nori, "Long-lasting quantum memories: Extending the coherence time of superconducting artificial atoms in the ultrastrong-coupling regime," Phys. Rev. A **97**, 033823 (2018).

[55] G. M. Andolina, F. M. D. Pellegrino, V. Giovannetti, A. H. MacDonald, and M. Polini, "Cavity quantum electrodynamics of strongly correlated electron systems: A no-go theorem for photon condensation," Phys. Rev. B **100**, 121109 (2019).

[56] N. M. Sundaresan, Y. Liu, D. Sadri, L. J. Szőcs, D. L. Underwood, M. Malekakhlagh, H. E. Türeci, and A. A. Houck, "Beyond strong coupling in a multimode cavity," Phys. Rev. X **5**, 021035 (2015).

[57] M. Malekakhlagh, A. Petrescu, and H. E. Türeci, "Cutoff-free circuit quantum electrodynamics," Phys. Rev. Lett. **119**, 073601 (2017).

[58] A. F. Kockum, V. Macrì, L. Garziano, S. Savasta, and F. Nori, "Frequency conversion in ultrastrong cavity QED," Sci. Rep. **7**, 5313 (2017).

[59] P. Forn-Díaz, J. J. García-Ripoll, B. Peropadre, J.-L. Orgiazzi, M. A. Yurtalan, R. Belyansky, C. M. Wilson, and A. Lupascu, "Ultrastrong coupling of a single artificial atom to an electromagnetic continuum in the nonperturbative regime," Nat. Phys. **13**, 39–43 (2017).

[60] C. K. Law, "Interaction between a moving mirror and radiation pressure: A Hamiltonian formulation," Phys. Rev. A **51**, 2537 (1995).

[61] V. Macrì, A. Ridolfo, O. Di Stefano, A. F. Kockum, F. Nori, and S. Savasta, "Nonperturbative dynamical Casimir effect in optomechanical systems: Vacuum Casimir-Rabi splittings," Phys. Rev. X **8**, 011031 (2018).

[62] E. A. Power and T. Thirunamachandran, "Quantum electrodynamics in a cavity," Phys. Rev. A **25**, 2473–2484 (1982).

[63] S. Franke, S. Hughes, M. K. Dezfouli, P. T. Kristensen, K. Busch, A. Knorr, and M. Richter, "Quantization of quasinormal modes for open cavities and plasmonic cavity quantum electrodynamics," Phys. Rev. Lett. **122**, 213901 (2019).

[64] E. del Valle, A. Gonzalez-Tudela, F. P. Laussy, C. Tejedor, and M. J. Hartmann, "Theory of frequency-filtered and time-resolved n-photon correlations," Phys. Rev. Lett. **109**, 183601 (2012).

[65] C. Schäfer, M. Ruggenthaler, V. Rokaj, and A. Rubio, "Relevance of the quadratic diamagnetic and self-polarization terms in cavity quantum electrodynamics," arXiv preprint

arXiv:1911.08427 (2019).

[66] R. Bianchetti, S. Filipp, M. Baur, J. M. Fink, M. Göppl, P. J. Leek, L. Steffen, A. Blais, and A. Wallraff, "Dynamics of dispersive single-qubit readout in circuit quantum electrodynamics," Phys. Rev. A **80**, 043840 (2009).

[67] S. Haroche, "Nobel lecture: Controlling photons in a box and exploring the quantum to classical boundary," Rev. Mod. Phys. **85**, 1083–1102 (2013).

[68] B. Peropadre, D. Zueco, D. Porras, and J. J. García-Ripoll, "Nonequilibrium and nonperturbative dynamics of ultrastrong coupling in open lines," Phys. Rev. Lett. **111**, 243602 (2013).

[69] M. Bamba, K. Inomata, and Y. Nakamura, "Superradiant phase transition in a superconducting circuit in thermal equilibrium," Phys. Rev. Lett. **117**, 173601 (2016).

[70] D. Lentrodt and J. Evers, "Ab initio few-mode theory for quantum potential scattering problems," (2018), arXiv:1812.08556.

6.3 Gauge invariance of the Dicke and Hopfield models

Gauge invariance of the Dicke and Hopfield models

Luigi Garziano,[1] Alessio Settineri,[2] Omar Di Stefano,[1,2] Salvatore Savasta,[2,*] and Franco Nori[1,3]
[1]*Theoretical Quantum Physics Laboratory, RIKEN Cluster for Pioneering Research, Wako-shi, Saitama 351-0198, Japan*
[2]*Dipartimento di Scienze Matematiche e Informatiche, Scienze Fisiche e Scienze della Terra, Università di Messina, I-98166 Messina, Italy*
[3]*Physics Department, The University of Michigan, Ann Arbor, Michigan 48109-1040, USA*

(Received 18 February 2020; revised 27 July 2020; accepted 3 August 2020; published 26 August 2020)

The Dicke model, which describes the dipolar coupling between N two-level atoms and a quantized electromagnetic field, seemingly violates gauge invariance in the presence of ultrastrong light-matter coupling, a regime that is now experimentally accessible in many physical systems. Specifically, it has been shown that, while the two-level approximation can work well in the dipole gauge, the Coulomb gauge fails to provide the correct spectra in the ultrastrong coupling regime. Here we show that, taking into account the nonlocality of the atomic potential induced by the two-level approximation, gauge invariance is fully restored for arbitrary interaction strengths, even in the $N \to \infty$ limit. Finally, we express the Hopfield model, a general description based on the quantization of a linear dielectric medium, in a manifestly gauge-invariant form, and show that the Dicke model in the dilute regime can be regarded as a particular case of the more general Hopfield model.

DOI: 10.1103/PhysRevA.102.023718

I. INTRODUCTION

Models describing the interaction between one or few modes of the electromagnetic field in a resonator and individual or ensembles of few level atoms are a cornerstone of quantum optics. The simplest examples are the quantum Rabi [1–3] and the Dicke Hamiltonians [4–7] describing, respectively, the interaction of a single-mode bosonic field with a two-level atom, and with an ensemble of N two-level atoms. Their simplified version obtained after the rotating wave approximation are the Jaynes-Cummings and Tavis-Cummings models [8,9], respectively.

Recently, it has been argued that truncations of the atomic Hilbert space, to obtain a two-level description, violate the gauge principle [10–12]. Such violations become particularly relevant in the case of ultrastrong (USC) light-matter coupling, a regime, now experimentally accessible in many physical systems, in which the coupling strength is comparable to the transition energies in the system [13,14]. In particular, it has been shown that, while in the electric dipole gauge the two-level approximation can be performed as long as the Rabi frequency remains much smaller than the energies of all higher-lying levels, it can drastically fail in the Coulomb gauge, even for systems with an extremely anharmonic spectrum [11]. The Dicke Hamiltonian, a model of key importance for the description of collective effects in quantum optics, shares analogous worrying problems, not only in the presence of a small number N of atoms, but also in the so-called dilute regime, where $N \to \infty$, while the coupling strength between the field and the resulting collective excitations remains finite [11]. Examples of realizations of the Dicke model in the USC dilute regime include intersubband organic molecules [15–20], intersubband polaritons [21–24], and Landau polaritons [25–29].

In quantum electrodynamics, the choice of gauge influences the form of light-matter interactions. However, gauge invariance implies that all physical results should be independent of this formal choice. As a consequence, the observation that the quantum Rabi and Dicke model provide gauge-dependent energy spectra casts doubts on the reliability of these widespread descriptions.

The source of these gauge violations has been recently identified and a general method for the derivation of light-matter Hamiltonians in truncated Hilbert spaces, able to produce gauge-invariant physical results, even for extreme light-matter interaction regimes, has been proposed [30]. According to the gauge principle, the coupling of the matter system with the electromagnetic field is introduced by the minimal replacement rule $\hat{\mathbf{p}} \to \hat{\mathbf{p}} - q\hat{\mathbf{A}}$, where $\hat{\mathbf{p}}$ is the momentum of an effective particle, $\hat{\mathbf{A}}$ is the vector potential of the field, and q is the charge. It has been known for decades that approximations in the description of a quantum system with space truncation can give rise to *nonlocal* potentials which can always be expressed as potentials depending on *both* position and momenta: $V(\mathbf{r}, \hat{\mathbf{p}})$ [31]. In these cases, in order not to ruin the gauge principle, the minimal coupling replacement has to be applied not only to the kinetic energy of the particles in the system, but also to the nonlocal potentials in the effective Hamiltonian of the matter system [31–33]. Once this procedure is applied, it is possible to obtain gauge-invariant models, even in the presence of extreme light-matter interaction regimes [30,34]. This method has been applied to obtain a quantum Rabi model satisfying the gauge principle [30]. In the following, we will refer to models not violating gauge invariance as gauge-invariant (GI) models, even if the form of the Hamiltonians change after a gauge transformation. The generalization to N two-level systems (Dicke model) is

*Corresponding author: ssavasta@unime.it

briefly discussed in the Supplemental Material of Ref. [34]. The resulting GI quantum Rabi and Dicke Hamiltonians in the Coulomb gauge differ significantly in form from the standard ones and both contain field operators to *all* orders. A recent overview of these gauge issues in TLSs can be found in Ref. [35].

Here, after revisiting the derivation of the GI Dicke model, we derive the corresponding dilute regime, also known as the thermodynamic limit [36–39]. In such a limit, applying the Holstein-Primakoff transformation [40], the standard Dicke Hamiltonians in the dipole and in the Coulomb gauges, both bilinear in the bosonic operators, are obtained (see, e.g., Ref. [36]). Such Hamiltonian can be diagonalized exactly, using a multimode Bogoliubov transformation. However, it has been shown that the effective Hamiltonians in the Coulomb and dipole gauge give rise to polariton eigenfrequencies (modes) which can significantly differ for large coupling strengths [11]. Although the form of the gauge-invariant Dicke model contains field operators to all orders and appears very different from a bilinear Hamiltonian, we show that, in the thermodynamic limit, a bilinear Hamiltonian very similar to the standard one is obtained. Specifically, the resulting Dicke Hamiltonian in the Coulomb gauge only differs from the standard one for the coefficient of the diamagnetic term (proportional to $\hat{\mathbf{A}}^2$). However, we show that such a difference is sufficient to restore gauge invariance.

Another widespread description of the interaction between the quantized electromagnetic field and collective excitations is the Hopfield model [41]. This model was initially introduced to describe the interaction of the electromagnetic field with a harmonic resonant polarization density of a three-dimensional (3D) dielectric crystal. Nowadays, it is used to describe the interaction between free or confined light and different kinds of collective excitations, such as optical phonons, excitons in nanostructures, magnons, and plasmonic crystals, which can be described as bosonic fields. We compare the (GI) Dicke and the Hopfield models and apply to the latter the concepts derived for obtaining the first. In doing so, we provide a method to derive in a simple way manifestly gauge-invariant Hopfield models, having only knowledge about the matter polarization field.

II. DICKE MODEL WITH FINITE NUMBER OF DIPOLES

For the following analysis, we consider a generic setting as shown in Fig. 1, where a finite number of electric dipoles are coupled to the single mode of the electromagnetic field in a resonator (see, e.g., Ref. [11]). The dipoles can be modeled as effective particles of mass m in potentials $V(x_i)$, where x_i is the separation between the charges q and $-q$ of the ith dipole. In the absence of any dipole-dipole interaction, and of the interaction with the electromagnetic field, the Hamiltonian describing a system of N effective particles can be written as $\hat{H}_0^{(N)} = \sum_{i=1}^{N} \hat{H}_0^{(i)}$, where

$$\hat{H}_0^{(i)} = \frac{\hat{p}_i^2}{2m} + V(x_i). \tag{1}$$

Assuming that the two lowest-energy levels ($\hbar\omega_0$ and $\hbar\omega_1$) are well separated by the higher-energy levels and considering the system of dipoles interacting with a field mode of frequency $\omega_c \sim \omega_x$, where $\omega_x \equiv \omega_{1,0}$ (here $\omega_{i,j} \equiv \omega_i - \omega_j$), we can truncate the Hibert space of each dipole by considering as a basis only the two lowest-energy levels. In this case, each dipole can be modeled as a pseudospin, and the Hamiltonian describing the system of N dipoles, in the absence of interaction with the electromagnetic field, can be written in terms of collective angular momentum operators $\hat{J}_\alpha = (1/2)\sum_{i=1}^{N} \hat{\sigma}_\alpha^{(i)}$ ($\alpha = x, y, z$) as

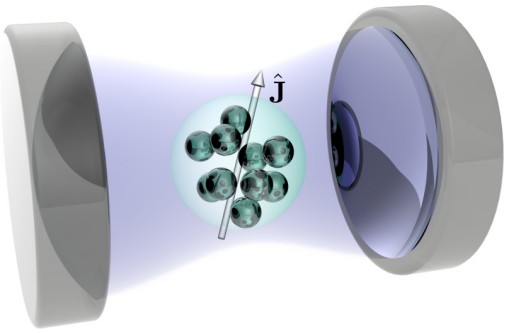

FIG. 1. Sketch of an optical resonator coupled to N identical, distinguishable, quantum emitters. We consider two-level emitters that can be described by means of collective operators $\hat{J}_\alpha$ with $\alpha \equiv \{x, y, z\}$, which obey the angular momentum commutation relations (with cooperation number $j = N/2$). These atoms interact with a bosonic mode of frequency ω_c via a dipole interaction. The resulting normalized collective coupling strength scales $\propto\sqrt{N}$.

$$\hat{\mathcal{H}}_0^{(N)} = \hat{\Pi}\hat{H}_0^{(N)}\hat{\Pi} = \hbar\omega_x(\hat{J}_z + j), \tag{2}$$

where $\hat{\sigma}_\alpha^{(i)}$ are Pauli matrices and $j = N/2$, and here $\hat{\Pi}$ is the operator projecting each effective particle into a two-level space. Notice that, after the projection, the operator $\hat{\Pi}$ represents the identity operator for the linear space constituted by the tensor product of all the N two-level spaces. Throughout this article we will use calligraphic symbols (as, for example, $\hat{\mathcal{H}}_0^{(N)}$) to indicate quantum operators in truncated Hilbert spaces. Notice that the ground state of the system corresponds to all the spins in their ground state: $|j, j_z = -j\rangle$, and it is an eigenstate of $\hat{\mathcal{H}}_0^{(N)}$ with eigenenergy equal to zero. When all the dipoles are in their excited state, the corresponding collective state $|j, j_z = j\rangle$ has energy $\hbar\omega_x N$.

A. Quantum Dicke model in the Coulomb gauge

By applying the minimal coupling replacement, the Hamiltonian for the system constituted by N dipoles and a single-mode electromagnetic resonator in the Coulomb gauge can be written as

$$\hat{H}_{\rm cg}^{(N)} = \sum_{i=1}^{N}\left[\frac{(\hat{p}_i - q\hat{A})^2}{2m} + V(x_i)\right] + \hat{H}_c, \tag{3}$$

where $\hat{H}_c = \hbar\omega_c\hat{a}^\dagger\hat{a}$ is the bare photonic Hamiltonian including a single mode with resonance frequency ω_c and annihilation (creation) operator $\hat{a}$ ($\hat{a}^\dagger$), and $\hat{A} = A_0(\hat{a} + \hat{a}^\dagger)$ is the vector potential along the x direction with a zero-point amplitude A_0. Notice that the vector potential has been assumed to be constant in the spatial region where the dipoles are

present. This approximation can be relaxed, even maintaining the dipole approximation.

It has been shown [30,42] that the minimal coupling replacement $\hat{p} \to \hat{p} - q\hat{A}$ determining Eq. (3) can also be implemented by applying to the matter system Hamiltonian the following unitary transformation:

$$\hat{H}_{\rm cg}^{(N)} = \hat{U}_N \hat{H}_0^{(N)} \hat{U}_N^\dagger + \hat{H}_c, \tag{4}$$

where

$$\hat{U}_N = \exp\left(i \frac{q}{\hbar} \hat{A} \sum_{i=1}^{N} x_i \right). \tag{5}$$

By expanding the kinetic terms, Eq. (3) can be written as the sum of three contributions:

$$\hat{H}_{\rm cg}^{(N)} = \hat{H}_0^{(N)} + \hat{H}_c + \hat{V}_{\rm cg}^{(N)}, \tag{6}$$

where $\hat{V}_{cg} = \hat{V}_{Ap} + \hat{V}_D$ describes the interaction terms

$$\hat{V}_{Ap}^{(N)} = \hat{A} \sum_{i=i}^{N} \frac{\hat{p}_i}{m} \tag{7}$$

and

$$\hat{V}_D^{(N)} = N \frac{q^2}{2m} \hat{A}^2 = D(\hat{a} + \hat{a}^\dagger)^2, \tag{8}$$

where $D = NA_0^2 q^2/(2m)$. Using the Thomas-Reiche-Kuhn (TRK) sum rule [43], the coefficient in the diamagnetic term can be written as $q^2/2m = \sum_k \omega_{k,j} |d_{k,j}|^2/\hbar$, where $d_{k,j} = \langle \psi_k | qx | \psi_j \rangle$ are the dipole matrix elements between two energy eigenstates of the effective particle, that in the following we assume to be real quantities. The TRK sum rule has a precise physical meaning, since it expresses the fact that the paramagnetic and diamagnetic contributions to the physical current-current response function cancel in the uniform static limit, which is a consequence of gauge invariance [44–46]. The physical current operator, corresponding to the Hamiltonian in Eq. (3), is

$$\hat{J}_{\rm phys} = \frac{\delta \hat{H}_{\rm cg}}{\delta \hat{A}} = q \sum_{i=1}^{N} \frac{\hat{p}_i}{m} + N \frac{q^2}{m} \hat{A}, \tag{9}$$

and the corresponding current-current response function in the uniform static limit is proportional to [46]

$$-2N \sum_k \omega_{k,j} |d_{k,j}|^2 + N \frac{\hbar q^2}{m} = 0. \tag{10}$$

This relationship expresses the fact that the paramagnetic (first term on the left-hand side) and diamagnetic (second term on the left-hand side) contributions to the physical current-current response function cancel out in the uniform and static limit [46]. It is interesting to observe that the TRK sum rule remains valid even in the presence of interatomic potentials [46]. Very recently, a TRK sum rule for the electromagnetic field coordinates, which holds even in the presence of USC interaction with a matter system, has been proposed [47].

Defining the adimensional coupling strengths $\eta_k = A_0 d_{k,0}/\hbar$, the diamagnetic coefficient can be written as

$$D = N\hbar \sum_k \omega_{k,0} \eta_k^2. \tag{11}$$

The standard Dicke Hamiltonian in the Coulomb gauge can be obtained from Eq. (3) truncating the Hilbert space of each dipole to include only two energy levels:

$$\hat{\mathcal{H}}_{\rm cg}^{\prime(N)} = \hat{\Pi} \hat{H}_{\rm cg}^{(N)} \hat{\Pi} = \omega_c \hat{a}^\dagger \hat{a} + \hbar\omega_x (\hat{J}_z + j) + 2\hbar\omega_x \eta (\hat{a}^\dagger + \hat{a}) \hat{J}_y + j \frac{q^2 \mathcal{A}_0^2}{m} (\hat{a}^\dagger + \hat{a})^2, \tag{12}$$

where $\eta \equiv \eta_1 = A_0 d_{1,0}/\hbar$, and the relation $i\hbar p_i/m = [x_i, H_0^{(i)}]$ has been used.

It has been shown that the two-level truncation for the effective particles ruins the gauge invariance [10]. In particular, it has been argued that the Coulomb-gauge Hamiltonian in Eq. (12) is not related by a unitary transformation (hence it is not gauge equivalent) to the corresponding Hamiltonian in the dipole gauge. Closely related developments have been presented in Refs. [11,12,30]. We will discuss this issue in detail below. Here we limit to showing that the Hamiltonian in Eq. (12) does not satisfy the gauge principle and how to solve this problem following Ref. [30]. This Hamiltonian can be obtained, projecting in two-level spaces the full Hamiltonian in Eq. (3). Using Eq. (4)

$$\hat{\mathcal{H}}_{\rm cg}^{\prime(N)} = \hat{\Pi} \hat{U}_N \sum_i \left[\frac{\hat{p}_i^2}{2m} + V(x_i) \right] \hat{U}_N^\dagger \hat{\Pi} + \hbar\omega_c \hat{a}^\dagger \hat{a}. \tag{13}$$

By applying the unitary operator to the kinetic and potential terms separately, observing that $[V(x_i), \hat{U}_N] = 0$, we obtain

$$\hat{\mathcal{H}}_{\rm cg}^{\prime(N)} = \hat{\Pi} \sum_i \frac{(\hat{p}_i - q\hat{A})^2}{2m} \hat{\Pi} + \hat{\Pi} \sum_i V(x_i) \hat{\Pi} + \hbar\omega_c \hat{a}^\dagger \hat{a}. \tag{14}$$

It has been shown that truncating the Hilbert space transforms a local operator like $V(x_i)$ into a nonlocal one which can be expressed as a function of both position and momentum [31]: $\hat{\Pi} V(x_i) \hat{\Pi} = W(x_i, \hat{p}_i)$. Therefore, the Hamiltonian in Eq. (14) contains operators $[W(x_i, \hat{p}_i)]$ depending also on the particle momenta, where the minimal coupling replacement, prescribed by the gauge principle, has not been applied.

In particular, we observe that, for a local potential, we have $\langle x' | V | x \rangle = V(x) \delta(x - x')$. By using the closure relation, it can be expressed as $V(x, x') = \sum_{n,n'} V_{n.n'} \psi_n(x) \psi_{n'}^*(x')$, where $\psi_n(x) = \langle x | \psi_n \rangle$ and $\{|\psi_n\rangle\}$ constitute a complete orthonormal basis. Notice that the Dirac delta function can be reconstructed only by keeping all the infinite vectors of the basis. Hence any truncation of the complete basis can transform a local potential into a nonlocal one. The action of the resulting nonlocal potential on a generic state $|\psi\rangle$ in the position representation is

$$\langle x | V | \psi \rangle = \int dx' \langle x | V | x' \rangle \langle x' | \psi \rangle = \int dx' V(x, x') \psi(x'). \tag{15}$$

Using the translation operator property, $\langle x | \hat{T}_a | \psi \rangle = \exp[i(a - x)\hat{p}] \psi(x)$, we obtain from Eq. (15)

$$\langle x | V | \psi \rangle = \int dx' V(x, x') e^{i(a-x)\hat{p}} \psi(x) = V(x, \hat{p}) \psi(x). \tag{16}$$

As an example, Fig. 2 shows as a local potential $V(x)$ (in this case a double-well potential) evolves into a nonlocal one when increasing the truncation of the Hilbert space. Here n indicates

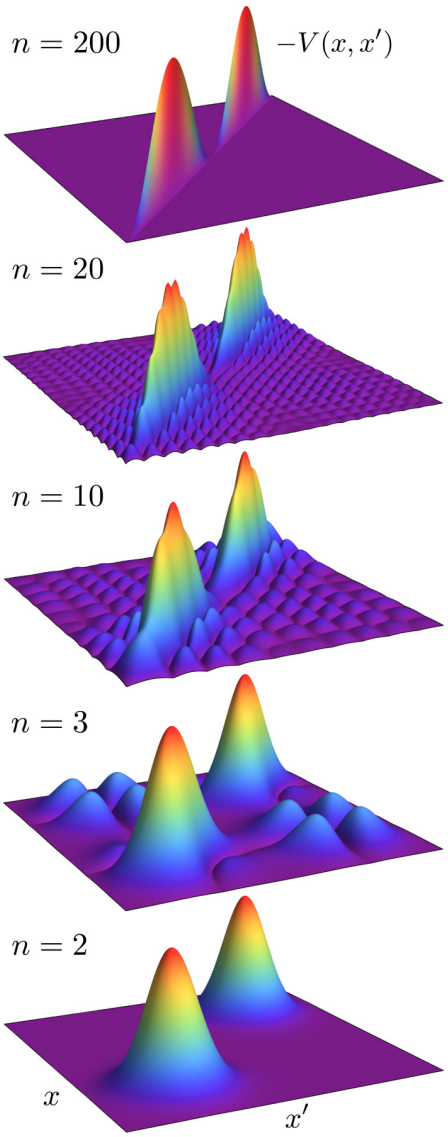

FIG. 2. Example of nonlocal potentials $V(x, x')$ originating from a local potential $V(x)$ (in this case a double well) after the truncation of the Hilbert space to the lowest n energy levels. Decreasing the number of levels, the degree of nonlocality increases. We considered the potential $V(\tilde{x}) = E_k[-(\beta/2)\tilde{x}^2 + (\gamma/4)\tilde{x}^4]$, where $\tilde{x}$ is a dimensionless coordinate [11], $\beta = 3.95$ and $\gamma = 2.08$ are dimensionless coefficients, and E_k is the kinetic-energy coefficient: $\hat{H}_0 = E_k\,\hat{\tilde{p}}^2/2 + V(\tilde{x})$. Note that only dimensionless quantities, as a function of dimensionless quantities, have been plotted and the three axes have been omitted.

the number of energy states included in the projection operator, starting from the ground state.

A formulation preserving the gauge principle can be obtained replacing in Eq. (14) the terms

$$\hat{\Pi} V(x_i)\hat{\Pi} = W(x_i, \hat{p}_i)$$

with

$$\hat{\Pi} W(x_i, \hat{p}_i - q\hat{A})\hat{\Pi}.$$

Hence this problem, arising from the truncation of the Hilbert space of the matter system, can be overcome by first applying to the matter system Hamiltonian (in the absence of interaction) $\hat{H}_0$ the projection operator $\hat{\Pi}$, and then the unitary operator $\hat{U}_N$ as follows:

$$\hat{H}_0^{(N)} \to \hat{\Pi}\hat{H}_0^{(N)}\hat{\Pi} \to \hat{U}_N\hat{\Pi}\hat{H}_0^{(N)}\hat{\Pi}\hat{U}_N^\dagger.$$

Finally, if one asks that the resulting Hamiltonian be within the truncated Hilbert space, one has to finally project:

$$\hat{U}_N\hat{\Pi}\hat{H}_0^{(N)}\hat{\Pi}\hat{U}_N^\dagger \to \hat{\Pi}\hat{U}_N\hat{\Pi}\hat{H}_0^{(N)}\hat{\Pi}\hat{U}_N^\dagger\hat{\Pi}.$$

This method is not limited to truncated two-level spaces but can be applied to any truncated Hilbert space to produce light-matter interaction Hamiltonians satisfying the gauge principle. Applying this procedure, we obtain

$$\hat{\mathcal{H}}_{\rm cg}^{(N)} = \hat{\mathcal{U}}_N\hat{\mathcal{H}}_0^{(N)}\hat{\mathcal{U}}_N^\dagger + \hbar\omega_c\hat{a}^\dagger\hat{a}, \tag{17}$$

where $\hat{\mathcal{U}}_N = \hat{\Pi}\hat{U}_N\hat{\Pi}$. Using repeatedly the properties of the identity operator $\hat{\Pi} = \hat{\Pi}^2$, we obtain

$$\hat{\mathcal{U}}_N = \exp\,[2i\eta(\hat{a} + \hat{a}^\dagger)\hat{J}_x]. \tag{18}$$

Here, once the Hilbert space is truncated, the operator Π is assumed to describe the identity operator in the truncated Hilbert space. This last procedure is essential in order to obtain unitary operators acting on $\hat{\mathcal{H}}_0$. According to the gauge principle, the coupling with the electromagnetic field has to compensate for the space- and time-dependent unitary transformations applied to the wave function of the particle. Field-dependent unitary operators can compensate for unitary transformations of the quantum state of the particle even in the presence of Hilbert space truncation. As shown in a very recent work [48], this procedure is essential to implementing the gauge principle in truncated Hilbert spaces.

The unitary transformation $\hat{\mathcal{U}}_N\hat{\mathcal{H}}_0\hat{\mathcal{U}}_N^\dagger$ describes the rotation of the system of pseudospins around the x axis by an angle $\hat{\phi} = 2\eta(\hat{a} + \hat{a}^\dagger)$. The resulting Hamiltonian is

$$\hat{\mathcal{H}}_{\rm cg}^{(N)} = \hbar\omega_c\hat{a}^\dagger\hat{a} + \hbar j\omega_x + \hbar\omega_x\{\hat{J}_z\cos[2\eta(\hat{a}^\dagger + \hat{a})] + \hat{J}_y\sin[2\eta(\hat{a}^\dagger + \hat{a})]\}. \tag{19}$$

This result shows that the occurrence of a nonlocal potential, arising from the truncation of the matter system Hilbert space, changes significantly the structure of the Coulomb-gauge interaction Hamiltonian (see, e.g., Ref. [49] for comparison). The price that one has to pay for preserving the gauge principle in such a truncated space is that the total Hamiltonian contains field operators at all orders, in contrast to the standard Coulomb gauge Hamiltonian in Eq. (12).

B. Dicke model in the dipole gauge

The Hamiltonian in the dipole gauge for a collection of N effective particles, $\hat{H}_{\rm dg}^{(N)}$, corresponds to the Power-Zienau-Woolley Hamiltonian after the dipole approximation. It can be obtained directly from the Hamiltonian in the Coulomb gauge with the electric dipole approximation Eq. (3) by means of a

gauge transformation, which is also a unitary transformation:

$$\hat{H}_{\rm dg}^{(N)} = \hat{T}_N \hat{H}_{\rm cg}^{(N)} \hat{T}_N^\dagger, \tag{20}$$

where $\hat{T}_N = \hat{U}_N^\dagger$. We obtain

$$\hat{H}_{\rm dg}^{(N)} = \hat{H}_0^{(N)} + \hat{T}_N \hat{H}_c T_N^\dagger. \tag{21}$$

Applying the Baker-Campbell-Hausdorff lemma, we have

$$\hat{H}_{\rm dg}^{(N)} = \hat{H}_0^{(N)} + \hat{H}_c + i\frac{qA_0}{\hbar}(\hat{a}^\dagger - \hat{a}) \sum_i x_i + \left(\frac{qA_0}{\hbar}\right)^2 \sum_{i,j} x_i x_j. \tag{22}$$

The standard Dicke Hamiltonian in the dipole gauge can be obtained from Eq. (22) truncating the Hilbert space of each dipole to include only two energy levels: $\hat{\mathcal{H}}_{\rm dg}^{(N)} = \hat{\Pi}\hat{H}_{\rm dg}^{(N)}\hat{\Pi}$. Observing that $q\hat{\Pi}\sum_i x_i \hat{\Pi} = 2d_{1,0}\hat{J}_x$, and using the fact that $\hat{\Pi}$ is the identity operator for the resulting collection of two-level systems, we obtain

$$\hat{\mathcal{H}}_{\rm dg}^{(N)} = \hbar\omega_c \hat{a}^\dagger \hat{a} + \hbar\omega_x(\hat{J}_z + j) + 2i\hbar\eta\,\omega_c(\hat{a}^\dagger - \hat{a})\hat{J}_x + 4\hbar\,\eta^2\,\omega_c\,\hat{J}_x^2. \tag{23}$$

Comparing Eq. (4) and Eq. (21) (notice that $\hat{T}_N = \hat{U}_N^\dagger$), we observe that, while the Coulomb-gauge Hamiltonian can be obtained by applying a unitary transformation to the bare matter Hamiltonian, the dipole-gauge Hamiltonian is obtained by applying the H.c. transformation to the bare photonic Hamiltonian.

We will show in the next subsection that, in contrast to the standard derivation of the Coulomb-gauge Dicke Hamiltonian, the dipole gauge Hamiltonian in Eq. (23) does not violate the gauge principle. This behavior can be understood by observing that a truncation on the number of modes in the photonic system, as a single-mode description of the resonator, despite determining a loss of spatial locality [50], does not introduce any spatial nonlocality in the quadratic potential of the single-mode Hamiltonian, since different normal modes are independent and correspond to different effective particles. On the contrary, truncating the Hilbert space of an individual mode, e.g., considering a few photon system, could produce issues analogous to those appearing in the Coulomb gauge.

Equation (23) describes the Dicke Hamiltonian in the dipole gauge. It includes a self-polarization term induced by the interaction with the electromagnetic field ($\propto \hat{J}_x^2$). Neglecting it can lead to unphysical results [51] and to the loss of gauge invariance. This Hamiltonian slightly differs from that derived in [11], where the intra-atom self-polarization terms $\propto x_i^2$ are included in the atomic potentials and give rise to a renormalization of the atomic transition frequency $\omega_{1,0}$ and of the coupling η. While the full inclusion of these terms into the qubit Hamiltonian might seem to be the most accurate approach to derive a reduced two-level Hamiltonian, it applies the two-level truncation to the different terms of the light-matter interaction Hamiltonian with a different level of accuracy. Specifically, while the terms $\propto x_i^2$ are included in the atomic potentials before the diagonalization of the atomic Hamiltonian, the other terms are taken into account only after the application of the two-level approximation. Moreover, the resulting self-polarization term $\hat{J}_x^2 = (1/4)\sum_{i,j}\hat{\sigma}_x^{(i)}\hat{\sigma}_x^{(j)}$ still includes the intra-atomic contributions ($i = j$), although these determine only a rigid shift of all the energy levels. In Ref. [11] it is shown that, when the coupling strength is quite high, including the intra-atom self-polarization terms in the atom potential before the diagonalization of the full atomic Hamiltonian, can result in less accurate results.

C. Gauge invariance of the Dicke model

The Dicke Hamiltonian in the dipole gauge in Eq. (23) can also be derived directly applying a gauge (unitary) transformation to the Dicke Hamiltonian in the Coulomb gauge in Eq. (17) [or alternatively in Eq. (19)]:

$$\hat{\mathcal{H}}_{\rm dg}^{(N)} = \hat{\mathcal{T}}_N \hat{\mathcal{H}}_{\rm cg}^{(N)} \hat{\mathcal{T}}_N^\dagger, \tag{24}$$

where $\hat{\mathcal{T}}_N = \hat{\mathcal{U}}_N^\dagger$. Equation (24) demonstrates that the two formulations of the Dicke model $\hat{\mathcal{H}}_{\rm cg}^{(N)}$ and $\hat{\mathcal{H}}_{\rm dg}^{(N)}$ are related by a gauge transformation. Such a relation is not fulfilled if $\hat{\mathcal{H}}_{\rm cg}^{(N)}$ is replaced by $\hat{\mathcal{H}}_{\rm cg}^{\prime(N)}$.

III. DICKE MODEL IN THE $N \to \infty$ LIMIT

The starting point for our analysis in the thermodynamic limit is the Holstein-Primakoff representation [40] of the angular momentum operators $\hat{J}_z = \hat{b}^\dagger\hat{b} - j$, $\hat{J}_+ = \hat{b}^\dagger\sqrt{2j - \hat{b}^\dagger\hat{b}}$, and $\hat{J}_- = \hat{J}_+^\dagger$ [notice that $\hat{J}_\pm = \hat{J}_x \pm i\hat{J}_y$]. Here $\hat{b}$ and $\hat{b}^\dagger$ are bosonic operators. This allows one to obtain effective Hamiltonians that are exact in the standard thermodynamic limit $N \to \infty$ and $\eta \to 0$, with $\eta\sqrt{N} \to \lambda$ remaining a finite quantity.

We proceed in the thermodynamic limit by replacing the angular momentum operators introduced in the previous section by using the Holstein-Primakoff representation, expanding the square roots, and finally neglecting terms with powers of j in the denominator, since these go to zero in the considered limit [52]. We can start from the Hamiltonian of the collective spin system in the absence of interaction with the electromagnetic field in Eq. (2). We obtain

$$\hat{\mathcal{H}}_0 = \hbar\omega_x \hat{b}^\dagger\hat{b}. \tag{25}$$

A. Dipole gauge

Applying the Holstein-Primakoff representation to Eq. (23) and performing the thermodynamic limit ($N \to \infty$, $\eta\sqrt{N} \to \lambda$), we obtain

$$\hat{\mathcal{H}}_{\rm dg} = \hbar\omega_c \hat{a}^\dagger\hat{a} + \hbar\omega_x \hat{b}^\dagger\hat{b} + i\hbar\lambda\,\omega_c(\hat{a}^\dagger - \hat{a})(\hat{b} + \hat{b}^\dagger) + \hbar\omega_c\,\lambda^2\,(\hat{b} + \hat{b}^\dagger)^2. \tag{26}$$

B. Coulomb gauge

In contrast to the Dicke Hamiltonians in the dipole gauge $\hat{\mathcal{H}}_{\rm dg}^{(N)}$, and in the standard Coulomb gauge $\hat{\mathcal{H}}_{\rm cg}^{\prime(N)}$, the correct Coulomb gauge Dicke Hamiltonian $\hat{\mathcal{H}}_{\rm cg}^{(N)}$ contains field operators at all orders. At a first sight, this feature prevents the possibility to obtain a harmonic Dicke Hamiltonian in the thermodynamic limit as obtained from $\hat{\mathcal{H}}_{\rm dg}^{(N)}$. Hence the thermodynamic limit, apparently, would destroy gauge invariance. Actually, as we are going to show, this is not the case.

Starting from Eq. (19), performing a series expansion of $\cos[2\eta(\hat{a}^\dagger+\hat{a})]$ and $\sin[2\eta(\hat{a}^\dagger+\hat{a})]$, we obtain

$$\hat{\mathcal{H}}_{\rm cg}^{(N)} = \hbar\omega_c\hat{a}^\dagger\hat{a} + \hbar\frac{N\omega_x}{2} + \hbar\omega_x(\hat{b}^\dagger\hat{b} - N/2) \times [1 - 2\eta^2(\hat{a}^\dagger+\hat{a})^2 + O(\eta^4)] - i\hbar\omega_x\frac{\sqrt{N}}{2}(\hat{b}^\dagger - \hat{b})[2\eta(\hat{a}^\dagger+\hat{a}) + O(\eta^3)]. \quad (27)$$

In the thermodynamic limit ($N\to\infty$, $\sqrt{N}\eta\to\lambda$), only terms up to the second order in η remain different from zero, and we finally obtain

$$\mathcal{H}_{\rm cg} = \hbar\omega_c\hat{a}^\dagger\hat{a} + \hbar\omega_x\hat{b}^\dagger\hat{b} - i\hbar\omega_x\lambda\,(\hat{b}^\dagger - \hat{b})(\hat{a}^\dagger + \hat{a}) + \hbar\mathcal{D}(\hat{a}^\dagger+\hat{a})^2, \quad (28)$$

where we defined $\mathcal{D} = \omega_x\lambda^2$. As a result, also the correct Coulomb gauge Hamiltonian $\mathcal{H}_{\rm cg}^{(N)}$ [Eq. (19)] reduces to a Hamiltonian which describes a harmonic system constituted by two interacting harmonic oscillators, like the dipole gauge Hamiltonian.

In the same limit, the standard Coulomb gauge Hamiltonian $\mathcal{H}_{\rm cg}^{\prime(N)}$, not satisfying the gauge principle, becomes

$$\mathcal{H}'_{\rm cg} = \hbar\omega_c\hat{a}^\dagger\hat{a} + \hbar\omega_x\hat{b}^\dagger\hat{b} - i\hbar\omega_x\lambda\,(\hat{b}^\dagger - \hat{b})(\hat{a}^\dagger + \hat{a}) + \hbar\mathcal{D}'(\hat{a}^\dagger+\hat{a})^2, \quad (29)$$

where we used Eq. (11), and defined $\mathcal{D}' = \sum_k \omega_{k,0}\lambda_k^2 = D/\hbar$. $\hat{\mathcal{H}}'_{\rm cg}$ in Eq. (29) is very similar to $\hat{\mathcal{H}}_{\rm cg}$ in Eq. (28). They only differ for the diamagnetic coefficient multiplying the term $(\hat{a}^\dagger+\hat{a})^2$. While the coefficient in Eq. (29) ($\mathcal{D}'$) contains a sum over all the allowed transitions from the ground state, the one in Eq. (28) ($\mathcal{D} < \mathcal{D}'$), more consistently, contains only the contribution from the single two-level transition considered in the two-level approximation leading to the Dicke model. As we will show in the next subsection, this difference determines the loss or the preservation of gauge invariance. Moreover, it has been observed that the value of the diamagnetic coefficient with respect to $\omega_x\lambda^2$ can prevent or allow a superradiant phase transition in Dicke models [53].

It is interesting and reassuring that also after the truncation of the Hilbert space of the atomic ensemble, using Eq. (28), the paramagnetic and diamagnetic contributions to the physical current-current response function [44–46] still cancel in the uniform static limit. In particular, in the present case, it is proportional to

$$-\frac{(\omega_x\lambda)^2}{\omega_x} + \mathcal{D} = 0. \quad (30)$$

This does not occur using the Hamiltonian in Eq. (29):

$$-\frac{(\omega_x\lambda)^2}{\omega_x} + \mathcal{D}' \neq 0. \quad (31)$$

C. Gauge invariance

In order to demonstrate that $\hat{\mathcal{H}}_{\rm cg}$ and $\hat{\mathcal{H}}_{\rm dg}$ are related by a unitary (gauge) transformation and hence display the same spectrum of eigenergies, we start applying the Holstein-Primakoff representation to the unitary operator which implements the minimal coupling replacement in Eq. (17), as well as the gauge transformation of the Dicke model [see Eq. (24)]. Taking the standard limits ($N\to\infty$, with $\sqrt{N}\eta = \lambda$ finite), we obtain

$$\hat{\mathcal{U}}_N \to \hat{\mathcal{U}} = \exp[i\lambda(\hat{a}+\hat{a}^\dagger)(\hat{b}+\hat{b}^\dagger)]. \quad (32)$$

The Dicke Hamiltonian in the Coulomb gauge $\hat{\mathcal{H}}_{\rm cg}$ can be readily obtained by applying the generalized minimal coupling replacement using Eq. (25) and Eq. (32):

$$\hat{\mathcal{H}}_{\rm cg} = \hat{\mathcal{U}}\hat{\mathcal{H}}_0\hat{\mathcal{U}}^\dagger + \hbar\omega_c\hat{a}^\dagger\hat{a}. \quad (33)$$

This approach is particularly interesting, since it provides a recipe to obtain the correct Coulomb-gauge light-matter interaction Hamiltonian starting from the knowledge of the unperturbed Hamiltonian of a bosonic excitation $\hat{\mathcal{H}}_0$ and its associated polarization operator, which in this case is $\hat{p} = \sqrt{N}d_{1,0}(\hat{b}+\hat{b}^\dagger)$. Notice that the unitary operator in Eq. (33) can be expressed as $\hat{\mathcal{U}} = \exp(i\hat{A}\hat{p}/\hbar)$. Thus, within this approach, it is not necessary to start explicitly considering a collection of effective two-level atoms, but it is sufficient to start from a bosonic Hamiltonian for the bare matter system and then to use the generalized minimal coupling replacement in Eq. (33). We will discuss further this point and its connection with the Hopfield model in the next section.

Applying to $\hat{\mathcal{H}}_{\rm cg}$ the unitary transformation $\hat{\mathcal{T}}\hat{\mathcal{H}}_{\rm cg}\hat{\mathcal{T}}^\dagger$, where $\hat{\mathcal{T}} = \hat{\mathcal{U}}^\dagger$, the corresponding Hamiltonian in the dipole gauge in Eq. (26) is easily recovered:

$$\hat{\mathcal{T}}\hat{\mathcal{H}}_{\rm cg}\hat{\mathcal{T}}^\dagger = \hat{\mathcal{H}}_{\rm dg}. \quad (34)$$

Equation (34) demonstrates that $\hat{\mathcal{H}}_{\rm dg}$ and $\hat{\mathcal{H}}_{\rm cg}$ are related by a unitary transformation as required by gauge invariance; hence they will display the same eigenvalues. In contrast, $\hat{\mathcal{H}}'_{\rm cg}$ is *not* related to $\hat{\mathcal{H}}_{\rm dg}$ by a unitary transformation and thus it will display *different* energy levels.

We now provide a direct check of the breakdown of gauge invariance of the Dicke model as described by the standard Hamiltonian in the Coulomb gauge Eq. (29). Specifically, we compare the resonance frequencies of the two collective polariton modes obtained by diagonalizing (using Bogoliubov-Hopfield transformations) the Hamiltonians Eqs. (26), (28), and (29). For the polariton frequencies, resulting from the diagonalization of Eq. (26), we obtain

$$\omega_{\rm dg\pm}^2 = \tfrac{1}{2}\left[\tilde{\omega}_x^2 + \omega_c^2 \pm \sqrt{\left(\tilde{\omega}_x^2 - \omega_c^2\right)^2 + 4\lambda^2\omega_x\omega_c}\right], \quad (35)$$

where $\tilde{\omega}_x = \sqrt{\omega_x(\omega_x + 4\lambda^2/\omega_c)}$.

Diagonalizing the Hamiltonian in Eq. (28) results in the polariton frequencies

$$\omega_{\rm cg\pm}^2 = \tfrac{1}{2}\left[\tilde{\omega}_c^2 + \omega_x^2 \pm \sqrt{\left(\tilde{\omega}_c^2 + \omega_x^2\right)^2 - 4\,\omega_c^2\omega_x^2}\right], \quad (36)$$

with $\tilde{\omega}_c = \sqrt{\omega_c(\omega_c + 4\mathcal{D})}$.

The polariton frequencies $\omega'_{\rm cg\pm}$ resulting from the diagonalization of the standard Coulomb-gauge Dicke Hamiltonian in Eq. (29) can be obtained from Eq. (36) after the replacement $\mathcal{D}\to\mathcal{D}'$.

The unitary gauge transformation in Eq. (34) implies that $\omega_{\rm dg\pm} = \omega_{\rm cg\pm}$. This relation can be explicitly shown after some algebraic manipulation. On the contrary, the polariton

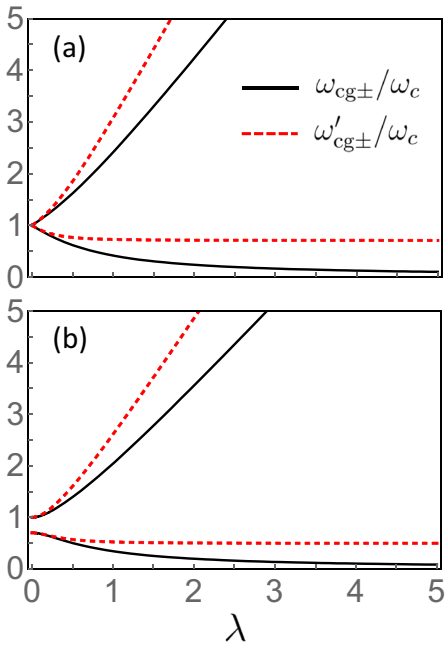

FIG. 3. Frequencies $\omega_{cg\pm} = \omega_{dg\pm}$ and $\omega'_{cg\pm}$ of the two polariton modes, obtained diagonalizing the Dicke model, in the limit $N \to \infty$, as a function of the normalized coupling strength λ for (a) the resonant case ($\omega_c = \omega_x$) and (b) for the detuned case with $\omega_x = 0.8\omega_c$.

frequencies obtained from $\hat{\mathcal{H}}'_{cg}$ are different:

$$\omega'_{cg\pm} \neq \omega_{cg\pm} = \omega_{dg\pm}.$$

Figure 3 displays $\omega_{cg\pm}/\omega_c = \omega_{dg\pm}/\omega_c$ and $\omega'_{cg\pm}/\omega_c$ as a function of λ, for $\mathcal{D}' = 2\mathcal{D}$. The choice of $\alpha \equiv \mathcal{D}'/\mathcal{D}$ depends on the specific system. Here we used the reasonable value $\alpha = 2$.

The differences are relevant, starting from normalized coupling strengths $\lambda \sim 0.4$. Hence we can conclude that for coupling strengths $\lambda \gtrsim 0.4$ the standard Coulomb-gauge Dicke Hamiltonian (in the thermodynamic limit) provides significantly wrong polariton frequencies in agreement with the results in Ref. [11].

D. Superradiant quantum phase transitions

In the past, it was shown [54] that, when the number of atoms tends to infinity, the Dicke model can undergo a transition to a superradiant phase, where the system exhibits a spontaneous coherent electromagnetic field. The initial prediction used the rotating wave approximation (Tavis-Cummings model). However, soon after, using a Hamiltonian similar to that in Eq. (26), it was shown that photon condensation is robust against the addition of counter-rotating terms [55,56]. These early studies soon stimulated great interest on the Dicke model as well as a long-standing and still ongoing debate and controversies (see Ref. [7] for a recent review). A thorough detailed description of the whole debate is beyond the scope of this article. Here we limit ourselves to briefly describing how the results presented here enter this debate.

The Dicke model Hamiltonian in Eq. (26) also exhibits a quantum phase transition [57], which can occur at zero temperature by tuning the light-matter coupling λ across a quantum critical point. Above the quantum critical point, the ground state of the cavity QED system is twice degenerate.

To the best of our knowledge, this phase transition has never been observed in thermal equilibrium systems. However, it has been realized with quantum simulators made of atoms in an optical cavity subject to both dissipation and driving [58,59].

Early on, it was pointed out that addition of the neglected diamagnetic term (proportional to $\hat{\mathbf{A}}^2$) in the Dicke model, naturally generated by applying minimal coupling, forbids the phase transition as a consequence of the TRK sum rule (no-go theorem for superradiant phase transition) [60,61]. Specifically, using the Hamiltonian in Eq. (29), it has been shown that the superradiant phase transition can occur only if

$$\omega_x \lambda^2 > \mathcal{D}' = D/\hbar,$$

where

$$D = N A_0^2 q^2/(2m).$$

However, the TRK sum rule, which can be expressed as

$$\mathcal{D}' = \sum_k \omega_{k,0} \lambda_k^2 = D/\hbar$$

(here $\omega_{k,0}$ and λ_k are the transition frequencies and coupling rates between the ground state and all the excited states of the atom), implies that $\omega_x \lambda^2 \leqslant \mathcal{D}'$.

More recently [53], it has been shown that the TRK sum rule also forbids the quantum phase transitions, in the case of cavity QED systems consisting of real atoms coupled to the field via minimal coupling Eq. (29). Such a no-go theorem does not apply to circuit QED systems. If this phase transition can be observed using superconducting circuit systems is still a subject of debate.

The general debate on a superradiant phase transition was enriched by a work providing a microscopic derivation of the Dicke model in the dipole gauge [62]. In this model [see, e.g., Eq. (26)], there is no diamagnetic term preventing the Dicke phase transition. Hence the authors claim that the basis of no-go argumentations concerning the Dicke phase transition with atoms in electromagnetic fields dissolves. Actually, this puzzling ambiguity was addressed in previous work [49]. In the electric dipole gauge, the system is described by the original Dicke Hamiltonian. As a consequence, in the dipole gauge, the quantum operator $-i\omega_c(\hat{a} - \hat{a}^\dagger)$ does not correspond, as in the Coulomb gauge, to the electric-field operator but to the displacement operator. Although above the critical coupling $\langle \hat{a} \rangle \neq 0$, the phase transition leads to a spontaneous polarization of the two-level systems, however, it does not lead to a spontaneous transverse electric field. This occurs because the electric-field operator in the dipole gauge is

$$\hat{E} = -i\omega_c[\hat{a} - \hat{a}^\dagger - \lambda(\hat{b} - \hat{b}^\dagger)].$$

More recent work [10] confirms this view and applies it to circuit QED systems.

This article, showing accurately that the Dicke model in the thermodynamic limit provides gauge-independent physical results, eliminates any gauge ambiguities in discussions on the

superradiant phase transition in cavity QED systems consisting of real atoms coupled to the field via minimal coupling. In particular, the same results obtained in the dipole gauge are obtained in the Coulomb gauge if the correct Coulomb-gauge Hamiltonian in Eq. (29) is adopted, and if the system operators $\hat{\mathcal{O}}$, as well the system states, are transformed according to the proper unitary transformation: $\hat{\mathcal{O}}_{\rm dg} = \hat{\mathcal{T}}\hat{\mathcal{O}}_{\rm cg}\hat{\mathcal{T}}^{\dagger}$ and $|\psi_{\rm dg}\rangle = \hat{\mathcal{T}}|\psi_{\rm cg}\rangle$. Finally, we observe that, using the Coulomb gauge Dicke model in Eq. (29), since the TRK sum rule is satisfied [see Eq. (30)], the superradiant phase transition is forbidden because (following, e.g., Ref. [53]) it would require $\omega_x\lambda^2 < \mathcal{D}$.

IV. GAUGE INVARIANCE OF THE HOPFIELD MODEL

The Hopfield model provides a full quantum description of the interaction between the electromagnetic field and a dielectric which is described by a harmonic polarization density. The original treatment considers a 3D uniform dielectric with a single resonance frequency describing dispersionless collective excitations. This exactly solvable model was initially applied to the case of excitonic polaritons. Afterwards, it has been applied and/or generalized to describe a great variety of systems with different dimensionalities and degrees of freedom, including quantum well [63] and cavity polaritons [64], phonon polaritons [65,66], and plasmonic nanoparticle crystals [67]. A generalized Hopfield model for inhomogeneous and dispersive media has been proposed [68]. Here we analyze the original model, its gauge properties, and its connection with the Dicke model in the thermodynamic limit.

The field operators are given in terms of the bosonic photonic operators $\hat{a}_{\mathbf{k},\lambda}$ and the bosonic operators $\hat{b}_{\mathbf{k},\lambda}$ describing the destruction of the polarization quanta by

$$\begin{aligned}\hat{A}(\mathbf{r}) &= \sum_{\mathbf{k},\lambda} A_k^{(0)}\mathbf{e}_{\mathbf{k},\lambda}(\hat{a}_{\mathbf{k},\lambda} + \hat{a}^{\dagger}_{-\mathbf{k},\lambda})e^{i\mathbf{k}\cdot\mathbf{r}},\\ \hat{\mathbf{P}}(\mathbf{r}) &= P^{(0)}\sum_{\mathbf{k},\lambda}\mathbf{e}_{\mathbf{k},\lambda}(\hat{b}_{\mathbf{k},\lambda} + \hat{b}^{\dagger}_{-\mathbf{k},\lambda})e^{i\mathbf{k}\cdot\mathbf{r}},\end{aligned} \tag{37}$$

where $\mathbf{k}$ is the wave vector, λ labels the two transverse polarizations, $\mathbf{e}_{\mathbf{k},\lambda}$ are the polarization unit vectors, and we have defined $A_k^{(0)} = \sqrt{\hbar/(2\epsilon_0 V\omega_k)}$ and $P^{(0)} = \sqrt{\hbar\omega_0\beta/(2V)}$. Here, V is the quantization volume, ω_k and ω_0 are the bare resonance frequencies of the photonic modes and of the matter system waves, respectively, and β is the polarizability [41].

The Hopfield Hamiltonian in the Coulomb gauge can be written as

$$\begin{aligned}\hat{H}_{\rm cg}^{\rm Hop} &= \hbar\sum_{\mathbf{k},\lambda}\omega_k\hat{a}^{\dagger}_{\mathbf{k},\lambda}\hat{a}_{\mathbf{k},\lambda} + \hbar\omega_0\sum_{\mathbf{k},\lambda}\hat{b}^{\dagger}_{\mathbf{k},\lambda}\hat{b}_{\mathbf{k},\lambda}\\ &\quad + i\hbar\omega_0\sum_{\mathbf{k},\lambda}\Lambda_k(\hat{a}_{\mathbf{k},\lambda} + \hat{a}^{\dagger}_{-\mathbf{k},\lambda})(\hat{b}_{\mathbf{k},\lambda} - \hat{b}^{\dagger}_{-\mathbf{k},\lambda})\\ &\quad + \hbar\omega_0\sum_{\mathbf{k},\lambda}\Lambda_k^2(\hat{a}_{\mathbf{k},\lambda} + \hat{a}^{\dagger}_{-\mathbf{k},\lambda})^2,\end{aligned} \tag{38}$$

where $\Lambda_k = VA_k^{(0)}P^{(0)}/\hbar$.

It is interesting to observe that this equation can be written in the compact form

$$\hat{H}_{\rm cg}^{\rm Hop} = \hbar\sum_{\mathbf{k},\lambda}\omega_k\hat{a}^{\dagger}_{\mathbf{k},\lambda}\hat{a}_{\mathbf{k},\lambda} + \hat{U}_{\rm Hop}\left(\hbar\omega_0\sum_{\mathbf{k},\lambda}\hat{b}^{\dagger}_{\mathbf{k},\lambda}\hat{b}_{\mathbf{k},\lambda}\right)\hat{U}^{\dagger}_{\rm Hop}, \tag{39}$$

where

$$\hat{U}_{\rm Hop} = \exp\left[i\sum_{\mathbf{k},\lambda}\Lambda_k(\hat{a}_{\mathbf{k},\lambda} + \hat{a}^{\dagger}_{-\mathbf{k},\lambda})(\hat{b}_{\mathbf{k},\lambda} - \hat{b}^{\dagger}_{-\mathbf{k},\lambda})\right]. \tag{40}$$

We observe that this unitary operator coincides with the Hermitian conjugate of the operator describing the Coulomb $\rightarrow$ dipole gauge transformation in a system with a polarization density operator given by Eq. (37):

$$\hat{U}_{\rm Hop} = \hat{T}^{\dagger}_{\rm Hop}, \tag{41}$$

where

$$\hat{T}_{\rm Hop} = \exp\left[\frac{i}{\hbar}\int d\mathbf{r}\,\hat{A}(\mathbf{r})\cdot\hat{P}(\mathbf{r})\right]. \tag{42}$$

This relationship implies that the Hopfield Hamiltonian in the dipole gauge can be easily obtained:

$$\begin{aligned}\hat{H}_{\rm dg}^{\rm Hop} &= \hat{T}_{\rm Hop}\hat{H}_{\rm cg}^{\rm Hop}\hat{T}^{\dagger}_{\rm Hop} = \hat{T}_{\rm Hop}\left(\hbar\sum_{\mathbf{k},\lambda}\omega_k\hat{a}^{\dagger}_{\mathbf{k},\lambda}\hat{a}_{\mathbf{k},\lambda}\right)\hat{T}^{\dagger}_{\rm Hop}\\ &\quad + \hbar\omega_0\sum_{\mathbf{k},\lambda}\hat{b}^{\dagger}_{\mathbf{k},\lambda}\hat{b}_{\mathbf{k},\lambda}.\end{aligned} \tag{43}$$

After simple algebra, we obtain

$$\begin{aligned}\hat{H}_{\rm dg}^{\rm Hop} &= \hbar\sum_{\mathbf{k},\lambda}\omega_k\hat{a}^{\dagger}_{\mathbf{k},\lambda}\hat{a}_{\mathbf{k},\lambda} + \hbar\omega_0\sum_{\mathbf{k},\lambda}\hat{b}^{\dagger}_{\mathbf{k},\lambda}\hat{b}_{\mathbf{k},\lambda}\\ &\quad -1\hbar\sum_{\mathbf{k},\lambda}\omega_k\Lambda_k(\hat{a}_{\mathbf{k},\lambda} - \hat{a}^{\dagger}_{-\mathbf{k},\lambda})(\hat{b}_{\mathbf{k},\lambda} + \hat{b}^{\dagger}_{-\mathbf{k},\lambda})\\ &\quad + \hbar\sum_{\mathbf{k},\lambda}\omega_k\Lambda_k^2(\hat{b}_{\mathbf{k},\lambda} + \hat{b}^{\dagger}_{-\mathbf{k},\lambda})^2.\end{aligned} \tag{44}$$

Equation (43) demonstrates that Eq. (38) and Eq. (44) are related by a unitary (gauge) transformation and hence display the same energy spectrum. The compact forms in Eq. (39) and Eq. (43) are manifestly gauge related. Moreover, being manifestly related by a unitary transformation, they provide the same energy spectra and the same matrix elements of physical observables. Of course, both the corresponding operators and the vector states have to be transformed accordingly, when changing from one gauge to the other. If needed, a continuous set of gauge transformations which depend on one parameter can be considered. It is sufficient to, e.g., start from the Hamiltonian in the Coulomb gauge and then consider a unitary transformation using modified unitary operators, where the exponent in Eq. (42) is multiplied by such a parameter (see, e.g., Ref. [12]).

These results open the way to the application of the generalized minimal coupling replacement [see Eqs. (39), (41), and (42)] to promptly derive general gauge-invariant Hopfield Hamiltonians. Given a generic polarization operator like that in Eq. (37), using the unitary operator in Eq. (42), it is possible to directly obtain the total Hamiltonian in the Coulomb or

dipole gauge by applying the corresponding transformation to the bare matter system Hamiltonian [see Eq. (39)] or to the bare photonic Hamiltonian [see Eq. (44)]. From this point of view, the Dicke model in the dilute regime can be regarded as a particular case of the Hopfield model where the polarization density operator is $\hat{P} = (\sqrt{N} d_{1,0}/V)(\hat{b} + \hat{b}^\dagger)$ (see Sec. III C).

V. CONNECTION WITH THE PEIERLS SUBSTITUTION

Throughout this work we considered ensembles of noninteracting atoms. It remains an open problem how to construct gauge-invariant model Hamiltonians for interacting atoms. Here we limit ourselves to briefly analyzing the simplest case of spinless electrons in a one-dimensional inversion-symmetric crystal with N sites (one atom per site) in a tight-binding approximation (see, e.g., Refs. [46,69]). In the absence of the interaction with the field, and considering a single orbital $\phi_j(x) = \phi(x - R_j)$ (here R_j indicates the site coordinate) per atom, the model Hamiltonian can be written as

$$\hat{\mathcal{H}}_0 = E_0 \sum_{j=1}^{N} |j\rangle\langle j| - t \sum_{j=1}^{N} (|j+1\rangle\langle j| + \text{H.c.}), \tag{45}$$

where $E_0 = \langle \phi_j | H_0 | \phi_j \rangle$ and $t = -\langle \phi_{j\pm1} | H_0 | \phi_j \rangle$. Considering the interaction with a uniform field, the model Hamiltonian becomes

$$\hat{\mathcal{H}} = \Pi \hat{U} \hat{\mathcal{H}}_0 \hat{U}^\dagger \Pi, \tag{46}$$

where $\hat{U} = \exp(iqx\hat{A})$ and $\Pi = \sum_j |j\rangle\langle j|$. Assuming that $\hat{U}$ is almost constant within the spatial range of the localized orbitals, we have $\langle \phi_j | \hat{U} | \phi_{j'} \rangle \simeq \delta_{j,j'} \exp(iqR_j\hat{A})$. We obtain

$$\hat{\mathcal{H}}_0 = E_0 \sum_{j=1}^{N} |j\rangle\langle j| - t \sum_{j=1}^{N} (e^{iqa\hat{A}} |j+1\rangle\langle j| + \text{H.c.}), \tag{47}$$

where $a = R_{j+1} - R_j$. This result corresponds to the so-called Peierls substitution and can be easily generalized to fields which are slowly varying on the lattice scale replacing the phase fators in Eq. (47) with $\exp\{iq\frac{a}{2}[\hat{A}(R_{j+1}) + \hat{A}(R_j)]\}$ [46,70–73]. If more than one orbital per atom is considered, in addition to the Peierls substitution [46], we expect the presence (also in the diagonal term proportional to E_0) of additional phase factors depending on the dipole moment matrix element between two orbitals at the same site, similar to those obtained for a single atom [30]. Such a development is left for future work. We conclude this section by observing that the Peierls substitution method and the results presented in this work are closely connected. They both implement the minimal coupling replacement applying unitary operators to the bare Hamiltonian of the material system. Such a connection is further explored in a very recent work [48].

VI. DISCUSSION AND OUTLOOK

We have investigated the gauge invariance of the Dicke model in the dilute regime. In particular, we started from the derivation of the correct (not violating the gauge principle) Dicke model in the Coulomb gauge for a finite number N of dipoles. After that, using the Holstein-Primakoff transformation, we obtained the Coulomb-gauge Dicke Hamiltonian in the dilute regime. We demonstrated that it is related by a gauge (unitary) transformation to the corresponding Hamiltonian in the dipole gauge. Hence the two gauges, as required, provide the same energy spectra, in contrast with the standard Dicke model. The standard Dicke Hamiltonian in the Coulomb gauge and the one derived here only differ for the diamagnetic coefficient multiplying the term $(\hat{a}^\dagger + \hat{a})^2$. This difference determines either the loss or the preservation of gauge invariance.

We also analyzed the Hopfield model, showing its gauge invariance. We provided a method to derive in a simple way manifestly gauge-invariant Hopfield models, having knowledge just of the matter polarization field. These results show that the Dicke model in the dilute regime can be regarded as a particular case of the more general Hopfield model.

Finally, we briefly discussed the connection of the gauge-invariant approach here discussed with the Peierls substitution used to introduce the interaction of crystals with the electromagnetic field. This brief analysis suggests a generalization of the present approach to many-body interacting electron systems.

Very recently, it has been shown that generalized Dicke models for two-level systems which do not display inversion symmetry can generate sizable spin squeezing and entanglement [74]. It would be interesting to apply the methods proposed here to eliminate gauge ambiguities from these models.

ACKNOWLEDGMENTS

We thank S. De Liberato for useful discussions and suggestions. F.N. is supported in part by NTT Research, Army Research Office (ARO) (Grant No. W911NF-18-1-0358), Japan Science and Technology Agency (JST) (via the Q-LEAP program and the CREST Grant No. JPMJCR1676), Japan Society for the Promotion of Science (JSPS) (via the KAKENHI Grant No. JP20H00134 and the JSPS-RFBR Grant No. JPJSBP120194828), and the Grant No. FQXi-IAF19-06 from the Foundational Questions Institute Fund (FQXi), a donor advised fund of the Silicon Valley Community Foundation. S.S. acknowledges the Army Research Office (ARO) (Grant No. W911NF1910065).

[1] I. I. Rabi, On the process of space quantization, Phys. Rev. **49**, 324 (1936).

[2] D. Z. Rossatto, C. J. Villas-Bôas, M. Sanz, and E. Solano, Spectral classification of coupling regimes in the quantum Rabi model, Phys. Rev. A **96**, 013849 (2017).

[3] O. Di Stefano, R. Stassi, L. Garziano, A. F. Kockum, S. Savasta, and F. Nori, Feynman-diagrams approach to the quantum Rabi model for ultrastrong cavity QED: Stimulated emission and reabsorption of virtual particles dressing a physical excitation, New J. Phys. **19**, 053010 (2017).

[4] R. H. Dicke, Coherence in spontaneous radiation processes, Phys. Rev. **93**, 99 (1954).
[5] T. Brandes, Coherent and collective quantum optical effects in mesoscopic systems, Phys. Rep. **408**, 315 (2005).
[6] B. M. Garraway, The Dicke model in quantum optics: Dicke model revisited, Philos. Trans. R. Soc. A **369**, 1137 (2011).
[7] P. Kirton, M. M. Roses, J. Keeling, and E. G. Dalla Torre, Introduction to the Dicke model: From equilibrium to nonequilibrium, and vice versa, Adv. Quantum Technol. **2**, 1800043 (2019).
[8] J. M. Fink, R. Bianchetti, M. Baur, M. Göppl, L. Steffen, S. Filipp, P. J. Leek, A. Blais, and A. Wallraff, Dressed Collective Qubit States and the Tavis-Cummings Model in Circuit QED, Phys. Rev. Lett. **103**, 083601 (2009).
[9] M. Feng, Y. P. Zhong, T. Liu, L. L. Yan, W. L. Yang, J. Twamley, and H. Wang, Exploring the quantum critical behavior in a driven Tavis–Cummings circuit, Nat. Commun. **6**, 7111 (2015).
[10] D. De Bernardis, T. Jaako, and P. Rabl, Cavity quantum electrodynamics in the nonperturbative regime, Phys. Rev. A **97**, 043820 (2018).
[11] D. De Bernardis, P. Pilar, T. Jaako, S. De Liberato, and P. Rabl, Breakdown of gauge invariance in ultrastrong-coupling cavity QED, Phys. Rev. A **98**, 053819 (2018).
[12] A. Stokes and A. Nazir, Gauge ambiguities imply Jaynes-Cummings physics remains valid in ultrastrong coupling QED, Nat. Commun. **10**, 499 (2019).
[13] A. F. Kockum, A. Miranowicz, S. De Liberato, S. Savasta, and F. Nori, Ultrastrong coupling between light and matter, Nat. Rev. Phys. **1**, 19 (2019).
[14] P. Forn-Díaz, L. Lamata, E. Rico, J. Kono, and E. Solano, Ultrastrong coupling regimes of light-matter interaction, Rev. Mod. Phys. **91**, 025005 (2019).
[15] T. Schwartz, J. A. Hutchison, C. Genet, and T. W. Ebbesen, Reversible Switching of Ultrastrong Light-Molecule Coupling, Phys. Rev. Lett. **106**, 196405 (2011).
[16] S. Kéna-Cohen, S. A. Maier, and D. D. C. Bradley, Ultrastrongly coupled exciton-polaritons in metal-clad organic semiconductor microcavities, Adv. Opt. Mater. **1**, 827 (2013).
[17] C. R. Gubbin, S. A. Maier, and S. Kéna-Cohen, Low-voltage polariton electroluminescence from an ultrastrongly coupled organic light-emitting diode, Appl. Phys. Lett. **104**, 233302 (2014).
[18] M. Mazzeo, A. Genco, S. Gambino, D. Ballarini, F. Mangione, O. Di Stefano, S. Patanè, S. Savasta, D. Sanvitto, and G. Gigli, Ultrastrong light-matter coupling in electrically doped microcavity organic light emitting diodes, Appl. Phys. Lett. **104**, 233303 (2014).
[19] S. Gambino, M. Mazzeo, A. Genco, O. Di Stefano, S. Savasta, S. Patanè, D. Ballarini, F. Mangione, G. Lerario, D. Sanvitto, and G. Gigli, Exploring light–matter interaction phenomena under ultrastrong coupling regime, ACS Photon. **1**, 1042 (2014).
[20] A. Genco, A. Ridolfo, S. Savasta, S. Patanè, G. Gigli, and M. Mazzeo, Bright polariton Coumarin-based OLEDs operating in the ultrastrong coupling regime, Adv. Opt. Mater. **6**, 1800364 (2018).
[21] A. A. Anappara, S. De Liberato, A. Tredicucci, C. Ciuti, G. Biasiol, L. Sorba, and F. Beltram, Signatures of the ultrastrong light-matter coupling regime, Phys. Rev. B **79**, 201303(R) (2009).
[22] G. Günter, A. A. Anappara, J. Hees, A. Sell, G. Biasiol, L. Sorba, S. De Liberato, C. Ciuti, A. Tredicucci, A. Leitenstorfer, and R. Huber, Sub-cycle switch-on of ultrastrong light–matter interaction, Nature (London) **458**, 178 (2009).
[23] Y. Todorov, A. M. Andrews, R. Colombelli, S. De Liberato, C. Ciuti, P. Klang, G. Strasser, and C. Sirtori, Ultrastrong Light-Matter Coupling Regime with Polariton Dots, Phys. Rev. Lett. **105**, 196402 (2010).
[24] B. Askenazi, A. Vasanelli, A. Delteil, Y. Todorov, L. C. Andreani, G. Beaudoin, I. Sagnes, and C. Sirtori, Ultra-strong light-matter coupling for designer Reststrahlen band, New J. Phys. **16**, 043029 (2014).
[25] G. Scalari, C. Maissen, D. Turcinkova, D. Hagenmuller, S. De Liberato, C. Ciuti, C. Reichl, D. Schuh, W. Wegscheider, M. Beck, and J. Faist, Ultrastrong coupling of the cyclotron transition of a 2D electron gas to a THz metamaterial, Science **335**, 1323 (2012).
[26] C. Maissen, G. Scalari, F. Valmorra, M. Beck, J. Faist, S. Cibella, R. Leoni, C. Reichl, C. Charpentier, and W. Wegscheider, Ultrastrong coupling in the near field of complementary split-ring resonators, Phys. Rev. B **90**, 205309 (2014).
[27] Q. Zhang, M. Lou, X. Li, J. L. Reno, W. Pan, J. D. Watson, M. J. Manfra, and J. Kono, Collective non-perturbative coupling of 2D electrons with high-quality-factor terahertz cavity photons, Nat. Phys. **12**, 1005 (2016).
[28] A. Bayer, M. Pozimski, S. Schambeck, D. Schuh, R. Huber, D. Bougeard, and C. Lange, Terahertz light-matter interaction beyond unity coupling strength, Nano Lett. **17**, 6340 (2017).
[29] X. Li, M. Bamba, Q. Zhang, S. Fallahi, G. C. Gardner, W. Gao, M. Lou, K. Yoshioka, M. J. Manfra, and J. Kono, Vacuum Bloch–Siegert shift in Landau polaritons with ultra-high cooperativity, Nat. Photon. **12**, 324 (2018).
[30] O. Di Stefano, A. Settineri, V. Macrì, L. Garziano, R. Stassi, S. Savasta, and F. Nori, Resolution of gauge ambiguities in ultrastrong-coupling cavity QED, Nat. Phys. **15**, 803 (2019).
[31] A. F. Starace, Length and velocity formulas in approximate oscillator-strength calculations, Phys. Rev. A **3**, 1242 (1971).
[32] R. Girlanda, A. Quattropani, and P. Schwendimann, Two-photon transitions to exciton states in semiconductors. application to CuCl, Phys. Rev. B **24**, 2009 (1981).
[33] S. Ismail-Beigi, E. K. Chang, and S. G. Louie, Coupling of Nonlocal Potentials to Electromagnetic Fields, Phys. Rev. Lett. **87**, 087402 (2001).
[34] A. Settineri, O. Di Stefano, D. Zueco, S. Hughes, S. Savasta, and F. Nori, Gauge freedom, quantum measurements, and time-dependent interactions in cavity and circuit QED, arXiv:1912.08548.
[35] A. Le Boité, Theoretical Methods for Ultrastrong Light–Matter Interactions, Adv. Quantum Technol. **3**, 1900140 (2020).
[36] C. Emary and T. Brandes, Quantum Chaos Triggered by Precursors of a Quantum Phase Transition: The Dicke Model, Phys. Rev. Lett. **90**, 044101 (2003).
[37] N. Lambert, C. Emary, and T. Brandes, Entanglement and the Phase Transition in Single-Mode Superradiance, Phys. Rev. Lett. **92**, 073602 (2004).
[38] N. Shammah, N. Lambert, F. Nori, and S. De Liberato, Superradiance with local phase-breaking effects, Phys. Rev. A **96**, 023863 (2017).
[39] N. Shammah, S. Ahmed, N. Lambert, S. De Liberato, and F. Nori, Open quantum systems with local and collective

incoherent processes: Efficient numerical simulations using permutational invariance, Phys. Rev. A **98**, 063815 (2018).
[40] T. Holstein and H. Primakoff, Field dependence of the intrinsic domain magnetization of a ferromagnet, Phys. Rev. **58**, 1098 (1940).
[41] J. J. Hopfield, Theory of the contribution of excitons to the complex dielectric constant of crystals, Phys. Rev. **112**, 1555 (1958).
[42] S. Savasta and R. Girlanda, The particle-photon interaction in systems descrided by model Hamiltonians in second quantization, Solid State Commun. **96**, 517 (1995).
[43] J. J. Sakurai, *Modern Quantum Mechanics* (Addison-Wesley Publishing Company, Inc., Redwood City, CA, 1994).
[44] D. Pines and P. Nozieres, *The Theory of Quantum Liquids* (W. A. Benjamin, New York, 1966).
[45] G. Giuliani and G. Vignale, *Quantum Theory of the Electron Liquid* (Cambridge University Press, Cambridge, UK, 2005).
[46] G. M. Andolina, F. M. D. Pellegrino, V. Giovannetti, A. H. MacDonald, and M. Polini, Cavity quantum electrodynamics of strongly correlated electron systems: A no-go theorem for photon condensation, Phys. Rev. B **100**, 121109(R) (2019).
[47] S. Savasta, O. Di Stefano, and F. Nori, TRK sum rule for interacting photons, arXiv:2002.02139.
[48] S. Savasta, O. Di Stefano, A. Settineri, D. Zueco, S. Hughes, and F. Nori, Gauge principle and gauge invariance in quantum two-level systems, arXiv:2006.06583.
[49] J. Keeling, Coulomb interactions, gauge invariance, and phase transitions of the Dicke model, J. Phys.: Condens. Matter **19**, 295213 (2007).
[50] C. S. Muñoz, F. Nori, and S. De Liberato, Resolution of superluminal signalling in non-perturbative cavity quantum electrodynamics, Nat. Commun. **9**, 1924 (2018).
[51] C. Schäfer, M. Ruggenthaler, V. Rokaj, and A. Rubio, Relevance of the quadratic diamagnetic and self-polarization terms in cavity quantum electrodynamics, ACS Photon. **7**, 975 (2020).
[52] E. Cortese, L. Garziano, and S. De Liberato, Polariton spectrum of the Dicke-Ising model, Phys. Rev. A **96**, 053861 (2017).
[53] P. Nataf and C. Ciuti, No-go theorem for superradiant quantum phase transitions in cavity QED and counter-example in circuit QED, Nat. Commun. **1**, 72 (2010).
[54] K. Hepp and E. H. Lieb, On the superradiant phase transition for molecules in a quantized radiation field: The Dicke maser model, Ann. Phys. (NY) **76**, 360 (1973).
[55] K. Hepp and E. H. Lieb, Equilibrium statistical mechanics of matter interacting with the quantized radiation field, Phys. Rev. A **8**, 2517 (1973).
[56] H. J. Carmichael, C. W. Gardiner, and D. F. Walls, Higher order corrections to the Dicke superradiant phase transition, Phys. Lett. A **46**, 47 (1973).
[57] K. Le Hur, *Understanding Quantum Phase Transitions* (Taylor and Francis, London, 2010), p. 217.
[58] A. T. Black, H. W. Chan, and V. Vuletić, Observation of Collective Friction Forces due to Spatial Self-Organization of Atoms: From Rayleigh to Bragg Scattering, Phys. Rev. Lett. **91**, 203001 (2003).
[59] Z. Zhiqiang, C. H. Lee, R. Kumar, K. J. Arnold, S. J. Masson, A. S. Parkins, and M. D. Barrett, Nonequilibrium phase transition in a spin-1 Dicke model, Optica **4**, 424 (2017).
[60] K. Rzażewski, K. Wódkiewicz, and W. Żakowicz, Phase Transitions, Two-Level Atoms, and the A^2 Term, Phys. Rev. Lett. **35**, 432 (1975).
[61] I. Bialynicki-Birula and K. Rzążewski, No-go theorem concerning the superradiant phase transition in atomic systems, Phys. Rev. A **19**, 301 (1979).
[62] A. Vukics, T. Grießer, and P. Domokos, Elimination of the *A*-Square Problem from Cavity QED, Phys. Rev. Lett. **112**, 073601 (2014).
[63] S. Savasta and R. Girlanda, Quantum description of the input and output electromagnetic fields in a polarizable confined system, Phys. Rev. A **53**, 2716 (1996).
[64] V. Savona, Z. Hradil, A. Quattropani, and P. Schwendimann, Quantum theory of quantum-well polaritons in semiconductor microcavities, Phys. Rev. B **49**, 8774 (1994).
[65] C. R. Gubbin, F. Martini, A. Politi, S. A. Maier, and S. De Liberato, Strong and Coherent Coupling between Localized and Propagating Phonon Polaritons, Phys. Rev. Lett. **116**, 246402 (2016).
[66] M. A. Sentef, M. Ruggenthaler, and A. Rubio, Cavity quantum-electrodynamical polaritonically enhanced electron-phonon coupling and its influence on superconductivity, Sci. Adv. **4**, eaau6969 (2018).
[67] S. Lamowski, C.-R. Mann, F. Hellbach, E. Mariani, G. Weick, and F. Pauly, Plasmon polaritons in cubic lattices of spherical metallic nanoparticles, Phys. Rev. B **97**, 125409 (2018).
[68] C. R. Gubbin, S. A. Maier, and S. De Liberato, Real-space Hopfield diagonalization of inhomogeneous dispersive media, Phys. Rev. B **94**, 205301 (2016).
[69] J. Li, D. Golez, G. Mazza, A. J. Millis, A. Georges, and M. Eckstein, Electromagnetic coupling in tight-binding models for strongly correlated light and matter, Phys. Rev. B **101**, 205140 (2020).
[70] R. Peierls, Zur theorie des diamagnetismus von leitungselektronen, Z. Phys. **80**, 763 (1933).
[71] J. M. Luttinger, The effect of a magnetic field on electrons in a periodic potential, Phys. Rev. **84**, 814 (1951).
[72] D. R. Hofstadter, Energy levels and wave functions of Bloch electrons in rational and irrational magnetic fields, Phys. Rev. B **14**, 2239 (1976).
[73] M. Graf and P. Vogl, Electromagnetic fields and dielectric response in empirical tight-binding theory, Phys. Rev. B **51**, 4940 (1995).
[74] V. Macrì, F. Nori, S. Savasta, and D. Zueco, Spin squeezing by one-photon–two-atom excitation processes in atomic ensembles, Phys. Rev. A **101**, 053818 (2020).

6.4 Gauge Principle and Gauge Invariance in Quantum Two-Level Systems

Gauge Principle and Gauge Invariance in Quantum Two-Level Systems

Salvatore Savasta,[1,*] Omar Di Stefano,[1] Alessio Settineri,[1] David Zueco,[2,3] Stephen Hughes,[4] and Franco Nori[5,6]

[1] *Dipartimento di Scienze Matematiche e Informatiche, Scienze Fisiche e Scienze della Terra, Università di Messina, I-98166 Messina, Italy*
[2] *Instituto de Ciencia de Materiales de Aragón and Departamento de Física de la Materia Condensada , CSIC-Universidad de Zaragoza, Pedro Cerbuna 12, 50009 Zaragoza, Spain*
[3] *Fundación ARAID, Campus Río Ebro, 50018 Zaragoza, Spain*
[4] *Department of Physics, Engineering Physics, and Astronomy, Queen's University, Kingston, Ontario K7L 3N6, Canada*
[5] *Theoretical Quantum Physics Laboratory, RIKEN Cluster for Pioneering Research, Wako-shi, Saitama 351-0198, Japan*
[6] *Physics Department, The University of Michigan, Ann Arbor, Michigan 48109-1040, USA*

The quantum Rabi model is a widespread description for the coupling between a two-level system and a quantized single mode of an electromagnetic resonator. Issues about this model's gauge invariance have been raised. These issues become evident when the light-matter interaction reaches the so-called ultrastrong coupling regime. Recently, a modified quantum Rabi model able to provide gauge-invariant physical results in any interaction regime was introduced [Nature Physics **15**, 803 (2019)]. Here we provide an alternative derivation of this result, based on the implementation in two-state systems of the gauge principle, which is the principle from which all the fundamental interactions in quantum field theory are derived. The adopted procedure can be regarded as the two-site version of the general method used to implement the gauge principle in lattice gauge theories. Applying this method, we also obtain the gauge-invariant quantum Rabi model for asymmetric two-state systems, and the multi-mode gauge-invariant quantum Rabi model beyond the dipole approximation.

I. INTRODUCTION

The ultrastrong and deep-strong coupling (USC and DSC) between individual or collections of effective two-level systems (TLSs) and the electromagnetic field has been realized in a variety of settings [1, 2]. In these extreme regimes of quantum light-matter interaction, the coupling strength becomes comparable to (USC) or larger than (DSC) the transition frequencies of the system.

Recently, it has been argued that truncations of the atomic Hilbert space, to obtain a two-level description of the matter system, violate the gauge principle [3–5]. Such violations become particularly relevant in the USC and DSC regimes. In particular, De Bernardis *et al.* [3] shows that, while in the electric dipole gauge, the two-level approximation can be performed as long as the Rabi frequency remains much smaller than the energies of all higher-lying levels, it can drastically fail in the Coulomb gauge, even for systems with an extremely anharmonic spectrum.

The impact of the truncation of the Hilbert space of the matter system to only two states was also studied by Stokes and Nazir [4], by introducing a one-parameter (α) set of gauge transformations. The authors found that each value of the parameter produces a distinct quantum Rabi model (QRM), providing distinct physical predictions. Investigating a *matter* system with a lower anharmonicity (with respect to that considered in Ref. [3]), they use the gauge parameter α as a sort of fit parameter to determine the optimal QRM for a specific set of system parameters, by comparing the obtained α-dependent lowest energy states and levels with the corresponding predictions of the non-truncated gauge invariant model. The surprising result is that, according to this procedure, in several circumstances the *optimal* gauge is the so-called Jaynes-Cummings (JC) gauge, a gauge where the counter-rotating terms are automatically absent.

Recently, the source of gauge violation has been identified, and a general method for the derivation of light-matter Hamiltonians in truncated Hilbert spaces able to produce gauge-invariant physical results has been developed [6] (see also related work [7–9]). This gauge invariance was achieved by compensating the non-localities introduced in the construction of the effective Hamiltonians. The resulting quantum Rabi Hamiltonian in the Coulomb gauge differs significantly from the standard one, but provides exactly the same energy levels obtained by using the dipole gauge, as it should be, because physical observable quantities must be gauge invariant. A recent overview of these gauge issues in TLSs can be found in Ref. [10].

Very recently, the validity of the gauge invariant QRM developed in Ref. [6] has been put into question by Stokes and Nazir [5]. Specifically, it is claimed that the results in Ref. [6] are not correct, and the truncation of the Hilbert space necessarily ruins gauge-invariance.

Here we present a detailed derivation of the results in Ref. [6] with an alternative, more direct and fundamental method. In our opinion, this approach demonstrates that the results in Ref. [6] [Eqs. (8) and (9) in particular] are indeed correct, and moreover, represent the implementation in a fully consistent and physically meaning-

* corresponding author: ssavasta@unime.it

ful way of the fundamental gauge principle in two-state systems. The derivation described here can be regarded as the two-site version of the general method for *lattice gauge theories* [11]. These represent the most advanced and commonly used tool for describing gauge theories in the presence of a truncated infinite-dimensional Hilbert space. When a gauge theory is regularized on the lattice, it is vital to maintain its invariance under gauge transformations [11]. An analogous approach has been developed as early as 1933 [12] for the description of tightly-bound electrons in a crystal in the presence of a slowly-varying magnetic vector potential (see, e.g., also Refs. [13–15]).

Applying this method, we also obtain the multi-mode gauge-invariant QRM beyond the dipole approximation.

The derivation presented here in Sect. IV, we believe, is already sufficient to eliminate any concerns about the validity of the results in Ref. [6]. However, in Sect. V, we also provide a reply to the key points raised by Stokes and Nazir [5].

II. THE GAUGE PRINCIPLE

In this section, we recall some fundamental concepts, which we will apply in the next sections.

In quantum field theory, the coupling of particles with fields is constructed in such a way that the theory is invariant under a gauge transformation [16]. Here, we limit the theoretical model to consider $U(1)$ invariance. This approach can be generalized to introduce non-abelian gauge theories [11, 16].

Let us consider the transformation of the particle field $\psi \to e^{iq\theta}\psi$. This transformation represents a symmetry of the free action of the particle (e.g., the Dirac action) if θ is a constant, but we want to consider a generic function $\theta(x)$ (*local* phase transformation). However, the free Dirac action is not invariant under local phase transformations, because the factor $e^{iq\theta(x)}$ does not commute with ∂_μ. At the same time, it is known that the action of the free electromagnetic field is invariant under the gauge transformation:

$$A_\mu \to A_\mu - \partial_\mu \theta \,. \tag{1}$$

It is then possible to replace, in the action, the derivative ∂_μ with a *covariant derivative* of ψ as

$$D_\mu \psi = (\partial_\mu + iqA_\mu)\,\psi \,, \tag{2}$$

so that

$$D_\mu \psi \to e^{iq\theta} D_\mu \psi \,, \tag{3}$$

even when θ depends on x. It is now easy to construct a Lagrangian with a local $U(1)$ invariance. It suffices to replace all derivatives ∂_μ with covariant derivatives D_μ.

The same procedure, leading to the well-known minimal coupling replacement, can be applied to describe the interaction of a non-relativistic particle with the electromagnetic field. Considering a particle of mass m with a geometrical coordinate x and a potential $V(x)$, the Hamiltonian of such a particle interacting with the electromagnetic field can be written as

$$\hat{H}_0^{\rm gi} = \frac{1}{2m}\left[\hat{p} - qA(x)\right]^2 + V(x) \,, \tag{4}$$

where $\hat{p} = -id/dx$ is the momentum of the particle (here $\hbar = 1$). It turns out that the expectation values $\langle\psi|\hat{H}_0^{\rm gi}|\psi\rangle$ are invariant under local phase transformations,

$$\psi(x) \to e^{iq\theta(x)}\psi(x) \,, \tag{5}$$

thanks to the presence of the gauge field $A(x)$.

Note that the function of a continuous degree of freedom $\psi(x)$ lives in the infinite-dimensional space of all square-integrable functions, and the local phase transformation transforms a state vector in this space into a different vector in the same space. Finally, we observe that the total Hamiltonian, in addition to $\hat{H}_0^{\rm gi}$, includes the free Hamiltonian for the gauge field.

III. DOUBLE-WELL SYSTEMS IN THE TWO-STATE LIMIT

The problem of a quantum-mechanical system whose state is effectively restricted to a two-dimensional Hilbert space is ubiquitous in physics and chemistry [17]. In the simplest examples, the system simply possesses a degree of freedom that can take only two values. For example, the spin projection in the case of a nucleus of spin-1/2 or the polarization in the case of a photon. Besides these *intrinsically* two-state systems, a more common situation is that the system has a continuous degree of freedom x, for example, a geometrical coordinate, and a potential energy function $V(x)$ depending on it, with two separate minima [17] (see Fig. 1). Let us assume that the barrier height V is large enough that the system dynamics can be adequately described by a two-dimensional Hilbert space spanned by the two *ground* states in the two wells $|L\rangle$ and $|R\rangle$.

The motion in the two-dimensional Hilbert space can be adequately described by the simple Hamiltonian:

$$\hat{\mathcal{H}}_0 = \sum_{j=L,R} E_j |j\rangle\langle j| - t\left(|R\rangle\langle L| + \text{h.c.}\right) \,, \tag{6}$$

where the tunneling coefficient is given by $t = \langle L|\hat{H}_0|R\rangle$, and

$$\hat{H}_0 = \frac{\hat{p}^2}{2m} + V(x) \tag{7}$$

is the usual system Hamiltonian.

If the potential is an even function of the geometrical coordinate, $V(x) = V(-x)$ (see Fig. 2), $E_L = E_R$, and we can fix $E_L = E_R = 0$. Introducing the Pauli operator $\hat{\rho}_x = |L\rangle\langle R| + \text{h.c.}$, we obtain

$$\hat{\mathcal{H}}_0 = -t\hat{\rho}_x \,, \tag{8}$$

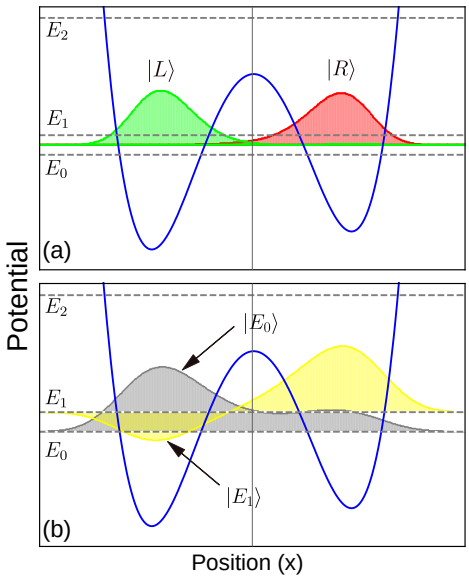

Figure 1. **A double-well system in the *two-state* limit**. The symbols E_0 and E_1 are the two lowest-energy levels, well separated in energy by the next higher energy level E_2. Panel (a) also shows the square modulus of the two wavefunctions localized in the well, obtained as linear combinations of the two lowest energy wavefunctions displayed in panel (b).

whose eigenstates, delocalized in the two wells, are the well-known symmetric- and antisymmetric combinations (see Fig. 2b),

$$|S\rangle = \frac{1}{\sqrt{2}}\left(|R\rangle + |L\rangle\right) ,$$
$$|A\rangle = \frac{1}{\sqrt{2}}\left(|R\rangle - |L\rangle\right) , \qquad (9)$$

with eigenvalues $E_{A,S} = \pm t$, so that $\Delta = E_A - E_S = 2t$, where we assume $t > 0$. The Hamiltonian in Eq. (6) can be written in diagonal form as

$$\hat{\mathcal{H}}_0 = (\Delta/2)\hat{\sigma}_z \, , \qquad (10)$$

where $\hat{\sigma}_z = -\hat{\rho}_x = |A\rangle\langle A| - |S\rangle\langle S|$. Note, to distinguish between the different basis states for the operator representations, we use $\hat{\sigma}_i$ for the $|A\rangle - |S\rangle$ basis, and $\hat{\rho}_i$ for the $|L\rangle - |R\rangle$ basis. Thus, for example, the diagonal $\hat{\sigma}_z$ operator becomes of nondiagonal form in the $|L\rangle - |R\rangle$ basis.

It is worth noticing that this elementary analysis is not restricted to the case of a double-well potential. Analogous considerations can be carried out for systems with different potential shapes, displaying two (e.g., lowest energy) levels well separated in energy from the next higher level. The wavefunctions $\psi_L(x) = \langle x|L\rangle$ and $\psi_R(x) = \langle x|L\rangle$ can be obtained from the symmetric and antisymmetric combinations of $\psi_S(x)$ and $\psi_A(x)$ (see Fig. 1), which can be obtained exactly as the two lowest energy eigenfunctions of the Schrödinger problem described by the Hamiltonian in Eq. (7). The gap $\Delta = 2t$ is obtained from the difference between the corresponding eigenvalues. This two-state tunneling model is a well known formalism to describe many realistic systems, including the ammonia molecule, coupled quantum dots, and superconducting flux-qubits.

The case of a potential of the effective particle which does not display inversion symmetry can also be easily addressed. For example, an asymmetric double well potential, as shown in Fig. 1, can be considered. In this case, Eq. (6) can be expressed as

$$\hat{\mathcal{H}}_0 = \frac{\epsilon}{2}\hat{\rho}_z - \frac{\Delta}{2}\hat{\rho}_x \, . \qquad (11)$$

The quantity ϵ is the *detuning* parameter, that is, the difference in the ground-state energies of the states localized in the two wells in the absence of tunneling. The Hamiltonian in Eq. (11) can be trivially diagonalized with eigenvalues $\pm\omega_q/2$, where $\omega_q = \sqrt{\Delta^2 + \epsilon^2}$.

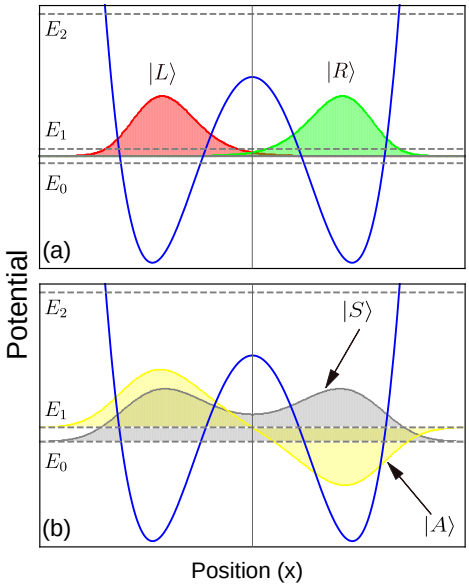

Figure 2. **A symmetric double-well system in the *two-state* limit**. The symbols E_0 and E_1 are the two lowest-energy levels, well separated in energy by the next higher energy level E_2. Panel (a) also shows the square modulus of the two wavefunctions localized in the well, obtained as symmetric and antysimmetric combinations of the two lowest energy wavefunctions displayed in panel (b).

IV. THE GAUGE PRINCIPLE IN TWO-LEVEL SYSTEMS

The question arises if it is possible to *save the gauge principle* when, under the conditions described above, such a particle is adequately described by states confined *in a two-dimensional complex space*. If we apply an arbitrary local phase transformation to, e.g., the wavefunction $\psi_A(x) = \langle x|A\rangle$: $\psi_A(x) \to \psi'_A(x) = e^{iq\theta(x)}\psi_A(x)$, it

happens that, in general, $\psi'_A(x) \neq c_S\psi_S(x) + c_A\psi_A(x)$, where c_A and c_S are complex coefficients. Thus the general local phase transformation does not guarantee that the system can still be described as a two state system. According to this analysis, those works claiming *gauge non-invariance due to material truncation in ultrastrong-coupling QED* [3–5] (we would say at any coupling strength, except negligible), at first sight, might appear to be correct.

The direct consequence of this conclusion would be that two-level models, widespread in physics and chemistry, are too simple to implement their interaction with a gauge field, according to the general principle from which the fundamental interactions in physics are obtained. Since adding to the particle system description a few additional levels does not change this point, the conclusion is even more dramatic. Moreover, according to Stokes and Nazir [4, 5], this leads to several non-equivalent models of light-matter interactions *providing different physical results*. One might then claim the death of the gauge principle and of gauge invariance in truncated Hilbert spaces, namely in almost all cases where theoreticians try to provide quantitative predictions to be compared with experiments.

Our view is drastically different: we find that the breakdown of gauge invariance is the direct consequence of the *inconsistent* approach of reducing the information (Hilbert space truncation) on the effective particle, without accordingly reducing the information, by the same amount, on the phase $\theta(x)$ determining the transformation in Eq. (5). In physics, the approximations must be done with care. These must be consistent.

We start by observing that the two-state system defined in Eq. (6) still has *a geometric coordinate*, which however *can assume only two values*: x_j (with $j = L, R$), that we can approximately identify with the position of the two minima of the double-well potential. More precisely, and more generally, they are:

$$\begin{aligned} x_R &= \langle R|x|R\rangle\,, \\ x_L &= \langle L|x|L\rangle\,. \end{aligned} \tag{12}$$

Here, parity symmetry implies $x_L = -x_R$. In the following we will use the shorthand $\langle R|x|R\rangle = a/2$. Hence, the operator describing the geometric coordinate can be written as [17] $\mathcal{X} = (a/2)\hat{\rho}_z$, where $\hat{\rho}_z \equiv |R\rangle\langle R| - |L\rangle\langle L|$.

We observe that the terms proportional to t in the Hamiltonian in Eq. (6) or Eq. (8), implies that these can be regarded as *nonlocal* Hamiltonians, i.e., with an effective potential depending on two distinct coordinates. Nonlocality here comes from the hopping term $t = \langle R|\hat{H}_0|L\rangle$, which is determined by the interplay of the kinetic energy term and of the potential energy in $\hat{H}_0$.

It is clear that the consistent and meaningful local gauge transformation corresponds to the following transformation

$$|\psi\rangle = c_L|L\rangle + c_R|R\rangle \to |\psi'\rangle = e^{iq\theta_L}c_L|L\rangle + e^{iq\theta_R}c_R|R\rangle\,, \tag{13}$$

where $|\psi\rangle$ is a generic state in the two-dimensional Hilbert space, and θ_j are arbitrary real valued parameters.

It is easy to show that the expectation values of $\hat{\mathcal{H}}_0$ are not invariant under the *local* transformation in Eq. (13). They are only invariant under a uniform phase change: $|\psi\rangle \to e^{iq\theta}|\psi\rangle$. However, one can introduce in the Hamiltonian field-dependent factors that compensate the difference in the phase transformation from one point to the other. Specifically, following the general procedure of lattice gauge theory, we can consider the *parallel transporter* (a unitary *finite-dimensional* matrix), introduced by Kenneth Wilson [11, 18, 19],

$$U_{x_k+a,x_k} = \exp\left[iq\int_{x_k}^{x_k+a} dx\, A(x)\right], \tag{14}$$

where $A(x)$ is the gauge field. After the gauge transformation of the field, $A'(x) = A(x)+d\theta/dx$, the transporter transforms as

$$U'_{x_k+a,x_k} = e^{iq\,\theta(x_k+a)}U_{x_k+a,x_k}e^{-iq\,\theta(x_k)}\,. \tag{15}$$

This property can be used to implement gauge invariant Hamiltonians in two-state systems.

A. Symmetric two-state systems

Introducing properly the parallel transporter in Eq. (14) into Eq. (8), we obtain a gauge-invariant two-level model:

$$\hat{\mathcal{H}}_0^{\rm gi} = -t\,|R\rangle\langle L|\,U_{x_R,x_L} + \text{h.c.}\,. \tag{16}$$

Gauge invariance can be directly verified:

$$\begin{aligned} &\langle\psi'|\left(|R\rangle\langle L|\,U'_{x_R,x_L} + \text{h.c.}\right)|\phi'\rangle = \\ &\langle\psi|\left(|R\rangle\langle L|\,U_{x_R,x_L} + \text{h.c.}\right)|\phi\rangle\,, \end{aligned}$$

where $|\psi\rangle$ and $|\phi\rangle$ are two generic states in the vector space spanned by $|L\rangle$ and $|R\rangle$. By neglecting the spatial variations of the field potential $A(x)$ on the distance $a = x_R - x_L$, (dipole approximation). The Hamiltonian in Eq. (16) can be written as

$$\hat{\mathcal{H}}_0^{\rm gi} = -t\,|R\rangle\langle L|\,e^{iqaA} + \text{h.c.}\,. \tag{17}$$

Using Eq. (9) and the Euler formula, it can be easily verified that the Hamiltonian in Eq. (17) can be expressed using the diagonal basis of $\hat{\mathcal{H}}_0$, as

$$\hat{\mathcal{H}}_0^{\rm gi} = \frac{\Delta}{2}\left[\hat{\sigma}_z\cos(qaA) + \hat{\sigma}_y\sin(qaA)\right], \tag{18}$$

where $\hat{\sigma}_y = -i\,(|A\rangle\langle S| - |S\rangle\langle A|)$. Using Eq. (9) and Eq. (12), then

$$qa/2 = q\langle A|x|S\rangle\,. \tag{19}$$

This precisely coincides with the transition matrix element of the dipole moment as in Ref. [6].

Considering a quantized field $\hat{A}$, the total light-matter Hamiltonian also contains the free-field contribution:

$$\hat{\mathcal{H}} = \frac{\Delta}{2}\left[\hat{\sigma}_z \cos\left(qa\hat{A}\right) + \hat{\sigma}_y \sin\left(qa\hat{A}\right)\right] + \hat{H}_{\rm ph}\,. \tag{20}$$

For the simplest case of a single-mode electromagnetic resonator, the potential can be expanded in terms of the mode photon destruction and creation operators. Around $x = 0$, $\hat{A} = A_0(\hat{a} + \hat{a}^\dagger)$, where A_0 (assumed real) is the zero-point-fluctuation amplitude of the field in the spatial region spanned by the effective particle. We also have: $\hat{H}_{\rm ph} = \omega_{\rm ph}\hat{a}^\dagger\hat{a}$, where $\omega_{\rm ph}$ is the resonance frequency of the mode. It can be useful to define the normalized coupling strength parameter [6]

$$\eta = q(a/2)A_0\,, \tag{21}$$

so that Eq. (20) can be written as

$$\hat{\mathcal{H}} = \frac{\Delta}{2}\left\{\hat{\sigma}_z \cos\left[2\eta(\hat{a} + \hat{a}^\dagger)\right] + \hat{\sigma}_y \sin\left[2\eta(\hat{a} + \hat{a}^\dagger)\right]\right\} + \omega_{\rm ph}\hat{a}^\dagger\hat{a}\,. \tag{22}$$

Using the relations $\hat{\rho}_z \equiv |R\rangle\langle R| - |L\rangle\langle L| = |A\rangle\langle S| + |S\rangle\langle A| \equiv \hat{\sigma}_x$, the Hamiltonian in Eq. (16) can also be expressed as

$$\hat{\mathcal{H}} = \hat{\mathcal{U}}\hat{\mathcal{H}}_0\hat{\mathcal{U}}^\dagger\,, \tag{23}$$

where

$$\hat{\mathcal{U}} = \exp\left(iqa\hat{A}\hat{\sigma}_x/2\right). \tag{24}$$

Equations (23) and (24) coincide with Eqs. (8) and (9) of Ref. [6], which represents the main results.

It is also interesting to rewrite the *coordinate*-dependent phase transformation in Eq. (13) as the application of a unitary operator on the system states. Defining $\phi = (\theta_R + \theta_L)/2$ and $\theta = (\theta_R - \theta_L)/2$, Eq. (13) can be written as

$$|\psi\rangle \to |\psi'\rangle = e^{iq\phi}e^{iq\theta\hat{\sigma}_x}|\psi\rangle\,. \tag{25}$$

This shows that the *coordinate*-dependent phase change of a generic state of a TLS is equivalent to a global phase change, which produces no effect, plus *a rotation in the Bloch sphere*, which can be compensated by introducing a gauge field as in Eq. (23). Notice also that Eq. (25) coincides with the result presented in the first section of the Supplementary Information of Ref. [6], obtained with a different, but equivalent approach.

In summary, the method presented here can be regarded as the two-site version (with the additional dipole approximation) of the general method for *lattice gauge theories* [11], which represents the most advanced and sophisticated tool for describing gauge theories in the presence of truncation of infinite-dimensional Hilbert spaces. These results eliminate any concern about the validity of the results presented in Ref. [6], raised by Stokes and Nazir [5].

We conclude this subsection by noting that Eq. (16) can be also used, without applying the dipole approximation, to obtain the (multi-mode) *gauge-invariant quantum Rabi model beyond the dipole approximation*. Specifically, without applying the dipole approximation to Eq. (16), after the same steps to obtain Eq. (22), we obtain

$$\hat{\mathcal{H}} = \frac{\Delta}{2}\left[\hat{\sigma}_z \cos\left(q\int_{x_L}^{x_R} dx\,\hat{A}(x)\right) + \hat{\sigma}_y \sin\left(q\int_{x_L}^{x_R} dx\,\hat{A}(x)\right)\right] + \hat{H}_{\rm ph}\,. \tag{26}$$

One interesting consequence of this result is that it introduces *a natural cut-off* for the interaction of high energy modes of the electromagnetic field with a TLS. In particular, owing to cancellation effects in the integrals in Eq. (26), the resulting coupling strength between the TLS and the mode goes rapidly to zero when the mode wavelength becomes shorter than $a/2 = \langle A|x|S\rangle$.

It is worth noticing that this derivation of the gauge-invariant QRM does not require the introduction of an externally controlled two-site *lattice* spacing, in contrast to general lattice gauge theories. In the present case, the effective spacing a between the two sites is only determined by the transition matrix element of the position operator between the two lowest energy states of the effective particle, $a = 2\langle A|x|S\rangle$, which in turn determines the dipole moment of the transition, $qa/2$.

B. Asymmetric two-state systems

The results in this section can be directly generalized to also address the case of a potential of the effective particle which does not display inversion symmetry. It has been shown that the interaction (in the USC and DSC limit) of these TLSs (without inversion symmetry) with photons in resonators can lead to a number of interesting phenomena [20–26]. In this case, Eq. (11) provides the bare TLS Hamiltonian. Note that the first term in Eq. (11) is not affected by the two-state local phase transformation in Eq. (13), hence the gauge invariant version of Eq. (11) can be written as

$$\hat{\mathcal{H}}_0^{\rm gi} = \frac{\epsilon}{2}\hat{\rho}_z - \frac{\Delta}{2}\left(|R\rangle\langle L|\,U_{x_R,x_L} + \text{h.c.}\right), \tag{27}$$

which, in the dipole approximation, reads:

$$\hat{\mathcal{H}}_0^{\rm gi} = \frac{\epsilon}{2}\hat{\rho}_z - \frac{\Delta}{2}\left(|R\rangle\langle L|\,e^{iqaA} + \text{h.c.}\right). \tag{28}$$

This can be expressed as

$$\hat{\mathcal{H}}_0^{\rm gi} = \frac{\epsilon}{2}\hat{\rho}_z - \frac{\Delta}{2}\left[\hat{\rho}_x \cos\left(qaA\right) - \hat{\rho}_y \sin\left(qaA\right)\right], \tag{29}$$

which can also be written in the more compact form

$$\hat{\mathcal{H}}_0^{\rm gi} = \hat{\mathcal{U}}\hat{\mathcal{H}}_0\hat{\mathcal{U}}^\dagger\,, \tag{30}$$

where

$$\hat{\mathcal{U}} = \exp\left[iqaA\hat{\rho}_z/2\right]. \tag{31}$$

Equations (30) and (31) represent the minimal coupling replacement for TLS, derived directly from the fundamental gauge principle.

We observe that the operator $\hat{\mathcal{X}} = a\hat{\rho}_z/2$ represents the geometrical-coordinate operator for the two-state system, with eigenvalues $\pm a/2$. The Hamiltonian in Eq. (29) can be directly generalized beyond the dipole approximation with the following replacement:

$$aA \to \int_{-a/2}^{a/2} dx\, A(x). \tag{32}$$

Considering a single-mode electromagnetic resonator, the total Hamiltonian becomes

$$\hat{\mathcal{H}} = \omega_{\rm ph}\hat{a}^\dagger\hat{a} + \frac{\epsilon}{2}\hat{\rho}_z - \frac{\Delta}{2}\left\{\hat{\rho}_x \cos\left[2\eta(\hat{a}+\hat{a}^\dagger)\right] - \hat{\rho}_y \sin\left[2\eta(\hat{a}+\hat{a}^\dagger)\right]\right\}. \tag{33}$$

Since the operator $\hat{\mathcal{X}}$ is the position operator in the two-state space, the unitary operator $\hat{\mathcal{U}}^\dagger = \hat{\mathcal{T}}$ also corresponds to the operator which implements the PZW unitary transformation [27], leading to the dipole-gauge representation,

$$\hat{\mathcal{H}}_d = \hat{\mathcal{U}}^\dagger\hat{\mathcal{H}}\hat{\mathcal{U}} = \omega_{\rm ph}\hat{a}^\dagger\hat{a} + \frac{\epsilon}{2}\hat{\rho}_z - \frac{\Delta}{2}\hat{\rho}_x - i\eta\omega_{\rm ph}(\hat{a}-\hat{a}^\dagger)\hat{\rho}_z + \eta^2\hat{\mathcal{I}}, \tag{34}$$

where we used: $\hat{\rho}_z^2 = \hat{\mathcal{I}}$, where $\mathcal{I}$ is the identity operator for the two-state system. Note that $\hat{\mathcal{H}}_d$ coincides with the Hamiltonian describing a flux qubit interacting with an LC oscillator [24].

V. DISCUSSION

In Sect. IV, we have derived from first principles the general QRM for TLSs. The results presented in Sect. IV exactly coincide with those obtained by Di Stefano *et al.* [6] for symmetric TLSs and in the dipole approximation. This derivation is already sufficient to eliminate any concern about the validity of the results in Ref. [6], recently raised Stokes and Nazir [5]. However, for completeness, here we address some of the specific criticisms that were raised.

A. The main issue raised by Stokes and Nazir in Ref. [5]

The gauge-invariant approaches developed in Sect. IV, and also in Ref. [6], are in contrast with the point of view adopted by Stokes and Nazir [4, 5]. According to them, gauge non-invariance is a necessary implication of the truncation of the Hilbert space of the material system. Moreover, it was claimed [5] that the approach proposed in Ref. [6] rests on an incorrect mathematical assertion and so does not resolve gauge non-invariance.

We have shown in Sect. IV, not only that the gauge-invariant QRM developed in Ref. [6] is correct, but also that it fits well in the spirit of lattice gauge theories initiated by Kenneth Wilson [11]. Hence it is clear that the claims in Refs. [4, 5] – that gauge non-invariance is a necessary implication of the truncation of the Hilbert space of the material system – are not correct.

Consistent with our approach, lattice gauge theories show that it is *vital* to maintain the gauge invariance of a theory after reducing the infinite amount of information associated to a continuous coordinate [11], contrary to the claims of Stokes and Nazir [4, 5].

In this section, we will also show that the method and the assumptions adopted in Ref. [6] to obtain a gauge invariant QRM and a general method to preserve gauge invariance in truncated Hilbert spaces are correct.

The apparent proof that the results in Ref. [6] rests on an incorrect mathematical assertion and does not resolve gauge non-invariance is presented in the section entitled "Material truncation".

According to the authors [5], the main issue is that Ref. [6] tacitly and incorrectly equates

$$\hat{P}\exp\left(iqx\hat{A}\right)\hat{P} = \exp\left[iq(\hat{P}x\hat{P})\hat{A}\right], \tag{35}$$

where $\hat{P}$ is the projection operator for the TLS. Since, they argue, $\hat{P} \neq \hat{I}$ (here $\hat{I}$ indicates the identity operator), in general, if $f(\hat{O})$ is a nonlinear function of a Hermitian operator $\hat{O}$, we have $\hat{P}f(\hat{O})\hat{P} \neq f(\hat{P}\hat{O}\hat{P})$.

Here, the key point from which all the criticisms descend, simply, is that Ref. [6] assumes $\hat{P} = \hat{I}$, while, according to Stokes and Nazir [5], $\hat{P} \neq \hat{I}$. Specifically, the results in Ref. [6], rely on the deliberate decision to treat the effective particle like a TLS, with its own identity. This is very clearly stated already below Eq. (5). Quoting directly from Ref. [6]: "$\hat{P} = |0\rangle\langle 0| + |1\rangle\langle 1|$ is the TLS identity operator". Clearly $\hat{P}$ is an operator with a 2×2 matrix representation. On the contrary, in Ref. [5], and using their different operator notation, P is an *infinite-dimensional* operator. From our perspective, the Hilbert space truncation occurs once and definitely. Moreover, once the matter system is described by a two-state system, any meaningful operator must act on this space and hence, it has a 2×2 matrix representation, and the properties of the identity operators can be legitimately used. As a consequence, operations like, e.g., $\hat{O}^2 = (\hat{P}\hat{O}\hat{P})^2$ are perfectly correct, in contrast to $\hat{O}^2 = (\hat{P}\hat{O}\hat{P})^2$, with $\hat{P}$ defined as in Ref. [5].

References [4, 5] both consider the two-level approximation in a partial and (in our view) inconsistent manner, with operators that repeatedly can *bring the system in and out of the "two-level" system.* Thus, strictly speaking, they do not have a rigorous two-level system, but one

coupled to other external levels. This unfortunate *mix-up* destroys gauge invariance as they show in their plots in Ref. [4].

In order to distinguish between the two different definitions of projection operators, from now on, we will indicate the projection operators as defined in Ref. [6] using calligraphic symbols. Reference [6] starts by using (specifying it from the beginning) $\hat{\mathcal{P}} \equiv \hat{\mathcal{I}}$ already when deriving the dipole-gauge Rabi Hamiltonian in Eq. (5), before presenting the main result [6]. A consequence of this choice, is that the equivalence $\hat{\mathcal{P}}\hat{U}(x)\hat{\mathcal{P}} = \hat{U}(\hat{\mathcal{P}}x\hat{\mathcal{P}})$ is legitimate. This result is obtained by expanding $\hat{U}(x)$ in a Taylor series and then using for each term the relation $\hat{\mathcal{P}}x^n\hat{\mathcal{P}} = (\hat{\mathcal{P}}x\hat{\mathcal{P}})^n$, which can be easily obtained using the properties of identity operators. This procedure is described in detail at the beginning of the Section I of the Supplementary Material of Ref. [6] for a generic operator $\hat{D}(\theta) = e^{iq\theta(x)}$.

In summary, Stokes and Nazir [5] strongly criticizes the consequences of the choice $\hat{\mathcal{P}} \equiv \hat{\mathcal{I}}$. They explain that for a non-linear function f, [see Eq. (20)], $\hat{P}f(\hat{O})\hat{P} \neq f(\hat{P}\hat{O}\hat{P})$, which is of course correct if $\hat{P}$ is not the identity operator. However, we are surprised to see that, a few lines before Eq. (20), Ref. [5] seems to contradict itself, by using $\hat{P}f(\hat{O})\hat{P} = f(\hat{P}\hat{O}\hat{P})$ to derive their Eq. (17). Specifically, following the procedure introduced in Ref. [4], Stokes and Nazir [5] start from the non-truncated total Hamiltonian H_α. Then, they apply the projection operator P to obtain their standard α-gauge two-level model. However, they treat in a *different* way the free atomic Hamiltonian H_m and the light-matter interaction term $\mathcal{V}_\alpha$. Specifically, they apply the first projection operator as PH_mP, but instead of applying the same procedure to the interaction term: $\mathcal{V}_\alpha \to P\mathcal{V}_\alpha P$, they use the non-equivalent (according to their definition of P) truncation: $\mathcal{V}_\alpha(x,p) \to \mathcal{V}_\alpha(PxP, PpP)$. Since $\mathcal{V}^\alpha(x,p)$ is a non-linear function of x (it contains a quadratic term), it is not at all clear why the authors used $\mathcal{V}^\alpha(PxP, PpP)$, instead of $P\mathcal{V}^\alpha(x,p)P$.

The same procedure is also adopted and briefly described by Stokes and Nazir in Ref. [4] (see the Methods section in particular). Below Eq. (12), (which is the same, in a slightly different notation of Eq. (16) in Ref. [5]), the authors write:
"If the interaction Hamiltonian V^α is linear in $\mathbf{r}$ and $\mathbf{p}_\alpha$ then the two-level model Hamiltonian can also be written $H_2^\alpha = P^\alpha H P^\alpha$. This is not the case for H in Eq. (11) due to the "$\hat{\mathbf{d}}^2$" term, which demonstrates the availability of different methods for deriving truncated models. Here we adopt the approach most frequently encountered in the literature, and outline other methods in Supplementary Note 2."

In summary, not only do Stokes and Nazir [5] use what a few lines below claim to be absolutely wrong, but, in a closely related work, the same authors also admit, after using this procedure, that it is "frequently encountered in the literature".

B. Gauge-ambiguities

Stokes and Nazir [5] (see also Ref. [28]) also point out that gauge-ambiguities are much broader than gauge non-invariance that results from an approximation. According to these references, subsystem predictions vary significantly with the gauge relative to which the subsystems are defined independent of model approximations.

Although it is true that features such as, e.g., the amount of light-matter entanglement and of bare excitations in the system eigenstates, are gauge-relative, in our opinion, this statement can be misleading and requires some comment. In particular, we observe that, as described in detail in Ref. [7], the approach developed in Ref. [6] can be applied to remove gauge ambiguities in all the experimentally observable quantities including the detectable light-matter entanglement in the ground state of cavity-QED systems, even in the presence of Hilbert space truncation. This is one of the main results of Ref. [7]. The main point here is that measurements (as, e.g., experimental clicks or transmission amplitudes) are numbers that do not care about our gauge discussions. Therefore, if our approximations are applied consistently, as theoreticians, we should provide these numbers. As theoreticians, we can play with different representations, but all of them must be consistent and unambiguous. Reference [7] shows that this is the case even under extreme conditions, as in the presence of deep ultrastrong light-matter interactions and/or non-adiabatic ultrafast switches of the interaction. These theories work well even in the presence of relevant approximations, if these are carried out in a consistent manner.

C. Other points raised by Ref. [5]

- **Bloch sphere rotation**

According to Stokes and Nazir [5], the models actually analysed in Ref. [4] are Bloch sphere rotations of the multipolar QRM.

As a matter of fact, the light-matter interaction is introduced, at a fundamental level, by invoking the gauge principle. This leads to the minimal coupling replacement. Then, a gauge (unitary) transformation can be applied to obtain the multipolar gauge Hamiltonian, which acquires a simple form in the dipole approximation. In Sect. I of the Supplementary Material of Ref. [6], it is explained how the results in Ref. [6] are indeed able to satisfy the gauge principle. Results in Sect. IV confirm this result in a very clear and precise way. Hence, from a fundamental point of view, the opposite is true: The multipolar QRM works fine because it is a Bloch sphere rotation (as required by gauge invariance in TLSs) of the Hamiltonian in Eqs. (8) and (9) of Ref. [6].

As a final remark on this point, we observe that in the Coulomb gauge and using the QRM of Ref. [6], the electric field operator can be expanded in terms of creation and destruction photon operators, as in the not-

truncated model, and as in the free electromagnetic theory (in the absence of interactions). On the contrary, after the gauge transformation in the multipolar QRM, the electric field operator also contains contributions from the atomic dipole, as a consequence of the PZW transformation. This is shown in detail in Ref. [7]. This view is further confirmed by Eq. (16) here, which can be used to derive the QRM beyond the dipole approximation in Eq. (26). A result that, to our knowledge, has never been obtained, so far within any gauge, including the multipolar gauge.

- **Non-equivalent models**

Stokes and Nazir [5] state:, "the idea of Ref. [4] (here Ref. [6]) to define two-level model gauge transformations as projections of gauge-fixing transformations does not resolve gauge non-invariance, because it does not produce equivalent models." The authors refuse our choice to regard the operator $\hat{\mathcal{P}}$ as the identity operator for the two-level space, although it seems that they also use it [4, 5] (see Sec. V). Then, they realize [5] that refusing this implies that gauge non-invariance in truncated Hilbert spaces cannot be resolved. This is not surprising, since in Sect. I of the Supplementary Material of Ref. [6], it has been shown that the gauge principle is satisfied using repeatedly the properties of the identity operator.

In our view, the conclusion reached in Ref. [5] is a direct consequence of an inconsistent choice attributed to Ref. [6]. Sect. IV here further confirms that only the choice $\hat{P} = \hat{I}$ can produce a gauge invariant theory in the spirit of lattice gauge theories.

D. Some consequences of renouncing gauge invariance

The consequence of the only possible choice, according to Refs. [4, 5], is that the gauge principle cannot be implemented in truncated Hilbert spaces, and gauge transformations provide non-equivalent light-matter interaction models. Since this remains true beyond TLSs, and since almost every practical calculation involving field-matter interactions is carried out cutting the infinite amount of information provided by exact infinite-dimensional Hilbert spaces, *the unpleasant conclusion of Stokes and Nazir [4, 5] is that gauge invariance and the gauge principle do not work in most practical cases.* Naturally, this would be a huge problem, not only in cavity QED, but also for a wide range of calculations, including the transport and optical properties of solids, especially in the presence of strong fields, and for the broad field of lattice gauge theories in quantum field theory and in condensed matter many-body quantum physics [11]. As shown, e.g., in Refs. [12–15, 18, 19], [11] and references therein, *luckily* this is not the case (see also Sect. IV).

VI. ON THE EXISTENCE OF SYSTEM-DEPENDENT *OPTIMAL* QUANTUM RABI MODELS

In Stokes and Nazir's Ref. [5], and also in their Ref. [4], the authors correctly admit that the dipole gauge is optimal when the anharmonicity is high. However, a system with high anharmonicity is just, as also discussed in Ref. [6], a system where the two level truncation can be safely performed, even in the presence of very high light-matter coupling strength.

On the contrary, when the anharmonicity, μ (with $\mu = (\omega_{2,1} - \omega_{1,0})/\omega_{10}$) is of the same order or lower than the normalized light-matter interaction strength η (i.e., $\mu \sim \eta$), the two level approximation becomes unreliable, because the detuning between the cavity frequency and the additional atomic transition frequencies becomes comparable with the coupling strength. This trivial and well-known issue has been described in detail in Sect. V of the Supplementary Information of Ref. [6].

In addition, if a strong positive detuning between the cavity-mode resonance frequency and the two-level transition frequency is considered, the coupling of additional atomic transitions with the cavity photons becomes even more relevant, and the two-level approximation becomes pointless. Indeed, this is the situation corresponding to a number of plots in Ref. [4].

Ref. [5], citing Ref. [4], explains that the multipolar-gauge (what we call dipole-gauge) does not work when the material system is an harmonic oscillator. In Ref. [4] the same concept is explained as: "We show further that if the material system is a harmonic oscillator, then it is possible to derive a JCM (Jaymes Cummings model) that is necessarily more accurate than any derivable QRM (quantum Rabi model) for finding ground-state averages."

It is well-known that the spectra and the physical properties of a harmonic system constituted by two coupled harmonic oscillators is very far from those of a system constituted of a two-level model interacting with a harmonic oscillator (QRM). Hence, the fact that the dipole-gauge QRM, which is an highly non-linear model is not able to describe harmonic oscillators is not surprising. However we are not able to catch the meaning of a highly nonlinear model, used as a fit to to reproduce only some very limited feature of the physics of two coupled harmonic oscillators (weak excitation limit).

We could elaborate in significantly more details and considerations, however, this is not the right place for a detailed analysis of the results in Ref. [4].

In the present work, we have shown how to apply the fundamental gauge principle to TLSs in order to derive a gauge-invariant QRM. Of course, this procedure works fine, until, taking also into account the interaction with the gauge field, the two-level approximation is meaningful. Naturally, if the detuning between the field and additional transitions becomes comparable with the coupling strength, these cannot be ignored anymore, and the two-

level approximation is no more adequate.

VII. CONCLUSIONS

In contrast with the claims of Stokes and Nazir [5], we have shown in Sect. IV of this work that the results presented in Ref. [6], and also used in Ref. [7], are correct, deriving them with an alternative, more direct and fundamental method. This derivation shows that the results in Ref. [6] are not only correct, but they constitute the only route (to our knowledge) to implement, in a fully consistent and physically meaningful way, the fundamental gauge principle in truncated Hilbert spaces. We have also extended the results in Ref. [6] to asymmetric two-state systems.

In addition, the method used here allowed us to obtain the gauge-invariant QRM beyond the dipole approximation, which is one of the main results of this work. Note that the problem of a quantum-mechanical system, whose state is effectively restricted to a two-dimensional Hilbert space and which interacts with the electromagnetic field in various regimes, is ubiquitous in physics and chemistry [17]. Hence, the availability of a general gauge-invariant model describing this widespread physics is highly desirable.

The results in Sect. IV shows that the results in Ref. [6] also fit well in the great tradition of lattice gauge theories opened by Kenneth Wilson [11]. Lattice gauge theories constitute a powerful reference example where it is possible and also *vital* to maintain the gauge invariance of a theory after reducing the infinite amount of information associated to a continuous coordinate [11], contrary to the claims of Refs. [4, 5].

A noteworthy feature of this derivation of the gauge-invariant QRM is that, in the present case, the two-site *lattice* spacing is not externally controlled, in contrast to general lattice gauge theories. Here, the effective spacing a between the two sites is only determined by the transition matrix element of the position operator between the two lowest energy states of the effective particle, which in turn determines the dipole moment of the transition.

In Sect. V we have also disproved the criticism by Stokes and Nazir [5], claiming that the results in Ref. [6] rest on an incorrect mathematical assertion.

We conclude with some key observations from Sect. V B, where we pointed out that the analysis here and in Refs. [6, 7] also remove gauge ambiguities in the experimentally observable quantities, including the detectable light-matter entanglement in the ground state of cavity-QED systems, even in the presence of Hilbert space truncation. This is one of the main results of Ref. [7]. The key point is that *measurements* (as, e.g., experimental clicks or transmission amplitudes) *are data that do not care about gauge representations*. Therefore, if our approximations are applied consistently, as theoreticians, we should provide numbers which are not affected by gauge transformations. Of course, as theoreticians we can play with different representations, but all of them must be consistent. Reference [7] shows that this is the case even under extreme conditions, as in the presence of deep ultrastrong light-matter interactions and/or non-adiabatic ultrafast switches of the interaction. All this works even in the presence of relevant approximations, if these are carried out in a consistent way.

If a theory is to be useful and meaningful, it should remove any ambiguities in the description of experimental data – so a theory that is introduced to be ambiguous and not gauge invariant, ultimately is not very useful; so claiming such a theory is more correct is futile.

ACKNOWLEDGMENTS

F.N. is supported in part by: NTT Research, Army Research Office (ARO) (Grant No. W911NF-18-1-0358), Japan Science and Technology Agency (JST) (via the CREST Grant No. JPMJCR1676), Japan Society for the Promotion of Science (JSPS) (via the KAKENHI Grant No. JP20H00134, and the grant JSPS-RFBR Grant No. JPJSBP120194828), and the Grant No. FQXi-IAF19-06 from the Foundational Questions Institute Fund (FQXi), a donor advised fund of the Silicon Valley Community Foundation. SH acknowledges funding from the Canadian Foundation for Innovation, and the Natural Sciences and Engineering Research Council of Canada. S.S. acknowledges the Army Research Office (ARO) (Grant No. W911NF1910065).

[1] A. F. Kockum, A. Miranowicz, S. De Liberato, S. Savasta, and F. Nori, "Ultrastrong coupling between light and matter," Nat. Rev. Phys. **1**, 19 (2019).
[2] P. Forn-Díaz, L. Lamata, E. Rico, J. Kono, and E. Solano, "Ultrastrong coupling regimes of light-matter interaction," Rev. Mod. Phys. **91**, 025005 (2019).
[3] D. De Bernardis, P. Pilar, T. Jaako, S. De Liberato, and P. Rabl, "Breakdown of gauge invariance in ultrastrong-coupling cavity QED," Phys. Rev. A **98**, 053819 (2018).
[4] A. Stokes and A. Nazir, "Gauge ambiguities imply Jaynes-Cummings physics remains valid in ultrastrong coupling QED," Nat. Commun. **10**, 499 (2019).
[5] A. Stokes and A. Nazir, "Gauge non-invariance due to material truncation in ultrastrong-coupling QED," Preprint at arXiv:2005.06499v1 (2020).
[6] O. Di Stefano, A. Settineri, V. Macrì, L. Garziano, R. Stassi, S. Savasta, and F. Nori, "Resolution of gauge ambiguities in ultrastrong-coupling cavity QED," Nat. Phys. **15**, 803 (2019).
[7] A. Settineri, O. Di Stefano, D. Zueco, S. Hughes, S. Savasta, and F. Nori, "Gauge freedom, quantum measurements, and time-dependent interactions in cavity and

circuit QED," Preprint at arxiv: 1912.08548 (2019).
[8] S. Savasta, O. Di Stefano, and F. Nori, "TRK sum rule for interacting photons," Preprint at arXiv:2002.02139 (2020).
[9] L. Garziano, A. Settineri, O. Di Stefano, S. Savasta, and F. Nori, "Gauge invariance of the Dicke and Hopfield models," Preprint at arXiv:2002.04241 (2020).
[10] Alexandre Le Boité, "Theoretical Methods for Ultrastrong Light–Matter Interactions," Adv. Quantum Technol. , 1900140 (2020).
[11] U.-J. Wiese, "Ultracold quantum gases and lattice systems: quantum simulation of lattice gauge theories," Ann. Phys. **525**, 777–796 (2013).
[12] R. Peierls, Z. Phys. **80**, 763–790 (1933).
[13] J. M. Luttinger, "The effect of a magnetic field on electrons in a periodic potential," Phys. Rev. **84**, 814–817 (1951).
[14] D. R. Hofstadter, "Energy levels and wave functions of Bloch electrons in rational and irrational magnetic fields," Phys. Rev. B **14**, 2239–2249 (1976).
[15] M. Graf and P. Vogl, "Electromagnetic fields and dielectric response in empirical tight-binding theory," Phys. Rev. B **51**, 4940–4949 (1995).
[16] M. Maggiore, *A modern introduction to quantum field theory*, Oxford Series in Physics No. 12 (Oxford University Press, 2005).
[17] A. J. Leggett, S. Chakravarty, A. T. Dorsey, M. P. A. Fisher, A. Garg, and W. Zwerger, "Dynamics of the dissipative two-state system," Rev. Mod. Phys. **59**, 1–85 (1987).
[18] K. G. Wilson, "Confinement of quarks," Phys. Rev. D **10**, 2445–2459 (1974).
[19] C. B. Lang, *Quantum chromodynamics on the lattice: an introductory presentation* (Springer, 2010).
[20] T. Niemczyk, F. Deppe, H. Huebl, E. P. Menzel, F. Hocke, M. J. Schwarz, J. J. Garcia-Ripoll, D. Zueco, T. Hümmer, E. Solano, A. Marx, and R. Gross, "Circuit quantum electrodynamics in the ultrastrong-coupling regime," Nat. Phys. **6**, 772–776 (2010).
[21] A. Ridolfo, M. Leib, S. Savasta, and M. J. Hartmann, "Photon blockade in the ultrastrong coupling regime," Phys. Rev. Lett. **109**, 193602 (2012).
[22] L. Garziano, R. Stassi, V. Macrì, A. F. Kockum, S. Savasta, and F. Nori, "Multiphoton quantum Rabi oscillations in ultrastrong cavity QED," Phys. Rev. A **92**, 063830 (2015).
[23] L. Garziano, V. Macrì, R. Stassi, O. Di Stefano, F. Nori, and S. Savasta, "One photon can simultaneously excite two or more atoms," Phys. Rev. Lett. **117**, 043601 (2016).
[24] F. Yoshihara, T. Fuse, S. Ashhab, K. Kakuyanagi, S. Saito, and K. Semba, "Superconducting qubit-oscillator circuit beyond the ultrastrong-coupling regime," Nat. Phys. **13**, 44–47 (2017).
[25] A. F. Kockum, A. Miranowicz, V. Macrì, S. Savasta, and F. Nori, "Deterministic quantum nonlinear optics with single atoms and virtual photons," Phys. Rev. A **95**, 063849 (2017).
[26] R. Stassi, V. Macrì, A. F. Kockum, O. Di Stefano, A. Miranowicz, S. Savasta, and F. Nori, "Quantum nonlinear optics without photons," Phys. Rev. A **96**, 023818 (2017).
[27] M. Babiker and R. Loudon, "Derivation of the Power-Zienau-Woolley Hamiltonian in quantum electrodynamics by gauge transformation," Proc. R. Soc. Lond. A **385**, 439–460 (1983).
[28] A. Stokes and A. Nazir, "Ultrastrong time-dependent light-matter interactions are gauge-relative," Preprint at arXiv:1902.05160 (2019).

6.5 Conclusions and Outlook

In this thesis work I presented the research activity developed during my Ph.D. program, mainly focused on several aspects of hybrid quantum systems. Specifically, I followed two lines of research. The first one concerns the study of dissipation and decoherence effects in open quantum systems entering the USC light-matter regime. The second line of research is devoted to the resolution of recently claimed gauge invariance issues in USC cavity- and circuit-QED. [79, 119, 120]. In the following I will draw a brief summary of the main results and achievements obtained in both this research activities.

Among the most relevant results obtained in the study of open quantum system dynamics in the USC regime, we presented a generalized dressed master equation [72], valid for arbitrary open hybrid quantum systems interacting with thermal reservoirs and for arbitrary strength of the coupling between the components of the hybrid system. The latter allowed us to study the dynamics of systems with harmonic, quasiharmonic, and anharmonic transitions. For example, exploiting this new theoretical tool, we demonstrated that mechanical quantum excitations can be coherently transferred among spatially separated mechanical oscillators through a dissipation-less quantum bus, due to the exchange of virtual Casimir photon pairs [121]. Moreover, a significant measurable flux of Casimir photons can be obtained in optomechanical systems also without a coherent pumping, suggesting another way for the experimental observation of the DCE [122]. Specifically, we demonstrated that an incoherently excited vibrating mirror can emit Casimir photon pairs, in analogy to atomic fluorescence or electroluminescence in semiconductor devices. The experimental demonstration of both of these processes could have important consequences. The first would show that the electromagnetic quantum vacuum is able to transfer mechanical energy somewhat like an ordinary fluid, opening up exciting possibilities of applying ideas from fluid dynamics in the study of the electromagnetic quantum vacuum. The experimental realization of this effect would make the DCE in high-frequency optomechanical systems a versatile and powerful new resource for the development of quantum-optomechanical technologies. On the other hand, the

possibility to observe a DCE by an incoherent thermal-like excitation would allow the parametric conversion of mechanical energy into electromagnetic energy in optomechanical systems where the mechanical frequency is usually much lower than the cavity frequency, eliminating the need for extremely high mechanical oscillation frequencies and ultrastrong single-photon optomechanical coupling. Furthermore, this new process could be exploited in order to achieve two-photon hyper-Raman scattering, where squeezed photons already present in an optical resonator are scattered into resonant cavity-photon pairs, in parametrically amplified optomechanical systems.

Gauge invariance is a general guiding principle in building the theory of fundamental interactions stating that all physical results must be independent of the gauge choice. In the recent years, different authors claimed that approximate models for light–matter interactions derived in different gauges may lead to different predictions, or can display different convergence properties in ultrastrongly coupled light-matter systems. After identifying the source of this gauge violation, we developed a method able to derive the correct gauge-invariant form of Hamiltonians in truncated Hilbert spaces valid even for extreme light–matter interaction regimes [123]. Exploiting this method, we derived the correct quantum Rabi Hamiltonian in the Coulomb gauge. Besides solving long-lasting controversies arising from gauge ambiguities in the quantum Rabi and Dicke models, these results could be also relevant for the study of systems with non-adiabatic time-dependent coupling strength and for the study of open quantum systems. For example, it turns out that when the interaction of the light and matter components of a quantum system is very strong (USC), the correct gauge dependence of the subsystem operators appearing in the master equation cannot be neglected as usual. Moreover, if the coupling between a subsystem (for example, the matter system) and the environment is described by a gauge interaction and the system–bath coupling strength is not weak, the preservation of the gauge principle should be ensured despite any truncation procedure. Furthermore, we have also investigated the gauge invariance of the Dicke model in the dilute regime, and deriving, also in this case, the correct gauge-invariant Dicke Hamiltonian in the Coulomb gauge for both a finite number N of dipoles and

in the dilute regimes with $N \to \infty$ [124]. Finally, by employing an *operational* approach based on the physical measurements of the system observables, we have investigated and solved a number of qualitative ambiguities in the theoretical description of cavity- and circuit-QED systems [125]. Among them we can highlight the proper definition of subsystem and their quantum measurements, the structure of light-matter ground states and the analysis of time-dependent interactions. In particular, even if we focused our attention on the quantum Rabi model, our results can be extended to matter systems including, multi-levels systems, a collection of quantum emitters, collective excitations, multi-mode resonators and atoms (natural or artificial) coupled to a continuum of light modes, finding possible applications even in cavity quantum optomechanics.

In a very recent preprint [126], we pointed out the relationship between the gauge-invariant quantum Rabi model and lattice gauge theories. This connection, I believe, will allow soon to obtain gauge-invariant models for the rigorous study of cavity-embedded 1D chains, and 2D systems, like graphene [127–129]. Furthermore, this approach, will allow the development of accurate models for studying topological quantum photonics and the cavity QED of interacting electron systems.

In conclusion, looking at the recent scientific literature, there is a great growing interest in studying light-matter interactions in the ultrastrong coupling regime. The results presented in this thesis have been so far very well received by the referees of various journals, and are receiving several citations. I am quite confident that my Ph.D. work will have a significant impact in the field of interacting quantum systems, and may contribute to the development of novel quantum technologies.

Bibliography

[1] F. Wolfgramm, C. Vitelli, F. A. Beduini, N. Godbout, and M. Mitchell, "Entanglement-enhanced probing of a delicate material system," *Nat. Phot.*, vol. 7, no. 1, pp. 28–32, 2013.

[2] C. Hempel, B. Lanyon, P. Jurcevic, R. Gerritsma, R. Blatt, and C. Roos, "Entanglement-enhanced detection of single-photon scattering events," *Nat. Phot.*, vol. 7, no. 8, pp. 630–633, 2013.

[3] C. Ockeloen, R. Schmied, M. Riedel, and P. Treutlein, "Quantum metrology with a scanning probe atom interferometer," *Phys. Rev. Lett.*, vol. 111, no. 14, p. 143001, 2013.

[4] G. Kurizki, P. Bertet, Y. Kubo, K. Mølmer, D. Petrosyan, P. Rabl, and J. Schmiedmayer, "Quantum technologies with hybrid systems," *Proceedings of the National Academy of Sciences*, vol. 112, no. 13, pp. 3866–3873, 2015.

[5] N. Gisin, G. Ribordy, W. Tittel, and H. Zbinden, "Quantum cryptography," *Rev. Mod. Phys.*, vol. 74, no. 1, p. 145, 2002.

[6] A. Sergienko, *Quantum communications and cryptography*. CRC Press, 2005.

[7] M. Nielsen and I. Chuang, *Quantum computation and quantum information*. Cambridge university press, 2010.

[8] A. Aspuru-Guzik and P. Walther, "Photonic quantum simulators," *Nat. Phys.*, vol. 8, no. 4, pp. 285–291, 2012.

[9] I. Bloch, J. Dalibard, and S. Nascimbène, "Quantum simulations with ultracold quantum gases," *Nat. Phys.*, vol. 8, no. 4, pp. 267–276, 2012.

[10] R. Blatt and C. Roos, "Quantum simulations with trapped ions," *Nat. Phys.*, vol. 8, no. 4, pp. 277–284, 2012.

[11] J. Morton and B. Lovett, "Hybrid solid state qubits: the powerful role of electron spins," *arXiv preprint arXiv:1103.0418*, 2011.

[12] P. C. Maurer, G. Kucsko, C. Latta, L. Jiang, N. Yao, S. Bennett, F. Pastawski, D. Hunger, N. Chisholm, M. Markham, *et al.*, "Room-temperature quantum bit memory exceeding one second," *Science*, vol. 336, no. 6086, pp. 1283–1286, 2012.

[13] J. Pla, K. Tan, J. Dehollain, W. Lim, J. Morton, F. Zwanenburg, D. Jamieson, A. Dzurak, and A. Morello, "High-fidelity readout and control of a nuclear spin qubit in silicon," *Nature*, vol. 496, no. 7445, pp. 334–338, 2013.

[14] R. J. Schoelkopf and S. M. Girvin, "Wiring up quantum systems," *Nature*, vol. 451, no. 7179, pp. 664–669, 2008.

[15] A. A. Houck, H. E. Türeci, and J. Koch, "On-chip quantum simulation with superconducting circuits," *Nat. Phys.*, vol. 8, no. 4, pp. 292–299, 2012.

[16] M. Poot and H. van der Zant, "Mechanical systems in the quantum regime," *Phys. Rep.*, vol. 511, no. 5, pp. 273–335, 2012.

[17] M. Aspelmeyer, T. J. Kippenberg, and F. Marquardt, "Cavity optomechanics," *arXiv preprint arXiv:1303.0733*, 2013.

[18] M. Wallquist, K. Hammerer, P. Rabl, M. Lukin, and P. Zoller, "Hybrid quantum devices and quantum engineering," *Phys. Scr.*, vol. 2009, no. T137, p. 014001, 2009.

[19] Z.-L. Xiang, S. Ashhab, J. You, and F. Nori, "Hybrid quantum circuits: Superconducting circuits interacting with other quantum systems," *Rev. Mod. Phys.*, vol. 85, no. 2, p. 623, 2013.

[20] P. Treutlein, C. Genes, K. Hammerer, M. Poggio, and P. Rabl, "Hybrid mechanical systems," in *Cavity Optomechanics*, pp. 327–351, Springer, 2014.

[21] I. Chiorescu, P. Bertet, K. Semba, Y. Nakamura, C. Harmans, and J. Mooij, "Coherent dynamics of a flux qubit coupled to a harmonic oscillator," *Nature*, vol. 431, no. 7005, pp. 159–162, 2004.

[22] J. You and F. Nori, "Superconducting circuits and quantum information," *Phys. Today*, vol. 58, no. 11, p. 42, 2005.

[23] J. Clarke and F. Wilhelm, "Superconducting quantum bits," *Nature*, vol. 453, no. 7198, pp. 1031–1042, 2008.

[24] S. Girvin, M. Devoret, and R. Schoelkopf, "Circuit QED and engineering charge-based superconducting qubits," *Phys. Scr.*, vol. 2009, no. T137, p. 014012, 2009.

[25] I. Buluta, S. Ashhab, and F. Nori, "Natural and artificial atoms for quantum computation," *Rep. Prog. Phys.*, vol. 74, no. 10, p. 104401, 2011.

[26] J. You and F. Nori, "Atomic physics and quantum optics using superconducting circuits," *Nature*, vol. 474, no. 7353, pp. 589–597, 2011.

[27] J. You, J. Tsai, and F. Nori, "Hybridized solid-state qubit in the charge-flux regime," *Phys. Rev. B*, vol. 73, no. 1, p. 014510, 2006.

[28] J. Koch, M. Terri, J. Gambetta, A. Houck, D. Schuster, J. Majer, A. Blais, M. Devoret, S. Girvin, and R. Schoelkopf, "Charge-insensitive qubit design derived from the cooper pair box," *Phys. Rev. A*, vol. 76, no. 4, p. 042319, 2007.

[29] J. You, X. Hu, S. Ashhab, and F. Nori, "Low-decoherence flux qubit," *Phys. Rev. B*, vol. 75, no. 14, p. 140515, 2007.

[30] V. E. Manucharyan, J. Koch, L. I. Glazman, and M. H. Devoret, "Fluxonium: Single cooper-pair circuit free of charge offsets," *Science*, vol. 326, no. 5949, pp. 113–116, 2009.

[31] M. Devoret, S. Girvin, and R. Schoelkopf, "Circuit-QED: How strong can the coupling between a josephson junction atom and a transmission line resonator be?," *Ann. Phys.*, vol. 16, no. 10-11, pp. 767–779, 2007.

[32] J. Bourassa, J. M. Gambetta, A. A. Abdumalikov Jr, O. Astafiev, Y. Nakamura, and A. Blais, "Ultrastrong coupling regime of cavity QED with phase-biased flux qubits," *Phys. Rev. A*, vol. 80, no. 3, p. 032109, 2009.

[33] T. Niemczyk, F. Deppe, H. Huebl, E. Menzel, F. Hocke, M. Schwarz, J. García-Ripoll, D. Zueco, T. Hümmer, E. Solano, A. Marx, and R. Gross, "Circuit quantum electrodynamics in the ultrastrong-coupling regime," *Nature Phys.*, vol. 6, no. 10, pp. 772–776, 2010.

[34] P. Forn-Díaz, J. Lisenfeld, D. Marcos, J. García-Ripoll, E. Solano, C. Harmans, and J. Mooij, "Observation of the Bloch-Siegert shift in a qubit-oscillator system in the ultrastrong coupling regime," *Phys. Rev. Lett.*, vol. 105, no. 23, p. 237001, 2010.

[35] G. Romero, D. Ballester, Y. Wang, V. Scarani, and E. Solano, "Ultrafast quantum gates in circuit QED," *Phys. Rev. Lett.*, vol. 108, no. 12, p. 120501, 2012.

[36] S. De Liberato, D. Gerace, I. Carusotto, and C. Ciuti, "Extracavity quantum vacuum radiation from a single qubit," *Phys. Rev. A*, vol. 80, no. 5, p. 053810, 2009.

[37] R. Stassi, A. Ridolfo, O. Di Stefano, M. Hartmann, and S. Savasta, "Spontaneous conversion from virtual to real photons in the ultrastrong-coupling regime," *Phys. Rev. Lett.*, vol. 110, no. 24, p. 243601, 2013.

[38] A. Ridolfo, S. Savasta, and M. Hartmann, "Nonclassical radiation from thermal cavities in the ultrastrong coupling regime," *Phys. Rev. Lett.*, vol. 110, no. 16, p. 163601, 2013.

[39] E. Jaynes and F. Cummings, "Comparison of quantum and semiclassical radiation theories with application to the beam maser," *Proceedings of the IEEE*, vol. 51, no. 1, pp. 89–109, 1963.

[40] J. Casanova, G. Romero, I. Lizuain, J. J. García-Ripoll, and E. Solano, "Deep strong coupling regime of the Jaynes-Cummings model," *Phys. Rev. Lett.*, vol. 105, no. 26, p. 263603, 2010.

[41] C. Ciuti, G. Bastard, and I. Carusotto, "Quantum vacuum properties of the intersubband cavity polariton field," *Phys. Rev. B*, vol. 72, no. 11, p. 115303, 2005.

[42] T. J. Kippenberg and K. J. Vahala, "Cavity optomechanics: backaction at the mesoscale," *Science*, vol. 321, no. 5893, pp. 1172–1176, 2008.

[43] I. Favero and K. Karrai, "Optomechanics of deformable optical cavities," *Nat. Photonics*, vol. 3, no. 4, pp. 201–205, 2009.

[44] F. Marquardt and S. M. Girvin, "Optomechanics," *Physics*, vol. 2, p. 40, May 2009.

[45] M. Aspelmeyer, T. J. Kippenberg, and F. Marquardt, "Cavity optomechanics," *Rev. Mod. Phys.*, vol. 86, pp. 1391–1452, Dec 2014.

[46] O. Arcizet, P. Cohadon, T. Briant, M. Pinard, and A. Heidmann, "Radiation-pressure cooling and optomechanical instability of a micromirror," *Nature*, vol. 444, no. 7115, pp. 71–74, 2006.

[47] A. Schliesser, P. Del'Haye, N. Nooshi, K. J. Vahala, and T. J. Kippenberg, "Radiation pressure cooling of a micromechanical oscillator using dynamical backaction," *Phys. Rev. Lett.*, vol. 97, p. 243905, Dec 2006.

[48] J. Thompson, B. Zwickl, A. Jayich, F. Marquardt, S. Girvin, and J. Harris, "Strong dispersive coupling of a high-finesse cavity to a micromechanical membrane," *Nature*, vol. 452, no. 7183, pp. 72–75, 2008.

[49] G. Anetsberger, O. Arcizet, Q. P. Unterreithmeier, R. Rivière, A. Schliesser, E. M. Weig, J. P. Kotthaus, and T. J. Kippenberg, "Near-field cavity optomechanics with nanomechanical oscillators," *Nature Physics*, vol. 5, no. 12, pp. 909–914, 2009.

[50] M. Eichenfield, R. Camacho, J. Chan, K. Vahala, and O. Painter, "A picogram-and nanometre-scale photonic-crystal optomechanical cavity," *Nature*, vol. 459, no. 7246, pp. 550–555, 2009.

[51] J. R. Johansson, G. Johansson, and F. Nori, "Optomechanical-like coupling between superconducting resonators," *Phys. Rev. A*, vol. 90, p. 053833, Nov 2014.

[52] R. C. Jaklevic, J. Lambe, A. H. Silver, and J. E. Mercereau, "Quantum interference effects in josephson tunneling," *Phys. Rev. Lett.*, vol. 12, pp. 159–160, Feb 1964.

[53] C. Wilson, G. Johansson, A. Pourkabirian, M. Simoen, J. Johansson, T. Duty, F. Nori, and P. Delsing, "Observation of the dynamical casimir effect in a superconducting circuit," *Nature*, vol. 479, no. 7373, pp. 376–379, 2011.

[54] G. T. Moore, "Quantum theory of the electromagnetic field in a variable-length one-dimensional cavity," *J. Math. Phys.*, vol. 11, p. 2679, 1970.

[55] J. R. Johansson, G. Johansson, C. Wilson, and F. Nori, "Dynamical Casimir effect in a superconducting coplanar waveguide," *Phys. Rev. Lett.*, vol. 103, no. 14, p. 147003, 2009.

[56] J. R. Johansson, G. Johansson, C. M. Wilson, and F. Nori, "Dynamical Casimir effect in superconducting microwave circuits," *Phys. Rev. A*, vol. 82, p. 052509, Nov 2010.

[57] P. D. Nation, J. R. Johansson, M. P. Blencowe, and F. Nori, "Stimulating uncertainty: Amplifying the quantum vacuum with superconducting circuits," *Rev. Mod. Phys.*, vol. 84, pp. 1–24, Jan 2012.

[58] M. Uhlmann, G. Plunien, R. Schützhold, and G. Soff, "Resonant cavity photon creation via the dynamical Casimir effect," *Phys. Rev. Lett.*, vol. 93, no. 19, p. 193601, 2004.

[59] M. Crocce, D. A. R. Dalvit, F. C. Lombardo, and F. D. Mazzitelli, "Model for resonant photon creation in a cavity with time-dependent conductivity," *Phys. Rev. A*, vol. 70, p. 033811, Sep 2004.

[60] A. Cleland and M. Geller, "Superconducting qubit storage and entanglement with nanomechanical resonators," *Phys. Rev. Lett.*, vol. 93, no. 7, p. 070501, 2004.

[61] M. LaHaye, J. Suh, P. Echternach, K. Schwab, and M. Roukes, "Nanomechanical measurements of a superconducting qubit," *Nature*, vol. 459, no. 7249, pp. 960–964, 2009.

[62] S. Etaki, M. Poot, I. Mahboob, K. Onomitsu, H. Yamaguchi, and H. Van der Zant, "Motion detection of a micromechanical resonator embedded in a dc squid," *Nat. Phys.*, vol. 4, no. 10, pp. 785–788, 2008.

[63] L. Wei, Y.-X. Liu, C. Sun, and F. Nori, "Probing tiny motions of nanomechanical resonators: classical or quantum mechanical?," *Phys. Rev. Lett.*, vol. 97, no. 23, p. 237201, 2006.

[64] M. Grajcar, S. Ashhab, J. Johansson, and F. Nori, "Lower limit on the achievable temperature in resonator-based sideband cooling," *Phys. Rev. B*, vol. 78, no. 3, p. 035406, 2008.

[65] J. Teufel, T. Donner, D. Li, J. Harlow, M. Allman, K. Cicak, A. Sirois, J. Whittaker, K. Lehnert, and R. Simmonds, "Sideband cooling of micromechanical motion to the quantum ground state," *Nature*, vol. 475, no. 7356, pp. 359–363, 2011.

[66] A. Armour, M. Blencowe, and K. Schwab, "Entanglement and decoherence of a micromechanical resonator via coupling to a cooper-pair box," *Phys. Rev. Lett.*, vol. 88, no. 14, p. 148301, 2002.

[67] Y.-X. Liu, L. Wei, and F. Nori, "Generation of nonclassical photon states using a superconducting qubit in a microcavity," *EPL*, vol. 67, no. 6, p. 941, 2004.

[68] M. Hofheinz, H. Wang, M. Ansmann, R. Bialczak, E. Lucero, M. Neeley, A. O'Connell, D. Sank, J. Wenner, J. Martinis, and A. Cleland, "Synthesizing arbitrary quantum states in a superconducting resonator," *Nature*, vol. 459, no. 7246, pp. 546–549, 2009.

[69] X.-W. Xu, H. Wang, J. Zhang, and Y.-x. Liu, "Engineering of nonclassical motional states in optomechanical systems," *Phys. Rev. A*, vol. 88, no. 6, p. 063819, 2013.

[70] C. K. Law, "Interaction between a moving mirror and radiation pressure: a hamiltonian formulation," *Phys. Rev. A*, vol. 51, pp. 2537–2541, Mar 1995.

[71] F. Beaudoin, J. Gambetta, and A. Blais, "Dissipation and ultrastrong coupling in circuit QED," *Phys. Rev. A*, vol. 84, no. 4, p. 043832, 2011.

[72] A. Settineri, V. Macrí, A. Ridolfo, O. Di Stefano, A. F. Kockum, F. Nori, and S. Savasta, "Dissipation and thermal noise in hybrid quantum systems in the ultrastrong-coupling regime," *Phys. Rev. A*, vol. 98, p. 053834, Nov 2018.

[73] V. Macrì, A. Ridolfo, O. Di Stefano, A. F. Kockum, F. Nori, and S. Savasta, "Nonperturbative dynamical Casimir effect in optomechanical systems: vacuum Casimir-Rabi splittings," *Phys. Rev. X*, vol. 8, p. 011031, Feb 2018.

[74] K. Hepp and E. H. Lieb, "On the superradiant phase transition for molecules in a quantized radiation field: the Dicke maser model," *Ann. Physics*, vol. 76, no. 2, pp. 360–404, 1973.

[75] Y. K. Wang and F. T. Hioe, "Phase transition in the Dicke model of superradiance," *Phys. Rev. A*, vol. 7, p. 831, Mar 1973.

[76] K. Rzażewski, K. Wódkiewicz, and W. Żakowicz, "Phase transitions, two-level atoms, and the A^2 term," *Phys. Rev. Lett.*, vol. 35, pp. 432–434, Aug 1975.

[77] N. Lambert, C. Emary, and T. Brandes, "Entanglement and the phase transition in single-mode superradiance," *Phys. Rev. Lett.*, vol. 92, no. 7, p. 073602, 2004.

[78] D. De Bernardis, P. Pilar, T. Jaako, S. De Liberato, and P. Rabl, "Breakdown of gauge invariance in ultrastrong-coupling cavity QED," *Phys. Rev. A*, vol. 98, p. 053819, Nov 2018.

[79] A. Stokes and A. Nazir, "Gauge ambiguities imply Jaynes-Cummings physics remains valid in ultrastrong coupling QED," *Nat. Commun.*, vol. 10, no. 1, p. 499, 2019.

[80] H. Kimble, "The quantum internet," *Nature*, vol. 453, no. 7198, pp. 1023–1030, 2008.

[81] A. Boca, R. Miller, K. M. Birnbaum, A. D. Boozer, J. McKeever, and H. J. Kimble, "Observation of the vacuum Rabi spectrum for one trapped atom," *Phys. Rev. Lett.*, vol. 93, no. 23, p. 233603, 2004.

[82] B. W. Shore, "Sir Peter Knight and the Jaynes–Cummings model," *J. Mod. Opt.*, vol. 54, no. 13-15, pp. 2009–2016, 2007.

[83] T. Schwartz, J. Hutchison, C. Genet, and T. Ebbesen, "Reversible switching of ultrastrong light-molecule coupling," *Phys. Rev. Lett.*, vol. 106, no. 19, p. 196405, 2011.

[84] A. A. Anappara, S. De Liberato, A. Tredicucci, C. Ciuti, G. Biasiol, L. Sorba, and F. Beltram, "Light-matter excitations in the ultra-strong coupling regime," *Phys. Rev. B*, vol. 79, p. 201303, 2009.

[85] G. Günter, A. A. Anappara, J. Hees, A. Sell, G. Biasiol, L. Sorba, S. De Liberato, C. Ciuti, A. Tredicucci, A. Leitenstorfer, *et al.*, "Sub-cycle switch-on of ultrastrong light–matter interaction," *Nature*, vol. 458, no. 7235, pp. 178–181, 2009.

[86] G. Scalari, C. Maissen, D. Turčinková, D. Hagenmüller, S. De Liberato, C. Ciuti, C. Reichl, D. Schuh, W. Wegscheider, M. Beck, and J. Faist, "Ultrastrong coupling of the cyclotron transition of a 2D electron gas to a THz metamaterial," *Science*, vol. 335, no. 6074, pp. 1323–1326, 2012.

[87] F. Yoshihara, T. Fuse, S. Ashhab, K. Kakuyanagi, S. Saito, and K. Semba, "Characteristic spectra of circuit quantum electrodynamics systems from the ultrastrong- to the deep-strong-coupling regime," *Phys. Rev. A*, vol. 95, p. 053824, May 2017.

[88] A. Bayer, M. Pozimski, S. Schambeck, D. Schuh, R. Huber, D. Bougeard, and C. Lange, "Terahertz Light-Matter Interaction beyond Unity Coupling Strength," *Nano Lett.*, vol. 17, p. 6340, oct 2017.

[89] D. Braak, "Integrability of the Rabi model," *Phys. Rev. Lett.*, vol. 107, no. 10, p. 100401, 2011.

[90] J.-F. Huang and C. Law, "Photon emission via vacuum-dressed intermediate states under ultrastrong coupling," *Phys. Rev. A*, vol. 89, no. 3, p. 033827, 2014.

[91] L. Garziano, A. Ridolfo, R. Stassi, O. Di Stefano, and S. Savasta, "Switching on and off of ultrastrong light-matter interaction: Photon statistics of quantum vacuum radiation," *Phys. Rev. A*, vol. 88, p. 063829, Dec 2013.

[92] L. Garziano, R. Stassi, A. Ridolfo, O. Di Stefano, and S. Savasta, "Vacuum-induced symmetry breaking in a superconducting quantum circuit," *Phys. Rev. A*, vol. 90, no. 4, p. 043817, 2014.

[93] C. Fabre, M. Pinard, S. Bourzeix, A. Heidmann, E. Giacobino, and S. Reynaud, "Quantum-noise reduction using a cavity with a movable mirror," *Physical Review A*, vol. 49, no. 2, p. 1337, 1994.

[94] S. Mancini and P. Tombesi, "Quantum noise reduction by radiation pressure," *Physical Review A*, vol. 49, no. 5, p. 4055, 1994.

[95] M. Pinard, C. Fabre, and A. Heidmann, "Quantum-nondemolition measurement of light by a piezoelectric crystal," *Physical Review A*, vol. 51, no. 3, p. 2443, 1995.

[96] D. Rugar, R. Budakian, H. Mamin, and B. Chui, "Single spin detection by magnetic resonance force microscopy," *Nature*, vol. 430, no. 6997, pp. 329–332, 2004.

[97] A. G. Krause, M. Winger, T. D. Blasius, Q. Lin, and O. Painter, "A high-resolution microchip optomechanical accelerometer," *Nature Photon.*, vol. 6, no. 11, pp. 768–772, 2012.

[98] M. Castagnino and R. Ferraro, "The radiation from moving mirrors: The creation and absorption of particles," *Ann. Phys.*, vol. 154, no. 1, pp. 1 – 23, 1984.

[99] S. Sarkar, "Photon statistics and moving mirrors," *Journal of the European Optical Society*, vol. 4, no. 6, p. 345, 1992.

[100] G. Barton and C. Eberlein, "On quantum radiation from a moving body with finite refractive index," *Ann. Phys.*, vol. 227, no. 2, pp. 222 – 274, 1993.

[101] S. Mancini, V. Giovannetti, D. Vitali, and P. Tombesi, "Entangling macroscopic oscillators exploiting radiation pressure," *Physical review letters*, vol. 88, no. 12, p. 120401, 2002.

[102] G. Plunien, B. Müller, and W. Greiner, "The casimir effect," *Phys. Rep.*, vol. 134, no. 2, pp. 87 – 193, 1986.

[103] P. W. Milonni, R. J. Cook, and M. E. Goggin, "Radiation pressure from the vacuum: Physical interpretation of the casimir force," *Phys. Rev. A*, vol. 38, pp. 1621–1623, Aug 1988.

[104] F. Haake, "Statistical treatment of open systems by generalized master equations," in *Springer tracts in modern physics*, pp. 98–168, Springer, 1973.

[105] C. Cohen-Tannoudji, B. Diu, and F. Laloë, *Quantum Mechanics: Volume II.* John Wiley & Sons, Inc., 1977.

[106] W. E. Lamb Jr, "Fine structure of the hydrogen atom. iii," *Physical Review*, vol. 85, no. 2, p. 259, 1952.

[107] W. E. Lamb, R. R. Schlicher, and M. O. Scully, "Matter-field interaction in atomic physics and quantum optics," *Phys. Rev. A*, vol. 36, pp. 2763–2772, Sep 1987.

[108] A. F. Starace, "Length and velocity formulas in approximate oscillator-strength calculations," *Phys. Rev. A*, vol. 3, pp. 1242–1245, Apr 1971.

[109] R. Girlanda, A. Quattropani, and P. Schwendimann, "Two-photon transitions to exciton states in semiconductors. application to CuCl," *Phys. Rev. B*, vol. 24, pp. 2009–2017, Aug 1981.

[110] S. Ismail-Beigi, E. K. Chang, and S. G. Louie, "Coupling of nonlocal potentials to electromagnetic fields," *Phys. Rev. Lett.*, vol. 87, p. 087402, Aug 2001.

[111] M. Babiker and R. Loudon, "Derivation of the Power-Zienau-Woolley Hamiltonian in quantum electrodynamics by gauge transformation," *Proc. R. Soc. Lond. A*, vol. 385, no. 1789, pp. 439–460, 1983.

[112] W. P. Healy, "Comment onelectric dipole interaction in quantum optics," *Phys. Rev. A*, vol. 22, pp. 2891–2893, dec 1980.

[113] E. A. Power and T. Thirunamachandran, "Comment on electric dipole interaction in quantum optics," *Phys. Rev. A*, vol. 22, pp. 2894–2895, Dec 1980.

[114] C. Cohen-Tannoudji, J. Dupont-Roc, and G. Grynberg, "Photons and atoms-introduction to quantum electrodynamics," *Wiley-VCH*, 1997.

[115] R. J. Glauber, "The quantum theory of optical coherence," *Phys. Rev.*, vol. 130, no. 6, p. 2529, 1963.

[116] M. Combescot and O. Betbeder-Matibet, "The exciton-polariton: Microscopic derivation of the phenomenological theory," *Solid State Commun*, vol. 80, no. 12, pp. 1011–1015, 1991.

[117] S. Savasta and R. Girlanda, "The particle-photon interaction in systems descrided by model Hamiltonians in second quantization," *Solid State Commun.*, vol. 96, no. 7, pp. 517–522, 1995.

[118] S. Savasta and R. Girlanda, "Quantum description of the input and output electromagnetic fields in a polarizable confined system," *Phys. Rev. A*, vol. 53, no. 4, p. 2716, 1996.

[119] D. De Bernardis, T. Jaako, and P. Rabl, "Cavity quantum electrodynamics in the nonperturbative regime," *Phys. Rev. A*, vol. 97, p. 043820, Apr 2018.

[120] A. Stokes and A. Nazir, "Ultrastrong time-dependent light-matter interactions are gauge-relative," *arXiv preprint arXiv:1902.05160*, 2019.

[121] O. Di Stefano, A. Settineri, V. Macrì, A. Ridolfo, R. Stassi, A. F. Kockum, S. Savasta, and F. Nori, "Interaction of mechanical oscillators mediated by the exchange of virtual photon pairs," *Phys. Rev. Lett.,*, vol. 122, p. 030402, Jan. 2019.

[122] A. Settineri, V. Macrì, L. Garziano, O. Di Stefano, F. Nori, and S. Savasta, "Conversion of mechanical noise into correlated photon pairs: Dynamical casimir effect from an incoherent mechanical drive," *Phys. Rev. A*, vol. 100, p. 022501, Aug 2019.

[123] O. Di Stefano, A. Settineri, V. Macrì, L. Garziano, R. Stassi, S. Savasta, and F. Nori, "Resolution of gauge ambiguities in ultrastrong-coupling cavity QED," *Nat. Phys.*, pp. 803–808, 2019.

[124] L. Garziano, A. Settineri, O. Di Stefano, S. Savasta, and F. Nori, "Gauge invariance of the dicke and hopfield models," *arXiv preprint arXiv:2002.04241*, 2020.

[125] A. Settineri, O. Di Stefano, D. Zueco, S. Hughes, S. Savasta, and F. Nori, "Gauge freedom, quantum measurements, and time-dependent interactions in cavity and circuit QED," *arXiv preprint arXiv:1912.08548*, 2019.

[126] S. Savasta, O. Di Stefano, A. Settineri, D. Zueco, S. Hughes, and F. Nori, "Gauge principle and gauge invariance in quantum two-level systems," *arXiv preprint arXiv:2006.06583*, 2020.

[127] J. Sabio, J. Nilsson, and A. H. Castro Neto, "f-sum rule and unconventional spectral weight transfer in graphene," *Phys. Rev. B*, vol. 78, p. 075410, Aug 2008.

[128] D. Hagenmüller and C. Ciuti, "Cavity QED of the graphene cyclotron transition," *Phys. Rev. Lett.*, vol. 109, no. 26, p. 267403, 2012.

[129] L. Chirolli, M. Polini, V. Giovannetti, and A. H. MacDonald, "Drude weight, cyclotron resonance, and the dicke model of graphene cavity QED," *Physical review letters*, vol. 109, no. 26, p. 267404, 2012.